

QUANTIFICATION AND EVALUATION OF THE BIOMECHANICAL
BEHAVIOUR OF THE TRUNK DURING FUNDAMENTAL TASKS:
SHOULD THE THORACIC SPINE BE CONSIDERED?

ALISON SCHINKEL-IVY

A DISSERTATION SUBMITTED TO
THE FACULTY OF GRADUATE STUDIES
IN PARTIAL FULFILLMENT OF THE REQUIREMENTS
FOR THE DEGREE OF
DOCTOR OF PHILOSOPHY

GRADUATE PROGRAM IN KINESIOLOGY & HEALTH SCIENCE
YORK UNIVERSITY
TORONTO, ONTARIO

September 2014

© Alison Schinkel-Ivy, 2014

Abstract

Thoracic spine research is sparse relative to the lumbar spine. A better understanding of thoracic spine mechanics may provide insight into pain mechanisms in both spine regions. This dissertation quantified and evaluated the biomechanical behaviour of the thoracic spine during fundamental tasks, to determine if monitoring the thoracic spine is necessary in the investigation of spine mechanics.

The number of trials required for repeatable and reliable trunk kinematic and muscle activation measures across maximal ranges-of-motion (ROM) were determined (Study #1). Thirty participants performed 10 trials of upright standing and maximal trunk ROM. Most measures demonstrated high repeatability, with two to five trials required.

The head and arm positions enabling maximal spinal ROM were determined in Study #2 using 24 participants, as relationships have been shown in head, arm, and upper back motion. The greatest angles were produced with the active head–loose arm, active head–crossed arm, and active head–abducted arm positions for maximum flexion, bending, and twisting, respectively.

Studies #3 and #4 determined the segments and superficial muscles that were necessary to quantify the motion and muscle activation characteristics of the trunk, specifically the thoracic spine. Thirty participants performed upright standing, maximum trunk ROM, and thoracic ROM. A four-cluster marker set quantified motion for most movement tasks. Of the 16 muscles tested, 10–14 were necessary to evaluate trunk muscle activation. These studies provided insight into thoracic function in relation to the lumbar spine.

Lumbar co-contraction was quantified during thoracic movements in Study #5. Thirty participants performed upright standing, maximum trunk ROM, and thoracic ROM. Thoracic flexion, bending, and twisting elicited 67%, 45%, and 55% greater co-contraction in the lumbar region than upright standing, demonstrating that the thoracic spine impacts the muscular response of the lumbar spine.

These studies quantified and characterized the biomechanical behaviour of the thoracic spine during fundamental tasks. As the thoracic spine demonstrated differences in motion and muscle activation characteristics along its length and compared to the lumbar spine, knowledge of thoracic spine behaviour and interactions may aid in clarifying the behaviour of and elucidating pain mechanisms within the thoracic and lumbar spine regions.

Dedication

I would like to dedicate this thesis to four of the most important people in my life:

My parents, John and Victoria Schinkel: Be it academics, gymnastics, or any other pursuits, you've always encouraged me to be my best. You've been amazing role models, and I owe you both so much. Thank you for your never-ending love and support, and for lending an ear when I needed it.

My best friend, Justine Stacey: Whether we're living in the same city, across the country, or on different continents, you're there for me with a good story and some laughs whenever I need a friend. It's been 23 years so far... here's to many more.

My husband, Ryan Ivy: My partner and teammate in this awesome journey called life. No matter the challenges I've faced, you have encouraged and supported me to overcome all of them. This would not have been possible without you. Don't forget... Seize the day! (oh... and push the fish, it's about to turn).

Acknowledgements

So many individuals have played an instrumental role in supporting me throughout this process. I won't be able to thank you enough, but I'll give it a shot.

Thanks to:

The Natural Sciences and Engineering Research Council of Canada, the Ontario Graduate Scholarship Program, and York University: For funding support for both myself and this research.

The Statistical Consulting Service at York University: For guidance regarding statistical analyses included in this project.

The Drake lab undergraduate volunteers: For help with data labelling.

The members of my Examining Committee, Dr. Stephan Milosavljevic and Dr. Jennifer Steeves: For your insightful comments during the defense, and for helping to strengthen this final product in the process.

My Supervisory Committee, Dr. William Gage and Dr. Anne Moore: For your support throughout my PhD, from courses and my comprehensive exam to this dissertation. The time you've taken to work with me was always appreciated. Thanks as well for the use of your lab equipment during data collection.

My supervisor, Dr. Janessa Drake: For your guidance, support, and friendship. Your constant encouragement, high expectations, and willingness to support me in professional development opportunities have pushed me to become a better and well-rounded academic and researcher, and I cannot thank you enough. Your open-door policy and willingness to take time for conversation were likewise much appreciated.

My MHK advisor, Dr. David Andrews: For all of your help in setting me up for success in this degree, and for your continuing support and belief in me.

My friends and colleagues from the University of Windsor, Dr. David Andrews, Michael Angelidis, Dr. Timothy Burkhart, and Michael Sonne: We worked hard, played hard (and partook in many a PBR Friday), and had an incredible time doing it. I would not have even considered a PhD if my Masters experience had not been so amazing.

All of my labmates in Biomechanics@York: I couldn't have asked for a better group of people to work with since I've been at York. All of you contributed to making my PhD the great experience that it was. Special thanks to:

- Brian Nairn: For being an amazing colleague and conference/travel buddy, and an even better friend; and for all the great times and bad jokes (2:30 will never be the same). The last four years have had many ups and downs, and you were there through all of them. I couldn't have done it without you.
- Corinne Babiolakis, Brendan Cotter, Jeev Kiriella, Graham Mayberry, and Dmitry Verniba: For being a huge part of my day-to-day support network. All of the laughs and random conversations kept me coming into school every day and helped get me through the rough patches.
- Aaron Siu and Susari Wanninayake: We didn't have a chance to work closely together for very long, but you were both always ready with a smile and a Friends or Whose Line Is It Anyways? quote or video to cheer me up when I needed it. TONK.

Finally, to all of my friends and family: Even if you didn't necessarily realize it, you were all a part of completing this project. Thank you all for your love and support.

Table of Contents

Abstract	ii
Dedication	iv
Acknowledgements	v
Table of Contents	vii
List of Tables	x
List of Figures	xiv
Glossary	xxii
Chapter 1: General Introduction	1
1.1 Thesis Layout	7
1.2 Global Thesis Objective and Hypothesis	10
1.3 Research Aims	10
1.4 Specific Purposes and Hypotheses	11
Chapter 2: Review of Literature	15
2.1 Low Back Pain: Consequences and Risk Factors	16
2.2 Why Study the Thoracic Spine?	18
2.3 Thoracic Spine Anatomy	20
2.4 Thoracic Spine <i>In Vitro</i> Properties	23
2.5 Thoracic Spine <i>In Vivo</i> Properties	25
2.5.1 Motion	25
2.5.2 Motion Patterns	29
2.5.3 Muscle Activation	30
2.5.4 Muscle Activation Patterns	33
2.6 Issues in Thoracic Spine Data Collection	36
2.6.1 Repeatability and Reliability of Motion and Muscle Activation	36
2.6.2 Position of Adjacent Segments	41
2.6.3 Thoracic Spine Data Collection Techniques	43
2.6.3.1 Motion	43
2.6.3.2 Muscle Activation	46
2.7 Literature Review Summary	47
Chapter 3: Repeatability of Kinematic and Electromyographical Measures During Standing and Trunk Motion: How Many Trials are Sufficient?	49
3.1 Introduction	52
3.2 Methods	55
3.2.1 Participants	55
3.2.2 Instrumentation	55
3.2.2.1 Kinematics	55
3.2.2.2 Electromyography	57
3.2.3 Procedures	59

3.2.4	Data Processing.....	61
3.2.5	Data Analysis	64
3.3	Results.....	68
3.4	Discussion.....	79
Chapter 4: Identification of Head and Arm Positions to Elicit Maximal Voluntary		
Trunk Range-of-Motion Measures.....		88
4.1	Introduction.....	90
4.2	Methods.....	93
4.2.1	Participants.....	93
4.2.2	Instrumentation	93
4.2.3	Procedures.....	93
4.2.4	Data Processing.....	97
4.2.5	Data Analysis	99
4.3	Results.....	100
4.4	Discussion.....	110
Chapter 5: Quantification of the Trunk Part I: Which Motion Segments are		
Required to Sufficiently Characterize its Kinematic Behaviour?.....		116
5.1	Introduction.....	118
5.2	Methods.....	121
5.2.1	Participants.....	121
5.2.2	Instrumentation	121
5.2.3	Procedures.....	122
5.2.4	Data Processing and Analysis.....	123
5.3	Results.....	127
5.4	Discussion.....	135
Chapter 6: Quantification of the Trunk Part II: Muscles Required to Represent		
Activation Characteristics During Range-of-Motion Tasks		143
6.1	Introduction.....	145
6.2	Methods.....	148
6.2.1	Participants.....	148
6.2.2	Instrumentation	149
6.2.3	Procedures.....	150
6.2.4	Data Processing and Analysis.....	151
6.3	Results.....	153
6.4	Discussion.....	161
Chapter 7: Does Thoracic Movement Influence Muscle Activation Patterns Around		
the Lumbar Spine?		169
7.1	Introduction.....	172
7.2	Methods.....	174
7.2.1	Participants.....	174

7.2.2	Instrumentation	175
7.2.2.1	Kinematics	175
7.2.2.2	Electromyography	175
7.2.3	Procedures.....	176
7.2.4	Data Processing.....	178
7.2.5	Data Analysis	182
7.3	Results.....	183
7.4	Discussion.....	194
Chapter 8:	General Discussion.....	202
8.1	Global Research Contributions	203
8.2	Specific Research Contributions.....	205
8.2.1	Study #1	205
8.2.2	Study #2	205
8.2.3	Study #3	206
8.2.4	Study #4	207
8.2.5	Study #5	208
8.3	General Limitations	209
8.4	Future Directions	212
8.5	Hypotheses Revisited.....	214
8.5.1	Global Thesis Objective.....	214
8.5.2	Specific Purposes	214
8.6	General Conclusions	218
References	220
Appendix A	247
Appendix B	255
Appendix C	287
Appendix D	292

List of Tables

Table 1:	Number of participants (<i>N</i> ; M: male; F: female) and movement tasks/conditions utilized in each study.....	8
Table 2:	General categories and specific risk factors for thoracic spine pain.....	20
Table 3:	Previous studies reporting repeatability and reliability statistics for kinematic measures	38
Table 4:	Previous studies reporting repeatability and reliability statistics for EMG measures	39
Table 5:	Instrumentation previously used for the measurement of thoracic motion.....	44
Table 6:	Electrode placements for the eight bilateral muscles tested	59
Table 7:	ANOVA results for the kinematic and EMG measures for each task.....	69
Table 8:	Mean (<i>SD</i>) angles (°) calculated using the different sets of trials. There was little change within each measure across the sets, indicating high repeatability.....	70
Table 9:	Number of trials required for each kinematic measure in each task. The intraclass correlation coefficient (ICC), normalized standard error of measurement (SEM) (% of grand mean), and unnormalized SEM (°) corresponding to that number of trials are also reported.....	73
Table 10:	Mean (<i>SD</i>) activation levels (%MVC) calculated using the different sets of trials. There was little change within each measure across the sets, indicating high repeatability.....	75
Table 11:	Number of trials required for each EMG measure in each task. The intraclass correlation coefficient (ICC), normalized standard error of measurement (SEM) (% of grand mean), and unnormalized SEM (°) corresponding to that number of trials are also reported.....	76
Table 12:	Mean (<i>SD</i>) root mean square differences (RMSDs) relative to each set of trials (‘reference’) in each task, collapsed across the ten trials and across measures. The RMSD values were very low, especially for the trial sets in which the averages of multiple trials were used, indicating strong agreement between the trial sets	78
Table 13:	Segments and marker clusters used to determine the angles of interest	98

Table 14:	Mean (<i>SD</i>), minimum, and maximum intraclass correlation coefficients (ICCs) across all angle measures for each movement condition	101
Table 15:	Mean (<i>SD</i>) maximum flexion angles (°) (rotations around the X axis) for each angle measure in the MaxFlex conditions.....	102
Table 16:	Mean (<i>SD</i>) maximum lateral bend angles (°) (rotations around the Y axis) for each angle measure in the MaxBend conditions.....	104
Table 17:	Mean (<i>SD</i>) maximum axial twist angles (°) (rotations around the Z axis) for each angle measure in the MaxTwist conditions.....	107
Table 18:	The head and arm positions that elicited the greatest angles for each measure during each movement task	110
Table 19:	Mean (<i>SD</i>) cross-correlation coefficients (R_{xy}) at zero lag, comparing the angle time series for each adjacent pairing of clusters in each movement task	128
Table 20:	Mean (<i>SD</i>) maximum angles for the movement tasks	128
Table 21:	Pearson product moment correlation coefficients (<i>r</i>) for the maximum angles achieved in each adjacent pairing of clusters in each movement task	129
Table 22:	Adjacent cluster pairings that met the criteria of very strong cross-correlations ($R_{xy}>0.90$) and very strong Pearson correlations ($r>0.80$) for each movement task, indicating that one of the clusters could be eliminated.....	130
Table 23:	To determine whether multiple adjacent clusters could be eliminated, the clusters that were involved in the adjacent pairings that initially met the criteria ($R_{xy}>0.90$, $r>0.80$) were eliminated one at a time, and the R_{xy} and <i>r</i> between the two clusters on either side of the eliminated cluster were determined	131
Table 24:	All identified marker sets for each movement task, consisting of the clusters that remained after applying the elimination criteria of very strong R_{xy} ($R_{xy}>0.90$) and very strong <i>r</i> ($r>0.80$)	132
Table 25:	Mean (<i>SD</i>) activation levels obtained during the holding phase of each movement task, along with the muscles that produced the minimum and maximum activation levels	155

Table 26:	Mean (<i>SD</i>), minimum, and maximum cross-correlation coefficients (R_{xy}) for each movement task, along with the number of pairings (out of 120 total) that resulted in very strong cross-correlations ($R_{xy}>0.90$).....	155
Table 27:	Mean (<i>SD</i>), minimum, and maximum correlation coefficients (<i>r</i>) for each movement task, along with the number of pairings (out of 120 total) that resulted in significant correlations ($p<0.05$).....	156
Table 28:	For pairings that met both criteria for all movement tasks within a movement direction, each muscle within the pairing was ‘eliminated’ and the mean (<i>SD</i>) cross-correlation coefficients (R_{xy}) and correlation coefficients (<i>r</i>) between the eliminated muscle and all other muscles were determined.....	159
Table 29:	Muscles that could be eliminated based on the results presented in Table 28. The muscle within each pairing that exhibited the highest mean cross-correlation coefficients (R_{xy}) and correlation coefficients (<i>r</i>) with all other muscles was eliminated. The remaining muscles required to capture the muscle activation characteristics of the trunk for each movement direction are also listed as Recommended Muscle Sets.....	160
Table 30:	Muscles (column 1) that met the criteria of $R_{xy}>0.90$ and <i>r</i> with $p<0.05$ with at least one other muscle (columns 2-4) for all directions of movement (top); muscle set recommendations common to all movement directions (bottom).....	161
Table 31:	Mean (<i>SD</i>) thoracic and lumbar angles ($^{\circ}$) obtained during each movement task in the plane of interest.....	184
Table 32:	Mean (<i>SD</i>), minimum, and maximum EMG levels (%MVC) for the lumbar muscles from the holding phase of each movement task.....	185
Table 33:	ANOVA statistics for all lumbar muscle pairings with a significant effect of task on co-contraction ($p<0.05$).....	187
Table 34:	Mean (<i>SD</i>), minimum, and maximum co-contraction index values (%MVC) from all possible pairings of lumbar muscles (28 total)	188
Table 35:	Mean (<i>SD</i>), minimum, and maximum difference (%) from Upright for all possible pairings of lumbar muscles (28 total)	189
Table 36:	ANOVA statistics for all upper muscle pairings with a significant effect of task on co-contraction ($p<0.05$).....	191

Table 37:	Mean (<i>SD</i>), minimum, and maximum co-contraction index values (%MVC) from all possible pairings of upper muscles (28 total).....	192
Table 38:	Mean (<i>SD</i>), minimum, and maximum difference (%) from Upright for all possible pairings of upper muscles (28 total).....	192
Table 39:	Significant correlations between thoracic angles and activation measures for the lumbar muscles (activation level (single muscle), CCI (muscle pairing)) for each direction of movement.....	194
Table 40:	Instructions given to participants prior to each trial with keywords describing the features of the task.....	248
Table 41:	Markers used to define the endpoints of each segment and cluster	291

List of Figures

Figure 1:	Mean (<i>SD</i>) range-of-motion (ROM) and neutral zone (NZ) for axial rotation in four spinal regions	24
Figure 2:	Mean (<i>SD</i>) ranges-of-motion (ROM) (°) of primary movements in each thoracic region.....	26
Figure 3:	Mean (<i>SD</i>) range of thoracic range-of-motion (ROM) (°) in axial twist and coupled lateral bend for neutral, flexed, and extended sagittal postures	28
Figure 4:	Percentage of participants displaying ipsilateral, contralateral, and variable lateral bend coupling during axial twist movements in neutral, flexed, and extended sagittal postures.....	29
Figure 5:	EMG amplitudes for the longissimus thoracis at T ₅ (L _{T5}), T ₈ (L _{T8}), and T ₁₁ (L _{T11}) during neutral sitting and seated axial twist, normalized to the peak axial twist amplitude.....	32
Figure 6:	Mean (<i>SD</i>) co-contraction (% maximum voluntary contraction; %MVC) of the left lower-thoracic erector spinae–left upper-thoracic erector spinae pairing per minute for 15 minute time intervals over 2 hours of prolonged sitting, comparing individuals who did (pain developers; PD) and did not (non-pain developers; NPD) develop pain.....	34
Figure 7:	Previous marker setup used to calculate a general thoracic angle	45
Figure 8:	Previous marker setup used to calculate angles for four thoracic regions	45
Figure 9:	Marker setup in the sagittal view	56
Figure 10:	Electrode placements for the abdominal musculature	58
Figure 11:	Electrode placements for the back musculature.....	58
Figure 12:	Collapsed 3D sagittal view of the markers in Visual3D.....	63
Figure 13:	Collapsed 3D sagittal view of the markers representing the calculation of each angle	64
Figure 14:	Graphical representation of the mean (<i>SD</i>) angles (°) for a) Upright and b) maximum trunk ROM movement tasks for each set of trials for the lumbar angle measure	71

Figure 15: Graphical representation of the mean (<i>SD</i>) EMG (%MVC) for each set of trials for the right lumbar erector spinae.....	72
Figure 16: Combinations of head and arm positions used for MaxFlex	95
Figure 17: Combinations of head and arm positions used for MaxBend.....	96
Figure 18: Combinations of head and arm positions used for MaxTwist.....	97
Figure 19: Collapsed 3D sagittal view of the markers representing the calculation of each angle	99
Figure 20: Graphical representation of the mean (<i>SD</i>) maximum angles in the upper regions during the MaxFlex conditions	102
Figure 21: Graphical representation of the mean (<i>SD</i>) maximum angles in the lower and global regions during the MaxFlex conditions.....	103
Figure 22: Graphical representation of the mean (<i>SD</i>) maximum angles in the head and cervico-thoracic regions during the MaxBend conditions	104
Figure 23: Graphical representation of the mean (<i>SD</i>) maximum angles in the thoracic regions during the MaxBend conditions	105
Figure 24: Graphical representation of the mean (<i>SD</i>) maximum angles in the lower and global regions during the MaxBend conditions	105
Figure 25: Graphical representation of the mean (<i>SD</i>) maximum angles in the head and cervico-thoracic regions during the MaxTwist conditions.....	108
Figure 26: Graphical representation of the mean (<i>SD</i>) maximum angles in the thoracic regions during the MaxTwist conditions.....	108
Figure 27: Graphical representation of the mean (<i>SD</i>) maximum angles in the lumbar region during the MaxTwist conditions.....	109
Figure 28: Graphical representation of the mean (<i>SD</i>) maximum angles in the trunk and pelvis during the MaxTwist conditions.....	109
Figure 29: Collapsed 3D sagittal view of the markers representing the calculation of each angle	124
Figure 30: The final marker set recommendation that was appropriate for the greatest number of movement tasks (6 of 7).....	135
Figure 31: a) Upright standing; b) Slumped standing	250

Figure 32: Combinations of head and arm positions used for MaxFlex	251
Figure 33: Combinations of head and arm positions used for MaxBend	252
Figure 34: Combinations of head and arm positions used for MaxTwist	253
Figure 35: a) Thoracic flexion; b) Thoracic bend; c) Thoracic twist. Participants kept the low back as neutral as possible while moving the head and thoracic spine	254
Figure 36: Orientation of the participant relative to the laboratory coordinate system.....	289
Figure 37: a) Posterior view of a cluster when adhered to the skin over the spine. b) Top view of a cluster when adhered to the skin over the spine	290
Figure 38: Sample time series data set of head, lumbar, pelvis, thoracic, and trunk flexion-extension angles during upright standing	293
Figure 39: Sample time series data set of head, lumbar, pelvis, thoracic, and trunk lateral bend angles during upright standing	294
Figure 40: Sample time series data set of head, lumbar, pelvis, thoracic, and trunk axial twist angles during upright standing	294
Figure 41: Sample time series data set of head, lumbar, pelvis, thoracic, and trunk flexion angles during MaxFlex	295
Figure 42: Sample time series data set of head, lumbar, pelvis, thoracic, and trunk lateral bend angles during MaxBend.....	295
Figure 43: Sample time series data set of head, lumbar, pelvis, thoracic, and trunk axial twist angles during MaxTwist	296
Figure 44: Sample time series data set of LEO, LIO, and LRA during upright standing.	296
Figure 45: Sample time series data set of LLES, LLTES, and LUTES during upright standing.....	297
Figure 46: Sample time series data set of LLD and LTR during upright standing	297
Figure 47: Sample time series data set of REO, RIO, and RRA during upright standing	298

Figure 48: Sample time series data set of RLES, RLTES, and RUTES during upright standing.....	298
Figure 49: Sample time series data set of RLD and RTR during upright standing	299
Figure 50: Time series data set of trunk angles in the flexion-extension, lateral bend, and axial twist directions during upright standing, as context for the EMG time series data sets	299
Figure 51: Sample time series data set of LEO, LIO, and LRA during MaxFlex	300
Figure 52: Sample time series data set of LLES, LLTES, and LUTES during MaxFlex	300
Figure 53: Sample time series data set of LLD and LTR during MaxFlex.	301
Figure 54: Sample time series data set of REO, RIO, and RRA during MaxFlex.	301
Figure 55: Sample time series data set of RLES, RLTES, and RUTES during MaxFlex	302
Figure 56: Sample time series data set of RLD and RTR during MaxFlex.....	302
Figure 57: Time series data set of trunk flexion angles during MaxFlex, as context for the EMG time series data sets	303
Figure 58: Sample time series data set of LEO, LIO, and LRA during MaxBend.....	303
Figure 59: Sample time series data set of LLES, LLTES, and LUTES during MaxBend	304
Figure 60: Sample time series data set of LLD and LTR during MaxBend.....	304
Figure 61: Sample time series data set of REO, RIO, and RRA during MaxBend	305
Figure 62: Sample time series data set of RLES, RLTES, and RUTES during MaxBend	305
Figure 63: Sample time series data set of RLD and RTR during MaxBend	306
Figure 64: Time series data set of trunk lateral bend angles during MaxBend, as context for the EMG time series data sets.....	306
Figure 65: Sample time series data set of LEO, LIO, and LRA during MaxTwist.....	307

Figure 66: Sample time series data set of LLES, LLTES, and LUTES during MaxTwist	307
Figure 67: Sample time series data set of LLD and LTR during MaxTwist	308
Figure 68: Sample time series data set of REO, RIO, and RRA during MaxTwist	308
Figure 69: Sample time series data set of RLES, RLTES, and RUTES during MaxTwist	309
Figure 70: Sample time series data set of RLD and RTR during MaxTwist.....	309
Figure 71: Time series data set of trunk axial angles during MaxTwist, as context for the EMG time series data sets	310
Figure 72: Sample time series data set of the head, CT, thoracic, UT, MT, and LT flexion angles during MaxFlex (neutral head, crossed arms)	311
Figure 73: Sample time series data set of the lumbar, pelvis, and trunk flexion angles during MaxFlex (neutral head, crossed arms).....	311
Figure 74: Sample time series data set of the head, CT, thoracic, UT, MT, and LT flexion angles during MaxFlex (active head, crossed arms).....	312
Figure 75: Sample time series data set of the lumbar, pelvis, and trunk flexion angles during MaxFlex (active head, crossed arms)	312
Figure 76: Sample time series data set of the head, CT, thoracic, UT, MT, and LT lateral bend angles during MaxBend (neutral head, crossed arms)	313
Figure 77: Sample time series data set of the lumbar, pelvis, and trunk lateral bend angles during MaxBend (neutral head, crossed arms)	313
Figure 78: Sample time series data set of the head, CT, thoracic, UT, MT, and LT lateral bend angles during MaxBend (active head, crossed arms).....	314
Figure 79: Sample time series data set of the lumbar, pelvis, and trunk lateral bend angles during MaxBend (active head, crossed arms).....	314
Figure 80: Sample time series data set of the head, CT, thoracic, UT, MT, and LT axial twist angles during MaxTwist (neutral head, crossed arms).....	315
Figure 81: Sample time series data set of the lumbar, pelvis, and trunk axial twist angles during MaxTwist (neutral head, crossed arms).....	315

Figure 82: Sample time series data set of the head, CT, thoracic, UT, MT, and LT axial twist angles during MaxTwist (active head, crossed arms).....	316
Figure 83: Sample time series data set of the lumbar, pelvis, and trunk axial twist angles during MaxTwist (active head, crossed arms)	316
Figure 84: Sample time series data set of the flexion angles of the C ₇ , T ₃ , T ₆ , T ₉ , T ₁₂ , and L ₅ clusters during MaxFlex.	317
Figure 85: Sample time series data set of the lateral bend angles of the C ₇ , T ₃ , T ₆ , T ₉ , T ₁₂ , and L ₅ clusters during MaxBend.....	317
Figure 86: Sample time series data set of the axial twist angles of the C ₇ , T ₃ , T ₆ , T ₉ , T ₁₂ , and L ₅ clusters during MaxTwist.	318
Figure 87: Sample time series data set of the flexion angles of the C ₇ , T ₃ , T ₆ , T ₉ , T ₁₂ , and L ₅ clusters during Slump	318
Figure 88: Sample time series data set of the flexion angles of the C ₇ , T ₃ , T ₆ , T ₉ , T ₁₂ , and L ₅ clusters during ThorFlex.....	319
Figure 89: Sample time series data set of the lateral bend angles of the C ₇ , T ₃ , T ₆ , T ₉ , T ₁₂ , and L ₅ clusters during ThorBend	319
Figure 90: Sample time series data set of the axial twist angles of the C ₇ , T ₃ , T ₆ , T ₉ , T ₁₂ , and L ₅ clusters during ThorTwist.....	320
Figure 91: Sample time series of the flexion angles of the T ₁₂ and L ₅ clusters during MaxFlex, used for the sample cross-correlation in Figure 92	320
Figure 92: Output of the cross-correlation performed between the T ₁₂ and L ₅ flexion angles during MaxFlex (shown in Figure 91). Positive values indicate that the clusters were moving in the same direction.....	321
Figure 93: Sample time series of the flexion angles of the T ₁₂ and L ₅ clusters during Slump, used for the sample cross-correlation in Figure 94	321
Figure 94: Output of the cross-correlation performed between the T ₁₂ and L ₅ flexion angles during Slump (shown in Figure 93). Negative values indicate that the clusters were moving in opposite directions.....	322
Figure 95: Sample time series data set of LEO, LIO, and LRA during Slump	323
Figure 96: Sample time series data set of LLES, LLTES, and LUTES during Slump	323

Figure 97: Sample time series data set of LLD and LTR during Slump	324
Figure 98: Sample time series data set of REO, RIO, and RRA during Slump	324
Figure 99: Sample time series data set of RLES, RLTES, and RUTES during Slump	325
Figure 100: Sample time series data set of RLD and RTR during Slump	325
Figure 101: Time series data set of trunk flexion angles during Slump, as context for the EMG time series data sets.....	326
Figure 102: Sample time series data set of LEO, LIO, and LRA during ThorFlex	326
Figure 103: Sample time series data set of LLES, LLTES, and LUTES during ThorFlex	327
Figure 104: Sample time series data set of LLD and LTR during ThorFlex	327
Figure 105: Sample time series data set of REO, RIO, and RRA during ThorFlex	328
Figure 106: Sample time series data set of RLES, RLTES, and RUTES during ThorFlex	328
Figure 107: Sample time series data set of RLD and RTR during ThorFlex	329
Figure 108: Time series data set of trunk flexion angles during ThorFlex, as context for the EMG time series data sets.....	329
Figure 109: Sample time series data set of LEO, LIO, and LRA during ThorBend ...	330
Figure 110: Sample time series data set of LLES, LLTES, and LUTES during ThorBend.....	330
Figure 111: Sample time series data set of LLD and LTR during ThorBend.....	331
Figure 112: Sample time series data set of REO, RIO, and RRA during ThorBend...	331
Figure 113: Sample time series data set of RLES, RLTES, and RUTES during ThorBend.....	332
Figure 114: Sample time series data set of RLD and RTR during ThorBend	332
Figure 115: Time series data set of trunk lateral bend angles during ThorBend, as context for the EMG time series data sets.....	333

Figure 116:	Sample time series data set of LEO, LIO, and LRA during ThorTwist...	333
Figure 117:	Sample time series data set of LEO, LIO, and LRA during ThorTwist...	334
Figure 118:	Sample time series data set of LLD and LTR during ThorTwist.....	334
Figure 119:	Sample time series data set of REO, RIO, and RRA during ThorTwist	335
Figure 120:	Sample time series data set of RLES, RLTES, and RUTES during ThorTwist	335
Figure 121:	Sample time series data set of RLD and RTR during ThorTwist	336
Figure 122:	Time series data set of trunk axial twist angles during ThorTwist, as context for the EMG time series data sets	336
Figure 123:	Sample time series of the activation of REO and RIO during MaxTwist, used for the sample cross-correlation in Figure 124.....	337
Figure 124:	Output of the cross-correlation performed between REO and RIO during MaxTwist (as shown in Figure 123). Positive values indicate that the muscles were activating at the same time.....	337
Figure 125:	Sample time series of the activation of RLES and RLTES during MaxFlex, used for the sample cross-correlation in Figure 126.....	338
Figure 126:	Output of the cross-correlation performed between REO and RIO during MaxTwist (as shown in Figure 125). Positive values indicate that the muscles were activating at the same time.....	338

Glossary

ASIS: Anterior superior iliac spine.

CCI: Co-contraction index; quantifies the extent of co-contraction between two muscles with respect to both activation magnitude and timing.

CT: Cervico-thoracic (relative angle between C₇ and T₃ marker clusters).

EMG: Electromyography.

EO: External oblique.

ES: Erector spinae.

GT: Greater trochanter.

IC: Iliac crest.

ICC: Intraclass correlation coefficient.

IO: Internal oblique.

LBP: Low back pain.

LD: Latissimus dorsi.

LT: Lower-thoracic (relative angle between T₉ and T₁₂ marker clusters).

MaxBend: Maximum trunk lateral bend.

MaxFlex: Maximum trunk flexion.

MaxTwist: Maximum trunk axial twist.

MT: Mid-thoracic (relative angle between T₆ and T₉ marker clusters).

MVC: Maximum voluntary contraction; used to normalize EMG signals from experimental tasks, yielding %MVC.

NPD: Non-pain developers; individuals who do not develop transient pain in response to a prolonged, low-level, static exposure.

PD: Pain developers; individuals who develop transient pain in response to a prolonged, low-level, static exposure.

RA: Rectus abdominis.

ROM: Range-of-motion.

SEM: Standard error of measurement; can be normalized to the grand mean, yielding SEM%.

Slump: Slumped standing.

ThorBend: Thoracic lateral bend.

ThorFlex: Thoracic flexion.

ThorTwist: Thoracic axial twist.

TR: Upper trapezius.

Upright: Upright standing.

UT: Upper-thoracic (relative angle between T₃ and T₆ marker clusters).

CHAPTER 1

General Introduction

CHAPTER 1

General Introduction

Back pain is a very common occupational-related musculoskeletal disorder, constituting one of the top ten causes for medical visits in the United States (Centers for Disease Control and Prevention, 2013). The lifetime prevalence of low back pain (LBP) has been estimated as 70% (Waters et al., 1993) and between 65% and 80% (Bird & Payne, 1999) in the general population, and as 63% in an occupational population (Thiese et al., 2014). Accordingly, the direct and indirect costs of back pain in industry are substantial (Makhsous et al., 2009). The lumbar spine has been more extensively researched due to the prevalence of pain in that region (Briggs et al., 2007; Edmondston & Singer, 1997). However, Briggs et al. (2009) found that the one-year prevalence of thoracic spine pain was approximately 30% for most occupational groups. Consequently, a better understanding of the behaviours of the thoracic spine may contribute to the identification of mechanisms of pain in this region. Furthermore, increased knowledge of thoracic spine behaviours, and the ways in which the thoracic and lumbar spine regions interact, may also enable a better understanding of the mechanisms of LBP.

To examine the mechanics of the thoracic spine, the repeatability and reliability of kinematic and electromyography (EMG) measures in that region must be understood. Within-session reliability has been investigated for kinematic measures during upright standing (Dunk et al., 2005), and EMG measures during maximal and submaximal isometric contractions (Dankaerts et al., 2004). Allison and Fukushima (2003) and Sparto

and Parnianpour (2001) put forth recommendations for the number of trials required to obtain repeatable measures for targeted trunk angles and contraction levels, respectively. However, within-session repeatability and reliability have not been investigated for unconstrained trunk movement tasks (upright standing and maximum trunk range-of-motion (ROM)) with the intent of providing recommendations for the minimum numbers of trials required for kinematic and EMG measures. Study #1 (Chapter 3) addressed this issue.

The nature of the interactions between various regions of the spine and adjacent segments, such as the head and arms, are also important to understand given the proximity of the head and arms to the thoracic spine. Past studies have reported relationships in the posture of the neck and thoracic spine, and upper-cervical and thoracic spine regions during upright standing (Kuo et al., 2009). Further, relationships have been shown in the motion of the cervical and upper-thoracic spine regions (Tsang et al., 2013) and the spine and arms (Crosbie et al., 2008; Theodoridis & Ruston, 2002). Therefore, it is essential that the effects of head and arm positions on trunk kinematics be quantified, and the positions that enable the elicitation of maximum trunk ROM be identified (Study #2, Chapter 4).

Similarly, gaps exist in the literature regarding the relationships in motion and muscle activation characteristics in the trunk (for the purposes of this dissertation, 'trunk' refers to the thoracic and lumbar spine regions together). Few studies have examined the coordination amongst the various regions of the spine. Notably, a study published by Johnson et al. (2010) determined the temporal relationships in head, cervical, upper-

thoracic (T₁–T₆), mid-thoracic (T₇–T₁₂), lumbar, and pelvis angles during sit-to-stand movement tasks. The motion patterns of adjacent regions showed high cross-correlations at zero time lag, ranging from $R_{xy}=0.71$ to $R_{xy}=0.98$, with the strongest cross-correlations between the thoracic spine regions (Johnson et al., 2010). Shan et al. (2014) identified strong relationships in the activation patterns of the bilateral lumbar ES muscles during trunk flexion and extension. Conversely, Lee et al. (2005) identified differences in activation levels at various spinal levels of the thoracic erector spinae (ES), indicating that single recording sites may not be sufficient to capture the muscle activation characteristics of the trunk. A comprehensive investigation of the relationships in motion and muscle activation characteristics within the thoracic spine, and between the thoracic and lumbar spine regions, is needed. This would be beneficial for elucidating a clear depiction of the behaviour of the trunk. Such an investigation was performed in Studies #3 and #4 (Chapters 5 and 6).

Standardization of the instrumentation used for thoracic spine data collection is also required for such investigations. Kinematically, the thoracic spine has been quantified as a single angle between the superior and inferior aspects (Dunk & Callaghan, 2005; Preuss & Popovic, 2010), or has been divided into two (Hidalgo et al., 2012; Johnson et al., 2010), three (Willems et al., 1996), or four (Lee et al., 2013; Preuss & Popovic, 2010) segments. Activation has been measured for the lower-thoracic ES (Drake et al., 2006; McGill, 1991; Nelson-Wong & Callaghan, 2010), latissimus dorsi (LD) (Drake et al., 2006; McGill, 1991), upper-thoracic ES (Burnett et al., 2009; Caneiro et al., 2010; Edmondston et al., 2011a), and upper trapezius (TR) (Burnett et al., 2009;

Caneiro et al., 2010). However, the segments and muscles necessary to adequately represent the motion and muscle activation characteristics of the thoracic spine remain to be determined, which was addressed in Studies #3 and #4 (Chapters 5 and 6).

Activation patterns within the trunk can also be quantified using a co-contraction measure. Co-contraction is a clinically important measure, with individuals with LBP exhibiting higher co-contraction relative to healthy participants (D'Hooge et al., 2013; Graham et al., 2014). Similar trends have also been identified in healthy individuals who develop transient LBP in response to a prolonged, low-level exposure (Nelson-Wong & Callaghan, 2010; Schinkel-Ivy et al., 2013). While co-contraction acts to stiffen and stabilize the spine, it is also associated with increased compressive forces in spinal joints (McGill et al., 2003) and increased metabolic cost (Cholewicki & McGill, 1996; Missenard et al., 2008), thereby contributing to long-term fatigue and injury risk. Previously, trunk muscle co-contraction has been examined during isometric trunk exertions (Brown & McGill, 2008; Granata et al., 2005a, b; Thelen et al., 1995), maximum trunk flexion-extension (Graham et al., 2014), and prolonged exposures (Nelson-Wong & Callaghan, 2010; Schinkel-Ivy et al., 2013). The co-contraction of the musculature in one region of the spine in response to non-neutral postures in another region has not yet been quantified. This issue was addressed in Study #5 (Chapter 7).

For the purposes of this dissertation, the term 'fundamental tasks' was used to refer to upright and slumped standing, maximum trunk ROM movement tasks, and thoracic ROM movement tasks. Subsets of these tasks were utilized for each of the five studies presented in this dissertation. These tasks were deemed to be fundamental for

several reasons. Firstly, the standing tasks (upright/slumped standing) represent postures that are commonly adopted in everyday life. The ROM tasks were performed predominantly in one plane of motion, and represent the ‘building blocks’ of trunk movement, in that components of these basic movements are incorporated into the complex movements that individuals use during activities of daily living as well as occupational tasks. Further, studies have identified differences in kinematic and EMG measures during these tasks between healthy participants and those with LBP (Ferguson et al., 1996a, b; Hidalgo et al., 2012; Geisser et al., 2005; Sheeran et al., 2012). As such, both types of measures have been suggested as potential screening or diagnosis tools for LBP (Geisser et al., 2005; Hidalgo et al., 2012), with additional potential for tracking rehabilitation progress as well as use in clinical intervention trials (Hidalgo et al., 2012; Marras et al., 1993b). Additionally, for research purposes, both upright and maximal angles may be used for data calibration and normalization purposes, to facilitate comparisons between individuals and groups (Edmondston et al., 2007b). Similarly, EMG levels from these tasks may be used as a submaximal value to normalize subsequent data. For all of these applications, an understanding of the behaviours of the trunk during the aforementioned tasks is critical as a precursor to the study of complex movements (those occurring in more than one plane of motion).

While studies regarding the thoracic spine have become more prevalent within the literature, gaps remain with respect to the muscle activation characteristics of the thoracic spine, along with relationships in the motion segments and muscles both within the thoracic spine and between the lumbar and thoracic spine regions. Therefore, this

dissertation aimed to quantify and evaluate these characteristics during fundamental tasks, as well as to address prevalent issues within the thoracic spine literature, to ultimately determine whether it is necessary to monitor or account for the thoracic spine during the investigation of spinal mechanics.

1.1 Thesis Layout

A literature review (Chapter 2) was undertaken to define the scope of the issues related to the thoracic spine, and to determine the most important directions for the present dissertation. Five studies are presented within Chapters 3 to 7 to address each of the specific research purposes listed below, in relation to the global thesis objective. All research purposes were addressed using data collected from the same group of 30 participants (young adults who were asymptomatic for back pain), during one collection session per participant. Different subsets of the data were used depending on the specific research question (Table 1). Where movement tasks overlapped between studies, the same 10 trials were utilized in each analysis (for example, the same 10 upright standing trials were used for both Study #1 and Study #5). Chapter 8 provides general discussion on the findings of the five studies, including the global and specific research contributions, common limitations, and future directions. The hypotheses posed in Chapter 1 are also revisited, and general conclusions are provided.

Table 1: Number of participants (*N*; M: male; F: female) and movement tasks/conditions utilized in each study. For specific instructions given to participants for each task, refer to Appendix A.

Study	<i>N</i>	Movement Tasks
1. Repeatability of Kinematic and Electromyographical Measures During Standing and Trunk Motion: How Many Trials are Sufficient?	<i>N</i> = 30 (15 M, 15 F)	Upright standing Maximum trunk flexion (active head, crossed arms) Maximum trunk lateral bend (active head, crossed arms) Maximum trunk axial twist (active head, crossed arms)
2. Identification of Head and Arm Positions to Elicit Maximal Voluntary Trunk Range-of-Motion Measures	<i>N</i> = 24 (12 M, 12 F)	Maximum trunk flexion (active head, crossed arms) Maximum trunk flexion (active head, loose arms) Maximum trunk flexion (neutral head, crossed arms) Maximum trunk flexion (neutral head, loose arms) Maximum trunk lateral bend (active head, crossed arms) Maximum trunk lateral bend (active head, loose arms) Maximum trunk lateral bend (neutral head, crossed arms) Maximum trunk lateral bend (neutral head, loose arms) Maximum trunk axial twist (active head, crossed arms) Maximum trunk axial twist (active head, abducted arms) Maximum trunk axial twist (active head, loose arms) Maximum trunk axial twist (neutral head, crossed arms) Maximum trunk axial twist (neutral head, abducted arms) Maximum trunk axial twist (neutral head, loose arms)
3. Quantification of the Trunk Part I: Which Motion Segments are Required to Sufficiently Characterize its Kinematic Behaviour?	<i>N</i> = 30 (15 M, 15 F)	Maximum trunk flexion (active head, crossed arms) Maximum trunk lateral bend (active head, crossed arms) Maximum trunk axial twist (active head, crossed arms) Thoracic flexion Thoracic lateral bend Thoracic axial twist Slumped standing
4. Quantification of the Trunk Part II: Muscles Required to Represent Activation Characteristics During Range-of-Motion Tasks	<i>N</i> = 30 (15 M, 15 F)	Maximum trunk flexion (active head, crossed arms) Maximum trunk lateral bend (active head, crossed arms) Maximum trunk axial twist (active head, crossed arms) Thoracic flexion Thoracic lateral bend Thoracic axial twist Slumped standing
5. Does Thoracic Movement Influence Muscle Activation Patterns Around the Lumbar Spine?	<i>N</i> = 30 (15 M, 15 F)	Upright standing Maximum trunk flexion (active head, loose arms) Maximum trunk lateral bend (active head, loose arms) Maximum trunk axial twist (active head, loose arms) Thoracic flexion Thoracic lateral bend Thoracic axial twist

As the data for all five studies were collected, processed, and analyzed in tandem, the recommendations from the first two studies were not yet available for application to Studies #3, #4, and #5. Although two trials may have been sufficient for some measures analyzed for the later studies, ten trials would still have been utilized to ensure the highest possible repeatability and reliability for all measures. Further, because different processing and analysis techniques were employed in Study #1 compared to Studies #3, #4, and #5, it was unknown whether two or three trials would provide sufficient repeatability for some of the analysis techniques used in the later studies. Study #2 identified an active head and loose arms, an active head and crossed arms, and an active head and abducted arms as the head and arm positions to produce the greatest spinal angles in maximum flexion, maximum lateral bend, and maximum axial twist movement tasks. However, other combinations of head and arm positions were employed in the later studies. For Studies #3 and #4, the active head and crossed arm positions were utilized for all maximum trunk ROM tasks. This combination of head and arm positions was selected for increased experimental control over the maximum ROM attained, as well as to ensure consistent activation patterns of the trunk muscles, especially those of the upper- and mid-back, to the greatest extent possible. For Study #5, the combination of active head and loose arms was selected for all maximum trunk ROM tasks, as these combinations were the most similar to those of the thoracic ROM tasks.

1.2 Global Thesis Objective and Hypothesis

Together, the studies of this dissertation seek to address one overarching, global objective:

To determine if it is necessary to monitor or account for the thoracic spine during the investigation of trunk and lumbar mechanics.

Rationale: Although the literature surrounding the thoracic spine is relatively sparse, knowledge of thoracic spine behaviours may assist in elucidating mechanisms of pain and injury in both the thoracic and lumbar spine regions. The thoracic spine is unique among the spine regions due to its size and articulations with the rib cage (Sizer et al., 2007), and displays both kinematic (White & Panjabi, 1990) and muscle activation (Lee et al., 2005) characteristics that differ from both the lumbar spine.

Hypothesis: It is hypothesized that it is necessary to monitor or account for these characteristics of the thoracic spine during the investigation of spinal mechanics.

1.3 Research Aims

The aims of this dissertation were:

- 1. To determine the best techniques for collecting kinematic and muscle activation data for the thoracic spine (Chapters 3, 4, 5, and 6).*
- 2. To understand factors contributing to thoracic spine motion characteristics (Chapter 4).*
- 3. To quantify the motion and muscle activation characteristics of the thoracic spine (Chapters 5 and 6).*

4. *To understand the effect of the thoracic spine on the lumbar spine, and/or the interactions between the two spine regions (Chapters 5, 6, and 7).*

1.4 Specific Purposes and Hypotheses

The specific purposes addressed by this dissertation were:

1. *To evaluate the repeatability and reliability of kinematic and EMG measures, and to determine the minimum number of trials required to achieve repeatability and reliability.*

Rationale: Upright standing is a commonly used posture throughout daily life, and it is likely that individuals have adopted a consistent posture that is the most comfortable for them. Maximum trunk ROM is limited by individuals' flexibility, and therefore it is not possible to over-shoot the 'target' posture. Further, posture-based instructions were provided to the participant, as opposed to task-based instructions. With respect to EMG measures, there are various activation strategies that an individual may employ to accomplish a movement outcome, and these may not be as consistent between multiple trials performed by an individual.

Hypothesis: It was hypothesized that the repeatability and reliability of both kinematic and EMG measures would be relatively high during upright standing and maximum trunk ROM movement tasks. It was further hypothesized that kinematic measures would demonstrate higher repeatability and reliability than EMG measures.

2. *To determine which head and arm positions enabled the greatest voluntary ROM in spine angle measures during maximum flexion, lateral bend, and axial twist.*

Rationale: Relationships have previously been established in the motion of the head and thoracic spine, and arms and thoracic spine (Crosbie et al., 2008, 2010; Kuo et al., 2009; Theodoridis & Ruston, 2002; Tsang et al., 2013). Lower and global regions may be limited in ROM by a finite amount of flexibility amongst the structures of the spinal column.

Hypothesis: It was hypothesized that the greatest angles would be elicited from the upper spinal regions (head, thoracic, and segmented thoracic measures) by the active head (moving the head in the direction of trunk motion) and crossed arm positions. Conversely, the neutral head (aligned with the trunk) and loose arm positions would elicit the greatest angles for the lower and global regions (lumbar, trunk, and pelvis) for maximum flexion and bending, and neutral head and abducted arms for maximum twist.

3. *To determine the set of segments necessary to sufficiently characterize the kinematics of the trunk and specifically the thoracic spine.*

Rationale: The thoracic spine exhibits varying motion characteristics along its length, in that flexion and lateral bend increase from the upper- to lower-thoracic regions, while the greatest amount of axial twist has been found in the mid-thoracic region (Willems et al., 1996).

Hypothesis: For this exploratory study, it was hypothesized that for each movement task examined, not all collected segments would be necessary to characterize the kinematics of the thoracic spine. However, due to the motion characteristics differing between the smaller thoracic spine regions (Willems et al., 1996), it was expected that in order to

sufficiently characterize thoracic spine motion in all directions, a marker set consisting of five to six clusters would be required.

4. *To investigate the interactions between the thoracic and lumbar musculature, and to determine which superficial muscles were necessary to adequately capture the gross trunk muscle activation characteristics.*

Rationale: EMG measures are generally accepted to be highly variable both within- and between-individuals, and are task-dependent. Often during trunk movements, muscles activate even when they do not contribute directly to the movement (Thelen et al., 1995).

Hypothesis: For this exploratory study, it was hypothesized that the majority of tested muscles would be required to quantify the muscle activation characteristics in the trunk, due to the wide range of functions of the tested muscles. Further, muscles from both the anterior (abdominal) and posterior sides of the body would be required to quantify the gross trunk muscle activation characteristics, due to the multi-directional nature of the movement tasks tested, but there would be some grouping within the abdominal and/or back musculature.

5. *To determine the extent of the increases in co-contraction in the lumbar musculature during deviation of the thoracic spine from an upright posture, and to determine whether a relationship exists between the angle of the thoracic spine and co-contraction within the lumbar spine.*

Rationale: While performing movement tasks requiring deviation of the thoracic spine from an upright posture, the lumbar region will remain in an upright position. Increased co-contraction in the lumbar spine will be necessary in order to maintain the upright,

neutral posture in that region during thoracic movement tasks, compared to upright standing.

Hypothesis: It was hypothesized that co-contraction in the lumbar spine would increase in response to thoracic movement tasks in which the thoracic spine deviated from an upright posture. Further, it was hypothesized that the thoracic angle would be positively associated with increased co-contraction in the lumbar spine.

CHAPTER 2

Review of Literature

CHAPTER 2

Review of Literature

2.1 Low Back Pain: Consequences and Risk Factors

It is well established that LBP accounts for a substantial portion of workplace injuries and associated disability, as well as increasing health care costs in North America (Nelson-Wong et al., 2008). For example, the annual lost productivity is approximated to be \$28 billion US, in addition to an estimated 100 million lost workdays per year in the United States (Makhsous et al., 2009). The lifetime prevalence of low back pain (LBP) has been estimated as 70% (Waters et al., 1993) and between 65% and 80% (Bird & Payne, 1999) in the general population. In addition, the lifetime prevalence in the working population has been found to be 63% (Thiese et al., 2014). With such far-reaching effects, it is not surprising that many research efforts have been devoted to the understanding of the mechanisms and prevention of LBP (Norman et al., 1998).

The origins of LBP are multifactorial (Stevenson et al., 2001) and complex. Identified risk factors fall into three main categories: personal, psychosocial, and occupational (Govindu & Babski-Reeves, 2014). Personal factors include age (Bigos et al., 1986; Govindu & Babski-Reeves, 2014; Hoy et al., 2010; Kopec et al., 2003; Stevenson et al., 2001), sex (Hoy et al., 2010), body mass index (Govindu & Babski-Reeves, 2014; Hoy et al., 2010), education status (Hoy et al., 2010), a long back (Adams et al., 1999), reduced lumbar lordosis (Adams et al., 1999), and previous non-serious LBP (Adams et al., 1999). Stress has commonly been identified as a psychosocial risk factor

in LBP (Govindu & Babski-Reeves, 2014; Hoy et al., 2010; Kopec et al., 2003), as have psychosocial workplace factors such as job dissatisfaction, monotonous tasks, and lack of social support (Hoy et al., 2010).

General occupational factors include force, repetition, non-neutral postures, and vibration (Govindu & Babski-Reeves, 2014), and are often encountered in manual material handling tasks (lifting, lowering, pushing, pulling, etc.). Specifically, Marras et al. (1995) identified lifting frequency, load moment, trunk lateral velocity, trunk twisting velocity, and trunk sagittal angle as predictive for medium risk and high risk occupational-related low back disorders. In addition, Norman et al. (1998) found that the integrated L₄–L₅ moment, usual hand force, peak L₄–L₅ shear force, and peak trunk velocity were independent risk factors for LBP. Lower level static exposures such as prolonged standing and sitting have also been implicated through epidemiological studies as an occupational risk factor (Tissot et al., 2009). Prolonged postures, including standing and sitting, impose static loads on the soft tissues and may result in discomfort (Pope et al., 2002). Prolonged standing has been shown to induce LBP in asymptomatic individuals, with 40-81% of participants developing LBP during a 2-hour standing protocol (Gregory & Callaghan, 2008; Gregory et al., 2008; Marshall et al., 2011; Nelson-Wong & Callaghan, 2010; Nelson-Wong et al., 2008, 2010). Gregory and Callaghan (2008) identified kinematic, kinetic, and muscle activation variables that were associated with LBP during prolonged standing. In addition, individuals who developed pain during prolonged standing (Nelson-Wong et al., 2008; Nelson-Wong & Callaghan, 2010) and sitting (Schinkel-Ivy et al., 2013) protocols displayed increased levels of co-contraction in

various pairings of muscles in the trunk and pelvis, relative to individuals who did not develop pain.

2.2 Why Study the Thoracic Spine?

The majority of previous work has been conducted with a focus on the lumbar spine. Substantially less emphasis has been placed on the thoracic spine, which is perhaps a consequence of the complexities in the thoracic spine as a result of anatomical characteristics or the far lower incidence of injury in the thoracic relative to lumbar spine (Briggs et al., 2007; Edmondston & Singer, 1997). For example, between 10-15% of spinal pain disorders in the general population are related to the thoracic spine (Edmondston et al., 2007a), while the lifetime prevalence of low back pain has been stated to be as high as 70% in the general population (Waters et al., 1993). Alternatively, that the role of the thoracic spine is often considered primarily as that of force transmission between the upper and lower body (Lee et al., 2005) may have led this region to be neglected. Despite the time, effort, and money that has been contributed to LBP research, the risk factors and mechanisms of LBP have yet to be clearly explained. Potentially, the traditional approach of examining the lumbar spine in isolation may have contributed to the current lack of clarity regarding LBP in the literature. The spine regions are biomechanically interrelated (Lau et al., 2010), and significant correlations have been observed between the thoracic and lumbar curvatures (Hellsing et al., 1987). In addition, Briggs et al. (2007) concluded that the extent of thoracic kyphosis affected spinal loading and trunk muscle forces in the lumbar spine, supporting an influence of the

thoracic spine on the lumbar spine. Therefore, it is possible that a thorough investigation of the behaviours of the thoracic spine (kinematics, muscle activation) and the interactions between the thoracic and lumbar spine regions may aid in improving the understanding of the mechanisms of LBP.

While the injury prevalence in the thoracic spine is less than that of the lumbar spine, Briggs et al. (2009) found that thoracic spine pain was still relatively widespread in a general population of workers, through a literature review of 52 studies which included manual labourers, office workers, health professionals, manufacturing and industrial workers, drivers, military personnel, and performing artists. Their results indicated that the one-year prevalence of thoracic spine pain ranged from 3-55%, with medians of around 30% for most occupational groups (Briggs et al., 2009). Further, significant odds ratios were reported for a variety of risk factors (Table 2). The high median prevalence rates suggest that thoracic spine pain may represent a substantial occupational health issue (Briggs et al., 2009). The thoracic spine has unique characteristics with respect to both anatomy and biomechanics (Fujimori et al., 2014). Motion (Hidalgo et al., 2012; Marras et al., 1999; Mayer et al., 1984; Shum et al., 2005a, b; Wong & Lee, 2004) and muscle activation (D'Hooze et al., 2013; Lariviere et al., 2000; Watson et al., 1997) characteristics have previously been identified as being related to pain in the low back, and similar trends may be present within the thoracic spine. Therefore, a better understanding of thoracic spine behaviours is crucial to elucidate the mechanisms and development of thoracic pain disorders, and to the prevention and treatment of these disorders.

Table 2: General categories and specific risk factors for thoracic spine pain (Table generated from results presented in: Briggs AM, Bragge P, Smith AJ, Govil D, Straker LM. Prevalence and associated factors for thoracic spine pain in the adult working population: A literature review. *Journal of Occupational Health* 2009;51:177-92).

Category	Risk Factor
Individual	Concurrent musculoskeletal disorders Exercising Pre-menstrual tension Female
General work-related	High work load High work intensity Perceiving ergonomic problems in the workplace Working in some specialized areas Performing boring/tedious work tasks Certain year levels of study Employment duration Driving specialized vehicles High number of flying hours
Physical work-related	Manual physiotherapy tasks Climbing stairs High physical stress
Psychosocial work-related	Perceived risk of injury High mental pressure

2.3 Thoracic Spine Anatomy

An understanding of thoracic spine anatomy is crucial to the study of thoracic spine motion and muscle activation. The spine consists of four primary sagittal curves: cervical lordosis, thoracic kyphosis, lumbar lordosis, and sacral kyphosis (Roussouly & Pinheiro-Franco, 2011). The curves function to increase the strength of the vertebral column, maintain upright standing posture, assist with shock absorption, and protect the vertebrae (Tortora, 2005). The cervical, thoracic, lumbar, and sacral curves are made up of seven, twelve, five, and one (made up of five fused vertebrae) vertebrae, respectively (Tortora, 2005). Vertebrae are identified as the first letter of the spine region (cervical,

thoracic, lumbar, sacral) and the number within that region, counting from superior to inferior. The spine regions are biomechanically interrelated (Lau et al., 2010), and as such, the thoracic kyphosis is influenced by the orientation of the lumbar and cervical spines (Roussouly & Pinheiro-Franco, 2011), with significant correlations identified between the thoracic and lumbar curvatures (Hellsing et al., 1987). The extent of thoracic kyphosis also affects spinal loading and trunk muscle force along the thoracic and lumbar spine regions in upright standing, with increased loading and muscle force identified in individuals with greater kyphosis (Briggs et al., 2007).

The thoracic spine has been referred to as a transitional zone between the cervical and lumbar spine regions (Fujimori et al., 2014; Sizer et al., 2007; Willems et al., 1996), and is often considered a region of force transmission between the lower and upper body (Lee et al., 2005). As such, the thoracic spine differs from the other spine regions both anatomically and biomechanically (Fujimori et al., 2014). The thoracic spine is unique within the spine regions because of the articulations with the rib cage (Sizer et al., 2007). While the paravertebral muscles, spinal ligaments, intervertebral discs, and facet joints provide stiffness and stability along the length of the spine (Edmondston & Singer, 1997; Fujimori et al., 2014; Watkins et al., 2005), the articulations with the rib cage increase the stiffness and stability of the thoracic spine specifically (Edmondston & Singer, 1997; Horton et al., 2005; Willems et al., 1996). Due to the interaction with the ribs and sternum, the number of articulations, the geometry, and the varied material properties of the comprising structures (Csernatony et al., 2011), the thoracic spine is a highly complex anatomical structure.

Spinal motion consists of movement in six degrees of freedom for each vertebra, with rotation around and translation along an axis as the vertebral body moves along one of the cardinal planes (Gibbons & Tehan, 1998). The thoracic spine is also unique among the spine regions because of its size (Sizer et al., 2007). Changes in morphological characteristics, mainly zygapophyseal joint orientation and vertebral body dimensions, along the length of the thoracic spine have led to it being divided into upper, middle, and lower regions (approximately T₁–T₄, T₄–T₈, T₈–T₁₂, respectively) (Willems et al., 1996). While the predominant motion of the thoracic spine is axial twist (Lee et al., 2005), there are differences within the smaller regions. The distribution of primary movements along the thoracic spine reflects the changes in vertebrae morphology along its length (Lee et al., 2005; Willems et al., 1996), in that axial rotation is greater in the upper and middle regions than in the lower region (greatest in mid-thoracic), while flexion and lateral bending increase inferiorly (Willems et al., 1996). The nature of motion coupling, or consistent appearance of a motion about one axis with motion about a second axis (White & Panjabi, 1990), is also influenced by morphological differences in the vertebrae (Willems et al., 1996). For example, the coupling of lateral bend and axial twist in the upper-thoracic spine occurs in opposite directions, while in the mid- and lower-thoracic spine regions, the direction of coupling is unclear and has been found to occur in both directions (White & Panjabi, 1990). Overall, the ROM in the thoracic spine is generally less than that of the other spine regions (Fujimori et al., 2014).

The thorax, namely the thoracic and lumbar spine regions, must withstand forces due to weight bearing and external loads, along with those from muscles (Andriacchi et

al., 1974). The muscles of the back may be organized into three groups: the longitudinal muscles, consisting of the iliocostalis, longissimus, and spinalis muscles; the oblique muscles, consisting of semispinalis, multifidus, and rotatores; and small intersegmental muscles such as interspinales and intertransversarii (Morris et al., 1962). The longitudinal ES muscles have been the most extensively examined, because of their superficial nature. The ES are typically not examined individually, but rather as a collective along with the other muscles at the same levels of the vertebral column, based on similar functions (Morris et al., 1962). Patterns of activity have been found to vary between the different levels of the thoracic spine musculature, due at least in part to biomechanical differences, such as variations in vertebral morphology and the associated mobility, between the regions of the thoracic spine (Lee et al., 2005). Muscle activity in the trunk may also be influenced by posture (Lee et al., 2005). The differences in activation patterns between the different levels of the thoracic musculature emphasize the complexity of thoracic muscle function (Lee et al., 2005).

2.4 Thoracic Spine *In Vitro* Properties

Early research examining the thoracic spine mainly encompassed in vitro investigations of thoracic spine anatomy, mechanical properties, and ROM. Panjabi et al. (1991) reported on the three-dimensional anatomy of the thoracic vertebrae. Panjabi et al. constructed three-dimensional load-displacement curves to define the mechanical properties (1976a) and the three-dimensional flexibility and stiffness (1976b) of each level of the thoracic spine. Busscher et al. (2009) quantified the ROM, neutral zone (zone

between the points of the largest changes in flexibility in the load-displacement curve), neutral zone stiffness (inverse of the slope of the load-displacement curve in the neutral zone), and flexibility of the upper-, mid-, and lower-thoracic regions, concluding that the former three measures varied amongst the regions (Figure 1). Oxland et al. (1992) investigated the three-dimensional motion of the intervertebral joints of the thoracolumbar spine (T₁₁–T₁₂, T₁₂–L₁) by applying flexion-extension, axial twist, and lateral bend moments. The effects of loading on these mechanical properties have also been examined. Stanley et al. (2004) and Tawackoli et al. (2004) subjected T₂–S₁ and T₉–L₃ segments, respectively, to compressive preloads, concluding that the ROM and flexibility of the segments decreased under preload.

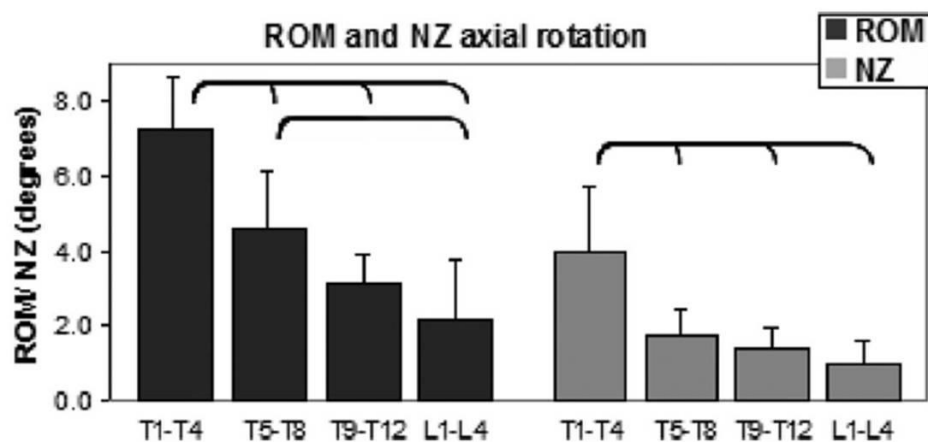


Figure 1: Mean (*SD*) range-of-motion (ROM) and neutral zone (NZ) for axial rotation in four spinal regions (Busscher I, van Dieen JH, Kingma I, van der Veen AJ, Gijsbertus V, Veldhuizen AG. Biomechanical characteristics of different regions of the human spine: An in vitro study on multilevel spinal segments. *Spine* 2009;34(26):2858-64. Figure 2, page 2860). For copyright permission, refer to Appendix B.

In order to verify the role of the rib cage and posterior tissues in thoracic spine stiffness and stability, various techniques involving fracture or removal of these components have been employed. The rib cage has been found to increase stability of the thoracic spine in all three planes (Oda et al., 1996, 2002; Watkins et al., 2005). The lateral aspects of the facet joints also contribute substantially to spinal stability (Oda et al., 2002). The intervertebral disc, costosternal joint, sternum, facets, and ligaments have also been shown to influence sagittal plane motion, and releasing those elements increased the thoracic spine ROM in that plane (Horton et al., 2005; Oda et al., 1996). Resection of the costovertebral joints likewise increased ROM in the lateral bend and axial twist planes (Oda et al., 1996). These in vitro studies provide the mechanical basis for understanding kinematic behaviours within the thoracic spine (for example, relationships between stiffness and ROM at different levels of the thoracic spine, and the influence of the rib cage on ROM). Further, this knowledge is required to understand muscle activation characteristics observed in the thoracic spine during in vivo research, as biomechanical changes along the length of the thoracic spine, such as vertebral morphology and associated mobility, influence patterns of muscle activity at different levels (Lee et al., 2005).

2.5 Thoracic Spine *In Vivo* Properties

2.5.1 Motion

In vivo thoracic spine kinematic studies have focused on ROM characteristics in the primary planes of motion, as well as coupling of motion in other planes (Edmondston

et al., 2007a; Fujimori et al., 2012, 2014; Gregersen & Lucas, 1967; Moon et al., 2014; Willems et al., 1996). Gregersen and Lucas (1967) used Steinmann pins inserted into the spinous processes of the thoracolumbar spine to examine trunk axial twist during various tasks. In sitting and standing, approximately 6° of rotation was observed in each thoracic joint, with greater rotation in the thoracic compared to lumbar spine (Gregersen & Lucas, 1967). In the upper-, mid-, and lower-thoracic regions, Willems et al. (1996) determined that flexion and lateral bend ROM increased inferiorly along the thoracic spine, while axial twist ROM was greatest in the mid-thoracic region (Figure 2). Similar trends with respect to lateral bend and axial twist were reported by Fujimori et al. (2014) and Fujimori et al. (2012), respectively, based on computed tomography.

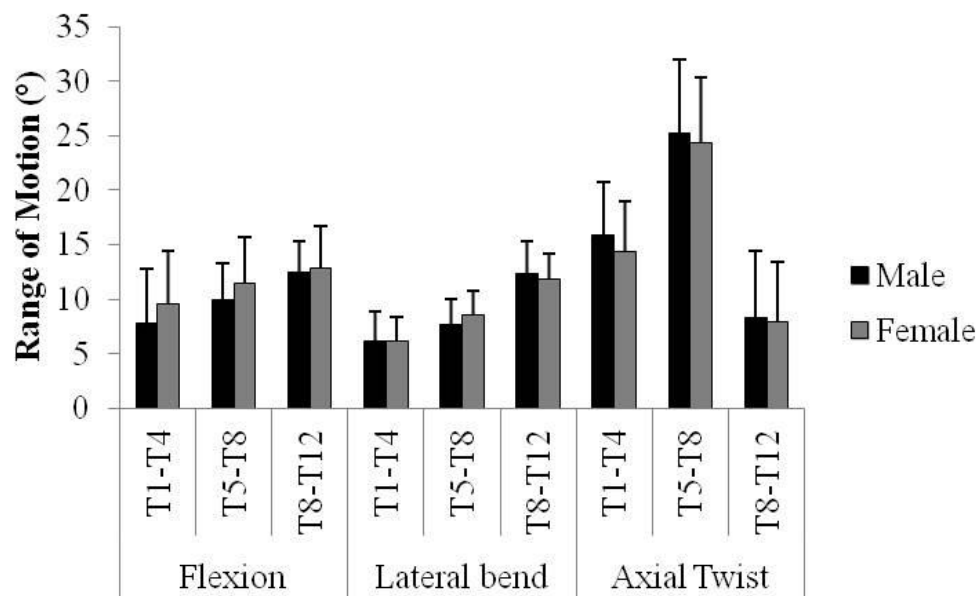


Figure 2: Mean (SD) range-of-motion (ROM) (°) of primary movements in each thoracic region (Graph generated from data presented in: Willems JM, Jull GA, Ng JKF. An in vivo study of the primary and coupled rotations of the thoracic spine. *Clinical Biomechanics* 1996;11(6):311-6. Table 1, page 314).

Patterns of coupled motion have also been examined in the thoracic spine, with the greatest focus on coupling between lateral bend and axial twist. Fujimori et al. (2012, 2014), Moon et al. (2014), and Willems et al. (1996) examined the coupling between these two movements in either three (upper-, mid-, lower-thoracic) or four (upper-, middle-upper, middle-lower, lower- thoracic) thoracic regions. Results ranged from ipsilateral coupling to contralateral coupling to variable patterns, depending on the region and primary motion (Fujimori et al., 2012, 2014; Moon et al., 2014; Willems et al., 1996) as well as the sagittal spine posture (Moon et al., 2014). Fujimori et al. (2014) also identified coupled flexion in the upper- and mid-thoracic regions during lateral bending movements, and coupled extension in the lower-thoracic region. Sizer et al. (2007) reviewed various studies on coupling behaviours in the thoracic spine, and concluded that previous findings were conflicting. A greater number of studies reviewed by Sizer et al. (2007) identified trends towards ipsilateral coupling, which is supported by more recent studies (Fujimori et al., 2012, 2014; Moon et al., 2014). Potentially, conflicting coupling behaviours reported across studies may be due to differences in study designs or measurement methods (Sizer et al., 2007). In addition, the starting spinal posture of participants may affect both the ROM and nature of coupled movement, as Edmondston et al. (2007a) found changes in thoracic rotation based on whether the trunk was sagittally neutral, flexed, or extended (Figure 3), and coupling patterns that were more common to each of the trunk postures (Figure 4). Alternatively, thoracic spine coupling behaviours may simply be inconsistent across individuals (Sizer et al., 2007), which is supported by

variability in coupling patterns within participants (Fujimori et al., 2012, 2014; Willems et al., 1996).

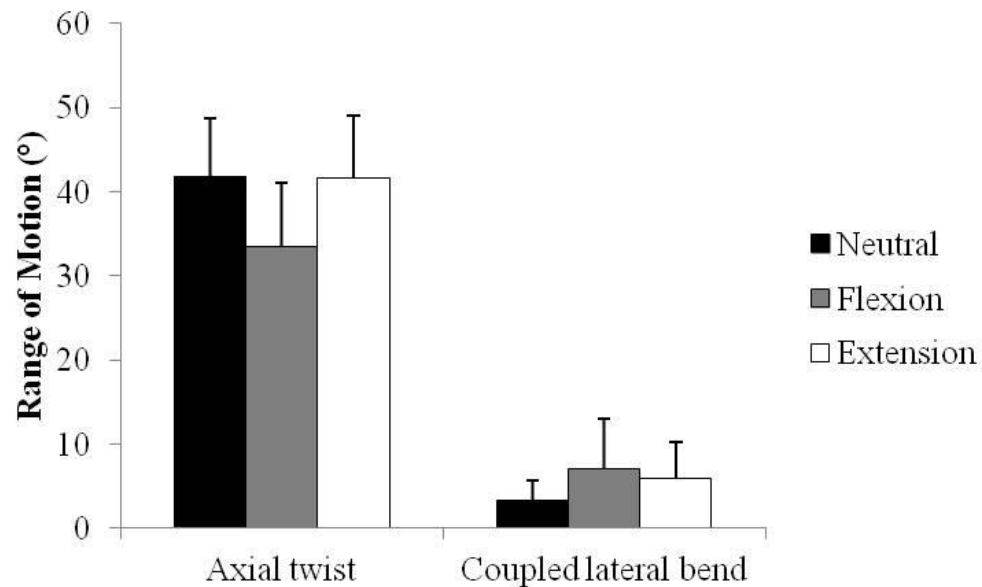


Figure 3: Mean (*SD*) thoracic range-of-motion (ROM) (°) in axial twist and coupled lateral bend for neutral, flexed, and extended sagittal postures (Graph generated from data presented in: Edmondston SJ, Aggerholm M, Elfving S, Flores N, Ng C, Smith R. Influence of posture on the range of axial rotation and coupled lateral flexion of the thoracic spine. *Journal of Manipulative and Physiological Therapeutics* 2007a;30:193-9. Table 1, page 195).

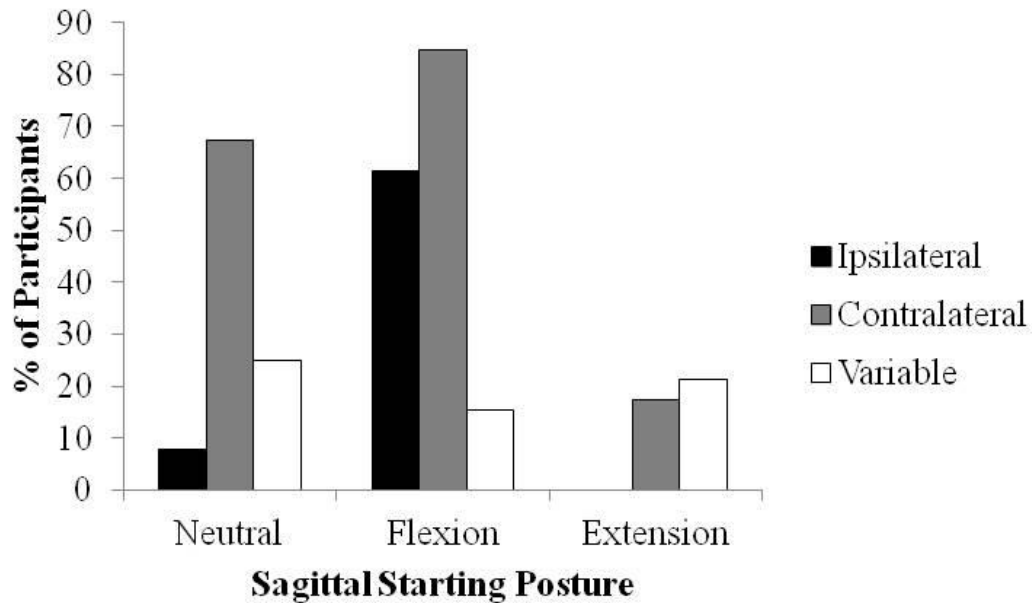


Figure 4: Percentage of participants displaying ipsilateral, contralateral, and variable lateral bend coupling during axial twist movements in neutral, flexed, and extended sagittal postures (Graph generated from data presented in: Edmondston SJ, Aggerholm M, Elfving S, Flores N, Ng C, Smith R. Influence of posture on the range of axial rotation and coupled lateral flexion of the thoracic spine. *Journal of Manipulative and Physiological Therapeutics* 2007a;30:193-9. Table 3, page 197).

2.5.2 Motion Patterns

Coordination in the movements of various body segments have been assessed previously, typically using cross-correlation analyses. Cross-correlation quantifies the extent to which two sets of time-varying data sets are correlated (Shum et al., 2007), to assess spatial and temporal similarities between sets of time series data (Nelson-Wong et al., 2009). The majority of these studies have focused on the coordination of a region of the spine and an adjacent joint. For example, Tsang et al. (2013) examined the coordination of cervical and upper-thoracic motion during neck flexion, extension, lateral bend, and axial twist. Similarly, Lee and Wong (2002) and Wong and Lee (2004)

assessed coordination of the lumbar spine and hip during trunk movements in all planes of motion, while Shum et al. (2005b, 2007) performed a similar analysis for activities of daily living. Johnson et al. (2010) employed a more localized approach, determining the temporal relationships in the head, cervical, upper-thoracic (T₁–T₆), mid-thoracic (T₇–T₁₂), lumbar, and pelvis angles during sit-to-stand movements. The findings revealed that the motion patterns of adjacent regions showed very high cross-correlations at zero time lag, ranging from $R_{xy}=0.71$ to $R_{xy}=0.98$ (Johnson et al., 2010). Cross-correlation coefficients tended to decrease when comparing non-adjacent regions (Johnson et al., 2010). Similar patterns were observed for maximum cross-correlation coefficients (Johnson et al., 2010). The thoracic spine regions (upper-thoracic and mid-thoracic) produced the strongest cross-correlations for both types of coefficients (Johnson et al., 2010).

Overall, movement capabilities of the thoracic spine are complex and non-uniformly distributed amongst the different levels (Preuss & Popovic, 2010). Therefore, an investigatory approach in which motion is investigated at different levels within the thoracic spine (as opposed to a single global thoracic measure) is necessary (Preuss & Popovic, 2010) to ensure that thoracic motion is being sufficiently represented.

2.5.3 *Muscle Activation*

Surface EMG has been used extensively within the literature to investigate muscle activation characteristics in the trunk. In addition to examining metrics such as average or maximum activation levels, data collection and processing techniques have been developed to utilize different characteristics of the EMG signal. For example, cross-

correlation of pairings of EMG signals has been used to quantify activation timing and sequencing (Nelson-Wong et al., 2012, 2013). Further, the EMG signal shows characteristic changes with fatigue (Beneck et al., 2013; Kumar et al., 2006), and is related to muscle forces and spine loading (Cholewicki & McGill, 1996; Granata & Marras, 2000). It has also been observed that differences in EMG variables exist between healthy individuals and individuals with LBP. For example, Nelson-Wong and Callaghan (2010) and Schinkel-Ivy et al. (2013) identified higher co-contraction levels during two hours of prolonged standing and sitting, respectively, in individuals who developed pain over the protocol compared to those who did not. Similarly, it has been well-established that individuals with LBP demonstrate higher activation levels in the lumbar ES during maximum trunk flexion movements (Colloca & Hinrichs, 2005; Watson et al., 1997).

Recent studies have begun to address the paucity of literature regarding the kinematics of the thoracic spine. However, few studies have aimed to specifically address muscle activation characteristics in the thoracic spine. Recently, studies by Nairn et al. (2013a, b) and Schinkel-Ivy et al. (2013) quantified activation characteristics of the LD (T₉), lower-thoracic ES (T₉), and upper-thoracic ES (T₄), and along with the external oblique (EO), internal oblique (IO), lumbar ES (L₃), and rectus abdominis (RA).

Activation levels of each of the aforementioned muscles (Nairn et al., 2013a), as well as co-contraction patterns within the various pairings of muscles (Schinkel-Ivy et al., 2013), have been documented for two hours of prolonged sitting, although comparisons between the muscles themselves were not necessary to address the research question. Activation levels have been compared between muscles for several postures in sitting (upright

sitting, slumped sitting, and maximum flexion), with differences identified between the LD and upper-thoracic ES during upright sitting (Nairn et al., 2013b). Lee et al. (2005) quantified the activation levels of the longissimus thoracis muscles at three levels (T₅, T₈, and T₁₁) during axial twist. Results were variable depending on the level of the muscle, in that the activation at the T₅ level either increased with ipsilateral rotation or decreased with contralateral rotation, while the T₈ and T₁₁ levels only decreased with contralateral rotation (Figure 5) (Lee et al., 2005). Taken together, these results suggest that muscle activation characteristics should be quantified at multiple levels throughout the thoracic spine. However, it has not yet been determined whether it is necessary to evaluate all of these muscles to properly represent the muscle activation characteristics of the trunk and specifically the thoracic spine.

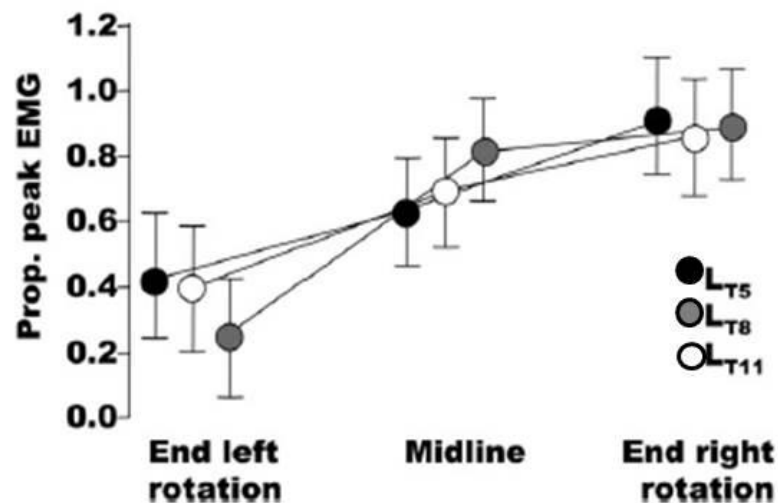


Figure 5: EMG amplitudes for the longissimus thoracis at T₅ (L_{T5}), T₈ (L_{T8}), and T₁₁ (L_{T11}) during neutral sitting and seated axial twist, normalized to the peak axial twist amplitude (Lee LJ, Coppieters MW, Hodges PW. Differential activation of the thoracic multifidus and longissimus thoracis during trunk rotation. Spine 2005;30(8):870-6. Figure 2b, page 872). For copyright permission, refer to Appendix B.

2.5.4 *Muscle Activation Patterns*

One measure of activation pattern that is commonly quantified for the trunk musculature is that of co-contraction, or the concurrent activation of the opposing muscles around a joint (Missenard et al., 2008). Co-contraction may serve a variety of functions, such as equilibrating the moments created by agonist muscles in other axes (Thelen et al., 1995); stiffening spinal joints (Brown et al., 2006; Stokes et al., 2011; Thelen et al., 1995); increasing spinal stability (Hubley-Kozey & Vezina, 2002; Thelen et al., 1995) and regulating stress distributions across the contact surface of the joint (Thelen et al., 1995). These benefits also come with several penalties, mainly increased compressive forces in spinal joints (McGill et al., 2003), increased metabolic cost (Cholewicki & McGill, 1996; Missenard et al., 2008), and inefficiency of movement (Gregory et al., 2008). The resulting fatigue may facilitate the beginning of a cycling effect, whereby fatigue impairs muscle coordination (Potvin & O'Brien, 1998), resulting in reduced spinal stiffness and stability (Granata et al., 2004; Grondin & Potvin, 2009). The appropriate levels of spinal stability are then maintained by increases in co-contraction at the expense of additional spinal compression (Granata et al., 2004).

The clinical importance of co-contraction is highlighted by studies that have demonstrated links between co-contraction and LBP, in that individuals with LBP tend to exhibit higher co-contraction relative to healthy participants during trunk flexion (D'Hooge et al., 2013; Graham et al., 2014). Similar trends have also been identified between individuals who did and did not develop transient back pain in response to a prolonged, low-level, static exposure. Nelson-Wong and Callaghan (2010) and Schinkel-

Ivy et al. (2013) observed greater trunk co-contraction in participants who developed pain over two hours of prolonged standing and sitting, respectively, compared to those who did not develop pain (Figure 6). In a follow-up study, Nelson-Wong and Callaghan (2014) determined that individuals who developed pain during prolonged standing were at higher risk of developing future clinical low back pain.

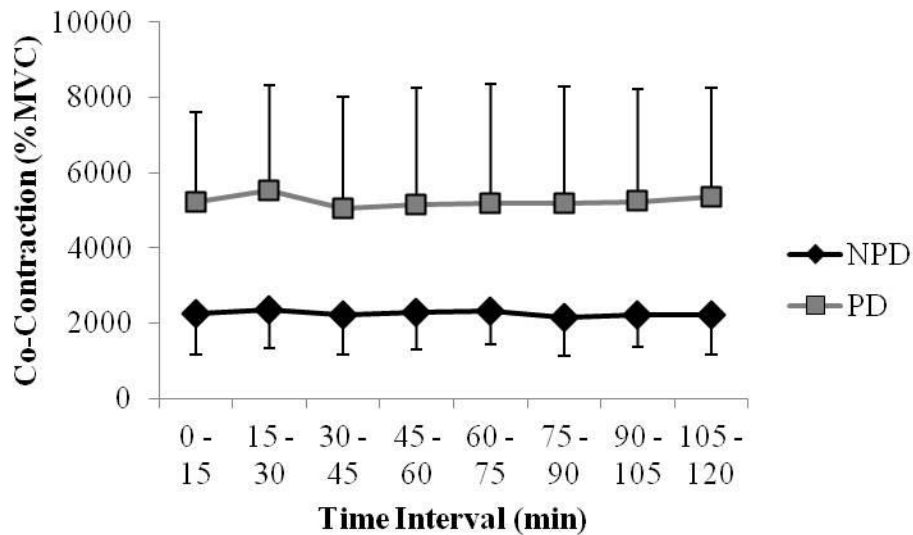


Figure 6: Mean (SD) co-contraction (%maximum voluntary contraction; %MVC) of the left lower-thoracic erector spinae–left upper-thoracic erector spinae pairing per minute for 15 minute time intervals over 2 hours of prolonged sitting, comparing individuals who did (pain developers; PD) and did not (non-pain developers; NPD) develop pain (Unpublished data; graph generated from data collected in association with: Schinkel-Ivy A, Nairn BC, Drake JDM. Investigation of trunk muscle co-contraction and its association with low back pain development during prolonged sitting. Journal of Electromyography and Kinesiology 2013;23:778-86).

The majority of studies regarding co-contraction in the trunk have focused on global trunk flexor-extensor co-contraction measures (Brown & McGill, 2008; D’Hooge

et al., 2013; Granata et al., 2005a, b; Thelen et al., 1995). Several studies have quantified co-contraction between various pairings of muscles in the trunk using the co-contraction index (Graham et al., 2014; Nelson-Wong & Callaghan, 2010; Schinkel-Ivy et al., 2013). However, the focus of these studies was on either the lumbar musculature (Graham et al., 2014) or general trunk musculature (Nelson-Wong & Callaghan, 2010; Schinkel-Ivy et al., 2013) in response to trunk ROM movement tasks or prolonged, low-level exposures. The effects of thoracic movement on co-contraction throughout the trunk have not yet been quantified.

Cross-correlation techniques have also been employed in the study of trunk muscle activation patterns. For example, Shan et al. (2014) used cross-correlation to quantify the similarities in activation patterns between the bilateral lumbar ES muscles during trunk flexion and extension, resulting in maximum cross-correlation coefficients ranging from $R_{xy}=0.822$ to $R_{xy}=0.913$. Cross-correlation can also be used to determine the temporal phase lag between the signals from two muscles (Nelson-Wong et al., 2012). This technique has been employed to quantify the activation sequences of various back, abdominal, and pelvic muscles during trunk extension movements from a flexed starting position (Nelson-Wong et al., 2012) and during assessments of lumbopelvic control (Nelson-Wong et al., 2013). Nelson-Wong et al. (2012) identified differences in activation strategies between individuals who did and did not develop pain in response to a prolonged standing protocol. Nelson-Wong et al. (2013) found similar trends between individuals with and without LBP. While the use of cross-correlation has recently become more prevalent in the trunk muscle activation literature, studies of activation

patterns throughout the trunk remain scarce, and a better understanding of the relationships in trunk muscle activation patterns is needed.

The works cited in this section, addressing both the motion and muscle activation characteristics of the thoracic spine in vivo, provide the foundation for the studies in the present dissertation. This dissertation will extend the knowledge base from the above studies with respect to the coordination of motion in the thoracic and lumbar spine regions, as well as relationships in muscle activation patterns between the regions.

2.6 Issues in Thoracic Spine Data Collection

2.6.1 Repeatability and Reliability of Motion and Muscle Activation

Repeatability and reliability represent the consistency of a measure (Webb et al., 2006; Weir, 2005), and have been extensively researched for trunk kinematics and EMG measures. An understanding of these measures is crucial, as the reliability of a test must be established before it can be considered valid (Carlsson & Rasmussen-Barr, 2013). Further, repeatability and reliability is necessary for the collection of data relating to the identification of LBP characteristics and the evaluation of treatment interventions, as tests must be performed similarly both within- and between-sessions. Past studies have identified differences in kinematic and EMG measures during these tasks between healthy participants and those with LBP (Ferguson et al., 1996a, b; Geisser et al., 2005; Hidalgo et al., 2012; Sheeran et al., 2012). As such, these measures may have utility as potential screening or diagnosis tools for LBP (Geisser et al., 2005; Hidalgo et al., 2012). With established reliability, there are also potential uses for tracking rehabilitation progress and

managing treatment, as well as for use in clinical intervention trials (Hidalgo et al., 2012; Marras et al., 1993b). In terms of utility in a research context, upright and maximal angles may both be used in the calibration and normalization of data, to enable comparisons between individuals and groups (Edmondston et al., 2007b). Submaximal EMG values from upright standing or maximum trunk ROM measures may also be used to normalize subsequent data. Therefore, repeatability and reliability are crucial to ensure appropriate tracking of rehabilitation progress and treatment in a clinical setting, and proper data processing and analysis in a research context.

Past work has assessed the repeatability and reliability characteristics of kinematic and EMG measures during different tasks, both within- and between-sessions, as well as within- and between-raters for subjective tests. Past research addressing the repeatability and reliability of kinematic and EMG measures has been more focused on between-sessions, with within-session repeatability and reliability examined to a lesser extent. Specific to the trunk, the between-session reliability of kinematic measures during maximum trunk ROM (Hidalgo et al., 2012; Montgomery et al., 2011) and upright standing (Dunk et al., 2005) has been evaluated, as has the between-session reliability of EMG measures during maximal and submaximal isometric trunk contractions (Dankaerts et al., 2004; Lariviere et al., 2014; Ng et al., 2003; Pitcher et al., 2008; Stevens et al., 2006). Within-session reliability has been assessed for kinematic measures of the trunk during upright standing (Dunk et al., 2005), and for EMG measures during maximal and submaximal isometric contractions (Dankaerts et al., 2004). Specific details regarding the

measures and associated repeatability and reliability outcomes can be found in Tables 3 and 4.

Table 3: Previous studies reporting repeatability and reliability statistics for kinematic measures. ICC: intraclass correlation coefficient.

Study	Task	Measure	Type of Repeatability / Reliability	Repeatability / Reliability Results
Dunk et al. (2005)	Upright standing	Angles: <ul style="list-style-type: none"> • Cervical • Thoracic • Lumbar 	Within-session Between-session	ICC = 0.55 to 0.98 ICC = 0.16 to 0.84
Hidalgo et al. (2012)	Trunk flexion, lateral bend, axial twist	Angles: <ul style="list-style-type: none"> • Upper thoracic • Lower thoracic • Upper lumbar • Lower lumbar • Total lumbar 	Between-session	ICC = 0.60 to 0.96
Montgomery et al. (2011)	Trunk axial twist	Angles: <ul style="list-style-type: none"> • Trunk 	Between-session	ICC = 0.82
Troke et al. (2007)	Lumbar flexion, lateral bend, axial twist	Angles: <ul style="list-style-type: none"> • Lumbar 	Between-session	ICC = 0.72 to 0.99

Table 4: Previous studies reporting repeatability and reliability statistics for EMG measures. ES: erector spinae; ICC: intraclass correlation coefficient; MVC: maximum voluntary contraction; Φ : dependability coefficient.

Study	Task	Measure	Type of Repeatability / Reliability	Repeatability / Reliability Results
Dankaerts et al. (2004)	Abdominal and back MVCs, submaximal contractions	Muscles: <ul style="list-style-type: none"> • External oblique • Internal oblique • Rectus abdominis • Multifidus • Iliocostalis lumborum • Thoracic ES 	Within-session Between-session	ICC = 0.75 to 0.98 ICC = 0.32 to 0.97
Ng et al. (2003)	Axial twist isometric MVCs, submaximal contractions	Muscles: <ul style="list-style-type: none"> • External oblique • Internal oblique • Rectus abdominis • Latissimus dorsi • Multifidus • Iliocostalis lumborum 	Between-session	ICC = 0.75 to 0.97
Pitcher et al. (2008)	Back MVCs, submaximal contractions	Muscles: <ul style="list-style-type: none"> • Upper lumbar ES • Lower lumbar ES 	Between-session	ICC = 0.74 to 0.97
Stevens et al. (2006)	Abdominal and back MVCs	Muscles: <ul style="list-style-type: none"> • External oblique • Internal oblique • Multifidus • Thoracic part of iliocostalis lumborum 	Between-session	ICC = 0.66 to 0.97

The repeatability and reliability characteristics of any given measure strongly influence the number of trials that need to be collected for a specific task or condition. Typically, three trials or less have been collected when measuring trunk motion and

muscle activation during unloaded trunk ROM tasks (Burnett et al., 2008; Dankaerts et al., 2009; Lariviere et al., 2000; Peach et al., 1998), loaded trunk ROM tasks (Lariviere et al., 2000), thoracic ROM tasks (Edmondston et al., 2007a; Willems et al., 1996), upright standing and sitting (Dankaerts et al., 2009), and slumped sitting (Dankaerts et al., 2009). Several authors have attempted to develop recommendations regarding the number of trials required for stable and repeatable measures (Allison & Fukushima, 2003; Sparto & Parnianpour, 2001). However, recommendations of this type pose a challenge, as the number of trials required to achieve repeatability and reliability differs based on the task and the specific measure.

Allison and Fukushima (2003) examined the repeatability of a trunk angle measure during targeted trunk flexion movements (20%, 50%, and 80% of available spinal flexion). The authors concluded that precision error stabilized at five trials, with the coefficient of variation and statistical power stabilizing after six trials.

Recommendations for repeatable EMG measures during isokinetic trunk extensions at 25%, 50%, 75%, and 100% of participants' maximum contraction level have also been established for the EO, IO, LD, lumbar ES, and RA (Sparto & Parnianpour, 2001).

Indices of dependability were calculated for each muscle for one, three, and five sessions and one, three, and five repetitions within each of those sessions. None of the muscles achieved a sufficient index of dependability within up to five repetitions and one session (Sparto & Parnianpour, 2001). Similar recommendations have not been developed for kinematic and EMG measures during unconstrained trunk movements, as the recommendations of both Allison and Fukushima (2003) and Sparto and Parnianpour

(2001) were based on highly constrained, targeted trunk angles and contraction levels, respectively. Further, both studies only included sagittal plane movements, which may not apply to other commonly performed movements such as those involving lateral bend, axial twist, or full ROM. As unconstrained trunk movements such as upright standing, maximum trunk flexion, maximum trunk lateral bend, and maximum trunk axial twist are often performed as a part of biomechanical data collection protocols, recommendations of the minimum number of trials required for these movements would be highly beneficial for researchers.

2.6.2 Position of Adjacent Segments

The reviewed literature provides evidence as to the wide ranges of previously reported maximum ROM and motion patterns, including coupling behaviours (Edmondston et al., 2007a; Fujimori et al., 2012, 2014; Gregersen & Lucas, 1967; Moon et al., 2014; Willems et al., 1996). These differences may originate from a variety of sources, including the instrumentation or measurement system used, such as motion capture (Lee et al., 2013; Nairn & Drake, 2014; Preuss & Popovic, 2010), electromagnetic tracking (Peach et al., 1998; Willems et al., 1996), or medical imaging techniques (Fujimori et al., 2012, 2014). Differences in the kinematic definition of the spine may also confound comparisons between studies, depending on whether authors reported trunk angles (Masset et al., 1998; McGregor et al., 1995), lumbar angles (Peach et al., 1998; Percy & Hindle, 1989; Van Herp et al., 2000), thoracic angles (Edmondston et al., 2007a; Fujimori et al., 2012, 2014), or partitioned thoracic angles (Hidalgo et al.,

2012; Lee et al., 2013; Nairn & Drake, 2014; Preuss & Popovic, 2010; Willems et al., 1996).

An additional issue which has been prevalent throughout the literature is a lack of control and/or reporting of the positions of the head and arms during maximum trunk ROM movement tasks. Often, the head and arm positions during these trials remains unspecified, and those studies that do provide specific details encompass a substantial amount of variation. Common head positions include maintaining a neutral (in line with the trunk) head position throughout the movement (Andersson et al., 1996; Peach et al., 1998), and moving the head in the same direction as trunk movement (i.e. for a trunk flexion movement, the head would be curled down towards the chest) (Alschuler et al., 2009; Willems et al., 1996). Arm positions that have been reported previously include crossed over the chest (Kaigle et al., 1998; Willems et al., 1996), hanging to the floor (Peach et al., 1998), and abducted to 90° (Edmondston et al., 2007a). The lack of standardization in head and arm positions may account for some of the differences in reported trunk ROM throughout the literature.

Studies that have examined the postures and motion of the upper portions of the spine have concluded that similarities exist between regions. Kuo et al. (2009) identified relationships between the thoracic spine and neck slope, and between the thoracic and upper-cervical spines during upright standing. The patterns of motion in the cervical and upper-thoracic regions during neck flexion, lateral bend, and axial twist have also been found to be related through the use of cross-correlation (Tsang et al., 2013). Therefore, it appears to be crucial to control for the positioning and movement of the head and neck

during trunk motion trials in order to minimize the influence of cervical movement on movement in the upper thoracic region (Willems et al., 1996). Similarly, consistent patterns of spinal motion occur during unilateral (Crosbie et al., 2008; Theodoridis & Ruston, 2002) and bilateral (Crosbie et al., 2008) arm elevations, along with consistent timing between thoracic and scapulohumeral movements during lifting (Crosbie et al., 2010). Taken together, the results of these studies suggest influences of head and arm positions on the kinematics of the trunk. Therefore, it is essential that the effects of head and arm positions on trunk kinematics be quantified, and the positions that enable the elicitation of maximum trunk ROM be identified.

2.6.3 Thoracic Spine Data Collection Techniques

2.6.3.1 Motion

Measurement of angles in the lumbar spine are typically quantified as the angle between the vertebrae bounding the region (T₁₂ or L₁ superiorly, L₅ or S₂ inferiorly) (Alexander et al., 2007; Cavanaugh et al., 1999; Gregory et al., 2006; Howarth et al., 2009; Pearcy, 1993; Shin & Mirka, 2007). The lumbar spine has also been subdivided into upper and lower divisions, using markers around L₃ (Astfalck et al., 2010; Claus et al., 2009). Means of quantifying the thoracic spine are less consistent between studies, however (Table 5). For example, past work has utilized individual markers at specific vertebral levels of the spine, such as T₂, T₆, and T₁₀ (Edmondston et al., 2007a), T₁, T₆, and T₁₂ (Edmondston et al., 2011b), or T₁, T₅, and T₁₀ (Claus et al., 2009). The resulting angle created by the three points was then calculated (Figure 7). Clusters of markers have also been placed at C₇ or T₁ and T₁₂, with the thoracic angle defined as the relative angle

between the two clusters (Dunk et al., 2005; Preuss & Popovic, 2010). Other research groups have divided the thoracic spine into smaller anatomical or functional regions. Hidalgo et al. (2012) and Johnson et al. (2010) each defined two thoracic regions, consisting of T₁–T₆ and T₇–T₁₂, and T₁–T₇ and T₇–T₁₂, respectively. Willems et al. (1996) subdivided the thoracic spine into three regions, from T₁ to T₄, T₄ to T₈, and T₈ to T₁₂. Further, in a multi-segmented model, Lee et al. (2013) and Preuss and Popovic (2010) defined four thoracic regions (C₇–T₃, T₃–T₆, T₆–T₉, and T₉–T₁₂) in addition to two lumbar (T₁₂–L₅ and L₅–S₁) regions (Figure 8).

Table 5: Instrumentation previously used for the measurement of thoracic motion.

Instrumentation	Study
Angle between markers at T ₂ , T ₆ , and T ₁₀	Edmondston et al., 2007a
Angle between markers at T ₁ , T ₆ , and T ₁₂	Edmondston et al., 2011b
Angle between markers at T ₁ , T ₅ , and T ₁₀	Claus et al., 2009
Angle between marker clusters at C ₇ or T ₁ and T ₁₂	Dunk et al., 2005; Preuss & Popovic, 2010
Two thoracic regions: T ₁ –T ₆ and T ₇ –T ₁₂	Hidalgo et al., 2012
Two thoracic regions: T ₁ –T ₇ and T ₇ –T ₁₂	Johnson et al., 2010
Three thoracic regions: T ₁ –T ₄ , T ₅ –T ₈ , and T ₉ –T ₁₂	Nairn & Drake, 2014
Three thoracic regions: T ₁ –T ₄ , T ₄ –T ₈ , and T ₈ –T ₁₂	Willems et al., 1996
Four thoracic regions: C ₇ –T ₃ , T ₃ –T ₆ , T ₆ –T ₉ , and T ₉ –T ₁₂	Lee et al., 2013; Preuss & Popovic, 2010

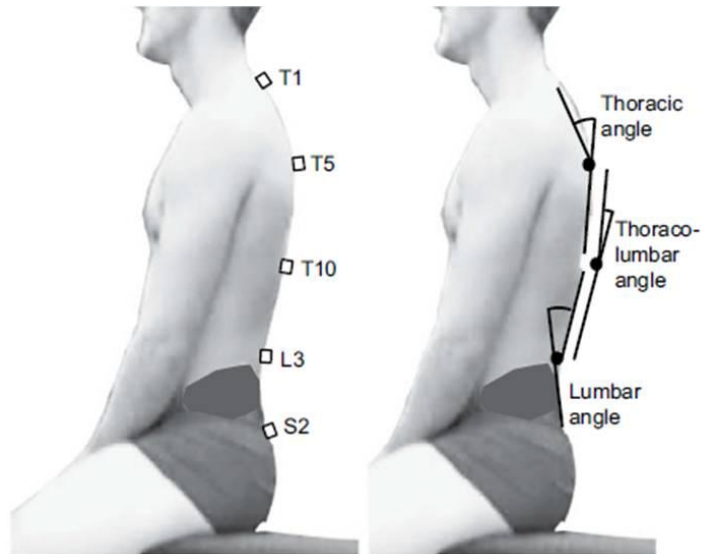


Figure 7: Previous marker setup used to calculate a general thoracic angle (angle between T₁, T₅, and T₁₀) (Claus AP, Hides JA, Mosely GL, Hodges PW. Is ‘ideal’ sitting posture real?” Measurement of spinal curves in four sitting postures. *Manual Therapy* 2009;14:404-8. Figure 1, page 405). For copyright permissions, refer to Appendix B.

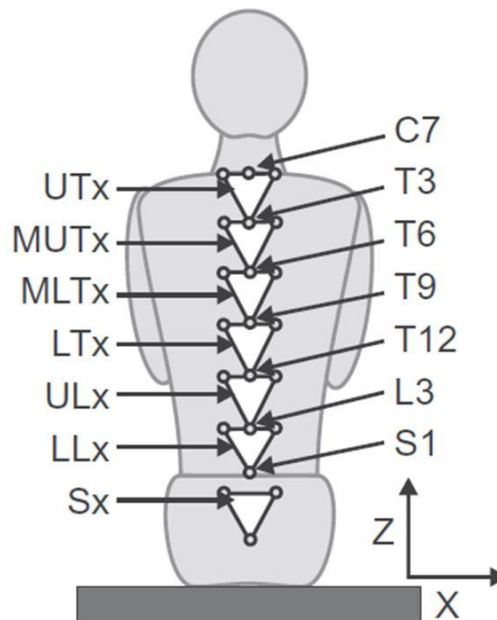


Figure 8: Previous marker setup used to calculate angles for four thoracic regions (T₃, T₆, T₉, and T₁₂) (Preuss RA, Popovic MR. Three-dimensional spine kinematics during multidirectional, target-directed trunk movement in sitting. *Journal of Electromyography and Kinesiology* 2010;20:823-32. Figure 1c, page 824). For copyright permissions, refer to Appendix B.

A recent study determined the least number of single markers required to adequately measure the sagittal and frontal curvatures of the whole spine, by placing 20 markers along the length of the spine from C₆ to S₁ (Ranavolo et al., 2013). The results of the study indicated that 9- and 10-marker sets showed the greatest number of valid marker configurations (Ranavolo et al., 2013). Further, the most common triads of markers that appeared in the analysis were C₇-T₂-T₃ and C₆-T₁-T₃ for the upper-thoracic region (C₆-T₄), T₅-T₇-T₈ and T₅-T₆-T₈ for the lower-thoracic region (T₅-T₁₂), and L₁-L₃-L₅ for the lumbosacral region (L₁-S₁) (Ranavolo et al., 2013). However, the minimum number and corresponding locations of segments (quantified using clusters of markers, as opposed to individual markers) necessary to characterize the thoracic spine has not yet been determined for maximum trunk ROM movement tasks.

2.6.3.2 Muscle Activation

Similarly to thoracic spine kinematics, the muscles needed to adequately represent the muscle activation characteristics of the trunk remain unclear. Although the musculature of the thoracic spine consists of different muscles and bundles within those muscles, the ES muscles are often considered as two large muscle groups, located on either side of the vertebral column (Morris et al., 1962). In part, this may be because it is difficult or impossible to definitively identify the individual back muscles through surface techniques (such as palpation), or because of the similar functions of the muscles during trunk movement (Morris et al., 1962). This strategy has generally been regarded as acceptable, as the total activity of the ES group has been found to be relatively consistent across participants for any given motion (Morris et al., 1962).

Generally, muscle activation characteristics of the thoracic spine have been reported in relation to either lumbar or cervical spine mechanics. The former tend to examine the LD (Drake et al., 2006; McGill, 1991) and lower-thoracic ES (Drake et al., 2006; McGill, 1991; Nelson-Wong & Callaghan, 2010), with both muscles often measured at the T₉ level. Conversely, for the purposes of cervical mechanics, the TR muscle between the C₇ spinous process and the acromion (Burnett et al., 2009; Caneiro et al., 2010) and the thoracic ES musculature at the T₄ level (upper-thoracic ES; Burnett et al., 2009; Caneiro et al., 2010; Edmondston et al., 2011a) tend to be of greater interest. Often, when the thoracic spine musculature is included to provide context to investigations of the lumbar or cervical muscles, only a subset of these muscles is examined. There is a paucity of work focusing on the integration of multiple muscles within the thoracic musculature as well as between the thoracic and lumbar musculature, which in turn would provide a better understanding of the biomechanical behaviours of the trunk.

2.7 Literature Review Summary

It is evident from the reviewed literature that research focusing on the thoracic spine remains relatively sparse compared to the lumbar spine. Recently, a greater proportion of work has begun to focus on the kinematics of the thoracic spine. However, gaps remain within the literature with respect to the muscle activation characteristics of the thoracic spine. Further, literature examining the relationships in the motion and muscle activation both within the thoracic spine and between the lumbar and thoracic

spine regions is lacking. Therefore, this dissertation aims to address these characteristics and relationships, along with issues reviewed above that are prevalent in the existing thoracic spine literature.

CHAPTER 3

Repeatability of Kinematic and Electromyographical Measures During Standing and Trunk Motion: How Many Trials are Sufficient?

CHAPTER 3

Repeatability of Kinematic and Electromyographical Measures During Standing and Trunk Motion: How Many Trials are Sufficient?

Summary

Previous studies have recommended a minimum of five trials to produce repeatable kinematic and EMG measures during target postures or contraction levels. This study examined the repeatability of kinematic and EMG measures during upright standing and maximum trunk ROM movement tasks, to determine the number of trials required to obtain repeatable and reliable measurements. Thirty participants performed ten trials of upright standing and maximum trunk ROM movement tasks. Mean (upright standing) and maximum (movement tasks) kinematic and EMG measures were assessed using ICCs, standard errors of measurement, and ANOVA, which were used to identify the minimum number of trials for each measure. An analysis of residuals was also employed to determine whether using a single trial or average of multiple trials demonstrated higher repeatability. The repeatability and reliability of the measures were generally high, with 59%, 68%, 78%, 86%, and 91% of measures producing repeatable and reliable values with two, three, four, five, and ten trials, respectively. Ten trials were not sufficient for several upright standing kinematic measures, maximum axial twist lumbar angles, and activation levels of muscles in the upper back in specific tasks. Generally, the measures requiring ten or more trials were those with very small amounts of motion or muscles that did not act in the role of prime mover. The results suggest that depending on the measure and movement task, between two and five trials are often

sufficient. These recommendations are intended to provide an acceptable trade-off between repeatable and reliable values and feasibility of the collection protocol.

3.1 Introduction

Extensive effort has been devoted to analyzing the factors associated with LBP. Kinematic and EMG assessments are frequently employed to gain a better understanding of characteristics of individuals with LBP (Ferguson et al., 2004; Lariviere et al., 2000; Sheeran et al., 2012), and to evaluate treatment interventions (Bruce-Low et al., 2012; Lomond et al., 2014; Mieritz et al., 2014; Neblett et al., 2010). The repeatability and reliability characteristics of these variables are important to the collection and interpretation of such studies, in order to ensure that tests are performed similarly both within- and between-sessions. Further, a test must first be considered reliable before it can be considered valid (Carlsson & Rasmussen-Barr, 2013).

The repeatability and reliability of kinematic and EMG measures have been researched in a variety of contexts. Regarding the trunk, between-session reliability has been investigated for kinematic measures during maximum trunk ROM (Hidalgo et al., 2012; Montgomery et al., 2011) and upright standing (Dunk et al., 2005), and for EMG measures during maximal and submaximal isometric trunk contractions (Dankaerts et al., 2004; Lariviere et al., 2014; Ng et al., 2003; Pitcher et al., 2008; Stevens et al., 2006). Within-session reliability has been assessed for kinematic measures of the trunk during gait (Chan et al., 2006; three trials) and upright standing (Dunk et al., 2005; five trials), and for EMG measures during maximal and submaximal isometric contractions (Dankaerts et al., 2004; three trials). However, knowledge of the within-session repeatability and reliability for a large number of trials (10) for kinematic and EMG measures during upright standing and maximum trunk ROM tasks is lacking.

An understanding of the repeatability and reliability of kinematic and EMG measures during these tasks is critical to facilitate the comparison of healthy participants and those with LBP. Past studies have identified differences in kinematic and EMG measures during these tasks between healthy participants and those with LBP (Ferguson et al., 1996a, b; Geisser et al., 2005; Hidalgo et al., 2012; Sheeran et al., 2012). As such, both types of measures have been suggested as potential screening or diagnosis tools for LBP (Geisser et al., 2005; Hidalgo et al., 2012). With established reliability, there are also potential uses for tracking rehabilitation progress and managing treatment, as well as for use in clinical intervention trials (Hidalgo et al., 2012; Marras et al., 1993b). Additionally, for research purposes, both upright and maximal angles may be used for data calibration and normalization purposes, to facilitate comparisons between individuals and groups (Edmondston et al., 2007b). Similarly, EMG levels from these tasks may be used as a submaximal value to normalize subsequent data. For all purposes, both clinical and research-based, repeatability and reliability are crucial to ensure appropriate tracking of rehabilitation progress and treatment, and data processing and analysis, respectively.

The work surrounding the number of trials needed to obtain representative measures within a session has produced differing results. A recommendation of this type is difficult to develop, as the minimum number of trials required to achieve repeatable and reliable values is likely to differ based on the task as well as the specific measure. Typically, three trials or less have been used when measuring trunk muscle activation and motion (Burnett et al., 2008; Dankaerts et al., 2009; Edmondston et al., 2007a; Lariviere et al., 2000; Peach et al., 1998; Willems et al., 1996). Allison and Fukushima (2003)

investigated the repeatability of trunk positioning with the eyes closed following a familiarization period (eyes open), and concluded that precision error stabilized at five trials, with the coefficient of variation and statistical power stabilizing after six trials. The movement tasks examined in this study were highly constrained to the mid-range of motion (20%, 50%, and 80% of available spinal flexion) and were performed in the sagittal plane, which may not translate to other commonly performed movements such as those involving lateral bend, axial twist, or full ROM. The number of trials required for repeatable measurements in various trunk muscles has been investigated during isokinetic trunk extensions at 25%, 50%, 75%, and 100% of participants' maximum contraction level, in which participants were provided with feedback of their torque output (Sparto & Parnianpour, 2001). Participants underwent a training session followed by three experimental sessions, one week apart, and indices of dependability were calculated for one, three, and five sessions and one, three, and five repetitions within each of those sessions. The authors concluded that one session of five repetitions was insufficient for repeatable EMG measurements (Sparto & Parnianpour, 2001). Although three trials are often used during data collection protocols, a set of recommendations has not been made for unconstrained trunk movement tasks, and it remains unclear whether three trials are either sufficient or necessary to produce repeatable kinematic and EMG measures in these tasks.

To the authors' knowledge, no study has examined repeatability and reliability of kinematic and EMG measures for upright standing and voluntary maximum trunk ROM movement tasks, with the intent of providing recommendations regarding the number of

trials required for these tasks. This study aimed to evaluate the repeatability and reliability of kinematic and EMG measures, and to determine the minimum number of trials required to achieve repeatability and reliability.

3.2 Methods

3.2.1 Participants

Participants included 30 right-hand dominant, recreationally active participants (15 males, 15 females). Participants had no history of back pain within one year prior to collection, in that they had not missed any days of school or work due to, nor sought treatment for, said pain. Mean (*SD*) age, body mass, and height were 25.0 years (3.8), 79.64 kg (8.75), and 1.80 m (0.05), respectively, for the males, and 22.8 years (2.7), 59.12 kg (6.38) and 1.66 m (0.05) for the females. All procedures were approved by the institution's Office of Research Ethics, and informed consent was obtained from all participants prior to collection.

3.2.2 Instrumentation

3.2.2.1 Kinematics

Fifty-nine passive-reflective markers were placed on the body using double-sided tape. Six clusters of five markers were attached to the skin over the C₇, T₃, T₆, T₉, T₁₂, and L₅ vertebrae (Figure 9). Each cluster consisted of a base from which four markers projected in a rectangular pattern (top left, top right, bottom left, bottom right), and a fifth marker projected posteriorly. The remaining 29 markers were placed on the head (left and right front and back of the head, middle back of the head; 5 total), pelvis (iliac crests, anterior superior iliac spines (ASIS); 4 total), trunk (acromia, sternum, T₁₀ vertebra; 4

total), and legs (greater trochanters, lateral and medial knee joint spaces, lateral malleoli, four on each thigh; 16 total). A seven-camera Vicon motion capture system (Vicon MX, Vicon Systems Ltd., Oxford, UK) tracked the markers' motion at a sampling rate of 50 Hz.

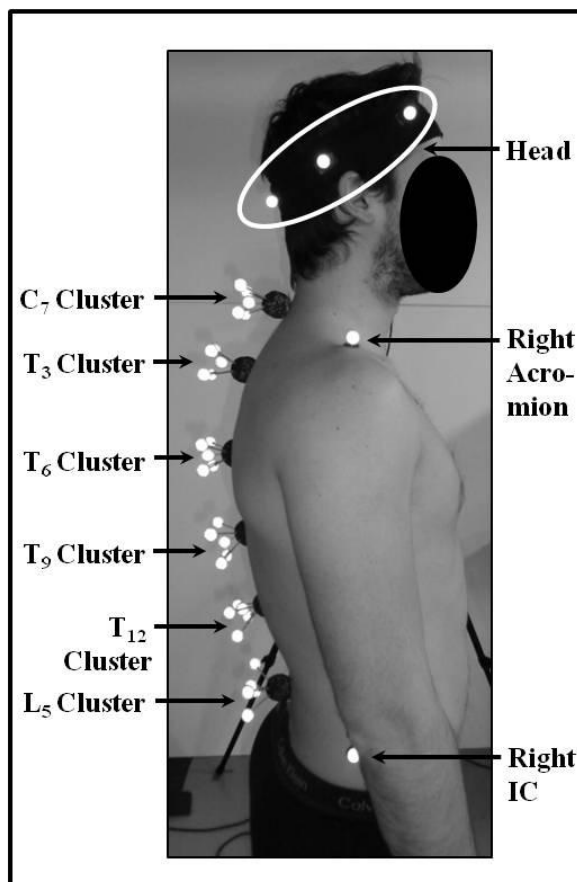


Figure 9: Marker setup in the sagittal view. IC: iliac crest (Adapted, by permission, from: Schinkel-Ivy A, Pardisnia S, Drake JDM. Head and arm positions that elicit maximal voluntary trunk range-of-motion measures. *Journal of Applied Biomechanics* 2014 (accepted July 1, 2014). Figure 2a. © Human Kinetics, Inc.). Written copyright permission not required for self-authored work; refer to Appendix B.

3.2.2.2 Electromyography

Electrode sites were shaved and swabbed with alcohol prior to electrode application. Pairs of disposable Ag/Ag-Cl electrodes (Ambu® Blue Sensor N, Ambu A/S, Denmark) were applied over the bilateral EO, IO, LD, lumbar ES, lower-thoracic ES, RA (Drake et al., 2006; McGill, 1991; Mirka & Marras, 1993; Nairn & Drake, 2014; Nelson-Wong & Callaghan, 2010; Schinkel-Ivy et al., 2013), TR (Burnett et al., 2009; Caneiro et al., 2010; McLean, 2005), and upper-thoracic ES (Burnett et al., 2009; Caneiro et al., 2010; Edmondston et al., 2011a; Nairn & Drake, 2014; Schinkel-Ivy et al., 2013) (Figures 10 and 11, Table 6). EMG signals were differentially amplified (frequency response 10-1000 Hz, common mode rejection 115 dB at 60 Hz, input impedance 10 G Ω ; AMT-8, Bortec, Calgary, Canada) and sampled at 2400 Hz (Vicon MX, Vicon Systems Ltd., Oxford, UK).

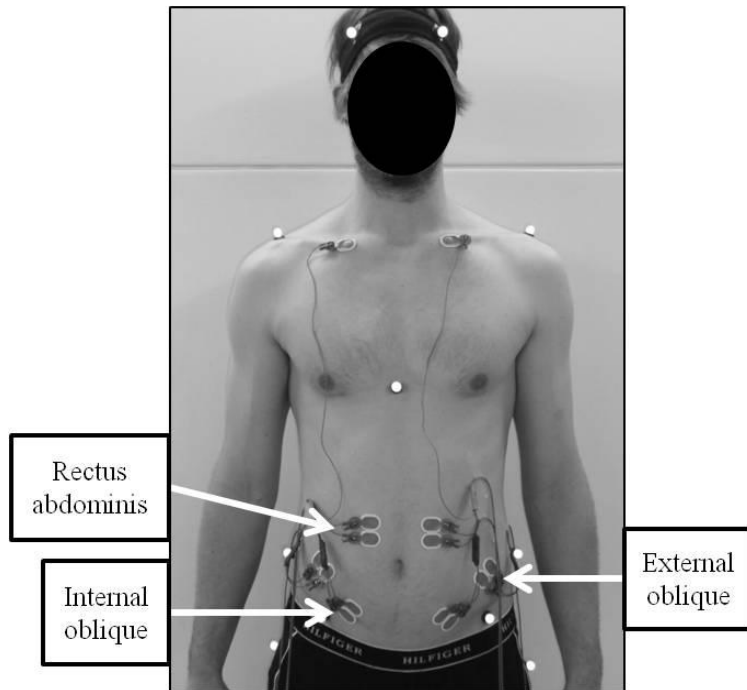


Figure 10: Electrode placements for the abdominal musculature.

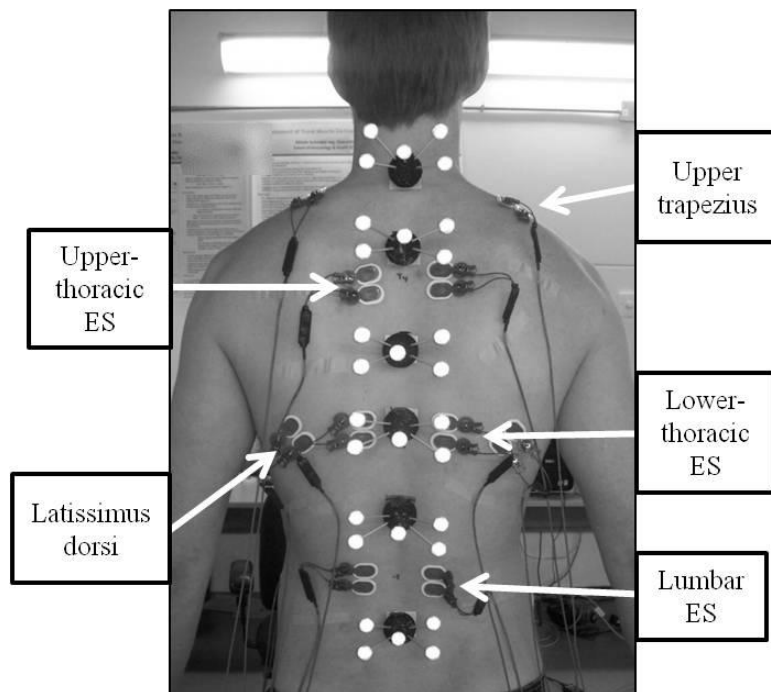


Figure 11: Electrode placements for the back musculature. ES: erector spinae.

Table 6: Electrode placements for the eight bilateral muscles tested.

Muscle	Location
External oblique (EO)	15 cm lateral to umbilicus (McGill, 1991), at an angle of 45° (Mirka & Marras, 1993)
Internal oblique (IO)	Below external oblique electrodes, superior to inguinal ligament (McGill, 1991)
Latissimus dorsi (LD)	Most lateral portion of muscle at the level of T ₉ (McGill, 1991)
Lumbar erector spinae (lumbar ES)	4 cm from the midline at the level of L ₃ (Mirka & Marras, 1993), or over the largest muscle mass at that level (Zipp, 1982)
Lower-thoracic erector spinae (lower-thoracic ES)	5 cm lateral from the midline at the level of T ₉ (McGill, 1991), or over the largest muscle mass at that level (Zipp, 1982)
Rectus abdominis (RA)	3 cm lateral to midline, 2 cm superior to umbilicus (Mirka & Marras, 1993)
Upper trapezius (TR)	2 cm lateral to the midpoint of a line drawn between the C ₇ spinous process and posterolateral acromion (Jensen et al., 1993)
Upper-thoracic erector spinae (upper-thoracic ES)	5 cm lateral from the T ₄ spinous process (Burnett et al., 2009, (adapted from Solomonow et al., 2003)), or over the largest muscle mass at that level (Zipp, 1982)

3.2.3 Procedures

Following electrode application, MVCs were completed. Trunk flexor MVCs were measured using a modified sit-up protocol where participants performed maximal isometric contractions involving trunk flexion, lateral bend, and axial twist against resistance (McGill, 1991, 1992). Trunk extensor MVCs were elicited with participants lying prone with their upper bodies hanging off the edge of a table and performing a maximal isometric back extension against resistance (McGill, 1991, 1992). The LD MVC was measured with participants sitting on a bench with the arm abducted to 90° and externally rotated, and the elbow flexed to 90° (upper arm parallel to the floor, forearm

almost perpendicular to the floor). Participants then performed a maximal isometric contraction downwards and posteriorly against resistance (Arlotta et al., 2011). The TR MVC was elicited with participants in a seated position with arms abducted at 90° while pushing the elbows upwards against resistance (McLean, 2005). For all MVC trials, participants were instructed to contract maximally against manual resistance (provided by an investigator) for 3-5 seconds while receiving verbal encouragement. Three trials of each procedure were performed, with rest (3 minutes, with confirmation from participants that they were sufficiently rested) between trials to minimize fatigue. The maximum EMG value from any of the three trials was designated as the MVC (see Section 3.2.4) (Knutson et al., 1994; Nairn & Drake, 2014; Schinkel-Ivy et al., 2013; Sparto & Parnianpour, 2001).

The passive-reflective markers were then applied. Participants performed a ‘T-pose’ (quiet standing with arms abducted to 90°), to be used later for data processing. Participants completed ten trials of each of four tasks in a random order, consisting of upright standing (Upright) and three movement tasks: maximum trunk flexion (MaxFlex), maximum trunk lateral bend (MaxBend), and maximum trunk axial twist (MaxTwist). The number of trials was selected based on a review of the literature. Typically, three trials or less have been used in previous literature (Burnett et al., 2008; Dankaerts et al., 2009; Edmondston et al., 2007a; Lariviere et al., 2000; Peach et al., 1998; Willems et al., 1996). While it may have been ideal to collect data for more than ten trials, the expectations for the time commitment of participants are limited to an extent (Sparto & Parnianpour, 2001). Additionally, in applications for LBP populations in research or

clinical settings, the length of the testing protocol may be limited by pain/discomfort. Complete instructions were provided prior to the beginning of the experimental protocol. Throughout the protocol, prompts were given to the participant prior to each trial so the participant understood what movement task was to be performed (this was necessary as the trials were performed in a random order). For the Upright trials, participants stood still for 10 seconds with the arms at the sides while looking straight ahead. During the maximum trunk ROM movement tasks, the participant moved their head in the direction of movement to the end of the ROM, and then continued to move the trunk to the maximal position in a smooth continuous motion. The arms were crossed over the chest, with the knees straight and feet flat on the floor. From upright standing, the participant moved into the position, held the position for 3 seconds, and moved back to upright standing, for a total duration of approximately 10 seconds per trial. Participants could rest at any time if needed; however, trials were performed consecutively in all cases.

3.2.4 Data Processing

Data were processed using Visual3D v.4 (C-Motion, Inc., Germantown, USA). All raw EMG signals were high-pass filtered with a dual-pass, fourth-order Butterworth filter (cutoff frequency: 30 Hz (Drake & Callaghan, 2006)) to eliminate heart rate contamination. EMG signals were full-wave rectified, then low-pass filtered with a dual-pass, fourth-order Butterworth filter (cutoff frequency: 2.5 Hz (Brereton & McGill, 1998; van Dieen & Kingma, 2005)). The MVC for each muscle was used to normalize the signals from the subsequent trials so that all EMG data were expressed as %MVC. Mean

activation levels were determined for each muscle for Upright, while maximum activation levels were determined for the movement trials.

From the marker data, the head (defined by five markers around the head and the acromia, although only the former were used to track motion), trunk (defined by the acromia, iliac crests, sternum, T₁₀, and spine clusters), pelvis (defined by the iliac crests, ASISs, and greater trochanters), and C₇, T₁₂, and L₅ clusters (defined by the five markers on each cluster) were defined as segments (Appendix C, Figures 12 and 13). A Cardan X-Y-Z (flexion/extension-lateral bend-axial twist) rotation sequence following orthopaedic convention (Preuss & Popovic, 2010; van Dieen & Kingma, 2005) was used to calculate angles in the three planes for the head (head relative to trunk), trunk (trunk relative to global coordinate system), thoracic (C₇ cluster relative to T₁₂ cluster), lumbar (T₁₂ cluster relative to L₅ cluster), and pelvis (pelvis relative to global coordinate system). Angle data were low-pass filtered with a dual-pass, fourth-order Butterworth filter (cutoff frequency: 2.5 Hz, determined by residual analysis on the angle data (Winter, 2005)). The mean angles during Upright were determined and used to zero the angles from the movement trials (however, the 'un-zeroed' angles were used for all analyses of Upright). Maximum angles in the primary plane of interest for each of the movement trials were then determined (flexion-extension, or rotations around the X axis, for MaxFlex; lateral bend, or rotations around the Y axis, for MaxBend; and axial twist, or rotations around the Z axis, for MaxTwist). For exemplar kinematic and EMG data, please refer to Appendix D.

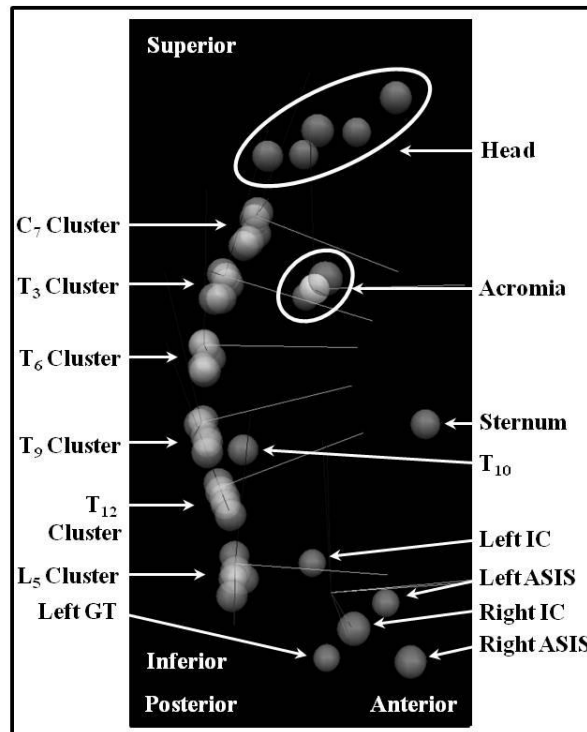


Figure 12: Collapsed 3D sagittal view of the markers in Visual3D. ASIS: anterior superior iliac spine; GT: greater trochanter; IC: iliac crest (Adapted, by permission, from: Schinkel-Ivy A, Pardisnia S, Drake JDM. Head and arm positions that elicit maximal voluntary trunk range-of-motion measures. *Journal of Applied Biomechanics* 2014 (accepted July 1, 2014). Figure 2b. © Human Kinetics, Inc.). Written copyright permission not required for self-authored work; refer to Appendix B.

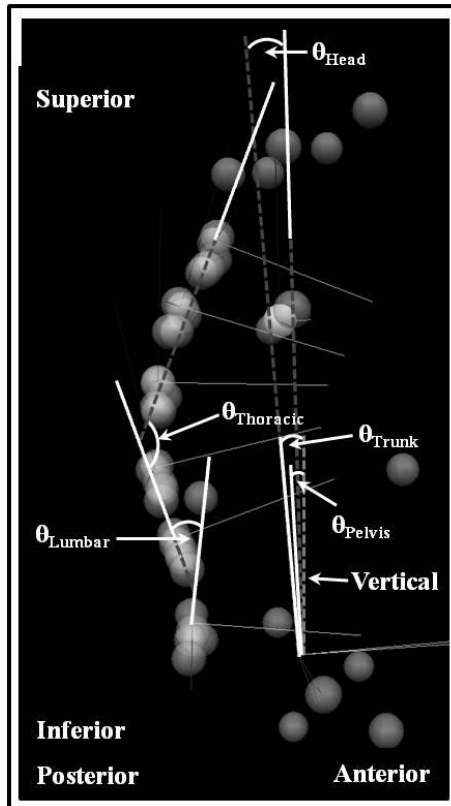


Figure 13: Collapsed 3D sagittal view of the markers representing the calculation of each angle. The angles represented in this collapsed 3D sagittal view are the equivalent of flexion-extension angles (Adapted, by permission, from: Schinkel-Ivy A, Pardisnia S, Drake JDM. Head and arm positions that elicit maximal voluntary trunk range-of-motion measures. *Journal of Applied Biomechanics* 2014 (accepted July 1, 2014). Figure 2c. © Human Kinetics, Inc.). Written copyright permission not required for self-authored work; refer to Appendix B.

3.2.5 Data Analysis

Statistical analyses were performed using IBM SPSS Statistics v.21 (IBM Corporation, Armonk, USA). Reliability, or the consistency of the measures (Webb et al., 2006; Weir, 2005), was assessed for the first two, three, four, and five trials, and all ten trials. Relative reliability was quantified using ICCs, while the standard error of measurement (SEM) was calculated to quantify absolute reliability (Atkinson & Nevill,

1998), which indicates the precision of the measure (Weir, 2005). These measures have been employed to assess the reliability of various kinetic, kinematic, neuromuscular, and performance measures in biomechanical research (Dankaerts et al., 2004; Hidalgo et al., 2012; Montgomery et al., 2011; Ng et al., 2003; Pitcher et al., 2008; Reeves et al., 2014; Stevens et al., 2006). ICCs range from 0.00 to 1.00, with higher values indicating greater reliability. Webb et al. (2006) characterized a coefficient of 0.80 to be sufficiently reliable for decision making (for example, in clinical trials), and therefore this was utilized in the present study as a threshold to identify sufficient reliability. The standard error of measurement was determined in two forms: unnormalized ($^{\circ}$ or %MVC for kinematic and EMG measures, respectively) (Lariviere et al., 2014; Montgomery et al., 2011) and normalized to the grand mean to yield SEM% (Dankaerts et al., 2004; Hidalgo et al., 2012; Stevens et al., 2006). The unnormalized SEM has the same units as the original measurement, and provides an indication of the magnitude of the error. Conversely, the SEM% (normalized to the grand mean) accounts for differences in the magnitude of the measures, thereby enabling comparisons of the errors between measures or to a threshold. To the authors' knowledge, a threshold has not been explicitly identified in the literature for acceptable SEM%. However, measures with SEM% of less than 25%, in conjunction with high ICCs, have been stated to demonstrate good to excellent reliability in previous work (Hidalgo et al., 2012; Stevens et al., 2006). Therefore, a criterion of SEM% of $\leq 25\%$ was selected.

To confirm repeatability of the measures, the mean (Upright) or maximum (movement tasks) measures for each participant were determined using 11 sets of trials:

First, Second, Third, Fourth, Fifth, Tenth, the averages of the FirstTwo, FirstThree, FirstFour, FirstFive, and AllTen. Single trials were included to assess whether a systematic effect was present in which values from early in the protocol were consistently different from those later in the protocol. The resulting values were then compared across the 11 sets of trials using analysis of variance (ANOVA), to determine if the values differed significantly across the various trials or sets of trials. Measures that differed significantly between the various trials or sets of trials indicated that the measures were not repeatable. For each task, three-way mixed-factor ANOVAs were used to analyze the kinematic measures, with repeated measures of angle measure (five levels: head, lumbar, pelvis, thoracic, trunk) and trial set (eleven levels), and between-group factor of sex. Four-way mixed-factor ANOVAs were used to analyze the EMG measures for each condition, with repeated measures of side (two levels: left, right), muscle (eight levels), and trial set, and between-group factor of sex. The factors of sex and region/muscle were initially included in the statistical models as differences in these factors have been identified previously (McGregor et al., 1995; Nairn & Drake, 2014), and therefore there was a possibility that repeatability and reliability would vary based on these factors. Data were collapsed where there were no significant effects involving these factors. When the assumption of sphericity was not met, degrees of freedom were determined using Greenhouse-Geisser corrections. Alpha was set to 0.05, and pairwise comparisons with Bonferroni corrections were used for post-hoc testing to establish whether any of the trial sets demonstrated significant differences from others. This component of the analysis, to establish whether the measures resulting from the various trial sets were significantly

different, was necessary to establishing repeatability (Essendrop et al., 2002). Similar techniques have been used previously (Dunk et al., 2005; Essendrop et al., 2001; Roe et al., 2006).

For each measure and movement task, the smallest number of trials meeting the three criteria ($ICC \geq 0.80$, $SEM\% < 25\%$, and no significant differences from other trial sets, based on the ANOVA results) was identified, indicating the minimum number of trials required for sufficient repeatability and reliability.

Finally, an analysis of residuals was employed to determine the preferable strategy with respect to using the measure from a single trial (First, Second, Third, Fourth, Fifth, or Tenth), or taking an average of multiple trials (FirstTwo, FirstThree, FirstFour, FirstFive, or AllTen). Root mean square differences (RMSDs) were calculated between each of the ten trials, relative to each of the sets of trials ('reference': First, Second, Third, Fourth, and Fifth trials, and the averages of the FirstTwo, FirstThree, FirstFour, FirstFive, and AllTen). The difference between each individual trial and each reference set of trials was determined and the square of the difference calculated. The mean of the square differences for that trial and all preceding trials were then calculated, followed by the square root of that value to obtain the RMSD. RMSDs for each individual trial, compared to each reference, were averaged across participants, then across the 10 individual trials to yield one value per reference, per angle measure or muscle. Finally, the RMSDs were averaged across all angle measures or muscles to obtain one value per reference set and task for kinematics and for EMG. Lower values indicated the best representation of all individual trials.

3.3 Results

Overall, the mean (*SD*) ICC and SEM% for all kinematic measures were 0.95 (0.04) and 33.7% (56.2). The ANOVAs for Upright flexion-extension and all movement tasks revealed significant effects involving the factor of trial set (Tables 7 and 8, Figures 14 and 15). However, the only significant pairwise comparisons within the factor of trial set were First and FirstFour for the head in Upright flexion-extension; First and Tenth, and Fifth and Tenth in MaxFlex; and Fifth and Tenth in males for MaxTwist. Of all kinematic measures in all tasks, 19 of 30 required only two trials to obtain repeatable and reliable values (Table 9). An additional four measures required five or less trials. For the remaining seven measures, ten trials were not sufficient to obtain acceptable repeatability and reliability. Six of the seven identified measures were for Upright. For all of the seven measures in which ten trials were not sufficient, while the SEM% was well above the threshold of 25%, this was likely due to the small magnitudes of the grand means. In examining the unnormalized SEM, these values were all equal to or less than 1.0°.

Table 7: ANOVA results for the kinematic and EMG measures for each task. The highest order interaction involving the factor of trial set is reported. The main effect statistic for trial set is reported when there were no significant effects of trial set. Where assumptions of sphericity were violated, degrees of freedom are reported using the Greenhouse-Geisser correction.

Task	Effect	<i>F</i> -Statistic
<i>Angles</i>		
Upright		
Flexion-extension	Trial set x angle measure ^a	$F_{40,1120}=1.586, p=0.012$
Lateral bend	Trial set ^b	$F_{10,290}=1.593, p=0.108$
Axial twist	Trial set ^a	$F_{10,280}=1.021, p=0.426$
MaxFlex	Trial set ^b	$F_{10,290}=4.505, p<0.001$
MaxBend	Trial set x sex ^a	$F_{10,280}=1.919, p=0.043$
MaxTwist	Trial set x sex ^a	$F_{10,280}=4.449, p<0.001$
<i>EMG</i>		
Upright	Trial set ^c	$F_{10,290}=0.265, p=0.968$
MaxFlex	Trial set ^c	$F_{10,260}=0.983, p=0.459$
MaxBend	Trial set x side ^d	$F_{10,290}=2.459, p=0.008$
MaxTwist	Trial set x side ^c	$F_{10,280}=2.807, p=0.002$
	Trial set x muscle ^c	$F_{9,817,274.88}=2.265, p=0.015$

^a Full kinematic statistical model (angle measure x trial set x sex)

^b Kinematic statistical model collapsed across sex (angle measure x trial set)

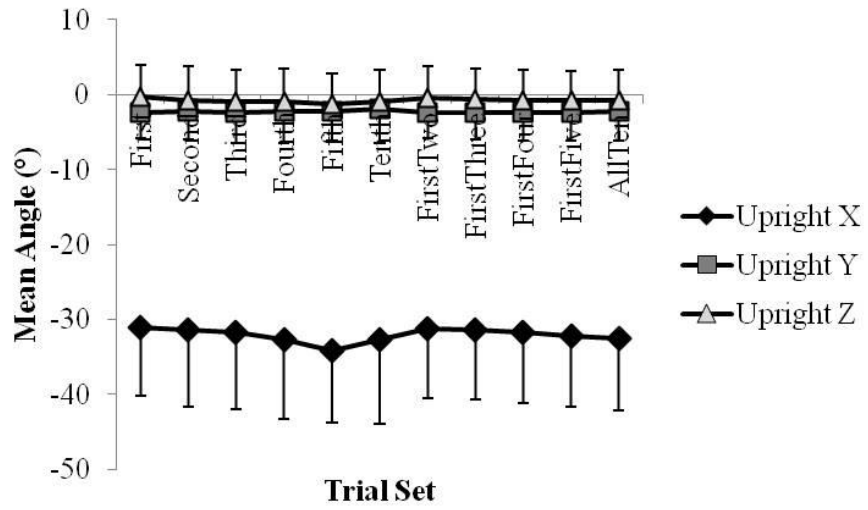
^c Full EMG statistical model (side x muscle x trial set x sex)

^d EMG statistical model collapsed across sex (side x muscle x trial set)

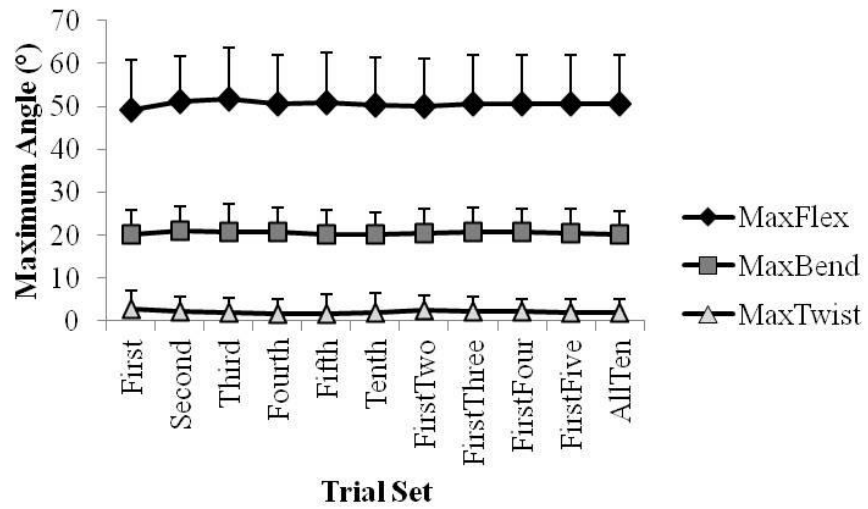
^e EMG statistical model collapsed across side and sex (muscle x trial set)

Table 8: Mean (*SD*) angles (°) calculated using the different sets of trials. There was little change within each measure across the sets, indicating high repeatability. Presented values are for a representative angle (lumbar angle; T₁₂ cluster relative to L₅ cluster). The trend for the lumbar angle (i.e. high repeatability) was displayed by most other angles. Values for Upright were not zeroed, while those for the movement tasks were zeroed to the Upright standing posture. Positive values indicate flexion (rotations around the X axis), lateral bend to the right (rotations around the Y axis), and axial twist to the right (rotations around the Z axis).

Task	Trial Set										
	First	Second	Third	Fourth	Fifth	Tenth	First Two	First Three	First Four	First Five	All Ten
<i>Upright</i>											
Flexion-extension	-31.0 (9.2)	-31.5 (10.3)	-31.8 (10.3)	-32.7 (10.7)	-34.1 (9.6)	-32.7 (11.2)	-31.2 (9.3)	-31.4 (9.4)	-31.7 (9.5)	-32.2 (9.4)	-32.5 (9.7)
Lateral bend	-2.4 (3.4)	-2.3 (3.7)	-2.5 (4.0)	-2.3 (4.2)	-2.2 (4.0)	-2.0 (4.5)	-2.3 (3.5)	-2.4 (3.6)	-2.4 (3.7)	-2.3 (3.7)	-2.2 (4.0)
Axial twist	-0.1 (4.2)	-0.6 (4.5)	-0.8 (4.1)	-0.8 (4.3)	-1.2 (4.0)	-0.9 (4.2)	-0.3 (4.3)	-0.5 (4.1)	-0.6 (4.1)	-0.7 (4.0)	-0.6 (4.0)
<i>Movement Tasks</i>											
MaxFlex	49.1 (11.8)	51.1 (10.5)	51.7 (12.1)	50.5 (11.4)	50.9 (11.5)	50.2 (11.1)	50.1 (11.0)	50.6 (11.2)	50.6 (11.2)	50.7 (11.2)	50.6 (11.4)
MaxBend	20.1 (5.9)	21.0 (5.9)	20.8 (6.4)	20.8 (5.5)	20.2 (5.7)	20.1 (5.2)	20.5 (5.5)	20.6 (5.7)	20.7 (5.6)	20.6 (5.5)	20.3 (5.3)
MaxTwist	3.0 (4.2)	2.3 (3.2)	2.0 (3.6)	1.7 (3.3)	1.9 (4.3)	1.8 (4.5)	2.7 (3.4)	2.5 (3.3)	2.3 (3.0)	2.2 (3.1)	2.1 (3.1)



a)



b)

Figure 14: Graphical representation of the mean (*SD*) angles (°) for a) Upright and b) maximum trunk ROM movement tasks for each set of trials for the lumbar angle measure.

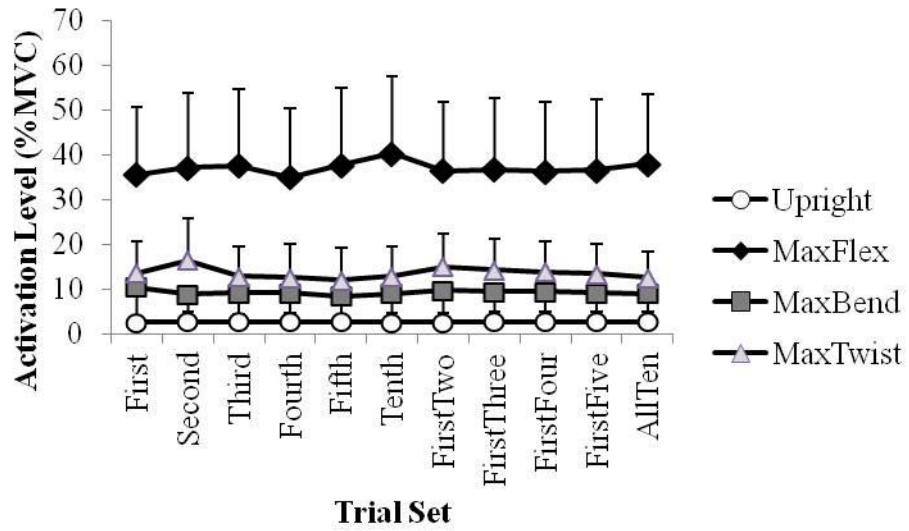


Figure 15: Graphical representation of the mean (*SD*) EMG (%MVC) for each set of trials for the right lumbar erector spinae.

Table 9: Number of trials required for each kinematic measure in each task. The intraclass correlation coefficient (ICC), normalized standard error of measurement (SEM) (% of grand mean), and unnormalized SEM (°) corresponding to that number of trials are also reported. For measures that did not achieve repeatability and reliability within ten trials, the ICC and SEMs for ten trials are reported.

Measure	Upright Standing											
	Flexion-Extension				Lateral Bend				Axial Twist			
	# Trials	ICC	SEM (%)	SEM (°)	# Trials	ICC	SEM (%)	SEM (°)	# Trials	ICC	SEM (%)	SEM (°)
Head	2	0.98	16.7	1.3	5	0.97	23.4	0.6	>10	0.97	135.4	0.8
Lumbar	2	0.90	9.7	3.0	4	0.98	23.1	0.5	>10	0.98	81.4	0.6
Pelvis	2	0.99	13.5	0.8	2	0.98	24.8	0.3	>10	0.96	58.7	0.7
Thoracic	2	0.97	3.1	1.3	>10	0.98	186.5	0.7	>10	0.98	28.3	0.9
Trunk	2	0.97	7.5	0.6	5	0.96	24.7	0.3	>10	0.97	47.1	0.7

Measure	Movement Tasks											
	Maximum Flexion				Maximum Bend				Maximum Twist			
	# Trials	ICC	SEM (%)	SEM (°)	# Trials	ICC	SEM (%)	SEM (°)	# Trials	ICC	SEM (%)	SEM (°)
Head	2	0.93	4.4	2.7	2	0.97	2.9	1.6	4	0.86	6.9	6.1
Lumbar	2	0.97	4.1	2.1	2	0.88	9.7	2.0	>10	0.93	47.7	1.0
Pelvis	2	0.96	4.5	3.0	2	0.86	13.6	1.7	2	0.86	11.6	6.1
Thoracic	2	0.88	14.1	3.8	2	0.96	5.8	2.0	2	0.95	5.5	2.9
Trunk	2	0.97	2.2	2.5	2	0.86	6.9	3.0	2	0.90	8.3	5.9

Regarding the EMG measures, the mean (*SD*) ICC and SEM% for all measures were 0.92 (0.08) and 17.5% (10.6). MaxBend and MaxTwist revealed significant interactions involving the factor of trial set (Tables 7 and 10). Within that factor, the EMG measures generally did not differ significantly, with the exceptions of Tenth and FirstFive for the right-side muscles in MaxTwist, and First and Tenth, First and AllTen, Tenth and FirstTwo, and FirstTwo and AllTen in the RA in MaxTwist. Of all EMG measures in all tasks, approximately 70% (45 of 64) required either two or three trials (Table 11). Of the remaining measures, seven required four trials, seven required five trials, three required ten trials, and two did not achieve acceptable repeatability and reliability within ten trials. Of the five measures requiring ten or more trials, unnormalized SEM ranged from 0.3%MVC (TR, Upright) to 7.0%MVC (upper-thoracic ES, MaxTwist).

Table 10: Mean (*SD*) activation levels (%MVC) calculated using the different sets of trials. There was little change within each measure across the sets, indicating high repeatability. Presented values for all conditions are for representative abdominal (right rectus abdominis) and back (right lumbar erector spinae) muscles. The trends for these muscles (i.e. high repeatability) were displayed by most other muscles.

Task	Trial Set										
	First	Second	Third	Fourth	Fifth	Tenth	First Two	First Three	First Four	First Five	All Ten
<i>Right rectus abdominis</i>											
Upright	5.3 (3.3)	5.4 (3.3)	5.3 (3.2)	5.4 (3.4)	5.3 (3.2)	5.4 (3.3)	5.4 (3.3)	5.3 (3.2)	5.4 (3.3)	5.3 (3.3)	5.3 (3.3)
MaxFlex	15.4 (17.0)	15.3 (13.2)	14.8 (13.9)	15.6 (16.3)	13.1 (11.0)	17.1 (16.7)	15.4 (14.2)	15.2 (13.7)	15.3 (13.7)	14.9 (13.0)	15.7 (14.3)
MaxBend	9.8 (9.1)	9.9 (8.0)	9.3 (6.2)	9.4 (7.3)	9.1 (6.7)	14.0 (24.2)	9.9 (8.5)	9.7 (7.6)	9.6 (7.3)	9.5 (7.1)	10.1 (8.5)
MaxTwist	12.5 (9.1)	11.7 (7.3)	11.2 (7.1)	10.8 (7.9)	10.5 (8.2)	10.0 (8.2)	12.1 (8.1)	11.8 (7.7)	11.5 (7.7)	11.3 (7.7)	10.5 (7.4)
<i>Right lumbar erector spinae</i>											
Upright	2.5 (1.5)	2.7 (1.6)	2.7 (1.5)	2.6 (1.6)	2.7 (1.6)	2.6 (1.6)	2.6 (1.5)	2.6 (1.5)	2.6 (1.5)	2.6 (1.5)	2.6 (1.5)
MaxFlex	35.5 (15.1)	37.2 (16.6)	37.5 (17.3)	34.9 (15.4)	37.7 (17.2)	40.3 (17.3)	36.4 (15.5)	36.7 (15.9)	36.3 (15.6)	36.6 (15.8)	37.9 (15.7)
MaxBend	10.4 (6.6)	8.8 (4.0)	9.1 (4.8)	9.1 (4.4)	8.5 (4.4)	9.0 (4.3)	9.6 (4.9)	9.4 (4.6)	9.3 (4.5)	9.2 (4.4)	9.0 (4.0)
MaxTwist	13.6 (7.0)	16.4 (9.5)	12.9 (6.7)	12.6 (7.6)	11.9 (7.3)	12.9 (6.6)	15.0 (7.5)	14.3 (7.0)	13.8 (6.7)	13.5 (6.5)	12.5 (5.8)

Table 11: Number of trials required for each EMG measure in each task. The intraclass correlation coefficient (ICC), normalized standard error of measurement (SEM) (% of grand mean), and unnormalized SEM (%MVC) corresponding to that number of trials are also reported. For measures that did not achieve repeatability and reliability within ten trials, the ICC and SEMs for ten trials are reported. EO: external oblique; IO: internal oblique; LD: latissimus dorsi; LES: lumbar ES; LTES: lower-thoracic ES; RA: rectus abdominis; TR: upper trapezius; UTES: upper-thoracic ES.

Measure	Task															
	Upright Standing				Maximum Flexion				Maximum Bend				Maximum Twist			
	# Trials	ICC	SEM (%)	SEM (%MVC)	# Trials	ICC	SEM (%)	SEM (%MVC)	# Trials	ICC	SEM (%)	SEM (%MVC)	# Trials	ICC	SEM (%)	SEM (%MVC)
<i>Left</i>																
EO	2	0.99	5.3	0.4	3	0.92	20.7	3.2	2	0.90	20.7	9.4	2	0.93	15.0	5.6
IO	2	0.99	8.1	0.6	5	0.88	21.8	3.6	2	0.97	15.0	4.5	2	0.96	16.9	3.3
LD	2	0.98	8.7	0.2	2	0.94	16.5	1.6	2	0.95	13.1	1.3	3	0.81	23.2	2.3
LES	2	0.98	8.1	0.2	2	0.93	9.9	3.9	2	0.92	14.2	2.8	2	0.92	17.3	2.3
LTES	2	0.96	9.4	0.2	4	0.84	19.3	3.6	2	0.85	16.6	2.1	5	0.82	24.0	1.9
RA	2	1.00	3.5	0.2	5	0.95	24.9	4.0	2	0.96	18.8	2.5	3	0.96	14.9	1.5
TR	5	0.95	24.0	0.4	2	0.95	16.8	1.9	2	0.91	18.6	2.2	4	0.93	21.5	2.9
UTES	2	0.93	13.7	0.3	5	0.88	23.4	2.1	5	0.89	24.6	2.5	>10	0.89	26.5	1.6
<i>Right</i>																
EO	2	0.99	4.9	0.3	3	0.84	20.3	2.4	2	0.94	18.2	3.2	2	0.98	9.0	4.4
IO	2	0.99	6.3	0.4	4	0.90	22.1	3.3	4	0.90	24.6	3.5	2	0.98	14.0	5.7
LD	2	0.99	4.6	0.1	2	0.87	21.7	2.3	3	0.89	22.9	1.8	4	0.91	24.1	3.8
LES	2	0.94	14.4	0.4	2	0.95	9.9	3.6	3	0.85	21.5	2.0	3	0.87	20.3	2.9
LTES	2	0.91	15.8	0.4	2	0.89	19.5	3.5	3	0.87	23.6	2.2	2	0.93	17.6	6.5
RA	2	1.00	2.7	0.1	5	0.94	23.8	3.5	2	0.98	13.1	1.3	3	0.97	10.7	1.3
TR	10	0.94	18.2	0.3	4	0.88	20.2	2.0	10	0.94	20.9	3.3	>10	0.86	36.8	5.7
UTES	2	0.89	15.0	0.4	2	0.89	18.1	1.7	4	0.81	21.7	1.5	10	0.91	21.6	7.0

The analysis of residuals showed strong agreement across the sets of trials for kinematic and EMG variables for all tasks. On average, the highest residuals (i.e. the least representative of the remaining trials) were found when calculating the RMSD relative to the First, Fifth, and Tenth trials (Table 12). The lowest residuals (the most representative of/similar to all other trials) were found for FirstFour and FirstFive. FirstTwo and FirstThree also produced very low residuals; on average (*SD*), the differences in residuals between FirstTwo and the lowest of FirstFour or FirstFive was 0.21 (0.15), and between FirstThree and the lowest of FirstFour or FirstFive was 0.05 (0.05). These results indicate that there was strong agreement between the different sets of trials, especially when using the averages of multiple trials.

Table 12: Mean (*SD*) root mean square differences (RMSDs) relative to each set of trials ('reference') in each task, collapsed across the ten trials and across measures. The RMSD values were very low, especially for the trial sets in which the averages of multiple trials were used, indicating strong agreement between the trial sets. Bolded and italicized values indicate the lowest and highest RMSDs, respectively.

Task	Trial Set									
	First	Second	Third	Fourth	Fifth	Tenth	First Two	First Three	First Four	First Five
<i>Angles (°)</i>										
Upright										
Flexion-extension	2.90 (1.56)	2.71 (1.43)	2.83 (1.58)	2.79 (1.42)	2.93 (1.52)	<i>3.21</i> (1.82)	2.09 (1.12)	1.99 (1.07)	1.98 (1.05)	1.97 (1.05)
Lateral bend	1.24 (0.61)	1.20 (0.65)	1.29 (0.72)	1.23 (0.69)	1.27 (0.68)	<i>1.50</i> (0.93)	0.92 (0.49)	0.88 (0.47)	0.86 (0.45)	0.86 (0.46)
Axial twist	2.38 (0.43)	2.38 (0.51)	2.52 (0.56)	2.52 (0.50)	2.51 (0.47)	2.62 (0.51)	1.80 (0.35)	1.68 (0.31)	1.67 (0.32)	1.67 (0.32)
MaxFlex	5.45 (1.12)	4.63 (1.06)	4.96 (1.17)	4.60 (1.18)	4.79 (1.07)	<i>5.71</i> (0.87)	3.69 (0.79)	3.52 (0.76)	3.41 (0.73)	3.39 (0.73)
MaxBend	3.70 (0.88)	3.27 (0.90)	3.45 (1.03)	3.34 (0.94)	3.65 (1.12)	3.98 (1.05)	2.53 (0.68)	2.47 (0.68)	2.42 (0.67)	2.42 (0.66)
MaxTwist	<i>8.91</i> (4.11)	7.99 (3.58)	8.09 (3.48)	7.51 (3.08)	8.63 (4.22)	7.84 (2.97)	6.18 (2.72)	5.89 (2.58)	5.75 (2.53)	5.79 (2.57)
<i>EMG (%MVC)</i>										
Upright	0.55 (0.25)	0.52 (0.25)	0.50 (0.24)	0.56 (0.29)	0.55 (0.27)	<i>0.62</i> (0.31)	0.40 (0.19)	0.38 (0.18)	0.37 (0.18)	0.37 (0.18)
MaxFlex	6.43 (3.48)	6.29 (3.44)	5.84 (3.17)	6.46 (4.03)	<i>7.01</i> (7.18)	6.74 (3.36)	4.70 (2.70)	4.50 (2.64)	4.43 (2.63)	4.51 (2.99)
MaxBend	5.15 (3.50)	4.83 (3.24)	4.95 (3.27)	4.69 (2.91)	4.84 (3.10)	<i>5.64</i> (3.10)	3.64 (2.44)	3.45 (2.24)	3.41 (2.24)	3.39 (2.22)
MaxTwist	8.11 (5.34)	7.57 (4.58)	7.44 (4.95)	7.84 (5.09)	7.97 (5.64)	8.22 (5.47)	5.86 (3.76)	5.52 (3.59)	5.42 (3.53)	5.41 (3.55)

3.4 Discussion

Overall, the repeatability and reliability of the kinematic and EMG measures were high, as evidenced by high ICCs, low SEM%, and few significant differences between the different sets of trials. Based on these criteria, of all measures for all tasks in the present study, 59%, 68%, 78%, 86%, and 91% produced repeatable and reliable values with two, three, four, five, and ten trials, respectively. The ANOVA results indicated that using an average measure from multiple trials provided more stable values than using a single trial, as did the results of the analysis of residuals in that the lowest RMSDs were found when calculating the RMSD relative to the average of multiple trials. These results suggest that this approach may be preferable to the use of a single value (for example, the last trial of a given set of repetitions). Researchers are encouraged to utilize these results in selecting the number of trials to be collected in an experimental protocol, depending on the measures of interest as well as the level of repeatability and reliability acceptable for the research question.

The mean angles and activation levels reported in the present study fell within previously reported ranges (Montgomery et al., 2011; Peach et al., 1998; Sheeran et al., 2012). Very few of the measures were affected by the trial set used, indicating that the measures remained relatively similar across the testing session. For the few kinematic measures in which ten trials was not sufficient to obtain repeatable and reliable values according to the criteria of the present study (thoracic Upright lateral bend angle, all Upright axial twist angles, lumbar MaxTwist angle), the largest differences between any of the trial sets ranged from 0.4° (FirstTrial and FourthTrial, head Upright axial twist

angle) to 1.2° (FirstTrial and FourthTrial, lumbar MaxTwist angle). Further, the unnormalized SEM values were less than 1.0°. As the differences and errors described above were all within 2° (Dos Santos et al., 2012; Troke et al., 2007), it is likely that differences were not clinically important (Troke et al., 2007). That is, the magnitude of errors were within a range that is considered clinically acceptable (Dos Santos et al., 2012), potentially due to lower precision of equipment used for these measures in a clinical setting. In addition, the small magnitudes may not be practically significant for research purposes, unless these measures are of primary interest. Similarly, the largest differences for EMG measures requiring more than ten trials were 1.9%MVC and 5.8%MVC for the left upper-thoracic ES (SecondTrial and TenthTrial) and right TR (FirstTrial and FourthTrial) in MaxTwist, respectively, with unnormalized SEMs ranging from 0.3%MVC (TR, Upright) to 7.0%MVC (upper-thoracic ES, MaxTwist). Considering the scale of these values and unnormalized SEM, especially for the kinematic measures, these differences may not be consequential enough to warrant the collection of ten or more trials per condition.

The reliability of the measures in the present study was high, with many ICCs greater than 0.80 and SEM% less than 25%. There have been wide variations in ICCs throughout the literature, depending on measure, task, and type of reliability. ICCs quantifying between-session reliability of trunk ROM have ranged from 0.39 to 0.93 (lumbar angle) (McGregor et al., 1995) and 0.60 (upper-thoracic angle) to 0.96 (lower-lumbar angle) (Hidalgo et al., 2012). Troke et al. (2007) reported between-session ICCs ranging from 0.72 to 0.99 for individual raters assessing lumbar ROM. Between- and

within-session reliability of spine angles in upright standing have been found to range from 0.64 to 0.84 and 0.55 to 0.98, respectively (Dunk et al., 2005). Within-session EMG reliability for maximal and submaximal trunk isometric contractions has ranged from 0.75 to 0.98 (Dankaerts et al., 2004), and between-session reliability from 0.32 to 0.97 (Dankaerts et al., 2004; Ng et al., 2003; Pitcher et al., 2008). While few studies have examined the within-session reliability of kinematic and EMG measures in upright standing and maximum trunk ROM movement tasks, the ICCs and SEM observed in the present study fall within the limited ranges reported in the literature.

The repeatability and reliability of Upright flexion-extension angles were very high, with only two trials necessary to obtain repeatable and reliable measures. Conversely, at least one measure in each of Upright lateral bend and Upright axial twist did not achieve repeatability and reliability within ten trials. Reliability has been previously identified as being positively related to ROM by Chan et al. (2006), who postulated that a larger ROM results in a higher signal-to-noise ratio, and therefore better reliability. The present results for the three planes in Upright agree with these findings, in that the Upright flexion-extension angles tended to exhibit greater magnitudes (AllTen mean (*SD*) of 32.5° (9.7) extension and 45.1° (8.4) flexion for the lumbar and thoracic angles, respectively) than the lateral bend (2.2° (4.0) and 0.5° (4.1) to the left) or axial twist (0.7° (4.0) and 2.8° (6.1) to the left) directions. The small magnitudes of these measures would have contributed to the high SEM%, although the unnormalized SEM values were all within a clinically acceptable range (Dos Santos et al., 2012).

Two trials were also found to be sufficient for all angle measures in the MaxFlex and MaxBend tasks. Similar to Upright flexion-extension, the large magnitudes of ROM for all measures in MaxFlex and MaxBend potentially resulted in a larger signal-to-noise ratio, contributing to high repeatability and reliability (Chan et al., 2006). Conversely, some measures for MaxTwist showed lower repeatability and reliability, and required a greater number of trials (head: 4, lumbar: >10). Maximum axial twist tasks have been found to exhibit lower ICCs than flexion and lateral bend tasks between sessions, for both lumbar and trunk ROM (McGregor et al., 1995; Troke et al., 2007). The lower repeatability and reliability of the kinematic measures in MaxTwist in the present study may potentially have been due to greater amounts of skin movement compared to MaxFlex or MaxBend, or that the MaxTwist position is simply more difficult for participants to replicate consistently due to redundancy in the musculoskeletal system or coupling of motion in the spine (White & Panjabi, 1990). The repeatability and reliability of the lumbar angle specifically may have been influenced by the relatively small magnitudes observed for this measure (thereby resulting in a high SEM%, even with a small unnormalized SEM), or the presence of coupled motion patterns in the lumbar spine (White & Panjabi, 1990), as the pattern of coupling in vitro has been shown to change from contralateral in the upper three lumbar levels to ipsilateral in the lower levels (Panjabi et al., 1989). In vivo, these patterns may show some within-participant variation during multiple repetitions, which would reduce the repeatability and reliability of the lumbar angle measure. Should this measure be of primary interest, additional markers

placed at the apex of the lumbar spine (approximately the L₃ vertebra) may assist in improving repeatability and reliability.

The repeatability and reliability of the EMG measures were slightly lower than those of the kinematic measures. This was to be expected, as there are many factors which can influence the EMG signal (De Luca, 1997), and EMG signals are inherently variable (German et al., 2008; Shaffer & Lauder, 1985). Further, kinematic measures represent the movement outcome, which is relatively fixed or constant, while EMG measures represent individual strategies to perform the movement task, which may vary both within and between individuals. While the repeatability and reliability of the EMG measures was slightly less than those of the kinematic measures, the ICC and SEM values were still acceptable, agreeing with previous work examining the within-session repeatability of EMG measures during trunk isometric contractions (ICCs ranging from 0.75 to 0.98) (Dankaerts et al., 2004). The generally high repeatability and reliability of the EMG measures suggest that while there may be differences in activation strategies that individuals adopt to achieve a specific movement task, the activation strategies used by the same individual over a series of repetitions may be relatively consistent. While the EMG measures were high overall, the MaxTwist measures tended to require the greatest number of trials to achieve repeatability and reliability. This finding may have been related to the lower reliability of the lumbar measure during MaxTwist, with potential changes in coupling patterns resulting from variations in activation strategies.

Of the EMG measures that required ten or more trials, three of the five measures originated from MaxTwist. This finding mirrors the kinematic measures, in that the

MaxTwist angles were less repeatable and reliable than those in MaxFlex or MaxBend. As well, the five measures were all muscles of the upper back (left and right upper-thoracic ES, right TR). These muscles would not have contributed substantially to the movement tasks performed in the present study, and their activation may have contributed more to stabilizing the spine through co-contraction (Thelen et al., 1995), or to maintaining the position of the arms. Therefore, the muscles would not necessarily have activated to the same extent during every trial, as opposed to the muscles that directly influenced the movement (for example, back extensors in MaxFlex, or obliques in MaxBend or MaxTwist). In addition, although the arm position for the movement tasks (arms crossed over the chest) was selected to ensure that participants maintained a consistent arm position, the activation of the upper back muscles may have been influenced by this position. Higher repeatability and reliability may be identified for these muscles during these tasks if using other arm positions, or if other tasks are examined that target these muscles more directly.

Previous work has recommended that one session of five to six trials produces stable kinematic measures (Allison & Fukushima, 2003), but is not sufficient for EMG measurements (Sparto & Parnianpour, 2001). The present study indicated that for many measures, as few as two to three trials are sufficient for repeatability and reliability. The discrepancies may be due to differences in tasks between the studies, in that previous work examined the repeatability of target trunk angles (20%, 50%, and 80% of available spinal flexion; Allison & Fukushima, 2003) and activation levels (25%, 50%, 75%, and 100% of MVC; Sparto & Parnianpour, 2001), whereas the present study utilized

unconstrained maximum trunk ROM movement tasks. For Upright, participants were asked to stand as they normally would, and were very consistent with respect to the angles in the flexion-extension plane. While the ICC and SEM% values for the lateral bend and axial twist planes were lower and higher, respectively, the differences in the magnitudes between the different trial sets, as well as the unnormalized SEM, were small. The ‘targets’ of the movement tasks in the present study were simply the maximum ROM in each plane, which would have been constrained in one direction by the flexibility of each participant, in contrast to target trunk angles in previous studies in which a participant could both over- and under-shoot the target. The discrepancy in the number of trials required for EMG measures between past and present studies may also be explained by task differences, in that the present maximum trunk ROM movement tasks may have required different motor control strategies compared to tasks in which participants were targeting angles at the mid-range of trunk motion.

The analysis of residuals agreed with the ANOVA findings, showing little variation within each measure across the sets of trials. Using the averages of multiple trials produced lower residuals, and therefore the best representation of all trials. Although the FirstFour and FirstFive methods produced the lowest residuals, the residuals of the FirstTwo and FirstThree were also very low. These findings suggest that regardless of the number of trials that have been recommended for a specific measure in the present study, the prudent approach is to calculate an average value across the trials, as opposed to using a value from one single trial (for example, the last trial of a set of repetitions).

The present study was limited by some methodological concerns. While the tasks in the present study were less targeted than in past work, the motion may not represent that of functional activities. Lower repeatability and reliability may be identified for tasks in which participants are given a task-oriented instruction (for example, 'lift the box') in which they are free to select the movement pattern required to accomplish the task, as opposed to the specific posture-based instructions in the present study. Additionally, the rotation sequence used to calculate the spine angles may have influenced the kinematic results, in that the higher variability of the axial twist angles may have partially been due to the Z axis being the third rotation in the sequence. However, this sequence is commonly used in biomechanical research as it follows orthopaedic convention (Preuss & Popovic, 2010) and the order in which importance is typically assigned to each plane of movement. Finally, the results may not generalize to individuals with LBP, as LBP populations demonstrate altered ROM (Hidalgo et al., 2012; Mayer et al., 1984), motion patterns (Marras et al., 1999; Shum et al., 2005a, b; Wong & Lee, 2004), muscle activation (D'Hooge et al., 2013; Lariviere et al., 2000; Watson et al., 1997), and variability relative to healthy control participants (Sheeran et al., 2012). Future work should establish similar recommendations for individuals with LBP.

In conclusion, the repeatability and reliability of kinematic and EMG measures was generally high, and indicated that approximately 59%, 68%, 78%, 86%, and 91% of measures produced repeatable and reliable values with two, three, four, five, and ten trials, respectively. Taking the average of values from the identified trial sets appeared to be preferable to the use of a single trial as a representative value. The exceptions for

which ten trials were not sufficient were Upright thoracic lateral bend angles, all Upright axial twist angles, MaxTwist lumbar angles, and EMG of the TR and upper-thoracic ES muscles in specific movement tasks. Recommendations regarding the minimum number of trials required for repeatable and reliable kinematic and EMG measures have been provided, ranging from two to five trials for most measures. These recommendations are intended to provide an acceptable trade-off between repeatable and reliable values and feasibility of the collection protocol, and to provide a guideline for researchers to select the number of trials most appropriate to their research question and measures of interest.

CHAPTER 4

Identification of Head and Arm Positions to Elicit Maximal Voluntary Trunk Range-of-Motion Measures

The work presented in Chapter 4 constitutes a paper that has been accepted for publication as of July 1, 2014 to the Journal of Applied Biomechanics:

Schinkel-Ivy A, Pardisnia S, Drake JDM. Head and arm positions that elicit maximum voluntary trunk range-of-motion measures. Journal of Applied Biomechanics, Accepted, July 2014.

CHAPTER 4

Identification of Head and Arm Positions to Elicit Maximal Voluntary Trunk Range-of-Motion Measures

Summary

Relationships have been shown between spinal motion and head and/or arm positions, yet there has been little standardization of the head and arm positions that elicit maximal voluntary spine angles during maximal trunk flexion, lateral bend, and axial twist. This study aimed to determine the head and arm positions that facilitated maximum voluntary ROM for various spine angle measures during these movement tasks. Twenty-four individuals performed maximal movement tasks in each plane with different combinations of head and arm positions (flexion and lateral bend: 4 combinations; axial twist: 6 combinations). Generally, greater angles were elicited for the upper spine measures when the head was moved in the direction of trunk motion, while the angles of the lower measures were either unaffected or greater when the head was kept in a neutral position. Arm positions also affected maximum spinal angles, in that angles were greatest when the arms were hanging to the floor (flexion), either hanging to the floor or crossed over the chest (lateral bend), and abducted to 90° (axial twist). These findings provide insight into the interplay between the spine and adjacent segments, and constituted an initial attempt to develop standardized positions during maximum trunk ROM movement tasks.

4.1 Introduction

Kinematic data (i.e. joint angles) are commonly normalized to the maximum ROM that can be obtained by a participant, in order to characterize the joint angles observed during experimental tasks as a percentage of maximum ROM. These normalization techniques are employed in order to account for individual differences, thereby facilitating comparisons between individuals and between groups (Edmondston et al., 2007b). For example, normalization has been employed to examine differences between healthy and patient groups (Dunk & Callaghan, 2010) and tasks (Callaghan & Dunk, 2002; Strahan et al., 2011), as well as changes over time (Howarth et al., 2013). Therefore, when collecting maximum ROM trials during the calibration portion of a data collection protocol, it is essential to elicit maximum ROM values of the trunk or spine regions of interest in each direction (flexion, lateral bend, and axial twist) to ensure that the normalized joint angles for the experimental tasks properly represent the absolute kinematic measures.

While spinal ROM in the flexion, lateral bend, and axial twist directions has been studied quite extensively (Edmondston et al., 2007a; Peach et al., 1998; Pearcy & Hindle, 1989; Tojima et al., 2013; Tsang et al., 2013; Van Herp et al., 2000; Willems et al., 1996), often the head and arm positions that participants are requested to maintain during these movement tasks are either unspecified or uncontrolled. Those studies that do specify head and/or arm positions exhibit substantial variation between protocols. With respect to head positions, participants have been asked to either maintain a neutral head position (in line with the trunk) throughout the movement task (Andersson et al., 1996; Peach et

al., 1998) or to move the head in the same direction of movement as the trunk (i.e. for a trunk flexion movement task, the head would be flexed towards the chest) (Alschuler et al., 2009; Willems et al., 1996); however, head positions often remain unspecified. Arm positions may also be unspecified or vary between studies. Positions that have been used previously include crossed over the chest (Kaigle et al., 1998; Willems et al., 1996), hanging to the floor (Peach et al., 1998), and abducted to 90° (Edmondston et al., 2007a). Taken together, it appears that there has been little standardization or consistency regarding head and arm positions during these movement tasks. The differences in head and arm positions used throughout the spinal ROM literature may account for some of the variation in maximum angles between studies. Further, an inability to attain maximum ROM may hinder any comparisons of normalized values, as normalizing to a value that is not actually a maximum would potentially result in a greater percentage of ROM than the true value. These issues highlight the need for the determination of a standardized series of head and arm positions to elicit maximal voluntary trunk ROM measures.

Although various head and arm positions have been employed in the past in quantifying maximum trunk ROM, recent work has shown relationships between the thoracic spine and neck slope and between the thoracic spine and upper-cervical spine during standing (Kuo et al., 2009). Relationships also exist in the timing of cervical and upper-thoracic motion as quantified by cross correlation (Tsang et al., 2013). Therefore, the necessity of controlling for the positioning and movement of the head and neck during trunk motion trials in order to minimize the influence of cervical movement on movement in the upper-thoracic segment (Willems et al., 1996) seems justified. Regarding arm

positions, previous work has indicated that consistent patterns of spinal motion can be observed during unilateral (Crosbie et al., 2008; Theodoridis & Ruston, 2002) and bilateral (Crosbie et al., 2008) arm elevations. Additionally, Crosbie et al. (2010) concluded that significant and consistent timing coherence was shown between thoracic and scapulohumeral movements during a lifting task. Given the relationships between spinal movement and adjacent segments, a further investigation of the influence of head and arm positions, specifically during maximum trunk ROM movement tasks, seems warranted. The aforementioned works establish that the position of adjacent segments or joints such as the head or shoulder influence thoracic position. However, little investigation has been conducted to determine whether this effect is exclusive or local to the thoracic spine, or if head and arm positions exert a more global influence over regions that are more removed from those spine regions, such as the lumbar spine or pelvis.

To the authors' knowledge, an investigation has not yet been conducted to determine which head and arm positions facilitate maximum voluntary spine ROM angles. Insight into the impact of head and arm positions on the amount of spinal motion is necessary to gain a better understanding of the interplay between the spine and adjacent regions, and for the study of ROM in special populations (for example, elderly or low back pain patients). Therefore, the purpose of this study was to determine which head and arm positions enabled the greatest voluntary ROM in various spinal regions during maximum trunk flexion, lateral bend, and axial twist.

4.2 Methods

4.2.1 Participants

Twenty-four individuals (12 males, 12 females) were recruited to participate in the study. The mean (*SD*) body mass, height, and age was 79.97 kg (9.38), 1.80 m (0.05), and 25.3 years (3.9) for the males, respectively, and 60.03 kg (6.56), 1.66 m (0.06), and 23.1 years (2.9) for the females. All participants were right-hand dominant, and had not been treated for back pain nor had missed any days of school or work due to back pain for at least 12 months prior to collection. All procedures were approved by the institution's Office of Research Ethics, and informed consent was obtained from all participants prior to collection.

4.2.2 Instrumentation

Fifty-nine passive-reflective markers were adhered to participants using double-sided tape. Six clusters of five markers each were placed over the C₇, T₃, T₆, T₉, T₁₂, and L₅ spinous processes. The 29 remaining markers were placed on the legs (greater trochanters, lateral and medial knee joint spaces, lateral malleoli, four on each thigh; 16 total), pelvis (iliac crests, anterior superior iliac spines; four total), trunk (acromia, sternum, 10th thoracic vertebra; four total), and head (left and right front and back of the head, mid-back of the head; five total). All kinematic data were sampled at 50 Hz by a seven-camera Vicon MX motion capture system (Vicon Systems Ltd., Oxford, UK).

4.2.3 Procedures

Once the markers were applied, a kinematic calibration trial was collected in the form of a 'T pose' (standing upright, with arms abducted to 90°). Participants then

performed a series of 150 movement trials (10 trials per condition; 15 conditions). The trials consisted of Upright and three movement tasks: MaxFlex, MaxBend, and MaxTwist (MaxBend and MaxTwist performed to the right side). For each of the movement tasks, various combinations of head and arm positions were used (Figures 16-18). MaxFlex and MaxBend consisted of four combinations; the head was either aligned with the trunk (neutral) or moved in the direction of trunk motion (active), and the arms were either crossed over the chest (crossed) or hanging freely to the floor (loose). The head positions were the same for MaxTwist (neutral/active), although an additional arm position was added such that there were six combinations for MaxTwist. The arms were either crossed (crossed), abducted to 90° (abducted), or hanging at the sides (loose). For the crossed position, the arms were elevated at the shoulder such that the upper arms were parallel with the floor, and the hands were placed on the contralateral shoulders. Prior to beginning the collection, participants were provided with complete instructions on each movement task, and practiced the movements with an investigator to ensure proper technique. Throughout the protocol, participants were prompted before each trial with brief instructions highlighting the key features of each movement so the movement was performed consistently at each occurrence. Movement tasks were initiated from the Upright position, following which participants moved into the position, held the position for three seconds, and moved back to Upright. All trials (including Upright) were completely randomized for each participant.

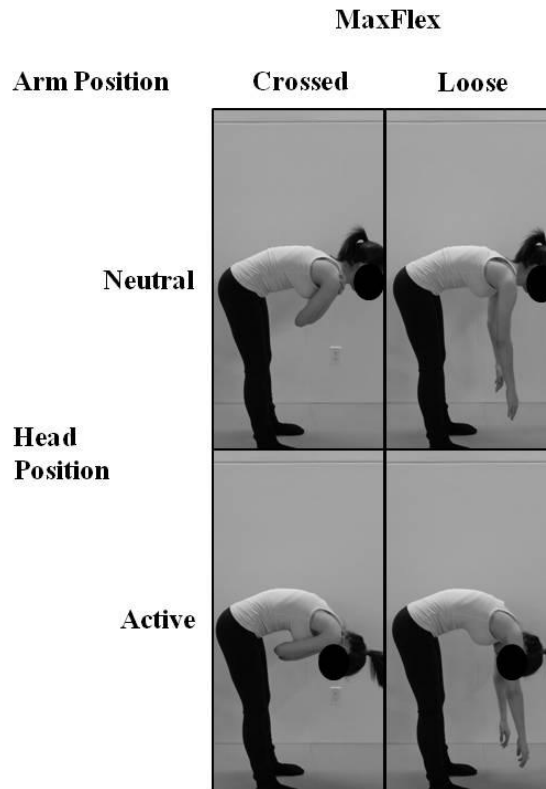


Figure 16: Combinations of head and arm positions used for MaxFlex (Adapted, by permission, from: Schinkel-Ivy A, Pardisnia S, Drake JDM. Head and arm positions that elicit maximal voluntary trunk range-of-motion measures. *Journal of Applied Biomechanics* 2014 (accepted July 1, 2014). Figure 1. © Human Kinetics, Inc.). Written copyright permission not required for self-authored work; refer to Appendix B.

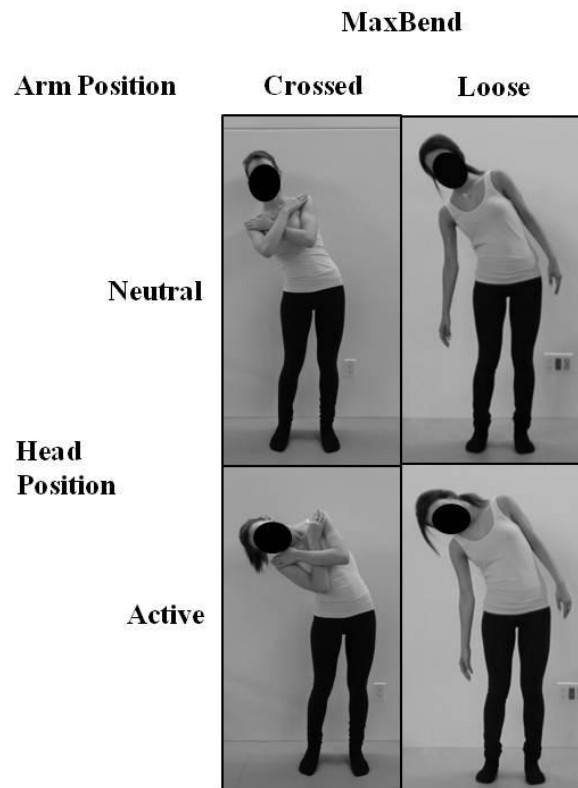


Figure 17: Combinations of head and arm positions used for MaxBend (Adapted, by permission, from: Schinkel-Ivy A, Pardisnia S, Drake JDM. Head and arm positions that elicit maximal voluntary trunk range-of-motion measures. *Journal of Applied Biomechanics* 2014 (accepted July 1, 2014). Figure 1. © Human Kinetics, Inc.). Written copyright permission not required for self-authored work; refer to Appendix B.

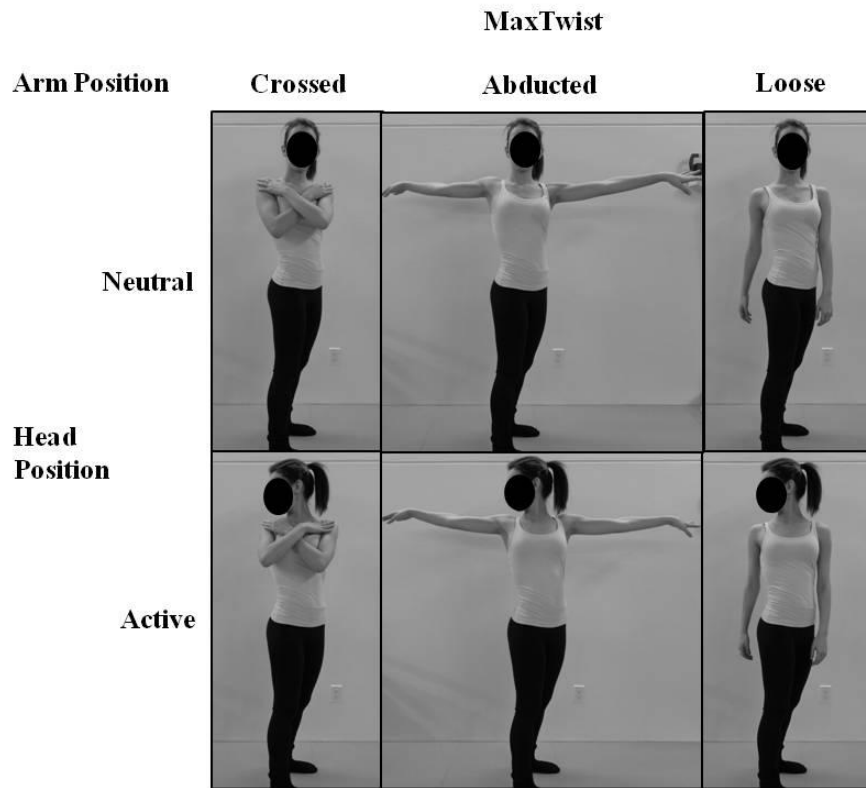


Figure 18: Combinations of head and arm positions used for MaxTwist (Adapted, by permission, from: Schinkel-Ivy A, Pardisnia S, Drake JDM. Head and arm positions that elicit maximal voluntary trunk range-of-motion measures. *Journal of Applied Biomechanics* 2014 (accepted July 1, 2014). Figure 1. © Human Kinetics, Inc.). Written copyright permission not required for self-authored work; refer to Appendix B.

4.2.4 Data Processing

Kinematic data were processed using Visual3D v.4 (C-Motion, Inc., Germantown, USA). The flexion-extension, lateral bend, and axial twist angles for the head, C₇, T₃, T₆, T₉, T₁₂, and L₅ clusters, trunk, and pelvis were calculated based on the marker data (Appendix C) using a Cardan X-Y-Z (flexion/extension-lateral bend-axial twist) rotation sequence (Preuss & Popovic, 2010; van Dieen & Kingma, 2005). The relative angles between specific segments were then determined (Table 13, Figure 19). Data were then

low-pass filtered with a dual-pass, fourth-order Butterworth filter with a cut-off frequency of 2.5 Hz, as determined by residual analysis (Winter, 2005). The mean angles in each direction for each angle measure during upright standing were determined to provide context for the maximum angles. Maximum angles in the plane of interest (MaxFlex: flexion-extension; MaxBend: lateral bend; MaxTwist: axial twist) were identified for each trial and averaged across the 10 trials for each condition. For exemplar kinematic data, please refer to Appendix D.

Table 13: Segments and marker clusters used to determine the angles of interest.

Angle Name	Segments and Markers Used for Calculation
Head	Head (defined by markers around the head circumference and acromia, although only the former were used to track motion) relative to trunk segment
Cervico-thoracic	C ₇ cluster relative to T ₃ cluster
Thoracic	T ₃ cluster relative to T ₁₂ cluster
Upper-thoracic	T ₃ cluster relative to T ₆ cluster
Mid-thoracic	T ₆ cluster relative to T ₉ cluster
Lower-thoracic	T ₉ cluster relative to T ₁₂ cluster
Lumbar	T ₁₂ cluster relative to L ₅ cluster
Trunk	Trunk (defined by the acromia and iliac crests) relative to laboratory coordinate system
Pelvis	Pelvis (defined by the iliac crests, anterior superior iliac spines, and greater trochanters) relative to laboratory coordinate system

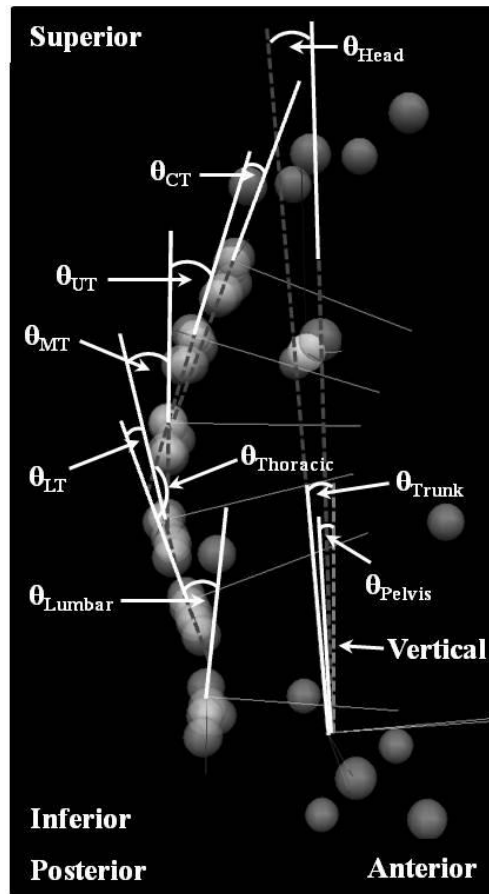


Figure 19: Collapsed 3D sagittal view of the markers representing the calculation of each angle. The angles represented in this collapsed 3D sagittal view are the equivalent of flexion-extension angles. CT: cervico-thoracic; UT: upper-thoracic; MT: mid-thoracic; LT: lower-thoracic (Adapted, by permission, from: Schinkel-Ivy A, Pardisnia S, Drake JDM. Head and arm positions that elicit maximal voluntary trunk range-of-motion measures. *Journal of Applied Biomechanics* 2014 (accepted July 1, 2014). Figure 2c. © Human Kinetics, Inc.). Written copyright permission not required for self-authored work; refer to Appendix B.

4.2.5 Data Analysis

All statistical analyses were performed using IBM SPSS Statistics v.21 (IBM Corporation, Armonk, USA). Intraclass correlation analyses (ICC(3,10)) were conducted to establish the reliability of the angle measures across the ten trials of each condition.

Four-factor mixed ANOVAs (one for each MaxFlex, MaxBend, and MaxTwist) with repeated measures of angle measure, head position, and arm position and between-group factor of sex were used to analyze differences between the various head and arm positions within each movement task. For ANOVAs in which there were no significant main effects or interactions of sex, data were collapsed across this factor. When the assumption of sphericity was not met, the degrees of freedom were determined using Greenhouse-Geisser corrections. Alpha was set to 0.05, and significant *F*-tests were further analyzed using pairwise comparisons, adjusted using Bonferroni. Due to the research question of interest of the present study, only the significant pairwise comparisons for the head and arm positions are reported.

4.3 Results

ICCs for each measure and movement condition ranged from ICC(3,10)=0.864 (lumbar, MaxTwist with active head and loose arms) to ICC(3,10)=0.996 (lumbar, MaxFlex with neutral head and loose arms) (Table 14). The vast majority of coefficients (122 of 126 total analyses) were of a magnitude of 0.900 or higher, indicating excellent reliability of the angle measures across the ten trials of each condition (Webb et al., 2006).

Table 14: Mean (*SD*), minimum, and maximum intraclass correlation coefficients (ICCs) across all angle measures for each movement condition.

Movement Task	Mean (<i>SD</i>) ICC	Minimum ICC	Maximum ICC
<i>MaxFlex</i>			
Neutral – Crossed	0.961 (0.025)	0.917	0.991
Neutral – Loose	0.967 (0.039)	0.878	0.996
Active – Crossed	0.986 (0.009)	0.964	0.995
Active – Loose	0.987 (0.005)	0.976	0.992
<i>MaxBend</i>			
Neutral – Crossed	0.969 (0.016)	0.931	0.981
Neutral – Loose	0.958 (0.030)	0.882	0.984
Active – Crossed	0.974 (0.012)	0.948	0.987
Active – Loose	0.972 (0.014)	0.939	0.987
<i>MaxTwist</i>			
Neutral – Crossed	0.961 (0.027)	0.901	0.990
Neutral – Abducted	0.969 (0.022)	0.922	0.994
Neutral – Loose	0.961 (0.028)	0.900	0.984
Active – Crossed	0.964 (0.038)	0.867	0.990
Active – Abducted	0.978 (0.021)	0.925	0.992
Active – Loose	0.964 (0.039)	0.864	0.988

For MaxFlex, there was a significant main effect of arm position ($F_{1,23}=17.716$, $p<0.001$), indicating that greater angles were attained with the loose arm position. A significant interaction between angle measure and head position ($F_{2,537,58,357}=257.08$, $p<0.001$) was also identified (Table 15, Figures 20 and 21), such that the active head position produced greater angles for the head, cervico-thoracic, thoracic, upper-thoracic, mid-thoracic, and lower-thoracic measures. There was no effect of head position for the lumbar, trunk, or pelvis measures.

Table 15: Mean (*SD*) maximum flexion angles (°) (rotations around the X axis) for each angle measure in the MaxFlex conditions. The mean flexion-extension angles in Upright are also provided for context. Positive values indicate flexion. *Significant difference between head position (collapsed across arm positions) for that angle measure ($p < 0.05$).

Measure	Upright	Neutral – Crossed	Neutral – Loose	Active – Crossed	Active – Loose
Head*	7.6 (9.3)	24.1 (14.2)	22.8 (15.0)	69.2 (11.5)	70.5 (11.7)
Cervico-thoracic*	14.0 (10.2)	17.3 (11.0)	17.5 (8.8)	27.8 (8.9)	29.0 (9.0)
Thoracic*	31.7 (10.1)	43.4 (8.0)	45.1 (7.6)	49.0 (6.9)	49.8 (6.1)
Upper-thoracic*	14.1 (5.6)	18.7 (5.3)	19.6 (5.5)	22.6 (5.0)	23.7 (4.6)
Mid-thoracic*	14.0 (6.2)	19.0 (5.7)	19.1 (5.6)	19.7 (6.2)	20.1 (5.8)
Lower-thoracic*	3.7 (7.3)	10.8 (6.4)	11.8 (6.8)	12.1 (6.5)	12.3 (6.6)
Lumbar	-32.4 (10.4)	17.1 (10.1)	18.4 (11.0)	17.6 (10.0)	17.9 (11.2)
Trunk	-7.6 (3.9)	105.6 (14.2)	108.6 (11.2)	106.8 (16.2)	107.9 (14.1)
Pelvis	5.6 (7.4)	71.8 (18.1)	75.3 (14.4)	70.8 (18.4)	72.3 (16.9)

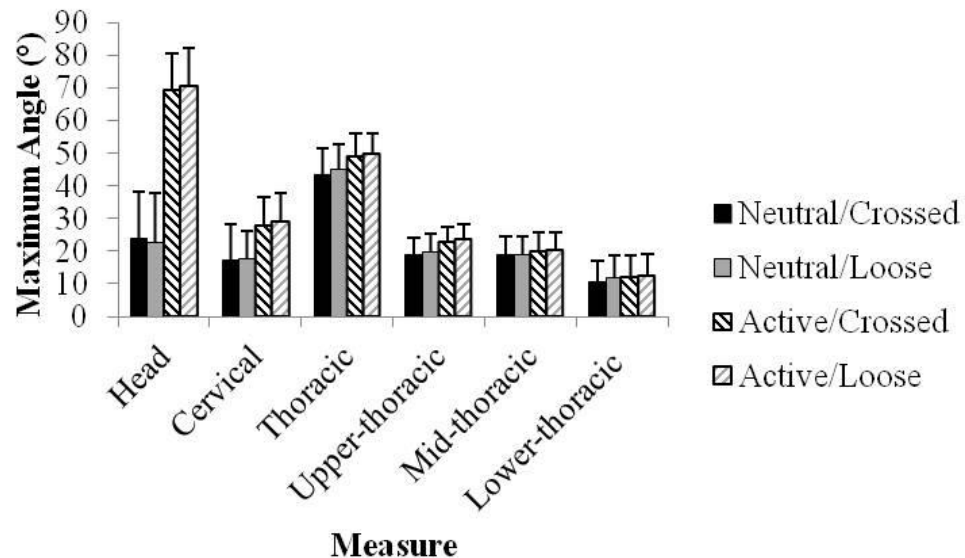


Figure 20: Graphical representation of the mean (*SD*) maximum angles in the upper regions during the MaxFlex conditions. Neutral head conditions are significantly different than the active head conditions, collapsed across arm positions ($p < 0.05$).

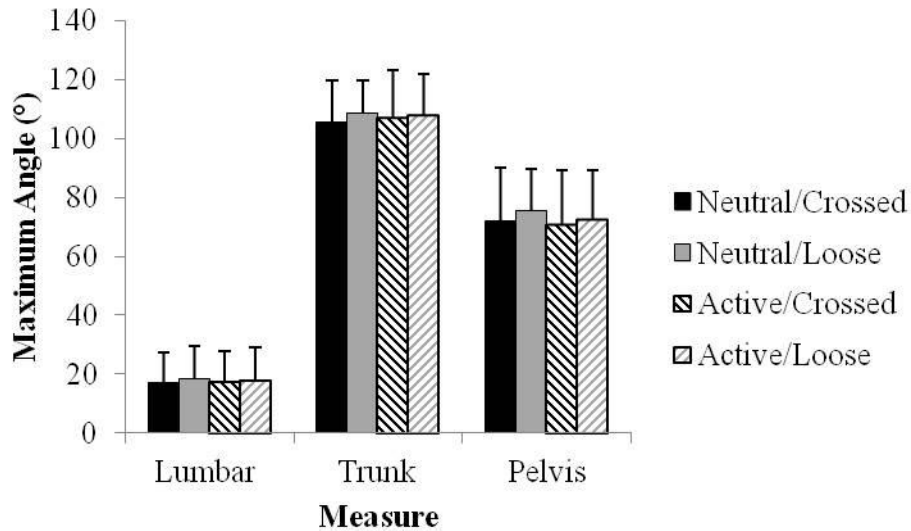


Figure 21: Graphical representation of the mean (*SD*) maximum angles in the lower and global regions during the MaxFlex conditions.

The MaxBend movement conditions displayed a significant interaction between angle measure, head position, and arm position ($F_{2,222,48.879}=3.255, p=0.042$) (Table 16, Figures 22-24). The active head position produced greater angles in the head, cervico-thoracic, thoracic, upper-thoracic, mid-thoracic, and lower-thoracic measures for at least one arm position. Conversely, for the lumbar, trunk, and pelvis measures, there was either no difference between head positions, or the neutral head position resulted in greater angles. Where significant pairwise comparisons were identified between arm positions, greater angles resulted from the crossed arm position for the head, cervico-thoracic, thoracic, upper-thoracic, mid-thoracic, and lower-thoracic angle measures, and from the loose arm position for the lumbar, trunk, and pelvis measures.

Table 16: Mean (*SD*) maximum lateral bend angles (°) (rotations around the Y axis) for each angle measure in the MaxBend conditions. The mean lateral bend angles in Upright are also provided for context. Positive values indicate lateral bending to the right. *Significant difference between arm positions within the same head position; shaded cells indicate a significant difference between head positions within the same arm position ($p<0.05$).

Measure	Upright	Neutral – Crossed	Neutral – Loose	Active – Crossed	Active – Loose
Head	2.5 (3.6)	30.6 (8.6)	30.1 (7.9)	57.6 (8.9)*	55.9 (9.7)
Cervico-thoracic	-0.8 (2.9)	7.5 (4.5)*	6.1 (4.7)	10.1 (5.0)*	9.0 (5.3)
Thoracic	0.9 (3.3)	22.4 (8.1)*	19.6 (6.7)	24.8 (7.4)*	20.3 (6.6)
Upper-thoracic	1.3 (2.9)	6.2 (3.3)*	5.7 (3.3)	6.6 (3.5)*	5.9 (3.1)
Mid-thoracic	2.1 (3.3)	7.5 (3.9)*	6.5 (4.0)	8.3 (3.8)*	7.0 (3.8)
Lower-thoracic	-2.7 (3.8)	6.7 (5.3)	6.0 (4.5)	7.9 (4.6)*	6.5 (4.1)
Lumbar	-2.4 (4.1)	18.6 (5.9)*	20.0 (5.9)	17.5 (5.7)*	19.8 (6.2)
Trunk	-1.2 (1.3)	42.5 (6.5)*	43.8 (6.3)	41.3 (7.0)*	43.1 (7.4)
Pelvis	-1.0 (2.1)	12.0 (4.0)*	13.0 (4.4)	10.9 (4.6)*	11.8 (4.8)

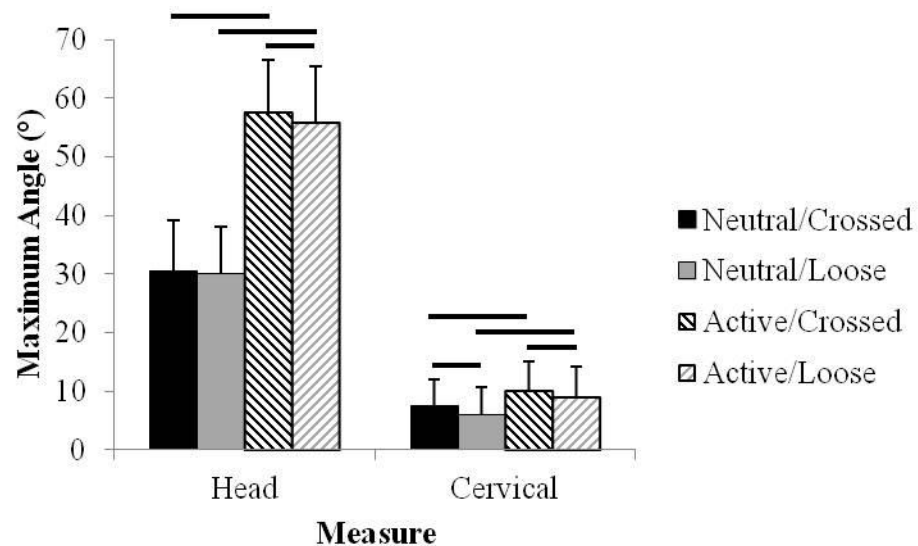


Figure 22: Graphical representation of the mean (*SD*) maximum angles in the head and cervico-thoracic regions during the MaxBend conditions. Horizontal bars indicate significant differences between conditions ($p<0.05$).

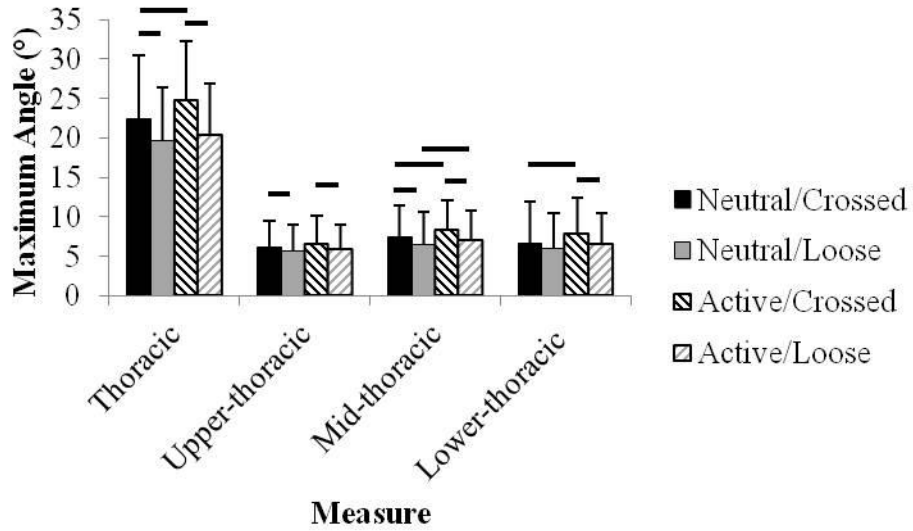


Figure 23: Graphical representation of the mean (*SD*) maximum angles in the thoracic regions during the MaxBend conditions. Horizontal bars indicate significant differences between conditions ($p < 0.05$).

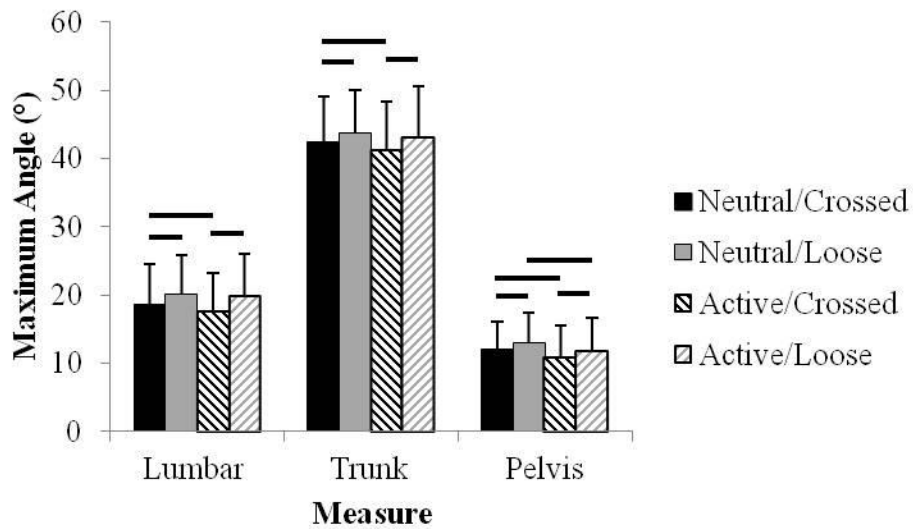


Figure 24: Graphical representation of the mean (*SD*) maximum angles in the lower and global regions during the MaxBend conditions. Horizontal bars indicate significant differences between conditions ($p < 0.05$).

A four-way interaction between sex, angle measure, head position, and arm position was identified for MaxTwist ($F_{4,582,100.796}=2.471$, $p=0.042$) (Table 17, Figures 25-28). Head position affected the head and cervico-thoracic measures in both sexes and lower-thoracic angles in males, with greater values produced in the active head position. The lumbar measure in females displayed the same trend, although the mean difference between the active and neutral head positions was less than 1.0° . For certain arm conditions, a neutral head position elicited greater mid-thoracic and trunk measures in males, and greater pelvis and trunk measures in females compared to an active head position. With respect to arm positions, the abducted position elicited the greatest angles in the thoracic, upper-thoracic, mid-thoracic, trunk, and pelvis measures for both males and females; these patterns were generally consistent across head positions. However, for the neutral head condition, the greatest values for the cervico-thoracic and lower-thoracic measures were achieved with the crossed arm position, and for the head with the loose arm position.

Table 17: Mean (*SD*) maximum axial twist angles ($^{\circ}$) (rotations around the Z axis) for each angle measure in the MaxTwist conditions. The mean axial twist angles in Upright are also provided for context. Positive values indicate axial twisting to the right. *Significant difference from the abducted arm position within the same head position; $^{\Delta}$ significant difference from the loose arm position within the same head position; shaded cells indicate a significant difference between head positions within the same arm position.

Sex	Measure	Upright	Neutral – Crossed	Neutral – Abducted	Neutral – Loose	Active – Crossed	Active – Abducted	Active – Loose
Male	Head	0.8 (2.9)	36.6 (9.0) $^{\Delta}$	32.2 (10.4) $^{\Delta}$	43.7 (11.5)	93.9 (11.5)	91.9 (13.5)	95.3 (11.8)
	Cervico-thoracic	-2.2 (2.8)	9.4 (7.5)*	-0.7 (9.7) $^{\Delta}$	9.0 (6.9)	23.0 (5.5)	20.7 (13.2)	22.0 (5.8)
	Thoracic	-3.9 (5.3)	41.5 (9.3)* $^{\Delta}$	52.9 (15.0) $^{\Delta}$	33.4 (10.4)	38.9 (7.5)* $^{\Delta}$	51.4 (13.9) $^{\Delta}$	33.4 (9.4)
	Upper-thoracic	-2.0 (4.5)	13.9 (5.5) $^{\Delta}$	16.5 (9.1) $^{\Delta}$	9.5 (3.3)	12.7 (4.0) $^{\Delta}$	15.4 (9.2) $^{\Delta}$	8.8 (2.9)
	Mid-thoracic	-3.0 (3.9)	17.3 (4.8)*	29.3 (13.3) $^{\Delta}$	17.3 (5.6)	16.5 (4.7)*	27.4 (12.3) $^{\Delta}$	16.5 (5.6)
	Lower-thoracic	0.5 (3.9)	14.7 (5.3)* $^{\Delta}$	12.0 (5.8)	10.8 (6.3)	15.3 (5.4)	13.7 (6.2)	12.6 (5.5)
	Lumbar	1.2 (3.4)	1.6 (4.7)	2.0 (3.2)	1.9 (3.2)	2.1 (5.1)	2.3 (2.9)	2.3 (3.1)
	Trunk	-0.9 (4.3)	70.1 (16.6)*	81.6 (15.4) $^{\Delta}$	67.1 (14.6)	66.7 (15.4)*	79.2 (14.8) $^{\Delta}$	65.5 (14.4)
	Pelvis	-0.9 (2.8)	53.1 (15.6)*	58.3 (15.7) $^{\Delta}$	53.2 (14.8)	51.4 (14.2)*	57.7 (13.6) $^{\Delta}$	51.6 (13.8)
Female	Head	-1.1 (3.5)	36.8 (14.3)	35.6 (17.6)	38.5 (17.1)	82.7 (13.3)	85.1 (13.9)	86.6 (11.7)
	Cervico-thoracic	-2.2 (4.1)	6.8 (6.0)	2.7 (5.7)	5.2 (5.7)	12.2 (5.3)	11.7 (8.2)	13.2 (5.9)
	Thoracic	2.9 (5.5)	37.5 (7.2)*	47.2 (12.4) $^{\Delta}$	33.3 (13.0)	38.5 (8.9)*	48.1 (12.1) $^{\Delta}$	34.8 (10.8)
	Upper-thoracic	-0.1 (4.0)	15.2 (4.9)*	21.1 (8.8) $^{\Delta}$	13.0 (7.8)	16.3 (6.3)* $^{\Delta}$	22.2 (8.7) $^{\Delta}$	13.8 (6.5)
	Mid-thoracic	0.8 (2.8)	14.7 (4.0)	20.6 (5.7)	15.0 (3.8)	14.5 (5.6)*	20.0 (6.3)	16.0 (3.5)
	Lower-thoracic	1.6 (3.5)	11.0 (3.1)	9.7 (3.8)	9.8 (4.7)	11.4 (3.2)	10.1 (3.2)	9.8 (4.6)
	Lumbar	-2.3 (4.4)	0.1 (4.9)	1.1 (5.2)	0.4 (5.4)	0.4 (4.5)	1.0 (5.1)	1.3 (5.7)
	Trunk	-0.6 (2.5)	70.6 (13.9)*	81.5 (14.4) $^{\Delta}$	70.4 (15.9)	68.0 (13.9)*	80.4 (15.4) $^{\Delta}$	65.7 (15.2)
	Pelvis	0.8 (6.0)	53.8 (13.2)*	59.7 (13.7) $^{\Delta}$	54.7 (15.9)	50.5 (13.7)*	57.9 (13.6) $^{\Delta}$	49.4 (15.6)

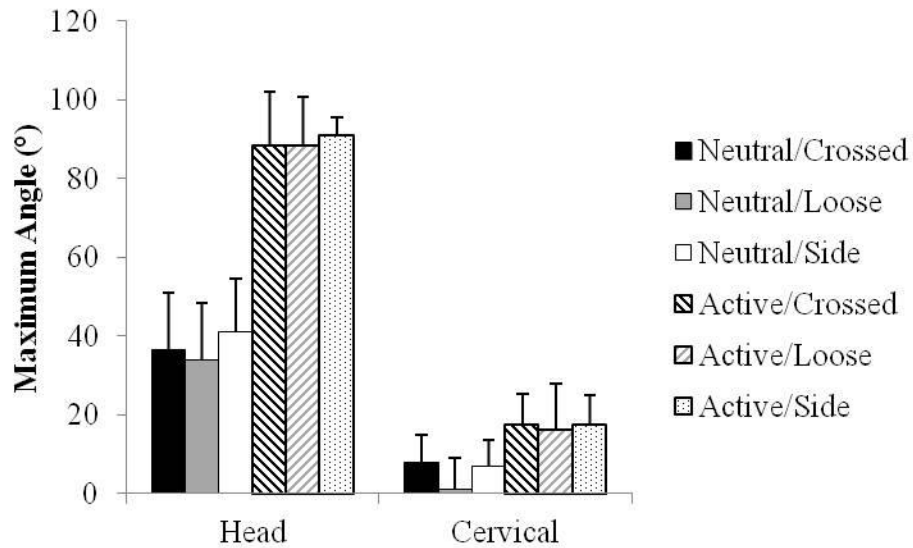


Figure 25: Graphical representation of the mean (*SD*) maximum angles in the head and cervico-thoracic regions during the MaxTwist conditions. Values have been collapsed across males and females; for significant differences between conditions, refer to Table 17.

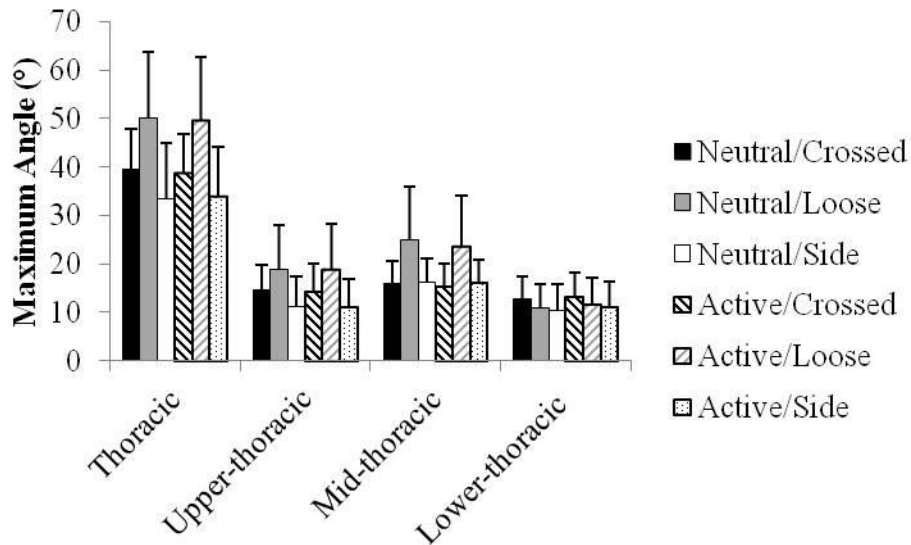


Figure 26: Graphical representation of the mean (*SD*) maximum angles in the thoracic regions during the MaxTwist conditions. Values have been collapsed across males and females; for significant differences between conditions, refer to Table 17.

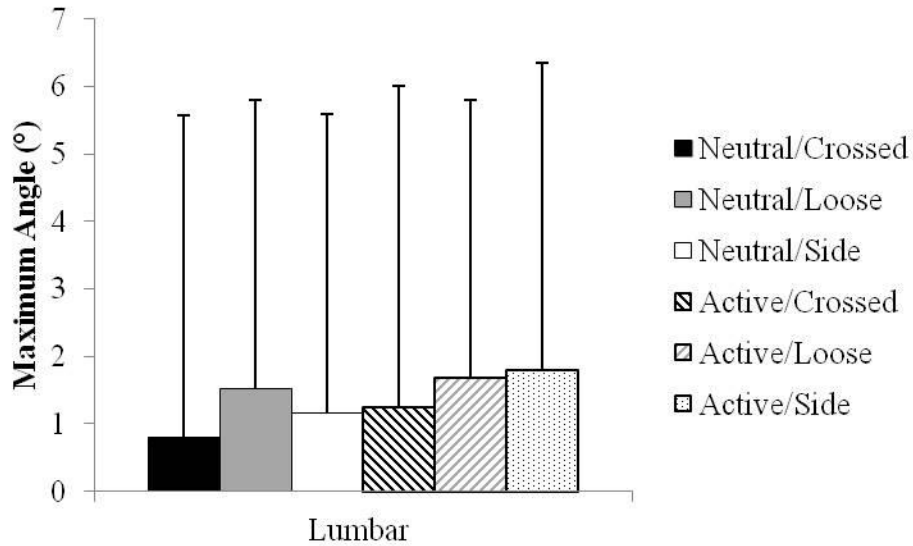


Figure 27: Graphical representation of the mean (*SD*) maximum angles in the lumbar region during the MaxTwist conditions. Values have been collapsed across males and females; for significant differences between conditions, refer to Table 17.

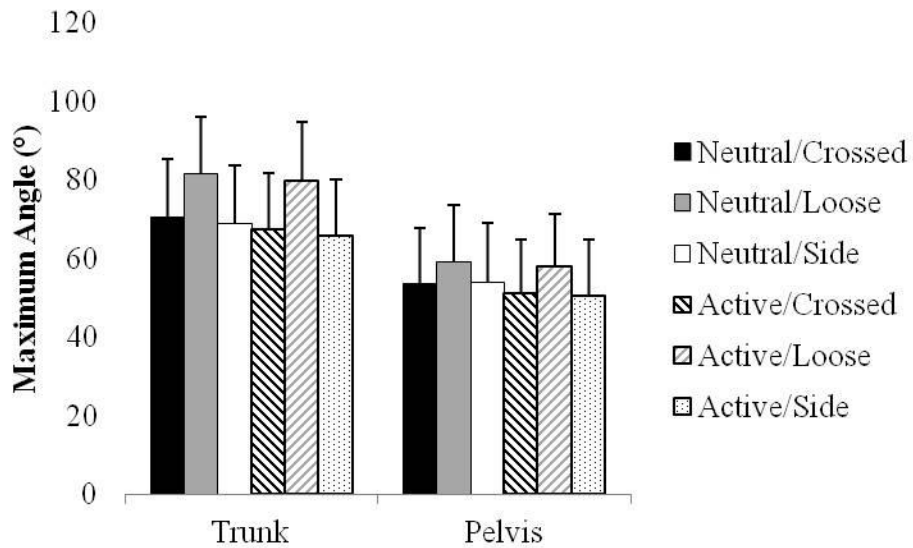


Figure 28: Graphical representation of the mean (*SD*) maximum angles in the trunk and pelvis during the MaxTwist conditions. Values have been collapsed across males and females; for significant differences between conditions, refer to Table 17.

4.4 Discussion

Overall, the findings of the present study supported the hypothesized results with respect to the effects of head position, in that for the upper regions (head, cervico-thoracic, thoracic, upper-thoracic, mid-thoracic, and lower-thoracic), an active head tended to elicit greater angles for all three movement tasks (Table 18). However, head position did not affect the maximum lumbar, trunk, or pelvis angles, with the exception of pelvis angles in MaxBend (greater angles with a neutral head position). The hypothesis with respect to arm position was supported for the MaxBend movement tasks, with greater angles for the upper regions with crossed arms and for the lower regions with loose arms. Conversely, for MaxFlex and MaxTwist, differences due to arm position generally resulted in greater angles with loose and abducted arms, respectively. These findings provide insight into the interplay between the spine and adjacent segments (head, arm), which is crucial to understand how the trunk functions as a system, as opposed to individual, isolated segments.

Table 18: The head and arm positions that elicited the greatest angles for each measure during each movement task. N/S: non-significant.

Measure	MaxFlex		MaxBend		MaxTwist	
	Head	Arms	Head	Arms	Head	Arms
Head	Active	Loose	Active	Crossed	Active	N/S
Cervico-thoracic	Active	Loose	Active	Crossed	Active	N/S
Thoracic	Active	Loose	Active	Crossed	N/S	Abducted
Upper-thoracic	Active	Loose	N/S	Crossed	N/S	Abducted
Mid-thoracic	Active	Loose	Active	Crossed	Neutral	Abducted
Lower-thoracic	Active	Loose	Active	Crossed	N/S	Crossed
Lumbar	N/S	Loose	N/S	Loose	N/S	N/S
Trunk	N/S	Loose	N/S	Loose	N/S	Abducted
Pelvis	N/S	Loose	Neutral	Loose	N/S	Abducted

The maximum spinal ROM values obtained in this study were comparable to those reported previously throughout the literature (Edmondston et al., 2007a; Peach et al., 1998; Percy & Hindle, 1989; Tojima et al., 2013; Tsang et al., 2013; Van Herp et al., 2000; Willems et al., 1996). Differences between the present and past data may potentially be due to differences in instrumentation or measurement systems (for example, motion capture versus electromagnetic tracking), or to differences in the definitions of spine angles (trunk, lumbar, thoracic, or partitioned thoracic). Based on the variations found in the present study between the conditions within each movement task, it is possible that some of the variability in spinal ROM between studies may be attributable to differences in head and arm positions between studies, or to not controlling these positions while participants performed the experimental tasks. These findings underscore the necessity of standardizing the positions used to elicit maximum voluntary ROM angles, or at the very least ensuring that care is taken to standardize positions between participants within the same study, and to specify the positions used during data reporting.

Previous work has shown relationships between the thoracic spine and neck slope ($r=-0.41$) and between the thoracic spine and upper-cervical spine ($r=0.32$) during standing (Kuo et al., 2009). Relationships have also been identified in the timing of cervical and upper-thoracic motion; cross-correlation coefficients of 0.965, 0.902, and 0.946 were reported by Tsang et al. (2013) for neck flexion-extension, rotation (twisting), and lateral bending, respectively. These same authors also noted considerable contributions of the thoracic spine to neck motion (Tsang et al., 2013). These

relationships suggest that movements of the head affect cervical and thoracic angles, and the present data agree in that the upper regions (head, cervico-thoracic, thoracic, upper-thoracic, mid-thoracic, and lower-thoracic) generally produced the greatest angles with the active head position in all three movement tasks. The only exception was the mid-thoracic measure in MaxTwist in males, in which greater angles were found for the neutral head position. However, as this region is more removed from the head, it is likely that the influence of head position is less compared to some of the more proximal regions, such as cervico-thoracic or upper-thoracic.

Conversely, for the lower regions, head position generally either did not influence the maximum values (lumbar, trunk), or greater values were found with a neutral head position (pelvis in MaxBend). The exception to this was the lumbar angle in females during MaxTwist, in that when the arms were loose at the sides, the active head position produced greater values, although the mean difference was less than 1.0° . The overall trends of no effect or greater values in a neutral head position for the lumbar, trunk, and pelvis angles may be attributable to the structure of the spinal connective tissues, specifically the ligaments and muscle tissue. The anterior and posterior longitudinal ligaments originate at attachment points on the skull and traverse the length of the spine to the sacrum and coccyx, respectively (White & Panjabi, 1990). Likewise, although in discontinuous bundles, the paraspinal muscles span the entire length of the spine from the occipital bone (spinalis capitis, semispinalis capitis) to the pelvis (iliocostalis lumborum) (Tortora, 2005). Assuming the ligaments and muscles can only deform to a certain length, the active head position would require a greater proportion of the available

deformation to accommodate the flexed, bent, or twisted head, concurrently reducing the maximum angle that could be elicited at the pelvis. Therefore, a neutral head position would enable a greater proportion of the deformation to be allocated to the pelvis.

While the head positions eliciting maximal angle measures were relatively consistent across movement tasks, arm positions were more variable depending upon the task. In MaxFlex, collapsed across all measures, loose arms tended to elicit greater angles. With the arms hanging to the floor, the mass of the arms (approximately 10% of body weight when combined (Winter, 2005)) is distributed further away from the body's center of mass than if the arms were crossed, thereby creating a greater moment around the axis of rotation (i.e. the hip joints) and contributing to a greater amount of trunk flexion. Alternatively, the loose arm position may have had a psychological effect in which participants subconsciously reached for the floor, thereby leading to greater angle measures. While it is intuitive that the same pattern would hold for MaxBend, the opposite was true for the upper regions (head, cervico-thoracic, thoracic, upper-thoracic, mid-thoracic, and lower-thoracic), in that greater angles were elicited from the crossed arm position. This position may have led participants to tuck the shoulder in the direction of the rib cage, enabling bending to a greater extent in the upper segments. Conversely, loose arms facilitated greater angles in the lower regions (lumbar, trunk, pelvis) in MaxBend. This effect could have resulted from the same mechanisms proposed for MaxFlex, of either a greater moment around the trunk due to the mass of the arms, or of participants subconsciously reaching for the floor. Finally, in MaxTwist, abducted arms tended to produce greater angles for the majority of regions (thoracic, upper-thoracic,

mid-thoracic, trunk, and pelvis), with the exception of lower-thoracic (crossed). This may be due to the nature of the twisting movement, in that the loose arm position constrained the twisting movement more than the abducted or crossed positions, which involved arm abduction and elevation, respectively, to 90°. Further, with the abducted arm position, participants tended to depress and retract the shoulder ipsilateral to the direction of movement, as opposed to the crossed arm position which tended to promote protraction of the shoulder through arm elevation in the sagittal plane. The depressed and retracted shoulder during the abducted arm position may have contributed, in part, increased rotation in the trunk during the twisting movement.

The findings of the present study are limited by several methodological considerations. All participants were asymptomatic for back pain within the previous year, in order to minimize the influence of pain status on the results. However, individuals with LBP typically exhibit lower ROM and modified movement patterns in the spine compared to healthy participants (Hidalgo et al., 2012; Mayer et al., 1984; Shum et al., 2005a, b; Wong & Lee, 2004), which may alter the effects of the positions of the head and arms in these individuals. Further, a maximum extension movement task was not included in the study due to the constraints inherent in a passive-reflective motion capture system, in that the cameras must have a direct view of the markers. As well, with the marker cluster set, an extended trunk posture would cause the marker clusters to touch or overlap, reducing the system's ability to distinguish between markers. Finally, maximum angles were only assessed during standing MaxFlex, MaxBend, and MaxTwist movement tasks, although greater maximum angles could potentially be elicited from

other body positions such as sitting (Edmondston et al., 2007a; Tsang et al., 2013) or supine (Fujimori et al., 2012), or from other functional tasks.

In conclusion, this study constituted an initial attempt to develop standardized positions during maximum ROM trials, in order to elicit maximal voluntary angles in each plane for various spinal regions. Standardized positions would be beneficial for the purposes of either comparing absolute angles during maximum trunk ROM trials, or normalizing kinematic data from other experimental tasks. For the maximum trunk ROM movement tasks assessed in the present study, the head and arm positions affected the maximum angles elicited from many of the spinal regions. The maximum angles of the upper regions were generally obtained from an active head position, while the lower regions were either not affected by head position or elicited greater angles with a neutral head. Loose and abducted arms generally produced the greatest angles for the MaxFlex and MaxTwist movement tasks, respectively, while those for MaxBend were recorded from the crossed and loose trials for the upper and lower regions, respectively. Ultimately, the choices of head and arm positions are dependent upon the spinal regions of interest. However, if it is only possible to collect one condition, the findings of the present study suggest that the optimal conditions to elicit maximum angles from the greatest number of regions would be an active head and loose arms for MaxFlex, active head and abducted arms for MaxTwist, and an active head and crossed arms for MaxBend.

CHAPTER 5

Quantification of the Trunk Part I: Which Motion Segments are Required to Sufficiently Characterize its Kinematic Behaviour?

CHAPTER 5

Quantification of the Trunk Part I: Which Motion Segments are Required to Sufficiently Characterize its Kinematic Behaviour?

Summary

Various kinematic definitions of the thoracic spine have been employed in past work. However, the segments necessary to sufficiently characterize the thoracic spine during trunk movement tasks in all three planes of motion have not yet been identified. This study aimed to determine the minimum number of segments necessary to adequately characterize the kinematics of the thoracic spine. Thirty individuals, asymptomatic for back pain, performed ten trials of maximum trunk flexion, lateral bend, and axial twist; thoracic flexion, lateral bend, and axial twist; and slumped standing. Marker clusters were applied over the C₇, T₃, T₆, T₉, T₁₂, and L₅ vertebrae. Three-dimensional angles of each cluster were calculated, and cross-correlation and correlation (r) analyses were employed to assess relationships in the motion patterns and maximum angles of adjacent clusters, respectively. The motion patterns of adjacent clusters were very strongly correlated ($R_{xy} > 0.90$ for 26 of 35 pairings), as were the maximum angles ($r > 0.80$ for 25 of 35 pairings). A four-cluster set (C₇, T₆, T₁₂, and L₅) represented quantified thoracic motion for six of the seven movement tasks tested. These results provide insight into thoracic movement coordination, with implications for predictive spinal modelling and clinical assessment practices.

5.1 Introduction

Kinematic measures are commonly-used tools in spine research, occupational settings, and clinical practice. Quantitative kinematic measures have been employed for such applications as comparing LBP patients and healthy controls (Esola et al., 1996; Marras et al., 1999) and assessing low back injury risk in occupational tasks (Marras et al., 1993a), while qualitative measures have utility for clinical assessments of LBP patients. The thoracolumbar and lumbar spine regions have been extensively characterized in terms of ROM, motion patterns, and resulting loading patterns during various postures, movements, and tasks (for example, Alexander et al., 2007; Callaghan & McGill, 2001; Drake & Callaghan, 2008; Lee & Wong, 2002; Percy & Tibrewal, 1984; Wong & Lee, 2004). The angle of lumbar lordosis, or relative orientation of the rib cage and pelvis, is also commonly employed as an input for predictive spine loading models (for example, Cholewicki & McGill, 1996). Emphasis has been placed on the lumbar spine due to its high injury incidence (Waters et al., 1993). Less research has been directed towards the thoracic spine, due to anatomical complexity and a lower incidence of injury (Briggs et al., 2007; Edmondston & Singer, 1997). Further, interactions between the thoracic and lumbar spine regions have not been well studied, even though the thoracic spine may substantially influence the lumbar spine through the potential for the thoracic spine to be a source of local and referred pain, and thoracic contributions to overall spinal posture and movement patterns in the lumbar spine, cervical spine, and shoulder girdle (Edmondston & Singer, 1997).

In addition to the potential influences of the thoracic spine on the lumbar spine and LBP (Edmondston & Singer, 1997), a better understanding of thoracic behaviours is crucial to address the issue of thoracic pain. Briggs et al. (2009) conducted a literature review of 52 studies of various occupational groups. Their results indicated that the one-year prevalence of thoracic spine pain ranged from 3-55%, with medians of around 30% for most occupational groups, suggesting that thoracic pain represents a significant occupational health problem in the general population (Briggs et al., 2009). While a limited body of literature has examined the thoracic spine, most studies focus on thoracic spine mechanical properties (Panjabi et al., 1976a, b) and ROM (Edmondston et al., 2007a, 2011b; Oda et al., 2002; Sizer et al., 2007; Willems et al., 1996), without a comprehensive investigation into movement coordination within the trunk, that is, relationships in the motion of different spinal levels. Although the thoracic spine is often considered as a single rigid segment, motion is not uniformly distributed throughout the region. Rather, flexion and lateral bend ROM tend to increase from the superior to inferior ends of the thoracic spine, while axial twist tends to be greatest in the mid-thoracic region (Willems et al., 1996). Additionally, coupling between lateral bend and axial twist vary throughout the thoracic spine (White & Panjabi, 1990). Determining the relationships in motion of different levels within the thoracic spine and trunk in general would provide insight into the kinematic data necessary to develop a predictive spine loading model incorporating the thoracic spine, and would also contribute qualitative information for use in clinical settings regarding functional motions of the spine and focal points for assessment to aid in identifying aberrant spinal motion. Therefore, a thorough

evaluation of spinal kinematics with an emphasis on the thoracic spine would be valuable and is warranted.

The characterization of motion in the thoracic spine is crucial to the investigation of mechanics in that region. The thoracic spine has been defined or partitioned in various ways in past work, which have generally been based on the anatomy of the region. For example, individual markers have been placed at specific vertebral levels on the spine, such as T₂, T₆, and T₁₀ (Edmondston et al., 2007a) or T₁, T₆, and T₁₂ (Edmondston et al., 2011b), and the resulting angle created by the three points calculated. A similar approach determines the relative angle between two clusters of markers placed at C₇ or T₁ and T₁₂ (Dunk & Callaghan, 2005; Preuss & Popovic, 2010). Other research groups have divided the thoracic spine into two (T₁–T₆, T₇–T₁₂; Johnson et al., 2010), three (T₁–T₄, T₄–T₈, and T₈–T₁₂; Willems et al., 1996), and four (C₇, T₃, T₆, and T₉; Lee et al., 2013; Preuss & Popovic, 2010) thoracic regions. A recent study (Ranavolo et al., 2013) determined the least number of single markers required to adequately measure the curvatures of the whole spine. However, to the authors' knowledge, no study to date has examined the minimum number of segments (defined by marker clusters) necessary to sufficiently characterize the thoracic spine during trunk movement tasks in all three planes of motion. Further, while previous work has described the motion of the whole spine and thoracic spine specifically, the locations at which motion should be described based on anatomical and functional evidence have not yet been established. Therefore, this study aimed to determine the set of segments necessary to sufficiently characterize the kinematics of the thoracic spine.

5.2 Methods

5.2.1 Participants

Thirty university-aged, right-hand dominant individuals (15 male, 15 female) participated in the study. Mean age, body mass, and height were 25.0 years (3.8), 1.80 m (0.05), and 79.64 kg (8.75), respectively, for the males and 22.8 years (2.7), 1.66 m (0.05), and 59.12 kg (6.38), respectively, for the females. Participants had not sought treatment for back pain, nor missed any days of school or work due to back pain, for twelve months prior to collection. All procedures were approved by the institution's Office of Research Ethics, and written informed consent was obtained from all participants prior to collection.

5.2.2 Instrumentation

Three-dimensional kinematics were collected using a Vicon MX motion capture system (Vicon Systems Ltd., Oxford, UK). Clusters of five passive-reflective markers were applied over the C₇, T₃, T₆, T₉, T₁₂, and L₅ vertebrae (determined by palpation) (Chapter 3, Section 3.2.2.1). The bases of the clusters were 2 cm in diameter. Although the C₇ and L₅ vertebrae are not located within the thoracic spine, these locations are often employed when examining the trunk as one segment. Individual markers were also placed on the head (5), trunk (4), pelvis (4), and legs (16). Surface markers have been found to introduce artefact from the movement of the soft tissue relative to the underlying bone (Heneghan & Balanos, 2010; Leardini et al., 2005). However, work addressing this issue has concluded that the motion of surface markers mounted over the spinous processes of the vertebrae is very strongly correlated to the position of the underlying

spinous processes (Morl & Blickan, 2006), likely due to the tight bonding of the overlying connective tissue to the bone (Gal et al., 1997; Lundberg, 1996). Artefact was minimized by ensuring proper adherence of the markers to the skin, and by mounting the clusters over the spinous processes. Kinematic data were sampled at 50 Hz. EMG data were also collected for eight trunk muscles bilaterally. Further information regarding EMG instrumentation, data collection procedures, and data processing can be found in Chapters 3 and 6.

5.2.3 *Procedures*

Following electrode application and EMG calibration protocols (Chapters 3 and 6), markers were applied and a kinematic calibration trial ('T-pose') was performed (upright standing, arms abducted to 90°). Participants then performed ten trials each of Upright and seven movement tasks: MaxFlex, MaxBend, and MaxTwist; slumped standing (rounding of the shoulders and back) (Slump); and thoracic flexion (ThorFlex), lateral bend (ThorBend), and axial twist (ThorTwist), in which participants were instructed to move their upper-/mid-back while maintaining a neutral, upright position in the low back to the best of their ability (Appendix A). All tasks were presented in a random order. Upright trials were each 10 seconds long. For all movement trials, participants moved to the position in a controlled manner, maintained the position for three seconds, and returned to their Upright position. All bending and twisting trials were performed to the right side. Participants were given complete instructions on all movement tasks prior to beginning the protocol, during which they were given time to practice each movement task. Prompts were also used before each trial during the

experimental protocol. A reliability analysis using intraclass correlation coefficients (ICC(3,10)) was conducted to ensure that the angle measures (see Section 5.2.4) demonstrated sufficient reliability between trials. Moderate to excellent reliability was demonstrated for all measures, with ICCs ranging from 0.70 to 0.99 and 97% of the measures yielding coefficients of 0.90 or above.

5.2.4 Data Processing and Analysis

Data were processed using Visual3D v.4 (C-Motion, Inc., Germantown, USA). The marker data were used to calculate three-dimensional angles of each spinal marker cluster relative to the laboratory coordinate system using a Cardan X-Y-Z (flexion/extension-lateral bend-axial twist) rotation sequence (Preuss & Popovic, 2010; van Dieen & Kingma, 2005) (Appendix C, Figure 29). A dual-pass, fourth-order low-pass Butterworth filter (cutoff frequency: 2.5 Hz, determined by residual analysis (Winter, 2005)) was then applied. The mean angles during Upright were determined and used to zero the angle signals from the movement trials.

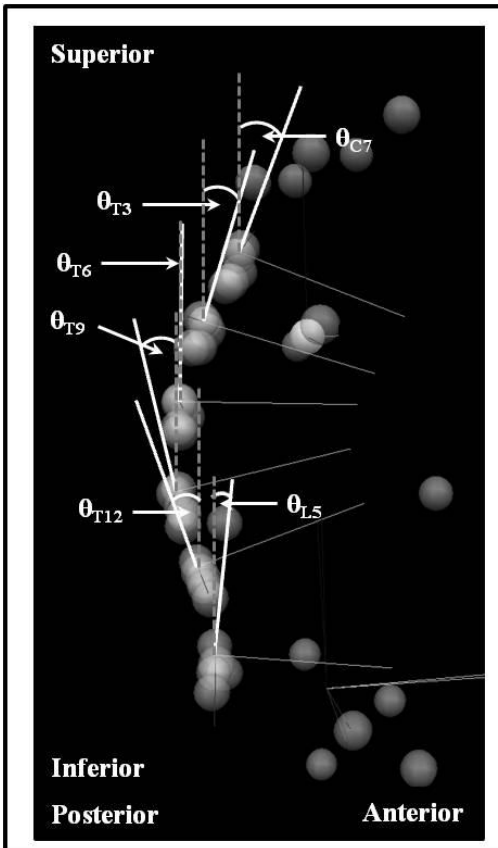


Figure 29: Collapsed 3D sagittal view of the markers representing the calculation of each angle. The angles represented in this collapsed 3D sagittal view are the equivalent of flexion-extension angles (Adapted, by permission, from: Schinkel-Ivy A, Pardisnia S, Drake JDM. Head and arm positions that elicit maximal voluntary trunk range-of-motion measures. *Journal of Applied Biomechanics* 2014 (accepted July 1, 2014). Figure 2c. © Human Kinetics, Inc.). Written copyright permission not required for self-authored work; refer to Appendix B.

For all movement trials, cross-correlations (Equation 1) were performed on the time series angle data of each possible pairing of clusters (15 in total) using a custom program written in Matlab v.R2012a (The MathWorks, Inc., Natick, USA). Cross-correlation determines the extent to which two time-varying data sets are correlated (Shum et al., 2007), to assess spatial and temporal similarities between the signals

(Nelson-Wong et al., 2009). The cross-correlation coefficient at a time lag of zero was extracted (Johnson et al., 2010), representing the strength of the relationship (Lee & Wong, 2002; Shum et al., 2005b, 2007; Wong & Lee, 2004) when the signals were aligned temporally. The mean values were then determined across the ten trials of each movement task and averaged across participants. Cross-correlation coefficients of 0.00-0.19 were considered very weak, 0.20-0.39 were considered weak, 0.40-0.59 were considered moderate (Swinscow, 1997), 0.60-0.89 were considered strong, and greater than 0.90 were considered very strong. While coefficients of 0.80 or above have been considered ‘very strong’ previously (Swinscow, 1997), given the relationship strengths in the present study, a more conservative criterion was required. Therefore, R_{xy} of 0.60–0.89 and greater than 0.90 were considered to be strong and very strong, respectively. For exemplar kinematic and cross-correlation data, please refer to Appendix D.

$$R_{xy}(\tau) = \frac{\frac{1}{T} \int_0^T x(t)y(t + \tau)dt}{\sqrt{R_{xx}(0)R_{yy}(0)}} \quad [1]$$

Where $R_{xy}(\tau)$ is the normalized cross-correlation of the two signals, $x(t)$ and $y(t)$, at a phase shift τ , with a potential range of values between ± 1 , and T is the length of the signal (Chatfield, 1984; Lee & Wong, 2002; Li & Caldwell, 1999; Nelson-Wong & Callaghan, 2010).

Further, for each segment, the maximum angles obtained in each cluster in the plane of movement during the movement trials were determined. Pearson product moment correlations between the maximum angles for each pairing of clusters were

calculated using IBM SPSS Statistics v.21 (IBM Corporation, Armonk, USA).

Significance was set at $p < 0.05$. The Pearson correlations provided an indication of the actual magnitude of the movements of each cluster, which was not accounted for by the cross-correlation technique. Pearson correlation coefficients (r) of 0.00-0.19, 0.20-0.39, 0.40-0.59, 0.60-0.79, and 0.80-1.00 were considered very weak, weak, moderate, strong, and very strong, respectively (Swinscow, 1997).

The results of the cross-correlation and Pearson correlation analyses were considered together to determine if and where there was redundancy in the clusters, and therefore identify which cluster(s) could be eliminated to reduce data collection requirements. Initially, adjacent pairings that exhibited very strong R_{xy} ($R_{xy} > 0.90$) and very strong r ($r > 0.80$) were identified, as these indicated that the motion of the two clusters was of similar magnitude, and of a strong spatial and temporal relationship. Any clusters within the thoracic spine (T_3, T_6, T_9, T_{12}) that were involved in a pairing that met the criteria were 'eliminated' one at a time, and the R_{xy} and r between the two clusters on either side of the eliminated cluster were determined. For example, if the T_3 - T_6 pairing met both the R_{xy} and r criteria (which was the case for all movement tasks (see Section 5.3)), the R_{xy} and r for the C_7 - T_6 and T_3 - T_9 pairings were examined (as if the T_3 and T_6 clusters were eliminated, respectively). The C_7 and L_5 clusters were deemed required as they represented the boundaries of recorded spinal motion, and were not evaluated for elimination. The elimination of multiple adjacent clusters was indicated if two adjacent remaining pairings both met the criteria. That is, if both the C_7 - T_6 (T_3 eliminated) and T_3 - T_9 (T_6 eliminated) pairings demonstrated very strong R_{xy} and r , then both the T_3 and

T₆ clusters were eliminated. This process was continued until the criteria were no longer met between the remaining clusters. All possible marker sets for each movement task were identified, consisting of the clusters that remained after applying the elimination criteria of very strong R_{xy} ($R_{xy}>0.90$) and very strong r ($r>0.80$). The smallest marker set that was suitable for as many of the movement tasks as possible was then determined.

5.3 Results

For the sagittal-plane movement tasks (MaxFlex, ThorFlex, Slump), the majority of cluster pairings tended to move in a very strongly correlated fashion, with mean (*SD*) cross-correlation coefficients ranging from $R_{xy}=0.91$ (0.26) to $R_{xy}=1.00$ (0.00) (Table 19). The exceptions were the T₉–T₁₂ ($R_{xy}=0.79$ (0.37)) and T₁₂–L₅ ($R_{xy}=-0.60$ (0.45)) pairings in ThorFlex and the C₇–T₃ ($R_{xy}=0.89$ (0.28)) and T₁₂–L₅ ($R_{xy}=-0.66$ (0.48)) pairings in Slump. Very strong Pearson correlations were identified between the maximum angles of the T₃ and T₆ clusters, the T₆ and T₉ clusters, and the T₉ and T₁₂ clusters for all three movement tasks, ranging from $r=0.81$ to $r=0.97$ (Tables 20 and 21). The C₇ and T₃ clusters for MaxFlex were also very strongly correlated ($r=0.84$). For MaxFlex, ThorFlex, and Slump, 4, 2, and 3 cluster pairings met the criteria for the elimination of one cluster, respectively.

Table 19: Mean (*SD*) cross-correlation coefficients (R_{xy}) at zero lag, comparing the angle time series for each adjacent pairing of clusters in each movement task. Shaded cells represent very strong cross-correlations ($R_{xy}>0.90$).

Movement Task	Cluster Pairing				
	C ₇ -T ₃	T ₃ -T ₆	T ₆ -T ₉	T ₉ -T ₁₂	T ₁₂ -L ₅
MaxFlex	0.98 (0.08)	1.00 (0.00)	1.00 (0.00)	1.00 (0.00)	0.99 (0.02)
ThorFlex	0.99 (0.01)	0.98 (0.05)	0.97 (0.05)	0.79 (0.37)	-0.60 (0.45)
Slump	0.89 (0.28)	0.99 (0.07)	0.99 (0.02)	0.91 (0.26)	-0.66 (0.48)
MaxBend	1.00 (0.00)	1.00 (0.00)	1.00 (0.00)	1.00 (0.01)	0.95 (0.15)
ThorBend	0.98 (0.04)	0.99 (0.01)	0.98 (0.04)	0.54 (0.48)	0.15 (0.48)
MaxTwist	1.00 (0.00)	1.00 (0.00)	0.97 (0.11)	0.97 (0.08)	0.95 (0.16)
ThorTwist	0.98 (0.03)	0.95 (0.12)	0.28 (0.67)	0.67 (0.33)	0.76 (0.22)

Table 20: Mean (*SD*) maximum angles for the movement tasks. Angles for MaxFlex, ThorFlex, and Slump represent rotations around the X axis; for MaxBend and ThorBend, rotations around the Y axis; and for MaxTwist and ThorTwist, rotations around the Z axis. Positive values indicate flexion, lateral bend to the right, and axial twist to the right.

Movement Task	Cluster					
	C ₇	T ₃	T ₆	T ₉	T ₁₂	L ₅
MaxFlex	138.89 (14.73)	131.11 (16.28)	126.95 (16.07)	124.81 (18.02)	118.90 (17.91)	69.37 (17.81)
ThorFlex	49.42 (11.56)	34.12 (8.89)	24.10 (8.76)	19.86 (8.41)	13.67 (7.86)	0.37 (2.12)
Slump	22.10 (10.35)	34.26 (12.21)	29.12 (11.12)	24.68 (10.40)	19.81 (10.78)	1.27 (4.89)
MaxBend	55.14 (8.86)	50.16 (6.76)	48.72 (6.58)	42.95 (6.63)	33.27 (6.46)	12.47 (4.12)
ThorBend	27.39 (6.59)	22.55 (7.03)	18.95 (6.84)	16.58 (5.51)	8.77 (5.18)	1.67 (1.10)
MaxTwist	102.96 (15.94)	86.44 (16.85)	71.12 (16.03)	54.91 (18.15)	43.27 (19.80)	50.14 (17.28)
ThorTwist	45.33 (12.21)	31.04 (10.94)	20.33 (9.37)	7.67 (8.02)	3.92 (5.61)	4.35 (5.77)

Table 21: Pearson product moment correlation coefficients (r) for the maximum angles achieved in each adjacent pairing of clusters in each movement task. Values in brackets indicate p -values. Shaded cells represent very strong correlations ($r>0.80$).

Movement Task	Cluster Pairing				
	C ₇ -T ₃	T ₃ -T ₆	T ₆ -T ₉	T ₉ -T ₁₂	T ₁₂ -L ₅
MaxFlex	0.84 (<0.001)	0.95 (<0.001)	0.97 (<0.001)	0.94 (<0.001)	0.79 (<0.001)
ThorFlex	0.70 (<0.001)	0.88 (<0.001)	0.89 (<0.001)	0.81 (<0.001)	0.03 (0.86)
Slump	0.56 (0.001)	0.91 (<0.001)	0.94 (<0.001)	0.91 (<0.001)	0.47 (0.009)
MaxBend	0.60 (<0.001)	0.89 (<0.001)	0.93 (<0.001)	0.88 (<0.001)	0.68 (<0.001)
ThorBend	0.83 (<0.001)	0.96 (<0.001)	0.97 (<0.001)	0.84 (<0.001)	0.52 (0.003)
MaxTwist	0.91 (<0.001)	0.96 (<0.001)	0.95 (<0.001)	0.93 (<0.001)	0.94 (<0.001)
ThorTwist	0.64 (<0.001)	0.87 (<0.001)	0.90 (<0.001)	0.82 (<0.001)	0.77 (<0.001)

Very strong cross-correlations were also observed for the C₇-T₃ and T₃-T₆ cluster pairings in the bending (MaxBend, ThorBend) and twisting movement tasks (MaxTwist, ThorTwist), ranging from $R_{xy}=0.95$ (0.15) to $R_{xy}=1.00$ (0.00). Similarly, the cross-correlation coefficients between the T₆-T₉, T₉-T₁₂, and T₁₂-L₅ pairings for MaxBend and MaxTwist were very strong, as was that for the T₆-T₉ pairing in ThorBend. All pairings for the bending and twisting tasks were very strongly correlated as well, ranging from $r=0.83$ to $r=0.97$, with the exceptions of C₇-T₃ in MaxBend and ThorTwist, and T₁₂-L₅ in MaxBend, ThorBend, and ThorTwist. These results indicated that 3, 2, 5, and 1 cluster pairings met the criteria for the elimination of one cluster for MaxBend, ThorBend, MaxTwist, and ThorTwist, respectively.

Instances where two adjacent clusters demonstrated motion patterns and maximum angles that were very strongly correlated ($R_{xy}>0.90$ and $r>0.80$, respectively) indicated that there was redundancy in the pairing, and one of the clusters in the pairing was unnecessary for quantifying the three-dimensional motion of the thoracic spine. The number of cluster pairings meeting these criteria ranged from 1 (ThorTwist) to 5 (MaxTwist) (Table 22). For MaxFlex, Slump, and MaxTwist, multiple adjacent pairings met the criteria, and therefore the removal of multiple clusters was possible for those movement tasks (Table 23). All possible marker sets for each movement task were identified, consisting of the clusters that remained after applying the elimination criteria (Table 24). From these movement task-specific sets, the four-cluster set containing the C₇, T₆, T₁₂, and L₅ clusters was identified as the set with the least number of marker clusters that would be sufficient for the greatest number of movement tasks (Figure 30). The only movement task for which this cluster set was not sufficient was ThorTwist, which required an additional cluster at T₉.

Table 22: Adjacent cluster pairings that met the criteria of very strong cross-correlations ($R_{xy}>0.90$) and very strong Pearson correlations ($r>0.80$) for each movement task, indicating that one of the clusters could be eliminated.

MaxFlex	ThorFlex	Slump	MaxBend	ThorBend	MaxTwist	ThorTwist
C ₇ -T ₃					C ₇ -T ₃	
T ₃ -T ₆	T ₃ -T ₆	T ₃ -T ₆	T ₃ -T ₆	T ₃ -T ₆	T ₃ -T ₆	T ₃ -T ₆
T ₆ -T ₉	T ₆ -T ₉	T ₆ -T ₉	T ₆ -T ₉	T ₆ -T ₉	T ₆ -T ₉	
T ₉ -T ₁₂		T ₉ -T ₁₂	T ₉ -T ₁₂		T ₉ -T ₁₂	
					T ₁₂ -L ₅	

Table 23: To determine whether multiple adjacent clusters could be eliminated, the clusters that were involved in the adjacent pairings that initially met the criteria ($R_{xy}>0.90$, $r>0.80$) were eliminated one at a time, and the R_{xy} and r between the two clusters on either side of the eliminated cluster were determined. Shaded cells represent pairings spanning the gap where a cluster was removed that met the criteria for elimination. If two adjacent remaining pairings both met the criteria ($R_{xy}>0.90$, $r>0.80$), multiple clusters could potentially be eliminated (bottom half of table).

Movement Task	Eliminated Cluster	Remaining Cluster Pairing	Mean (<i>SD</i>) R_{xy}	r (p -value)
<i>One Cluster Eliminated</i>				
MaxFlex	T ₃	C ₇ -T ₆	0.84 (0.42)	0.85 (<0.001)
	T ₆	T ₃ -T ₉	1.00 (0.00)	0.90 (<0.001)
	T ₉	T ₆ -T ₁₂	1.00 (0.00)	0.94 (<0.001)
	T ₁₂	T ₉ -L ₅	0.99 (0.03)	0.72 (<0.001)
ThorFlex	T ₃	C ₇ -T ₆	0.96 (0.07)	0.69 (<0.001)
	T ₆	T ₃ -T ₉	0.93 (0.14)	0.71 (<0.001)
	T ₉	T ₆ -T ₁₂	0.75 (0.42)	0.83 (<0.001)
Slump	T ₃	C ₇ -T ₆	0.88 (0.31)	0.35 (0.055)
	T ₆	T ₃ -T ₉	0.97 (0.09)	0.80 (<0.001)
	T ₉	T ₆ -T ₁₂	0.90 (0.26)	0.88 (<0.001)
	T ₁₂	T ₉ -L ₅	-0.75 (0.44)	0.40 (0.03)
MaxBend	T ₃	C ₇ -T ₆	0.99 (0.01)	0.64 (<0.001)
	T ₆	T ₃ -T ₉	1.00 (0.00)	0.76 (<0.001)
	T ₉	T ₆ -T ₁₂	0.99 (0.01)	0.85 (<0.001)
	T ₁₂	T ₉ -L ₅	0.94 (0.16)	0.70 (<0.001)
ThorBend	T ₃	C ₇ -T ₆	0.97 (0.05)	0.79 (<0.001)
	T ₆	T ₃ -T ₉	0.97 (0.06)	0.91 (<0.001)
	T ₉	T ₆ -T ₁₂	0.49 (0.53)	0.84 (<0.001)
MaxTwist	T ₃	C ₇ -T ₆	0.99 (0.01)	0.90 (<0.001)
	T ₆	T ₃ -T ₉	0.96 (0.13)	0.91 (<0.001)
	T ₉	T ₆ -T ₁₂	0.92 (0.24)	0.90 (<0.001)
	T ₁₂	T ₉ -L ₅	0.98 (0.09)	0.93 (<0.001)
ThorTwist	T ₃	C ₇ -T ₆	0.88 (0.25)	0.49 (0.006)
	T ₆	T ₃ -T ₉	0.17 (0.70)	0.76 (<0.001)
<i>Multiple Clusters Eliminated</i>				
MaxFlex	T ₆ , T ₉	T ₃ -T ₁₂	1.00 (0.00)	0.88 (<0.001)
Slump	T ₆ , T ₉	T ₃ -T ₁₂	0.88 (0.29)	0.69 (<0.001)
MaxTwist	T ₃ , T ₆	C ₇ -T ₉	0.95 (0.15)	0.82 (<0.001)
	T ₆ , T ₉	T ₃ -T ₁₂	0.90 (0.26)	0.91 (<0.001)
	T ₉ , T ₁₂	T ₆ -L ₅	0.98 (0.08)	0.94 (<0.001)
	T ₃ , T ₆ , T ₉	C ₇ -T ₁₂	0.89 (0.28)	0.80 (<0.001)
	T ₆ , T ₉ , T ₁₂	T ₃ -L ₅	0.97 (0.08)	0.95 (<0.001)

Table 24: All identified marker sets for each movement task, consisting of the clusters that remained after applying the elimination criteria of very strong R_{xy} ($R_{xy}>0.90$) and very strong r ($r>0.80$).

Movement Task	Potential Marker Sets	Eliminated Clusters	Remaining Representative Clusters	
MaxFlex	C ₇ -T ₃ -T ₆ -T ₉ -L ₅	T ₁₂	T ₉	
	C ₇ -T ₃ -T ₆ -T ₁₂ -L ₅	T ₉	T ₆ , T ₁₂	
	C ₇ -T ₃ -T ₉ -T ₁₂ -L ₅	T ₆	T ₃ , T ₉	
	C ₇ -T ₆ -T ₉ -T ₁₂ -L ₅	T ₃	C ₇ , T ₆	
	C ₇ -T ₃ -T ₉ -L ₅	T ₆	T ₃ , T ₉	
		T ₁₂	T ₉	
	C ₇ -T ₃ -T ₁₂ -L ₅	T ₆	T ₃	
		T ₉	T ₁₂	
	C ₇ -T ₆ -T ₉ -L ₅	T ₃	C ₇ , T ₆	
		T ₁₂	T ₉	
	C ₇ -T ₆ -T ₁₂ -L ₅	T ₃	C ₇ , T ₆	
		T ₉	T ₆ , T ₁₂	
	ThorFlex	C ₇ -T ₃ -T ₆ -T ₁₂ -L ₅	T ₉	T ₆
		C ₇ -T ₃ -T ₉ -T ₁₂ -L ₅	T ₆	T ₃ , T ₉
C ₇ -T ₆ -T ₉ -T ₁₂ -L ₅		T ₃	T ₆	
C ₇ -T ₆ -T ₁₂ -L ₅		T ₃	T ₆	
Slump		T ₉	T ₆	
	C ₇ -T ₃ -T ₆ -T ₉ -L ₅	T ₁₂	T ₉	
	C ₇ -T ₃ -T ₆ -T ₁₂ -L ₅	T ₉	T ₆ , T ₁₂	
	C ₇ -T ₃ -T ₉ -T ₁₂ -L ₅	T ₆	T ₃ , T ₉	
	C ₇ -T ₆ -T ₉ -T ₁₂ -L ₅	T ₃	T ₆	
	C ₇ -T ₃ -T ₉ -L ₅	T ₆	T ₃ , T ₉	
		T ₁₂	T ₉	
	C ₇ -T ₃ -T ₁₂ -L ₅	T ₆	T ₃	
		T ₉	T ₁₂	
	C ₇ -T ₆ -T ₉ -L ₅	T ₃	T ₆	
		T ₁₂	T ₉	
C ₇ -T ₆ -T ₁₂ -L ₅	T ₃	T ₆		
	T ₉	T ₆ , T ₁₂		

Table 24 (cont.): All identified marker sets for each movement task, consisting of the clusters that remained after applying the elimination criteria of very strong R_{xy} ($R_{xy}>0.90$) and very strong r ($r>0.80$).

Movement Task	Potential Marker Sets	Eliminated Clusters	Remaining Representative Clusters
MaxBend	C ₇ -T ₃ -T ₆ -T ₉ -L ₅	T ₁₂	T ₉
	C ₇ -T ₃ -T ₆ -T ₁₂ -L ₅	T ₉	T ₆ , T ₁₂
	C ₇ -T ₃ -T ₉ -T ₁₂ -L ₅	T ₆	T ₃ , T ₉
	C ₇ -T ₆ -T ₉ -T ₁₂ -L ₅	T ₃	T ₆
	C ₇ -T ₃ -T ₉ -L ₅	T ₆	T ₃ , T ₉
		T ₁₂	T ₉
	C ₇ -T ₆ -T ₉ -L ₅	T ₃	T ₆
		T ₁₂	T ₉
	C ₇ -T ₆ -T ₁₂ -L ₅	T ₃	T ₆
		T ₉	T ₆ , T ₁₂
ThorBend	C ₇ -T ₃ -T ₆ -T ₁₂ -L ₅	T ₉	T ₆
	C ₇ -T ₃ -T ₉ -T ₁₂ -L ₅	T ₆	T ₃ , T ₉
	C ₇ -T ₆ -T ₉ -T ₁₂ -L ₅	T ₃	T ₆
	C ₇ -T ₆ -T ₁₂ -L ₅	T ₃	T ₆
		T ₉	T ₆

Table 24 (cont.): All identified marker sets for each movement task, consisting of the clusters that remained after applying the elimination criteria of very strong R_{xy} ($R_{xy}>0.90$) and very strong r ($r>0.80$).

Movement Task	Potential Marker Sets	Eliminated Clusters	Remaining Representative Clusters
MaxTwist	$C_7-T_3-T_6-T_9-L_5$	T_{12}	T_9, L_5
	$C_7-T_3-T_6-T_{12}-L_5$	T_9	T_6, T_{12}
	$C_7-T_3-T_9-T_{12}-L_5$	T_6	T_3, T_9
	$C_7-T_6-T_9-T_{12}-L_5$	T_3	C_7, T_6
	$C_7-T_3-T_9-L_5$	T_6	T_3, T_9
		T_{12}	T_9, L_5
	$C_7-T_3-T_{12}-L_5$	T_6	T_3
		T_9	T_{12}
	$C_7-T_6-T_9-L_5$	T_3	C_7, T_6
		T_{12}	T_9, L_5
	$C_7-T_6-T_{12}-L_5$	T_3	C_7, T_6
		T_9	T_6, T_{12}
	$C_7-T_3-L_5$	T_6	T_3
		T_9	T_3
	$C_7-T_6-L_5$	T_{12}	L_5
		T_3	C_7, T_6
		T_9	T_6
		T_{12}	L_5
	$C_7-T_9-L_5$	T_3	C_7
		T_6	T_9
$C_7-T_{12}-L_5$	T_{12}	L_5	
	T_3	C_7	
	T_6	C_7, T_{12}	
ThorTwist	$C_7-T_3-T_9-T_{12}-L_5$	T_9	T_{12}
		T_6	T_3
	$C_7-T_6-T_9-T_{12}-L_5$	T_3	T_6

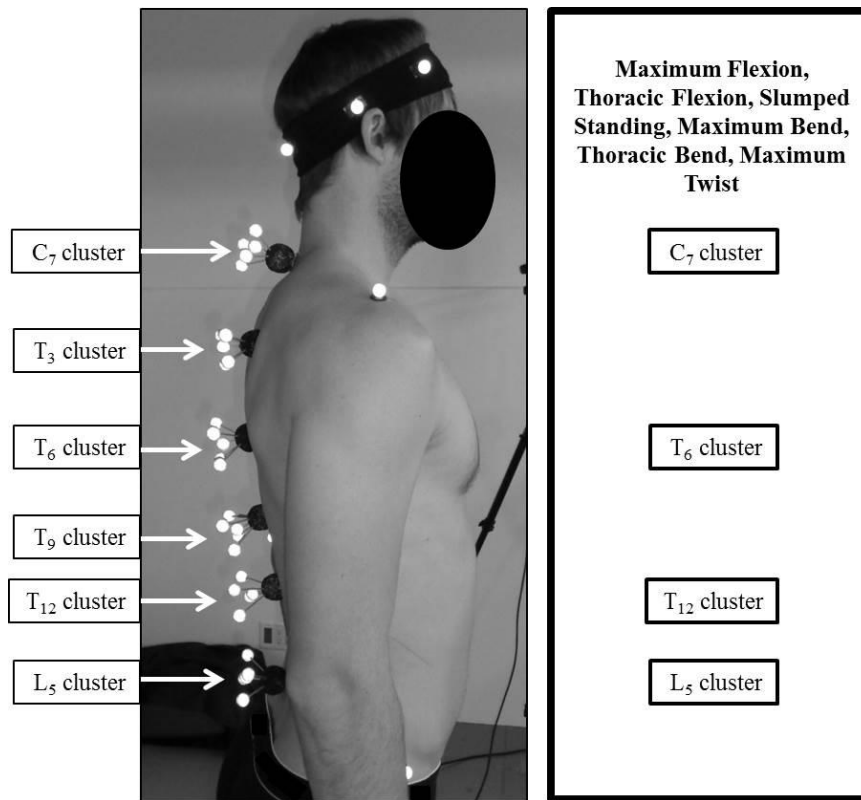


Figure 30: The final marker set recommendation that was appropriate for the greatest number of movement tasks (6 of 7) (Adapted from: Schinkel-Ivy A, Drake JDM.

Quantification of the trunk: Which motion segments are required to sufficiently characterize its kinematic behaviour? *Journal of Electromyography and Kinesiology* (in review, manuscript ID JEK-D-14-00129.R1). Figure 1). Written copyright permission not required for self-authored work; refer to Appendix B.

5.4 Discussion

The results of the present study indicated that for most of the movement tasks tested (MaxFlex, ThorFlex, Slump, MaxBend, ThorBend, and MaxTwist), a marker set consisting of four clusters at C₇, T₆, T₁₂, and L₅ provided a trade-off between feasibility of instrumentation and data processing, and the ability to capture the necessary information relating to thoracic motion. These findings provide insight into the relationships in

regional motion within the thoracic spine and between the thoracic and lumbar spine regions, as well as best practices recommendations for measuring thoracic motion. As the motion of the L₅ cluster was not strongly related to motion in the thoracic spine (including the next adjacent cluster, T₁₂), this suggests that the thoracic spine should be considered as its own separate entity. These results also have implications for modeling with respect to kinematic data that should be incorporated into predictive joint loading models, posture-matching-based approaches, and digital human modeling, and provide qualitative information regarding functional spine motion for use in clinical assessments.

The maximal spinal ROM values exhibited in the present study were comparable to previously reported values (Edmondston et al., 2007a; Peach et al., 1998; Tojima et al., 2013; Tsang et al., 2013; Van Herp et al., 2000; Willems et al., 1996). Discrepancies between the present results and past literature may be attributable to differences in data collection (for example, using an active head position in which the head was moved in the direction of trunk motion, compared to a neutral head position (Schinkel-Ivy et al., 2014)) and data processing (for example, in the present study, angles were measured with respect to the laboratory coordinate system, as opposed to relative angles calculated between two segments). Absolute angles were selected as opposed to relative angles because of the potential for artificial inflation of the cross-correlation and Pearson correlation results, since two adjacent relative angles would be utilizing data from the same cluster. Standardized instructions regarding head and arm positions were employed to control for effects of the movement of these segments on the movement of the spinal segments (Schinkel-Ivy et al., 2014). Participants were also given identical prompts prior to each

trial to ensure consistent performance within- and between- participants. A reliability analysis (ICC(3,10)) of the angle measures confirmed that each measure demonstrated good to excellent reliability. ICCs ranged from 0.70 to 0.99 and all but two measures resulted in ICCs of greater than 0.90, indicating that the trials were performed in a consistent manner throughout the protocol.

Cross-correlation techniques have previously been applied to kinematic data to examine coordination between body segments during various tasks. Tsang et al. (2013) reported cross-correlation results relating cervical and upper-thoracic movements during neck flexion, extension, lateral bend, and axial twist. Coordination between the lumbar spine and hip has also been assessed during activities of daily living (Shum et al., 2005b, 2007), and trunk flexion, extension, lateral bend, and axial twist (Lee & Wong, 2002; Wong & Lee, 2004). Further, Johnson et al. (2010) cross-correlated the motion of various trunk regions during sit-to-stand movements. Reported cross-correlation coefficients have ranged from $R_{xy}=0.53$ (lumbar and right hip lateral bend angles; Lee & Wong, 2002) to $R_{xy}=0.99$ (lumbar and hip flexion angles; Shum et al., 2007). The majority of these studies have used cross-correlation to relate the movements of distinctive anatomical regions (for example, lumbar spine and hip). However, to the authors' knowledge, it has not been used to examine the relationships between smaller regions within the spine.

As very strong cross-correlations have been identified between the global spine regions (Johnson et al., 2010; Lee & Wong, 2002; Shum et al., 2005b, 2007; Tsang et al., 2013; Wong & Lee, 2004), it is intuitive that smaller regions representing the movement of fewer vertebrae would also be strongly related. This was confirmed in the cross-

correlation coefficients for the movement tasks. Of the 35 initial cross-correlations performed between adjacent clusters for the movement tasks, 26 (74%) resulted in coefficients of $R_{xy} > 0.90$, with the majority of remaining coefficients equal to or greater than 0.50 (either positive or negative). Although this was likely due in part to the design of the movement tasks, the present results provide evidence of very strong relationships in the temporal characteristics of the motion of the clusters. Further, of the 35 Pearson correlations calculated for the maximum angles in each pairing of clusters, 25 (71%) of the coefficients were classified as very strong ($r > 0.80$), indicating that the magnitude of the maximum angles obtained were also closely related. While the strengths of the Pearson correlations were generally slightly lower than those of the cross-correlations, this was likely due to the nature of Pearson correlation analyses in which two single data points for each participant were analyzed, as opposed to cross-correlation analysis, which analyzed the similarities in motion patterns over a time series of data points.

A marker set with clusters at the C₇, T₆, T₁₂, and L₅ spinous processes was sufficient to characterize motion in six of the seven tested movement tasks (MaxFlex, ThorFlex, Slump, MaxBend, ThorBend, and MaxTwist). The identified marker cluster locations corresponded approximately with locations of anatomical significance, in that three of the clusters (C₇, T₁₂, and L₅) demarcated the bounds of the thoracic and lumbar spine regions. Further, the fourth cluster (T₆) was located around the apex of the thoracic kyphotic curve. On the surface, these results differed somewhat from those of Ranavolo et al. (2013), who determined that for individual markers along the spine, 9- and 10-marker sets showed the greatest number of valid marker configurations. For the cervical–

upper-thoracic region (C₆-T₄), the most common triads of markers were C₇-T₂-T₃ and C₆-T₁-T₃; for the lower-thoracic region (T₅-T₁₂), T₅-T₇-T₈ and T₅-T₆-T₈; and for the lumbosacral region (L₁-S₁), L₁-L₃-L₅ (Ranavolo et al., 2013). While the exact vertebrae differed slightly from those of the present study, the general landmarks are very similar, indicating that these approximate areas of the spine are critical for accurately measuring spinal posture and motion. That the marker sets recommended by Ranavolo et al. (2013) were obtained for the purpose of characterizing spinal curvature, and that single markers were used as opposed to marker clusters, may account for specific differences between recommended marker locations.

MaxTwist was the only movement task in which three clusters were sufficient to quantify motion (C₇, any thoracic vertebra, and L₅). That the primary motion of the thoracic spine is axial twist (Lee et al., 2005) may have contributed to this finding. Conversely, one extra cluster was required for ThorTwist in addition to the four-cluster marker set (C₇, T₆, T₁₂, and L₅ spinous processes) identified for the majority of movement tasks, which is likely warranted to use for collection as the mean differences between T₉ and the adjacent clusters (T₆/T₁₂) were relatively large (12.66° difference between T₆ and T₉, 3.75° difference between T₉ and T₁₂). This may be attributable to the novelty of the ThorTwist movement task, in that participants focused more on the instruction to keep the low back neutral, as opposed to focusing on the twisting movement itself. Further work will be required to elucidate the mechanism of the differences in the coordination of motion in the thoracic spine during twisting movements.

As the participants of the present study comprised a relatively young, asymptomatic sample, the results may provide a baseline which could be used to compare motion characteristics of other populations in which altered spinal motion has been identified, such as older populations (McGill et al., 1999) and LBP patients (Marras et al., 1999). In the context of clinical examination, the relationships in the patterns and magnitudes of motion may be weaker or aberrant compared to asymptomatic individuals. Future work should seek to determine the extent to which the findings of the present study differ in these populations. As dynamic motion characteristics have been identified as having utility in the assessment and classification of LBP patients (Ferguson et al., 1996a, b; Marras et al., 1993b), the identification of specific regions of the spine that demonstrate deviations from the results reported in the present study, in terms of both motion patterns and magnitudes, may be valuable for clinical examination.

Several methodological concerns limit the generalizability of the results of the present study. It was not possible to place the clusters on adjacent or every second vertebra due to technical limitations of the Vicon motion capture system. This has been identified as a limitation of cluster marker sets (as opposed to individual markers) by Ranavolo et al. (2013). Additionally, spinal motion was measured using surface markers, thereby introducing artefact from the movement of the soft tissue (Heneghan & Balanos, 2010; Leardini et al., 2005). While resources were not available to directly quantify the amount of soft tissue artefact, previous work has concluded that surface markers mounted over the spinous processes of the vertebrae are very strongly correlated to the positions of the spinous processes (Morl & Blickhan, 2006), likely due to the tight bonding of the

overlying connective tissue to the bone (Gal et al., 1997; Lundberg, 1996). Further, during the pilot stages of the study, the clusters were visually observed to be minimally affected by skin movement. Finally, the strong relationships in the present study may have been due to the design of the movement tasks, and therefore are expected to be lower in functional tasks (for example, activities of daily living). The relationships in the motion of the clusters may be less consistent or weaker during functional tasks in which participants are given task-based instructions (as opposed to posture-based instructions) and are free to select the movement strategies they deem most appropriate. However, that the general landmarks or regions of interest identified in the present study are consistent with previous results (Ranavolo et al., 2013) suggests that there is potential for these marker cluster sites to hold for functional tasks as well. Future work should seek to address these limitations to determine if the recommendations in the present study apply in these scenarios.

In conclusion, the results indicated that the motion of marker clusters at different vertebral levels along the trunk and specifically the thoracic spine was very strongly correlated, and also provided insight into the interactions between the thoracic and lumbar spine regions. Based on these results, a four-cluster marker set was sufficient to represent thoracic motion for the majority (six of seven) of movement tasks examined. Motion of the L₅ cluster was not strongly related to the motion of the thoracic vertebrae, indicating that with respect to motion characteristics, the thoracic spine should be considered as a separate entity. These findings aid in identifying the kinematic data required for predictive spinal loading models incorporating the thoracic spine, and provide guidance

for clinical assessments considering qualitative movement coordination at different spinal levels to aid in the identification of aberrant spinal motion.

CHAPTER 6

Quantification of the Trunk Part II: Muscles Required to Represent Activation Characteristics During Range-of-Motion Tasks

CHAPTER 6

Quantification of the Trunk Part II: Muscles Required to Represent Activation Characteristics During Range-of-Motion Tasks

Summary

The lower-thoracic erector spinae and latissimus dorsi are often examined in relation to lumbar spine mechanics, while studies investigating cervical mechanics have measured the upper-thoracic erector spinae and/or trapezius. Few studies have examined the interactions between the thoracic and lumbar musculature. This study aimed to investigate interactions between thoracic and lumbar musculature, and to determine which superficial muscles (recorded via surface EMG) were necessary to adequately capture gross trunk muscle activation characteristics. Surface EMG was recorded for eight trunk muscles bilaterally during maximum trunk ROM movement tasks in 30 participants. Cross-correlation and Pearson correlation were used to assess similarities in activation patterns and levels between muscles. Very strong cross-correlation coefficients and significant correlations were observed for seven, four, and six muscle pairings for flexion, lateral bend, and axial twist movement tasks, respectively. Further, four muscles were consistently strongly related to at least one other muscle. Recommended muscle sets ranged from 10–14 muscles, indicating what muscles were required to characterize different sections of the trunk. These findings contribute to the understanding of trunk muscle functioning and relationships in activation characteristics in the trunk musculature. The results may have implications for the modeling of the thoracic and lumbar spine regions. Further work should determine the best strategies for incorporating the recommended muscle sets into predictive loading models.

6.1 Introduction

Studies employing surface EMG to evaluate trunk muscle function are numerous throughout the literature. Various techniques may be employed during data collection and processing to examine different characteristics of the EMG signal, such as activation timing and sequencing (Nelson-Wong et al., 2012, 2013) and changes with fatigue (Beneck et al., 2013). Further, it has been established that EMG variables can be used to distinguish between healthy individuals and individuals with low back pain (Nelson-Wong & Callaghan, 2010; Watson et al., 1997). As a result of the insight provided by the EMG signal into various physiological processes (De Luca, 1997) and the potential relationships to injury in the lumbar spine, the lumbar musculature has been extensively researched with respect to many of these characteristics.

With the traditional focus on the lumbar musculature in spine biomechanics research, there is a relative paucity of work relating to muscle activation patterns and levels in the thoracic spine. However, the thoracic spine may exert substantial influence over postures and motion patterns in the whole spine and in the cervical and lumbar spine regions (Edmondston & Singer, 1997). Further, thoracic spine pain has been identified as a substantial occupational health problem in the general population by Briggs et al. (2009), who concluded that the median one-year prevalence for thoracic spine pain was approximately 30% for the occupational groups studied. As muscle activation differences have been observed between individuals with LBP and healthy participants (D'Hooge et al., 2013; Lariviere et al., 2000; Watson et al., 1997), a better understanding of thoracic activation characteristics is crucial to understanding pain and injury mechanisms in the

whole spine, as well as the thoracic spine specifically. While muscle activation in the lumbar spine is commonly characterized by the EO, IO, lumbar ES, and RA, there has been less standardization of muscles needed to capture the activation characteristics of the thoracic spine.

Past work has documented activation levels in several muscles in the thoracic spine, such as the LD (Drake et al., 2006; McGill, 1991) and lower-thoracic ES (Drake et al., 2006; McGill, 1991; Nelson-Wong & Callaghan, 2010), both often characterized at the T₉ level. These muscles are often examined in relation to lumbar spine mechanics. Conversely, for studies with a focus on the mechanics of the cervical or cervico-thoracic spine, activation levels have been recorded for the TR muscle between the C₇ spinous process and the acromion (Burnett et al., 2009; Caneiro et al., 2010), and for the thoracic ES musculature at the T₄ level (upper-thoracic ES; Burnett et al., 2009; Caneiro et al., 2010; Edmondston et al., 2011a). The majority of studies incorporating the musculature of the upper- and mid-back have focused on one to two of these four muscles, with little work done to integrate multiple muscles within the thoracic musculature itself, or across the thoracic and lumbar spine regions. Nairn et al. (2013a, b) and Schinkel-Ivy et al. (2013) presented three such studies, investigating activation levels of the surface trunk musculature during short-duration slumped sitting (Nairn et al., 2013b) and prolonged sitting (Nairn et al., 2013a), and co-contraction between the various muscles of the trunk during prolonged sitting (Schinkel-Ivy et al., 2013). In these studies, the bilateral LD (T₉), lower-thoracic ES (T₉), and upper-thoracic ES (T₄) activation levels were measured along with the EO, IO, lumbar ES (L₃), and RA muscles. However, whether it is

necessary to evaluate all of these muscles to properly represent the muscle activation characteristics of the thoracic spine along with the lumbar spine remains to be determined. A reduction in the number of muscles required would reduce the instrumentation necessary to quantify gross trunk muscle activation characteristics, thereby increasing portability of the system, or enabling the collection of additional muscles.

EMG recordings can also be used to provide insight into spinal loading variables through predictive modeling techniques (Cholewicki & McGill, 1996; Granata & Marras, 2000). While the relationship between muscle activation and muscle force is highly complex, muscle activation variables may be integrated into spine loading models to improve the realism of the model outputs. For example, the model presented by Granata and Marras (1993) included surface EMG measurements of the EO, IO, LD, lumbar ES, and RA. Alternatively, the lower-thoracic portion of ES has also been incorporated into spinal loading models (Cholewicki & McGill, 1996; McGill & Norman, 1986), indicating a potential influence of these muscles on the lumbar spine. Existing EMG-driven models have been developed specifically for the lumbar spine. These models include subsets of the thoracic musculature and lumbar or general trunk angles, and have not yet been modified to include sufficient detail regarding the thoracic spine. The development of a model to extend to the prediction of compression and shear in the thoracic spine would also enable the investigation of loading pathways along the length of the spine (i.e. both thoracic and lumbar), as well as the relationship between loading variables and pain in the thoracic spine. While it is intuitive (given their anatomical location) that these muscles

all contribute to loading in the thoracic and/or lumbar spine, it is unknown whether all muscles are required for loading estimates, or if a subset of muscles may be sufficient.

To the authors' knowledge, there is currently no recommendation regarding which muscle groups in the thoracic spine and trunk in general should be evaluated in order to provide the most representative activation characteristics. Therefore, this study aimed to investigate the interactions between the thoracic and lumbar musculature, to better understand the behaviour of the trunk musculature, and to determine the superficial muscles that were necessary to adequately capture gross trunk muscle activation characteristics.

6.2 Methods

6.2.1 Participants

Thirty individuals (15 male, 15 female) participated in the study, with mean (*SD*) age, height, and body mass, respectively, of 25.0 years (3.8), 1.80 m (0.05), and 79.64 kg (8.75) for the males and 22.8 years (2.7), 1.66 m (0.05), and 59.12 kg (6.38) for the females. All participants were right-hand dominant and asymptomatic for low back pain in that none had sought treatment for back pain, nor missed any days of school or work due to back pain, for twelve months prior to collection. All procedures were approved by the institution's Office of Research Ethics, and written informed consent was obtained from all participants prior to collection.

6.2.2 Instrumentation

Pairs of Ag/Ag-Cl electrodes (Ambu® Blue Sensor N, Ambu A/S, Denmark) were applied bilaterally over the bellies of the muscles of interest: EO, IO, LD, lumbar ES, lower-thoracic ES, RA (Drake et al., 2006; McGill, 1991; Mirka & Marras, 1993; Nairn & Drake, 2014; Nelson-Wong & Callaghan, 2010; Schinkel-Ivy et al., 2013), TR (Burnett et al., 2009; Caneiro et al., 2010; McLean, 2005), and upper-thoracic ES (Burnett et al., 2009; Caneiro et al., 2010; Edmondston et al., 2011a; Nairn & Drake, 2014; Schinkel-Ivy et al., 2013) (see Chapter 3, Section 3.2.2.2). Morris et al. (1962) acknowledged that the ES muscles are usually pooled together into functional groupings due to the difficulties in identifying individual muscles through surface landmarks and palpation. Therefore, the ES muscles were pooled by level as opposed to separated by muscle (i.e. iliocostalis thoracis versus longissimus thoracis). Through an assessment of the muscle activities of various individual components of the ES, Morris et al. (1962) concluded that although the investigated muscles did not always exhibit identical activity, the total activity of the muscles as a group was consistent across participants. EMG signals were differentially amplified (frequency response 10-1000 Hz, common mode rejection 115 dB at 60 Hz, input impedance 10 G Ω ; model AMT-8, Bortec, Calgary, Canada) and sampled at 2400 Hz (Vicon MX, Vicon Systems Ltd., Oxford, UK). Three-dimensional kinematics were also collected using a seven-camera Vicon MX motion capture system (Vicon MX, Vicon Systems Ltd., Oxford, UK). Further information regarding kinematics instrumentation, data collection procedures, and data processing can be found in Chapter 5.

6.2.3 *Procedures*

Following shaving and swabbing of electrode sites with rubbing alcohol, isometric MVC protocols were performed to elicit the maximum activation of each muscle. All protocols were performed against manual resistance provided by an investigator. For the trunk flexors, participants sat in a slightly reclined, bent-knee sit-up position at the edge of a therapy table with the arms crossed over the chest and performed maximal isometric trunk flexion, lateral bend, and axial twist against resistance (McGill, 1991, 1992). The trunk extensor MVCs entailed participants lying prone on a therapy table with the upper body cantilevered over the edge and feet restrained, and attempting to extend the trunk against resistance applied to the shoulders (McGill, 1991, 1992). For the LD MVC, participants abducted the arm to 90°, flexed the elbow to 90°, and externally rotated so the forearm was in an almost-vertical position. Participants then pulled their elbow downwards and backwards against resistance applied under the elbow (Arlotta et al., 2011). To elicit the TR MVC, participants abducted the arm to 90° and attempted to continue abducting the arm past this angle against resistance applied to the lateral aspect of the elbow (McLean, 2005). MVC trials lasted 3-5 seconds, with verbal encouragement provided by an investigator. Three trials were performed for each protocol, with rest between trials to minimize the effect of fatigue. The maximum value of the three trials was designated the MVC for that muscle (see Section 6.2.4).

Participants then performed ten trials of upright standing (used for kinematic calibration in Chapter 5) and seven movement tasks: MaxFlex, MaxBend, and MaxTwist; ThorFlex, ThorBend, and ThorTwist; and Slump. For the maximum trunk ROM tasks,

participants crossed the arms over the chest. The trial consisted of head movement followed by trunk movement in a smooth, continuous motion. The thoracic movement tasks entailed participants moving their head and thoracic spine while maintaining a neutral, upright position in the lumbar spine as much as possible. Bending and twisting trials were performed to the right side, and trials were presented in a random order. All movement trials lasted approximately 10 seconds, during which participants moved to the position in a controlled manner, held the position for 3 seconds, and moved back to upright standing. Participants received full instructions and time to practice the tasks prior to beginning the protocol, as well as brief prompts prior to each trial.

6.2.4 Data Processing and Analysis

Data were processed using Visual3D v.4 (C-Motion, Inc., Germantown, USA). Data were high-pass filtered using a fourth-order, dual-pass Butterworth filter (cutoff frequency: 30 Hz (Drake & Callaghan, 2006)), full-wave rectified, and low-pass filtered using a fourth-order, dual-pass Butterworth filter (cutoff frequency: 2.5 Hz (Brereton & McGill, 1998; van Dieen & Kingma, 2005)). The maximum value of any of the three MVC trials (see Section 6.2.3) was designated the MVC for that muscle. The signals from the movement tasks were then normalized to the MVC value by dividing all samples in the signal by that value, resulting in EMG data expressed as %MVC.

Cross-correlation analyses (see Chapter 5, Section 5.2.4, Equation 1) were conducted on the time series activation data to examine relationships in activation patterns of all possible pairings of muscles (120 total) over the trial durations, using a custom program written in Matlab v.R2012a (The MathWorks, Inc., Natick, USA).

Cross-correlation quantifies the extent to which two sets of time-varying data sets are correlated (Shum et al., 2007), to assess spatial and temporal similarities between the signals (Nelson-Wong et al., 2009). The cross-correlation coefficient at a time lag of zero was extracted (Johnson et al., 2010), representing the strength of the relationship (Lee & Wong, 2002; Shum et al., 2005b, 2007; Wong & Lee, 2004) when the signals were aligned temporally. For each movement task, the mean values were then averaged across trials and participants. Cross-correlation coefficients of 0.00-0.19 were considered very weak, 0.20-0.39 were considered weak, 0.40-0.59 were considered moderate (Swinscow, 1997), 0.60-0.89 were considered strong, and greater than 0.90 were considered very strong. While R_{xy} of 0.80 or above have been considered ‘very strong’ (Swinscow, 1997), a more conservative criterion was required given the strength of the relationships in the present data. Therefore, R_{xy} of 0.60–0.89 and greater than 0.90 were considered to be strong and very strong, respectively. For exemplar EMG and cross-correlation data, please refer to Appendix D.

The mean activation levels during the holding phase of the movement tasks were also determined, in order to provide an indication of the similarities in activation levels between each possible pairing of muscles. IBM SPSS Statistics v.21 (IBM Corporation, Armonk, USA) was used to calculate Pearson product moment correlations between the activation levels of each possible pairing of muscles, with significance set to $p < 0.05$.

Pairings of muscles exhibiting very strong cross-correlations ($R_{xy} > 0.90$) in activation patterns and significant Pearson correlations in activation levels ($p < 0.05$) were determined for each movement task. The pairings that met both criteria for all movement

tasks within a direction (flexion: MaxFlex, Slump, ThorFlex; bending: MaxBend, ThorBend; twisting: MaxTwist, ThorTwist) were then identified. For each of the muscles in these pairings, the mean R_{xy} and r were determined between that muscle and all other muscles (15 total) for all movement tasks in the direction of interest (flexion, bending, or twisting). The muscle of the pairing that exhibited the highest mean R_{xy} and r was selected for elimination, as its activation patterns and levels were more closely related to those of the rest of the muscles. The remaining muscles were then compiled into recommended muscle sets for the flexion, bending, and twisting movement tasks.

6.3 Results

Activation levels ranged from 5.15%MVC (left upper-thoracic ES, ThorBend) to 47.00%MVC (left EO, MaxBend) (Table 25). For the sagittal-plane movement tasks, 38, 40, and 59 of the possible muscle pairings demonstrated very strong R_{xy} in MaxFlex, Slump, and ThorFlex, respectively, with mean (*SD*) R_{xy} across all pairings of $R_{xy}=0.82$ (0.10), $R_{xy}=0.88$ (0.06), and $R_{xy}=0.90$ (0.05) (Table 26). While the mean (*SD*) r between the holding phase activation levels were substantially lower (0.12 (0.21), 0.22 (0.23), and 0.12 (0.26) for MaxFlex, Slump, and ThorFlex, respectively), a number of the pairings still demonstrated significant Pearson correlations (16, 31, and 22 pairings for MaxFlex, Slump, and ThorFlex, respectively) (Table 27). Of all possible muscle pairings for each movement task, the numbers of pairings that met both criteria ($R_{xy}>0.90$, r with $p<0.05$) for MaxFlex, Slump, and ThorFlex were 13, 26, and 14, respectively. Seven pairings

were common across all three movement tasks, indicating that there was potential for several muscles to be eliminated for the flexion movement direction.

Table 25: Mean (*SD*) activation levels obtained during the holding phase of each movement task, along with the muscles that produced the minimum and maximum activation levels. EO: external oblique; IO: internal oblique; LD: latissimus dorsi; LES: lumbar erector spinae; RA: rectus abdominis; TR: upper trapezius; UTES: upper-thoracic erector spinae.

Movement Task	Mean (<i>SD</i>) Hold Phase Activation of All Muscles	Minimum (<i>SD</i>) Activation Level (%MVC) and Muscle	Maximum (<i>SD</i>) Activation Level (%MVC) and Muscle
MaxFlex	17.00 (9.35)	8.33 (3.92); left UTES	40.13 (14.77); left LES
Slump	9.66 (2.67)	5.79 (4.68); left LD	15.08 (14.37); left RA
ThorFlex	10.63 (3.83)	5.74 (3.61); left LD	17.73 (20.39); left IO
MaxBend	15.45 (10.20)	6.75 (2.52); right UTES	47.00 (28.32); left EO
ThorBend	10.14 (5.38)	5.15 (2.90); left UTES	21.38 (19.68); left IO
MaxTwist	19.16 (11.59)	5.48 (1.91); left UTES	41.46 (23.96); right EO
ThorTwist	13.95 (9.17)	5.28 (4.40); right TR	30.90 (20.97); right UTES

Table 26: Mean (*SD*), minimum, and maximum cross-correlation coefficients (R_{xy}) for each movement task, along with the number of pairings (out of 120 total) that resulted in very strong cross-correlations ($R_{xy}>0.90$). EO: external oblique; LD: latissimus dorsi; LES: lumbar erector spinae; LTES: lower-thoracic erector spinae; RA: rectus abdominis; TR: upper trapezius; UTES: upper-thoracic erector spinae.

Movement Task	Mean (<i>SD</i>) R_{xy} of All Pairings	Minimum (<i>SD</i>) R_{xy} and Pairing	Maximum (<i>SD</i>) R_{xy} and Pairing	# $R_{xy}>0.90$
MaxFlex	0.82 (0.10)	0.57 (0.18); left LES–left RA	0.97 (0.01); left LD–right LD	38
Slump	0.88 (0.06)	0.78 (0.17); left RA–right TR	0.98 (0.01); left RA–right RA	40
ThorFlex	0.90 (0.05)	0.82 (0.13); left LTES–left RA	0.99 (0.01); left RA–right RA	59
MaxBend	0.89 (0.04)	0.75 (0.15); left EO–right LES	0.97 (0.03); left RA–right RA	54
ThorBend	0.94 (0.02)	0.89 (0.08); right LTES–right TR	0.98 (0.02); left RA–right RA	116
MaxTwist	0.91 (0.04)	0.78 (0.13); left TR–right UTES	0.99 (0.01); left RA–right RA	87
ThorTwist	0.92 (0.04)	0.78 (0.15); left TR–right UTES	0.99 (0.02); left RA–right RA	91

Table 27: Mean (*SD*), minimum, and maximum correlation coefficients (*r*) for each movement task, along with the number of pairings (out of 120 total) that resulted in significant correlations ($p < 0.05$). EO: external oblique; IO: internal oblique; LD: latissimus dorsi; LES: lumbar erector spinae; LTES: lower-thoracic erector spinae; RA: rectus abdominis; TR: upper trapezius; UTES: upper-thoracic erector spinae.

Movement Task	Mean (<i>SD</i>) <i>r</i> of All Pairings	Minimum <i>r</i> and Pairing	Maximum <i>r</i> and Pairing	# Significant Correlations
MaxFlex	0.12 (0.21)	-0.35; left IO–right TR	0.78; left LD–right LD	16
Slump	0.22 (0.23)	-0.25; left LTES–right IO	0.87; left LES–right LES	31
ThorFlex	0.12 (0.26)	-0.33; left UTES–right IO	0.83; left EO–right EO	22
MaxBend	0.10 (0.19)	-0.31; left LTES–right RA	0.61; left LES–right LES	13
ThorBend	0.20 (0.22)	-0.29; left LTES–right IO	0.73; right LTES–right UTES	30
MaxTwist	0.11 (0.20)	-0.39; left IO–right UTES	0.62; right TR–right UTES	16
ThorTwist	0.21 (0.19)	-0.26; left IO–left TR	0.76; left RA–right RA	27

The lateral bend and axial twist movement tasks tended to result in slightly higher R_{xy} and similar r to those of the sagittal-plane movement tasks. Mean (SD) R_{xy} ranged from 0.75 (0.15) (left EO–right lumbar ES, MaxBend) to 0.99 (0.01) (left RA–right RA, MaxTwist), with 54, 116, 87, and 91 of the possible muscle pairings meeting the criteria of $R_{xy}>0.90$ (very strong) for MaxBend, ThorBend, MaxTwist, and ThorTwist, respectively. In addition, for the same movement tasks, 13, 30, 16, and 27 of the possible muscle pairings produced significant Pearson correlations, with r ranging from -0.39 ($p=0.032$) (left IO–right upper-thoracic ES, MaxTwist) to 0.87 ($p<0.001$) (left lumbar ES–right lumbar ES, Slump). The numbers of pairings meeting both criteria were 7, 30, 12, and 22 for MaxBend, ThorBend, MaxTwist, and ThorTwist, respectively. Of the pairings identified for the bending tasks and the twisting tasks, 4 were common to both MaxBend and ThorBend, and 6 were common to both MaxTwist and ThorTwist. As in the flexion movement direction described above, these results indicated that there was potential for several muscles to be eliminated for the lateral bend and axial twist directions.

For each of the muscle pairings common to all movement tasks within a movement direction, the mean R_{xy} and r were determined between that muscle and all other muscles (15 total) (Table 28). The muscle of the pairing that exhibited the highest mean R_{xy} and r was then selected for elimination, as its activation patterns and levels were more closely related to those of the rest of the muscles. The remaining muscles were then compiled into recommended muscle sets (Table 29). For the flexion movement tasks, it was possible to eliminate 6 muscles, with 10 remaining in the recommended set. For the

lateral bend tasks, 3 muscles could be eliminated with 13 remaining, and for the axial twist tasks, 4 muscles could be eliminated with 12 remaining.

Table 28: For pairings that met both criteria for all movement tasks within a movement direction, each muscle within the pairing was ‘eliminated’ and the mean (*SD*) cross-correlation coefficients (R_{xy}) and correlation coefficients (r) between the eliminated muscle and all other muscles were determined. The muscle in the pairing exhibiting higher R_{xy} and r on average, indicating that muscle was more suitable for elimination (represented by shaded cells). *Although the muscles have the same or slightly lower R_{xy} and r than the other muscle in the pairing, these were selected for elimination as they were already eliminated on the basis of another pairing. EO: external oblique; IO: internal oblique; LD: latissimus dorsi; LES: lumbar erector spinae; LTES: lower-thoracic erector spinae; RA: rectus abdominis; TR: upper trapezius; UTES: upper-thoracic erector spinae.

Muscle Pairings	Eliminated Muscle	Mean (<i>SD</i>) R_{xy}	Mean (<i>SD</i>) r
<i>Flexion</i>			
Left EO–right EO	Left EO	0.89 (0.08)	0.20 (0.23)
	Right EO	0.90 (0.08)	0.20 (0.19)
Left LD–right LD	Left LD	0.90 (0.06)	0.19 (0.19)
	Right LD	0.90 (0.06)	0.15 (0.22)
Left LES–right LES	Left LES	0.82 (0.11)	0.15 (0.23)
	Right LES	0.82 (0.11)	0.14 (0.25)
Left LTES–right LTES	Left LTES	0.85 (0.05)	0.14 (0.27)
	Right LTES	0.85 (0.05)	0.16 (0.25)
Left RA–right IO	Left RA	0.87 (0.10)	0.12 (0.25)
	Right IO	0.89 (0.08)	0.15 (0.27)
Left TR–right TR	Left TR	0.82 (0.05)	0.14 (0.22)
	Right TR	0.82 (0.05)	0.15 (0.26)
Right IO–right RA	Right IO	0.89 (0.08)	0.17 (0.24)
	Right RA	0.88 (0.09)	0.15 (0.27)
<i>Lateral Bend</i>			
Left LTES–left UTES	Left LTES	0.91 (0.03)	0.08 (0.22)
	Left UTES	0.92 (0.04)	0.05 (0.19)
Left RA–right IO	Left RA	0.93 (0.03)	0.16 (0.23)
	Right IO	0.92 (0.03)	0.11 (0.20)
Left RA–right RA	Left RA*	0.93 (0.03)	0.16 (0.23)
	Right RA	0.94 (0.03)	0.17 (0.24)
Right LD–right LTES	Right LD	0.93 (0.03)	0.21 (0.21)
	Right LTES	0.90 (0.05)	0.15 (0.22)
<i>Axial Twist</i>			
Left EO–right LES	Left EO	0.92 (0.04)	0.23 (0.19)
	Right LES	0.93 (0.03)	0.26 (0.16)
Left EO–right LTES	Left EO	0.92 (0.04)	0.23 (0.19)
	Right LTES	0.90 (0.05)	0.26 (0.22)
Left LES–right IO	Left LES*	0.93 (0.03)	0.15 (0.18)
	Right IO	0.93 (0.04)	0.15 (0.18)
Left LES–right LES	Left LES	0.93 (0.03)	0.15 (0.18)
	Right LES	0.93 (0.03)	0.26 (0.16)
Left RA–right RA	Left RA	0.94 (0.03)	0.14 (0.24)
	Right RA	0.94 (0.03)	0.21 (0.21)
Right LTES–right UTES	Right LTES	0.90 (0.05)	0.26 (0.22)
	Right UTES	0.89 (0.05)	0.19 (0.23)

Table 29: Muscles that could be eliminated based on the results presented in Table 28. The muscle within each pairing that exhibited the highest mean cross-correlation coefficients (R_{xy}) and correlation coefficients (r) with all other muscles was eliminated. The remaining muscles required to capture the muscle activation characteristics of the trunk for each movement direction are also listed as Recommended Muscle Sets. EO: external oblique; IO: internal oblique; LD: latissimus dorsi; LES: lumbar erector spinae; LTES: lower-thoracic erector spinae; RA: rectus abdominis; TR: upper trapezius; UTES: upper-thoracic erector spinae.

Movement Direction	Eliminated Muscles	Recommended Muscle Sets
Flexion	Left LD, LES; right EO, IO, LTES, TR	Left EO, IO, LTES, RA, TR, UTES; right LD, LES, RA, UTES
Lateral Bend	Left LTES, RA; right LD	Left EO, IO, LD, LES, TR, UTES; right EO, IO, LES, RA, TR, UTES
Axial Twist	Left EO, LES, RA; right UTES	Left IO, LTES, TR, UTES; right EO, IO, LD, LES, LTES, RA, TR

Ideally, the same pairings of muscles with very strong R_{xy} and significant r would have been identified across all movement tasks, regardless of direction, in order to develop one recommended set of muscles common to all movement tasks. This was not the case with the present data (Tables 28 and 29). However, it is important to note that for all directions of interest, the left RA, right IO, right lower-thoracic ES, and right RA met the criteria of $R_{xy} > 0.90$ and r with $p < 0.05$ with at least one other muscle (Table 28). Therefore, a different, more generalized approach was possible in eliminating some of these muscles, although not all of the aforementioned abdominal muscles could be eliminated due to the overlap between the left RA, right IO, and right RA. This approach would result in the elimination of 2 muscles, with 14 muscles remaining.

Table 30: Muscles (column 1) that met the criteria of $R_{xy} > 0.90$ and r with $p < 0.05$ with at least one other muscle (columns 2-4) for all directions of movement (top); muscle set recommendations common to all movement directions (bottom). EO: external oblique; IO: internal oblique; LD: latissimus dorsi; LES: lumbar erector spinae; LTES: lower-thoracic erector spinae; RA: rectus abdominis; TR: upper trapezius; UTES: upper-thoracic erector spinae.

Potential Eliminated Muscle	Movement Direction		
	Flexion	Bending	Twisting
Left RA	Right IO	Right IO Right RA	Right RA
Right IO	Left RA Right RA	Left RA	Left LES
Right LTES	Left LTES	Right LD	Left EO Right UTES
Right RA	Right IO	Left RA	Left RA
Eliminated Muscles	Recommended Muscle Sets		
Left RA, right LTES	Left EO, IO, LD, LES, LTES, TR, UTES; right EO, IO, LD, LES, RA, TR, UTES		
Right IO, LTES	Left EO, IO, LD, LES, LTES, RA, TR, UTES; right EO, LD, LES, RA, TR, UTES		
Right LTES, RA	Left EO, IO, LD, LES, LTES, RA, TR, UTES; right EO, IO, LD, LES, TR, UTES		

6.4 Discussion

The present study aimed to investigate the interactions between the thoracic and lumbar musculature, to better understand the behaviour of the trunk musculature, and to determine the superficial muscles that were necessary to adequately capture the gross trunk muscle activation characteristics. The final recommended muscle sets varied substantially amongst movement task. However, several muscles were strongly correlated with at least one other muscle in all directions of movement (flexion, lateral bend, and axial twist), and therefore could be eliminated. These results provide insight into the synergy of the trunk musculature that produces trunk movements in the three

planes of motion, along with a preliminary indication of the superficial muscles that best represent the muscle activation characteristics of the trunk during these movements. A reduction in the number of muscles required would reduce the instrumentation necessary to quantify gross trunk muscle activation characteristics, thereby increasing portability of the collection system or enabling the collection of additional muscles. Further, these results can ultimately be applied to predictive joint loading models for the thoracic and lumbar spine regions, with respect to determining the best techniques by which to integrate the recommended muscle sets. These approaches may include ‘lumping’ muscles together, in that a specified muscle represents the activation of one or more other muscles, or including solely the recommended muscles identified for each task.

The cross-correlation technique has been employed previously in electromyography studies for the purposes of examining neuromuscular control and movement coordination (Nelson-Wong et al., 2012), and quantifying the extent of co-activation between two muscles (Nelson-Wong & Callaghan, 2010). As cross-correlation quantifies the extent of the similarities between two signals, it was selected as a means to identify the superficial muscles which best characterize the trunk with respect to muscle activation patterns. These results were incorporated with Pearson correlation analyses, in order to represent not only muscle activation patterns, but also the magnitude aspect of muscle activation. The activation levels reported in the present study are comparable to those previously documented in the literature (Peach et al., 1998), as are the cross-correlation results. For example, Shan et al. (2014) examined activation patterns of the bilateral lumbar ES muscles during flexion and extension, and obtained maximum cross-

correlation coefficients ranging from $R_{xy}=0.822$ to $R_{xy}=0.913$, which were within the range of values reported in the present study.

The strengths of the Pearson correlations were substantially lower than those of the cross-correlations, and were also much more variable across muscle pairings. Cross-correlations varied between $R_{xy}=0.57$ (left lumbar ES–left RA, MaxFlex) and $R_{xy}=0.99$ (left RA–right RA, MaxTwist), while Pearson correlations varied from $r=-0.39$ (left IO–right upper-thoracic ES, MaxTwist) to $r=0.87$ (left lumbar ES–right lumbar ES, Slump). This may potentially be explained by the types of inputs used for each of the analyses. Cross-correlation analyses utilize two time series of data and quantify the similarities in activation patterns over the entire time series, while Pearson correlations specifically compare two single data points for each participant. It appears that the similarities in activation characteristics between muscles are captured to a larger extent when the time-varying information is incorporated, as opposed to values averaged across a time series, which provides little indication of phase or amplitude characteristics. A limitation of the present study was the Pearson correlation criterion of a significant p -value (as opposed to a criterion relating to the r value itself, as in Chapter 5). This was necessitated by the expectation that correlations between the activation levels of different muscles would be substantially lower than between kinematic measures at different levels of the spine, due to the inherent variability of the EMG signal (German et al., 2008; Shaffer & Lauder, 1985). Although the magnitudes of the Pearson correlations were generally less than those observed in Chapter 5 for the kinematic measures, cross-correlation was also

employed as a criterion for elimination, which ensured that the eliminated muscles were strongly related to remaining muscles in terms of the timing and patterns of activation.

For the movement direction-specific recommendations, the remaining muscles for all directions constituted a mixture of abdominal and back muscles, and left and right sides. These findings indicate that multiple muscles acting on both sides of a movement are necessary to characterize any of the movement directions. Further supporting this conclusion, the majority of the cluster pairings meeting the R_{xy} and r criteria for elimination consisted of muscles performing similar actions. For symmetric movement tasks, it is intuitive that bilateral muscles activate with similar patterns and levels, and this was confirmed in the cluster pairings meeting the criteria for elimination for the flexion movement tasks (Table 26). Similar trends were observed to a lesser extent for the lateral bend and axial twist directions, with 2 of 4 (left lower-thoracic ES–left upper-thoracic ES, right LD–right lower-thoracic ES) and 3 of 6 (left EO–right lumbar ES, left EO–right lower-thoracic ES, right lower-thoracic ES–right upper-thoracic ES) pairings, respectively, representing muscles contributing to the same action. This indicated that to an extent, synergistic muscle co-contraction (i.e. concurrent activation of multiple muscles performing the same action) occurred, which aids in movement control as well as increasing spine stiffness and/or stability (Brown & McGill, 2008; Granata & Marras, 2000). These findings provide insight into the means by which the trunk musculature is recruited to accomplish movement tasks in all three planes of motion.

It is important to note that all bending and twisting tasks were performed towards the right side. Therefore, the recommendations for these muscles are specific to that

direction. Should movements to the left side be of interest, it would likely be necessary to use the muscles on the opposite side of the body from those recommended by the present results. The only instance in which both sides of a muscle were identified for elimination was the RA in the generalized recommendation, implying that recording from either the left or right RA should represent the activation characteristics of the opposite side, regardless of whether the movement is performed to the left or right side.

Although the movement direction-specific recommendations encompassed the elimination of both abdominal and back muscles, the generalized approach of identifying muscles that were strongly related to at least one other muscle for each direction of movement suggested that there were a greater number of abdominal muscles than back muscles for potential elimination (left RA, right IO, and right RA versus right lower-thoracic ES). The two approaches focused on different aspects of the relationships between the muscles, with the movement direction-specific recommendations identifying the muscles with the highest average cross-correlations and Pearson correlations, as opposed to those that were consistently present in strongly related muscle pairings across all movement directions. That the generalized approach identified a greater proportion of the abdominal muscles for elimination highlights the interrelationships amongst the activation characteristics of the abdominal musculature in all planes of movement (Thelen et al., 1995).

There were several methodological concerns that must be acknowledged regarding the present results. The participant sample consisted of young adults asymptomatic for back pain. As pain status affects EMG measures (D'Hooge et al.,

2013; Schinkel-Ivy et al., 2013; Watson et al., 1997), these results may not apply to individuals with LBP. The tasks of the present study were selected to promote a relatively consistent movement pattern. For example, the LD and TR muscles also contribute to arm movements as well as movement of the trunk (Ng et al., 2002; Tortora, 2005). Arm positions were standardized across participants, which would have minimized the influence of varied arm positions upon the results of the present study. However, future work should seek to determine whether these results generalize to ROM tasks with different arm positions, or to more functional activities with multiple movement strategies and greater involvement from both the upper and lower extremities. The cross-correlation function is such that only two signals can be included, as opposed to a global measure of activation pattern similarities incorporating various muscles. Finally, kinetic data were not collected as a part of the present study, as the necessary equipment was not available at the time of collection. These data would not necessarily have contributed to the final marker set recommendations, but instead could have enabled the evaluation of changes in estimated spinal loading as a function of the different muscle set recommendations. Potentially, a follow-up study could be conducted to determine the effects of the recommended muscle sets on estimated spinal compression and shear, compared to models incorporating all muscles or negating muscle activation. In addition, as most existing EMG-driven biomechanical models use only subsets of thoracic musculature and either lumbar or general trunk angles, a future direction of research is to incorporate the motion and muscle activation characteristics of the thoracic spine into existing biomechanical models.

While the number of required channels was not reduced substantially from the original data collection (16), the insights gained from the present study contribute to the understanding of trunk muscle functioning and relationships in activation characteristics between the musculature of the thoracic and lumbar spines. Due to the anatomical nature of the ES muscles (i.e. muscle segments that span overlapping portions of the spine) and the fact that these muscles generally perform similar functions (predominantly trunk extension (Tortora, 2005)) during a task, it is likely that there is some common drive in the innervations of these muscles, and thereby similar activation patterns. This was suggested by Morris et al. (1962) in that the overall activity of the tested ES muscles (longissimus dorsi, iliocostalis dorsi, and iliocostalis lumborum) remained relatively constant during standing and trunk ROM movement tasks. The results reflect the increased complexity and interaction of the neuromuscular characteristics both within the thoracic spine and between the lumbar and thoracic spine regions compared to kinematic measures. The measurement of kinematics at four levels along the spine was sufficient to quantify the motion characteristics in the thoracic spine (outcome measure) (Chapter 5). Conversely, it was necessary to retain between 10 and 14 muscles to capture trunk muscle activation characteristics, which are the driving mechanism behind the kinematic outcome measures.

In conclusion, this study aimed to improve the understanding of the behaviour of the trunk musculature. The recommended muscle sets varied substantially amongst the movement tasks, although there were similarities in identified muscle pairings within movement directions. Further, several muscles were strongly correlated with at least one

other muscle all directions of movement, and were therefore identified as potential candidates for elimination. The present study has implications for spine modeling in the thoracic and lumbar spine regions, with respect to identifying the muscles necessary and sufficient to use as inputs into predictive joint loading models. Overall, these findings will enable researchers to better quantify the muscle activation characteristics of and relationships between the thoracic and lumbar spine regions in future studies, and to determine the sets of muscles required as inputs for predictive joint loading models to obtain the most accurate estimates of spinal loading.

CHAPTER 7

Does Thoracic Movement Influence Muscle Activation Patterns Around the Lumbar Spine?

CHAPTER 7

Does Thoracic Movement Influence Muscle Activation Patterns Around the Lumbar Spine?

Summary

While the body of literature surrounding the thoracic spine has steadily increased, the nature of the interactions between the thoracic and lumbar spine regions remains unclear. Co-contraction has been related to pain and injury development, spinal compression, and fatigue, and provides a means of indirectly quantifying the demand on the lumbar musculature. Therefore, the purpose of this study was to determine the extent of the increases in co-contraction in the lumbar musculature during deviation of the thoracic spine from an upright posture. Thirty participants performed ten trials each of upright standing, maximum trunk ROM movement tasks, and thoracic movement tasks. Co-contraction was calculated between each possible pairing within the lumbar musculature (28 pairings) and upper musculature (28 pairings) and compared between tasks. Significant pairwise comparisons between upright standing and a movement task indicated greater co-contraction in the movement task. On average, co-contraction in the lumbar musculature was approximately 67%, 45%, and 55% greater than upright standing for ThorFlex, ThorBend, and ThorTwist, respectively. Generally, the thoracic movement task demonstrated greater co-contraction than the maximum task in the same direction. These findings provide insight into the interactions between the thoracic and lumbar spine regions, as well as the synergy within the trunk muscles to accomplish tasks. The increased co-contraction that occurred in the lumbar spine during tasks with a non-neutral thoracic spine may be associated with increased metabolic cost and fatigue. Therefore,

educating workers to maintain a neutral trunk (both lumbar and thoracic) may aid in reducing unnecessary co-contraction and the associated risk of long-term injury.

7.1 Introduction

The vast majority of studies have focused on the mechanics and motion of the lumbar spine, in part due to the high incidence of injury in that region (Briggs et al., 2007; Edmondston & Singer, 1997). The body of literature surrounding the thoracic spine is growing (Briggs et al., 2007; Edmondston et al., 2007a, 2011b; Edmondston & Singer, 1997; Sizer et al., 2007; Willems et al., 1996), although currently little work has been completed to investigate the effects of the thoracic spine on the lumbar spine. As the thoracic and lumbar spine regions are closely linked and function in tandem to achieve specific motion patterns, it is intuitive that thoracic motion may affect the behaviour of the lumbar spine (Edmondston & Singer, 1997). However, the majority of studies have focused specifically on lumbar (for example, Burnett et al., 2008; Drake & Callaghan, 2008) or general trunk motion, in which the trunk is considered as a single entity (for example, Cavanaugh et al., 1999; Graham et al., 2014; Peach et al., 1998). Thoracic motion tasks may provide an opportunity to more clearly elucidate the nature of the interactions between the thoracic and lumbar spine regions, specifically the influence of thoracic motion on muscle activations patterns in the lumbar spine.

Muscle co-contraction, or the concurrent activation of the opposing muscles around a joint (Missenard et al., 2008), is a measure of activation patterns that has been extensively researched in the trunk. Co-contraction has been theorized to serve a variety of functions, such as equilibrating the moments created by agonist muscles in other axes (Thelen et al., 1995); stiffening spinal joints (Brown et al., 2006; Stokes et al., 2011; Thelen et al., 1995); increasing spinal stability (Hubley-Kozey & Vezina, 2002; Thelen et

al., 1995); and regulating stress distributions across the contact surface of the joint (Thelen et al., 1995). While beneficial to the spine in some respects, there are also penalties to co-contraction, such as increased compressive forces in spinal joints (McGill et al., 2003), increased metabolic cost (Cholewicki & McGill, 1996; Missenard et al., 2008), and inefficiency of movement (Gregory et al., 2008). However, the resulting fatigue may impair muscle coordination (Potvin & O'Brien, 1998), which may reduce spinal stiffness and stability (Granata et al., 2004; Grondin & Potvin, 2009). An increase in co-contraction is then necessary to maintain an appropriate level of spinal stability, at the expense of additional spinal compression (Granata et al., 2004). Therefore, it appears that a balance between too little and too much co-contraction is necessary, in order to maintain sufficient spinal stability without excessive levels of loading or fatigue, which may constitute a risk factor for injury.

There is general agreement within the literature that individuals with LBP, as well as those in remission from LBP, demonstrate altered neuromuscular control during various tasks (D'Hooge et al., 2013; Graham et al., 2014; Hubley-Kozey & Vezina, 2002; Radebold et al., 2001; van Dieen et al., 2003b). Those focusing on co-contraction have identified increased global (D'Hooge et al., 2013) and localized lumbar (Graham et al., 2014) co-contraction in individuals with LBP relative to healthy participants. Further, links between co-contraction and both transient and clinical LBP have been identified using a model of prolonged low-level exposures. Nelson-Wong and Callaghan (2010) and Schinkel-Ivy et al. (2013) assessed co-contraction in prolonged standing and sitting exposures, respectively. In both contexts, individuals who developed pain over the

course of the exposure (2 hours) demonstrated greater co-contraction within the trunk musculature (Nelson-Wong & Callaghan, 2010; Schinkel-Ivy et al., 2013). In a follow-up study, Nelson-Wong and Callaghan (2014) determined if individuals who developed pain during 2 hours of standing would report clinical LBP in the following 3 years. The results indicated that pain development during prolonged standing was predictive of future clinical LBP (Nelson-Wong & Callaghan, 2014).

To the authors' knowledge, no study to date has examined the influence of thoracic movement on lumbar mechanics with respect to muscle activation patterns. Due to the potential clinical implications relating to spine injury risk, measures of co-contraction in both spine regions provide crucial information with respect to neuromuscular control, and warrant further investigation. Therefore, the purpose of this study was to determine the extent of the increases in co-contraction in the lumbar musculature during deviation of the thoracic spine from an upright posture, and to determine whether a relationship exists between the angles of the thoracic spine and co-contraction within the lumbar spine.

7.2 Methods

7.2.1 Participants

Fifteen males and fifteen females participated in the study (mean (*SD*) age, height, and body mass for males/females were 25.0 years (3.8)/22.8 years (2.7), 79.64 kg (8.75)/59.12 kg (6.38), and 1.80m (0.05)/1.66 m (0.05), respectively). All participants were right-hand dominant and had been asymptomatic for back pain for at least one year

prior to the collection, in that they had not missed any days of school or work due to, nor sought treatment for, back pain. All procedures were approved by the institution's Office of Research Ethics, and informed consent was obtained from all participants prior to collection.

7.2.2 *Instrumentation*

7.2.2.1 *Kinematics*

Clusters of five markers were attached to the skin using double-sided tape over the spinous processes of the C₇, T₃, T₆, T₉, T₁₂, and L₅ vertebrae. Markers were also placed on the head (left and right front and back of the head, middle back of the head; 5 total), pelvis (iliac crests, anterior superior iliac spines (ASIS); 4 total), trunk (acromia, sternum, T₁₀ vertebra; 4 total), and legs (greater trochanters, lateral and medial knee joint spaces, lateral malleoli, four on each thigh; 16 total). For the present study, the clusters at the C₇, T₁₂, and L₅ vertebrae were utilized in the subsequent calculation of thoracic and lumbar angles (see Section 7.2.4). Marker motion was recorded using a seven-camera Vicon motion capture system (Vicon MX, Vicon Systems Ltd., Oxford, UK) at a sampling rate of 50 Hz.

7.2.2.2 *Electromyography*

Participants were instrumented with 16 pairs of disposable Ag/Ag-Cl electrodes (Ambu® Blue Sensor N, Ambu A/S, Denmark) over eight muscles bilaterally: EO, IO, LD, lumbar ES, lower-thoracic ES, RA (Drake et al., 2006; McGill, 1991; Mirka & Marras, 1993; Nairn & Drake, 2014; Nelson-Wong & Callaghan, 2010; Schinkel-Ivy et al., 2013), TR (Burnett et al., 2009; Caneiro et al., 2010; McLean, 2005), and upper-

thoracic ES (Burnett et al., 2009; Caneiro et al., 2010; Edmondston et al., 2011a; Nairn & Drake, 2014; Schinkel-Ivy et al., 2013) (see Chapter 3, Section 3.2.2.2). The EO, IO, lumbar ES, and RA were of primary interest as muscles whose function predominantly affected the lumbar region, while the LD, lower-thoracic ES, upper-thoracic ES, and TR were considered to be the muscles of the upper back. EMG signals were differentially amplified (frequency response 10-1000 Hz, common mode rejection 115 dB at 60 Hz, input impedance 10 G Ω ; AMT-8, Bortec, Calgary, Canada) and sampled at 2400 Hz (Vicon MX, Vicon Systems Ltd., Oxford, UK).

7.2.3 Procedures

Electrode sites were shaved and swabbed with rubbing alcohol prior to electrode application to promote adherence and reduce skin impedance. Participants then underwent a series of exercises designed to elicit the maximum voluntary contraction (MVC) of each muscle. For the trunk flexors, a modified sit-up protocol was performed in which participants isometrically flexed, bent, and twisted the trunk against manual resistance (McGill, 1991, 1992). For the trunk extensors, the trunk was cantilevered off the end of a therapy table, and participants performed a resisted isometric back extension (McGill, 1991, 1992). The MVC for LD entailed participants abducting the shoulder to 90°, externally rotating the arm, and flexing the elbow to 90°, following which they pulled the elbow in a downwards direction against manual resistance (Arlotta et al., 2011). Finally, for the TR MVC, participants abducted the arms to 90° and pushed the elbow in an upwards direction against resistance (McLean, 2005). Three trials lasting 3-5 seconds were performed for each exercise, with rest between each trial to minimize the

effects of fatigue. The MVC for each muscle consisted of the maximum EMG value from any of the three trials.

Following marker application, participants performed a kinematic calibration trial consisting of quiet standing with the arms abducted to 90° ('T-pose'). Participants then performed 70 experimental trials, consisting of 10 trials each of Upright, three standing maximum trunk ROM tasks (MaxFlex, MaxBend, and MaxTwist), and three standing thoracic ROM movement tasks (ThorFlex, ThorBend, and ThorTwist). Trials were presented in a random order, and all bending and twisting was performed to the right side. The Upright trials were 10 seconds in length, in which participants stood still with the arms at the sides and head facing forward. For the maximum trunk ROM movement trials, participants first moved the head in the direction of motion (flexing, bending, or twisting) then continued to move the trunk until they reached the maximum position. The arms hung loose to the floor for the MaxFlex and MaxBend trials, and were held loose at the sides for the MaxTwist trials. For the thoracic ROM movement tasks, participants moved the head in the direction of motion then continued to move the thoracic spine ('upper- and mid-back') in that direction, in a smooth and continuous motion. They were also asked to maintain the lumbar spine ('low back') in as close to an upright, neutral position as possible (Appendix A). Arms were held at the sides for all thoracic movement trials. Each movement trial lasted for approximately 10 seconds, during which participants moved to the position, held the position for 3 seconds, and moved back to their starting upright position. Full instructions for each task were given to participants prior to the protocol, along with time to practice each movement task. Throughout the

protocol, prompts were given to the participant prior to each trial so the participant understood what movement task was to be performed (this was necessary as the trials were performed in a random order).

7.2.4 Data Processing

Kinematic data were processed using Visual3D v.4 (C-Motion, Inc., Germantown, USA). Thoracic and lumbar angles were defined as the relative angles between the C₇ and T₁₂ clusters (thoracic) and T₁₂ and L₅ clusters (lumbar) (Appendix C, Section 3.2.4). A Cardan X-Y-Z (flexion/extension-lateral bend-axial twist) rotation sequence (Preuss & Popovic, 2010; van Dieen & Kingma, 2005) was used to calculate thoracic and lumbar angles in the three planes. The angle time-series data were low-pass filtered with a dual-pass, fourth-order Butterworth filter (cutoff frequency: 2.5 Hz, determined by residual analysis (Winter, 2005)). The mean thoracic and lumbar angles for upright standing were calculated and all experimental trials were zeroed to these values. The mean angles during the holding phase of each movement trial were then determined.

Initial processing of EMG data was also completed using Visual3D v.4 (C-Motion, Inc., Germantown, USA). Contamination from heart rate within the raw EMG data was minimized by applying a dual-pass, fourth-order Butterworth filter (cutoff frequency: 30 Hz (Drake & Callaghan, 2006)). Data were then full-wave rectified and low-pass filtered using a dual-pass, fourth-order Butterworth filter (cutoff frequency: 2.5 Hz (Brereton & McGill, 1998; van Dieen & Kingma, 2005)). The MVC for each muscle was identified and used to normalize the EMG signals from the experimental trials, yielding a percentage of each individual's maximum activation levels (%MVC). EMG

data were then downsampled as a data reduction measure (Nelson-Wong & Callaghan, 2010) from 2400 Hz to 50 Hz (Schinkel-Ivy et al., 2013). Mean activation levels were determined for upright standing and the holding phase of each movement trial.

For the purpose of the present study, co-contraction was defined as the concurrent activation of two muscles (Lewek et al., 2004; Missenard et al., 2008; Rudolph et al., 2000). Co-contraction was selected as a measure of interest in addition to discrete measures in order to account for time-varying information in the signals and therefore better characterize the behaviours of the muscles. The co-contraction index (CCI; Equation 2) quantifies the extent to which a pairing of muscles is concurrently activating (Graham et al., 2014; Lewek et al., 2004; Nelson-Wong & Callaghan, 2010; Schinkel-Ivy et al., 2013) over a specified number of data points (Lewek et al., 2004; Nelson-Wong & Callaghan, 2010). The CCI quantifies the extent of co-contraction of the two muscles in terms of two characteristics: the activation level (%MVC) and the timing of activation (Rudolph et al., 2000; Schinkel-Ivy et al., 2013). The equation is calculated on a frame-by-frame basis and is cumulative over time (Rudolph et al., 2000). The output of the CCI is a single value for the specified time period which incorporates both characteristics, but does not offer a means of quantifying either characteristic separately. Higher values represent similar activation timing between the two muscles over a large time interval, relatively high activation of one or both muscles, or a combination thereof. The highest outputs are produced when two muscles activate with similar timing over the time interval and at high magnitudes (Rudolph et al., 2000). The maximum CCI that can be obtained in a single frame occurs when both muscles activate to 100% (assuming that

neither is activating to greater than their maximum level), resulting in a CCI of 200%MVC ($[100/100][100+100]$). To provide context, the maximum value that could possibly be attained for a task in the present study was 20,000%MVC, as CCIs were assessed over 100 frames in the present study. The tasks producing the highest co-contraction in the present study represented approximately 10-15% of this value.

$$CCI = \sum_{i=1}^N \left(\frac{EMG_{low}(i)}{EMG_{high}(i)} \right) [EMG_{low}(i) + EMG_{high}(i)] \quad [2]$$

Where N is the number of data points, and EMG_{low} and EMG_{high} are the relative magnitudes of the normalized EMG for the two muscles in the pairing (EMG_{high} is the signal with the higher magnitude at each sample in time) (Lewek et al., 2004; Nelson-Wong & Callaghan, 2010).

The CCI equation is limited by the inability to discriminate between its two components (activation level and activation timing), in terms of which aspect contributes to a greater extent to the final co-contraction value. There are, however, several benefits to the use of the equation. By assigning ‘low’ and ‘high’ labels to each muscle on a frame-by-frame basis, the equation does not require a global assignment of agonist and antagonist muscles (Kellis et al., 2003), which is advantageous as muscles may change roles during a movement. In addition, the formulation of the equation with ‘ EMG_{high} ’ as the denominator will generally avoid errors created by dividing by zero (Rudolph et al., 2000). Finally, co-contraction is often calculated as a relative measure between the activity level of the antagonist relative to the total activity level (Winter, 2005). The

normalization of antagonist activity to the total muscle activity may be problematic in some scenarios when attempting to compare co-contraction between various tasks, and relate co-contraction to spinal loading and fatigue. While the magnitude of co-contraction is included in the calculation of a relative measure, the output itself does not directly include the magnitude of the co-contraction; rather, the output indicates that the antagonist activity is, for example, 50% of that of the agonists. However, this ratio would apply whether the co-contraction was very low (for example, 1%MVC and 2%MVC) or very high (for example, 50%MVC and 100%MVC). Conversely, the CCI equation accounts, at least in part, for the magnitude of the activation levels through the $[EMG_{low}+EMG_{high}]$ term. This information is necessary if co-contraction is to be subsequently related to spinal loading and fatigue measures.

As the CCI used in the present chapter and the analysis employed in Chapter 6 (cross-correlation and correlation) both assess aspects of timing and magnitude of activation, it may initially appear that the two analyses provide similar information. The analyses in Chapter 6 assess the strength of the relationships between the activation patterns and magnitudes of each pairing of muscles, with outputs being values representing the relative strength of the relationship. Conversely, the CCI analysis of the present chapter provides a measure of the extent of co-contraction which is cumulative over time. This analysis quantifies the extent of co-contraction between two muscles, but does not quantify the strength of the relationship between the two signals directly. Further, Chapters 6 and 7 addressed two very different research questions to present

related but different information. Therefore, the two studies are complementary but by no means interchangeable.

For the present analysis, CCIs (expressed as %MVC) were calculated for every possible pairing within the lumbar spine (left and right EO, IO, lumbar ES, and RA) using a custom program written in Matlab v.2012a (The MathWorks, Inc., Natick, USA), for a total of 28 pairings. The same was done for all pairings of the upper musculature (28 in total), although the study focused on the lumbar musculature. A standardized number of frames (Graham et al., 2014; Lewek et al., 2004; O'Bryan et al., 2014) were used to ensure that CCI values were comparable between tasks. For the Upright trials, 100 frames (Lewek et al., 2004) from the middle portion of the trial were extracted for analysis. For the movement trials, the hold phase was time-normalized to 200 frames, with the middle 100 frames used for CCI calculation to avoid the transitional stage between the movement and the holding phase. The analysis yielded 56 CCI values for each trial, and each CCI was then averaged across the 10 trials for each of the seven movement tasks.

7.2.5 Data Analysis

Statistical analyses were performed using IBM SPSS Statistics v.21 (IBM Corporation, Armonk, USA). The angles, activation levels, and CCIs were input into mixed-factor ANOVAs with within-participant factor of task (Upright, MaxFlex, MaxBend, MaxTwist, ThorFlex, ThorBend, ThorTwist), and between-group factor of sex. While the measures from the maximum trunk ROM movement tasks are provided for context and a reference for the thoracic ROM tasks, the primary focus of the Results and

Discussion will be the thoracic ROM tasks in comparison with Upright. Data were collapsed across sex when there was no significant effect of that factor. Greenhouse-Geisser corrections were used to calculate the degrees of freedom when the assumption of sphericity was not met. Alpha was set to 0.05, and pairwise comparisons with Bonferroni corrections were used for post-hoc testing. In addition, the relationships between the thoracic angles during the hold phase in each direction of movement and the activation measures (activation level, CCI) for the lumbar muscles were determined using Pearson product moment correlations. Pearson coefficients (r) were considered to be very weak, weak, moderate, strong, and very strong when falling into the ranges of 0.00-0.19, 0.20-0.39, 0.40-0.59, 0.60-0.79, and 0.80-1.00, respectively (Swinscow, 1997).

7.3 Results

Significant main effects of task or interactions of task and sex were identified for both thoracic and lumbar angles for all movement directions (Table 31). Generally, the angles achieved in the maximum trunk and thoracic movement tasks were significantly greater than those in Upright. Between the maximum trunk and thoracic movement tasks in the same direction, thoracic angles were greater in ThorFlex than MaxFlex, while lumbar angles in the flexion and lateral bend directions were greater for the maximum trunk movement task compared to the thoracic movement task.

Table 31: Mean (*SD*) thoracic and lumbar angles (°) obtained during each movement task in the plane of interest. Angles for MaxFlex, ThorFlex, and Slump represent rotations around the X axis; for MaxBend and ThorBend, rotations around the Y axis; and for MaxTwist and ThorTwist, rotations around the Z axis. Positive values indicate flexion, lateral bend to the right, and axial twist to the right. *Significant difference from Upright; ^Δsignificant difference from maximum trunk movement task ($p < 0.05$).

Measure	Sex	Task		
<i>Flexion</i>		Upright	MaxFlex	ThorFlex
Thoracic	–	-0.07 (0.25)	18.53 (10.64)*	36.11 (10.82)* ^Δ
Lumbar	–	-0.02 (0.17)	49.52 (11.99)*	22.32 (9.45)* ^Δ
<i>Lateral Bend</i>		Upright	MaxBend	ThorBend
Thoracic	–	0.00 (0.11)	26.53 (7.64)*	27.95 (6.48)*
Lumbar	Male	-0.02 (0.05)	20.32 (4.41)*	3.79 (3.91) ^Δ
	Female	0.01 (0.10)	23.55 (6.26)*	5.44 (6.10)* ^Δ
<i>Axial Twist</i>		Upright	MaxTwist	ThorTwist
Thoracic	Male	-0.02 (0.17)	56.78 (10.87)*	51.16 (12.20)*
	Female	0.00 (0.13)	39.78 (9.22)*	35.84 (7.70)*
Lumbar	Male	0.00 (0.10)	-8.70 (6.11)*	-5.88 (3.44)*
	Female	-0.02 (0.14)	-1.81 (5.30)	1.06 (6.08)

Significant main effects of task were also identified for the average EMG levels for all muscles with the exception of right IO, which demonstrated a significant interaction between task and sex (Table 32). Activation levels of individual muscles ranged from 1.27%MVC (1.29) (right TR, MaxFlex) to 23.96%MVC (7.55) (right IO, MaxTwist, males). In all instances where post-hoc testing identified significant differences between Upright and movement tasks, the movement tasks exhibited greater activation levels than those of Upright. Comparisons of maximum trunk and thoracic movement tasks in the same direction were significantly different for the left and right lumbar ES (ThorFlex greater) for the flexion tasks; and for the left and right EO and lumbar ES (MaxTwist greater) for the axial twist tasks.

Table 32: Mean (*SD*), minimum, and maximum EMG levels (%MVC) for the lumbar muscles from the holding phase of each movement task. Sex is specified for ANOVAs in which a significant interaction between task and sex was identified. EO: external oblique; IO: internal oblique; LES: lumbar erector spinae; RA: rectus abdominis.

Task	Overall Mean (<i>SD</i>) Activation Level (%MVC)	Minimum Activation Level (%MVC)		Maximum Activation Level (%MVC)	
		Mean (<i>SD</i>)	Muscle	Mean (<i>SD</i>)	Muscle
Upright	3.71 (1.99)	2.50 (1.35)	Left LES	6.87 (4.29)	Left IO
MaxFlex	5.06 (2.62)	3.70 (3.18)	Right LES	9.29 (7.89)	Left RA
MaxBend	5.83 (3.78)	3.33 (2.28)	Right LES	15.27 (8.56)	Left EO
MaxTwist	9.30 (6.23)	5.85 (4.51)	Left LES	23.96 (7.55)	Right IO (males)
ThorFlex	5.95 (3.34)	6.72 (3.37)	Right LES	11.60 (14.18)	Left IO
ThorBend	6.34 (3.51)	3.84 (2.71)	Right LES	13.61 (12.87)	Left IO
ThorTwist	8.72 (5.66)	4.37 (3.44)	Left LES	19.24 (13.25)	Right IO (males)

For the CCIs for the lumbar musculature, significant main effects of task were identified for 16 of the 28 pairings, and significant interactions between task and sex for five pairings (Table 33). Co-contraction within the lumbar muscle pairings ranged from 255.83%MVC (177.87) (right lumbar ES–right RA, males, MaxFlex) to 2781.97%MVC (1927.40) (left EO–right IO, males, MaxTwist) (Table 34). CCIs were always greater in movement tasks compared to Upright when significant differences were identified. For the flexion and lateral bend directions, significant pairwise comparisons indicated that the thoracic movement task displayed greater levels of co-contraction than the corresponding maximum trunk movement task, while the opposite trend was observed for the axial twist direction. CCIs ranged from 16.46% (16.31) (MaxFlex) to 86.92% (48.80) (MaxTwist) greater than Upright (Table 35).

Table 33: ANOVA statistics for all lumbar muscle pairings with a significant effect of task on co-contraction ($p<0.05$). EO: external oblique; IO: internal oblique; LES: lumbar erector spinae; RA: rectus abdominis.

Muscle Pairing	Effect	F-Statistic
Left EO–left IO	Task	$F_{3.585,103.951}=5.195, p=0.001$
Left EO–left LES	Task	$F_{3.125,90.616}=11.272, p<0.001$
Left EO–left RA	Task	$F_{3.217,93.292}=3.134, p=0.026$
Left EO–right EO	Task	$F_{2.326,67.451}=15.587, p<0.001$
Left EO–right IO	Task x sex	$F_{2.622,73.420}=7.695, p<0.001$
Left EO–right LES	Task	$F_{3.305,95.843}=19.344, p<0.001$
Left EO–right RA	Task	$F_{3.387,98.231}=1.589, p=0.191$
Left IO–left LES	Task x sex	$F_{3.659,102.464}=2.903, p=0.029$
Left IO–left RA	Task	$F_{2.158,62.573}=1.543, p=0.221$
Left IO–right EO	Task	$F_{3.451,100.080}=2.890, p=0.033$
Left IO–right IO	Task	$F_{2.838,82.301}=2.600, p=0.061$
Left IO–right LES	Task	$F_{3.711,107.605}=15.466, p<0.001$
Left IO–right RA	Task	$F_{2.386,69.208}=1.947, p=0.142$
Left LES–left RA	Task x sex	$F_{3.312,92.745}=3.822, p=0.010$
Left LES–right EO	Task	$F_{2.817,81.679}=12.226, p<0.001$
Left LES–right IO	Task x sex	$F_{3.027,84.743}=3.110, p=0.030$
Left LES–right LES	Task	$F_{2.997,86.924}=18.290, p<0.001$
Left LES–right RA	Task	$F_{3.302,95.767}=13.880, p<0.001$
Left RA–right EO	Task	$F_{3.105,90.041}=3.351, p=0.021$
Left RA–right IO	Task	$F_{2.172,62.985}=1.258, p=0.293$
Left RA–right LES	Task	$F_{2.536,73.548}=16.747, p<0.001$
Left RA–right RA	Task	$F_{2.615,75.834}=5.005, p=0.005$
Right EO–right IO	Task	$F_{1.510,43.788}=10.040, p=0.001$
Right EO–right RLES	Task	$F_{2.697,78.205}=21.063, p<0.001$
Right EO–right RA	Task	$F_{3.551,102.991}=2.308, p=0.070$
Right IO–right RLES	Task	$F_{2.556,74.126}=26.528, p<0.001$
Right IO–right RA	Task	$F_{2.610,75.679}=1.932, p=0.139$
Right RLES–right RA	Task x sex	$F_{2.669,74.741}=3.591, p=0.021$

Table 34: Mean (*SD*), minimum, and maximum co-contraction index values (%MVC) from all possible pairings of lumbar muscles (28 total). Sex is specified for ANOVAs in which a significant interaction between task and sex was identified. EO: external oblique; IO: internal oblique; LES: lumbar erector spinae; RA: rectus abdominis.

Task	Overall Mean (<i>SD</i>) CCI	Minimum CCI		Maximum CCI	
		Mean (<i>SD</i>)	Pairing	Mean (<i>SD</i>)	Pairing
Upright	601.84 (226.87)	331.91 (192.81)	Right LES–right RA (males)	972.90 (760.35)	Left EO–right IO (females)
MaxFlex	723.62 (329.05)	255.83 (177.87)	Right LES–right RA (males)	1154.21 (546.26)	Left EO–right IO (females)
MaxBend	771.49 (346.68)	338.34 (171.44)	Right LES–right RA (males)	1558.87 (1113.11)	Left EO–left IO
MaxTwist	1063.80 (395.63)	493.75 (162.09)	Left IO–left LES (females)	2781.97 (1927.40)	Left EO–right IO (males)
ThorFlex	917.88 (185.78)	560.38 (209.61)	Left LES–left RA (females)	1429.61 (1210.34)	Left RA–right RA
ThorBend	847.57 (291.48)	476.44 (206.48)	Left IO–left LES (females)	1554.90 (1037.18)	Left EO–left IO
ThorTwist	900.05 (322.67)	444.17 (174.55)	Left LES–left RA (females)	1939.81 (1701.30)	Left EO–right IO (males)

Table 35: Mean (*SD*), minimum, and maximum difference (%) from Upright for all possible pairings of lumbar muscles (28 total). Sex is specified for ANOVAs in which a significant interaction between task and sex was identified. EO: external oblique; IO: internal oblique; LES: lumbar erector spinae; RA: rectus abdominis.

Movement Task	Mean (<i>SD</i>) % Difference from Upright	Minimum % Difference		Maximum % Difference	
		% Difference	Pairing	% Difference	Pairing
MaxFlex	16.46 (16.31)	-22.92	Right LES–right RA (males)	51.11	Left RA–right RA
MaxBend	25.70 (18.68)	-0.08	Left EO–right LES	75.74	Left EO–left IO
MaxTwist	86.92 (48.80)	14.26	Left IO–left RA	259.29	Left EO–right IO (males)
ThorFlex	66.78 (44.98)	15.61	Left IO–right EO	185.69	Right LES–right RA (males)
ThorBend	45.03 (22.41)	13.59	Left RA–right IO	147.28	Left IO–left LES (males)
ThorTwist	55.26 (30.27)	6.47	Left IO–left RA	150.53	Left EO–right IO (males)

The CCIs of the upper musculature were also analyzed, although not the focus of the present study. For 27 of the 28 pairings of thoracic muscles, significant main effects of task were observed for CCIs, along with a significant task-by-sex interaction for the left lower-thoracic ES–right LD pairing (Table 36). Mean (*SD*) CCIs ranged from 134.12%MVC (109.34) to 2139.14%MVC (1577.92) (Table 37). Of all comparisons between Upright and a movement task that were considered significant, the movement task demonstrated the greater CCI. Further, for all comparisons between the maximum trunk and thoracic movement task in the same direction, greater CCIs were identified for the thoracic movement task. On average (*SD*) across all pairings, CCIs ranged from 10.59% (28.20) (MaxFlex) to 94.97% (136.70) (ThorTwist) greater than Upright (Table 38).

Table 36: ANOVA statistics for all upper muscle pairings with a significant effect of task on co-contraction ($p < 0.05$). LD: latissimus dorsi; LTES: lower-thoracic erector spinae; TR: upper trapezius; UTES: upper-thoracic erector spinae.

Muscle Pairing	Effect	<i>F</i> -Statistic
Left LD–left LTES	Task	$F_{2,720,78.876}=3.005, p=0.040$
Left LD–left TR	Task	$F_{3,109,90.166}=5.807, p=0.001$
Left LD–left UTES	Task	$F_{3,389,98.279}=10.186, p<0.001$
Left LD–right LD	Task	$F_{3,688,103.259}=10.728, p<0.001$
Left LD–right LTES	Task	$F_{2,846,79.686}=4.928, p=0.004$
Left LD–right TR	Task	$F_{3,702,103.646}=5.978, p<0.001$
Left LD–right UTES	Task	$F_{3,275,94.988}=5.949, p=0.001$
Left LTES–left TR	Task	$F_{4,557,132.147}=11.909, p<0.001$
Left LTES–left UTES	Task	$F_{3,174,88.862}=6.737, p<0.001$
Left LTES–right LD	Task x sex	$F_{2,627,73.560}=2.991, p=0.043$
Left LTES–right LTES	Task	$F_{1,751,49.033}=6.666, p=0.004$
Left LTES–right TR	Task	$F_{3,698,103.543}=9.804, p<0.001$
Left LTES–right UTES	Task	$F_{2,685,77.877}=3.162, p=0.034$
Left TR–left UTES	Task	$F_{4,015,116.440}=13.567, p<0.001$
Left TR–right LD	Task	$F_{2,686,77.892}=7.203, p<0.001$
Left TR–right LTES	Task	$F_{2,169,62.891}=8.302, p<0.001$
Left TR–right TR	Task	$F_{2,052,57.454}=8.410, p=0.001$
Left TR–right UTES	Task	$F_{2,241,64.987}=7.957, p=0.001$
Left UTES–right LD	Task	$F_{3,626,101.536}=7.949, p<0.001$
Left UTES–right LTES	Task	$F_{3,150,88.197}=9.150, p<0.001$
Left UTES–right TR	Task	$F_{3,872,108.420}=10.437, p<0.001$
Left UTES–right UTES	Task	$F_{2,766,77.458}=3.688, p=0.018$
Right LD–right LTES	Task	$F_{1,445,41.917}=23.400, p<0.001$
Right LD–right TR	Task	$F_{2,977,83.360}=9.478, p<0.001$
Right LD–right UTES	Task	$F_{1,562,45.301}=22.611, p<0.001$
Right LTES–right TR	Task	$F_{2,305,64.529}=8.654, p<0.001$
Right LTES–right UTES	Task	$F_{1,400,40.602}=35.597, p<0.001$
Right TR–right UTES	Task	$F_{2,657,74.393}=10.717, p<0.001$

Table 37: Mean (*SD*), minimum, and maximum co-contraction index values (%MVC) from all possible pairings of upper muscles (28 total). Sex is specified for ANOVAs in which a significant interaction between task and sex was identified. LD: latissimus dorsi; LTES: lower-thoracic erector spinae; TR: upper trapezius; UTES: upper-thoracic erector spinae.

Task	Overall Mean (<i>SD</i>) CCI	Minimum CCI		Maximum CCI	
		Mean (<i>SD</i>)	Pairing	Mean (<i>SD</i>)	Pairing
Upright	258.24 (61.15)	171.46 (103.83)	Left TR–right TR	364.95 (212.59)	Left LTES–right LD (females)
MaxFlex	300.68 (140.80)	134.12 (109.34)	Left TR–right TR	613.00 (331.00)	Left LD–right LD
MaxBend	342.09 (102.21)	200.45 (134.09)	Left TR–left UTES	507.63 (290.99)	Left LD–left UTES
MaxTwist	472.80 (376.42)	187.01 (108.54)	Left TR–right TR	1806.45 (1267.18)	Right LTES–right UTES
ThorFlex	328.73 (86.82)	210.52 (112.45)	Left TR–right TR	546.08 (331.80)	Left LD–right LD
ThorBend	410.73 (68.59)	298.17 (177.73)	Left LTES–left-TR	565.14 (347.89)	Right LD–right LTES
ThorTwist	524.88 (447.64)	218.13 (136.14)	Left TR–right TR	2139.14 (1577.92)	Right LTES–right UTES

Table 38: Mean (*SD*), minimum, and maximum difference (%) from Upright for all possible pairings of upper muscles (28 total). Sex is specified for ANOVAs in which a significant interaction between task and sex was identified. LD: latissimus dorsi; LTES: lower-thoracic erector spinae; TR: upper trapezius; UTES: upper-thoracic erector spinae.

Movement Task	Mean (<i>SD</i>) % Difference from Upright	Minimum % Difference		Maximum % Difference	
		% Difference	Pairing	% Difference	Pairing
MaxFlex	10.59 (28.20)	-28.31	Right LTES–right TR	70.28	Left LD–right LD
MaxBend	31.19 (17.45)	-2.19	Left TR–right LTES	76.84	Left LD–left UTES
MaxTwist	76.13 (114.31)	9.07	Left TR–right TR	517.17	Right LTES–right UTES
ThorFlex	27.11 (12.03)	3.75	Left LTES–right LD (females)	53.21	Left LD–left TR
ThorBend	64.53 (32.70)	8.69	Left LTES–right LD (females)	131.25	Left TR–right TR
ThorTwist	94.97 (136.70)	16.49	Left LTES–right LD (females)	630.83	Right LTES–right UTES

Regarding the correlation analysis, significant weak positive relationships were identified between thoracic angle and activation level for two muscles in each movement direction (left and right lumbar ES for flexion; right EO and right lumbar ES for lateral bend and axial twist) (Table 39). Of the 28 pairings within the lumbar musculature, the CCIs for 8, 9, and 3 pairings were significantly correlated to the thoracic angle for the flexion, lateral bend, and axial twist movements, respectively. All significant correlations between were of weak or moderate strength, ranging from $r=0.267$ (left IO–left LES) to $r=0.459$ (right LES–right RA). Taken together, these results suggest a relationship between the positioning of the thoracic spine and the magnitude of muscle activation and co-contraction, in that increases in thoracic spine angles are associated with increases in the activation measures.

Table 39: Significant correlations between thoracic angles and activation measures for the lumbar muscles (activation level (single muscle), CCI (muscle pairing)) for each direction of movement. EO: external oblique; IO: internal oblique; LES: lumbar erector spinae; RA: rectus abdominis.

Muscle/Muscle Pairing	r (p -value)
<i>Flexion</i>	
Left LES	0.365 (0.004)
Right LES	0.271 (0.036)
Left IO–left LES	0.267 (0.039)
Left LES–left RA	0.306 (0.018)
Left LES–right EO	0.290 (0.024)
Left LES–right LES	0.380 (0.003)
Left LES–right RA	0.439 (<0.001)
Left RA–right LES	0.332 (0.010)
Right EO–right LES	0.327 (0.011)
Right LES–right RA	0.459 (<0.001)
<i>Lateral Bend</i>	
Right EO	0.323 (0.012)
Right LES	0.341 (0.008)
Left EO–right LES	0.348 (0.006)
Left IO–right EO	0.294 (0.023)
Left IO–right LES	0.328 (0.010)
Left LES–right LES	0.282 (0.029)
Left RA–right LES	0.319 (0.013)
Right EO–right IO	0.295 (0.022)
Right EO–right LES	0.321 (0.012)
Right IO–right LES	0.375 (0.003)
Right LES–right RA	0.371 (0.003)
<i>Axial Twist</i>	
Right EO	0.323 (0.012)
Right LES	0.341 (0.008)
Left EO–right LES	0.348 (0.006)
Left IO–right EO	0.294 (0.023)
Left IO–right LES	0.328 (0.010)

7.4 Discussion

Overall, participants displayed higher levels of co-contraction in the movement tasks compared to Upright, by approximately 16% (MaxFlex) to 87% (MaxTwist) for the

lumbar musculature and 11% (MaxFlex) to 95% (ThorTwist) for the upper musculature when averaged across all pairings. These findings provide insight into the interplay between the thoracic and lumbar spine regions (that is, the effects of a non-neutral thoracic spine posture on lumbar muscle activation), and imply that thoracic movement has a substantial impact on activation behaviours within the musculature of the lumbar spine. As the results of this study indicated that non-neutral thoracic spine postures are associated with increased co-contraction among the lumbar muscles, care must be taken to not simply recommend that workers maintain a neutral low back posture during work tasks as a sole means of attempting to decrease injury incidence. Rather, educating workers to maintain a neutral trunk, in both the lumbar and thoracic regions, may be more appropriate in reducing unnecessary co-contraction and the associated risk of long-term injury.

The present study differed from past investigations in the tasks examined and the method of co-contraction calculation. Previously, trunk muscle co-contraction has been examined during isometric trunk exertions (Brown & McGill, 2008; Granata et al., 2005a, b; Thelen et al., 1995), maximum trunk flexion-extension (Graham et al., 2014), and prolonged low-level exposures (Nelson-Wong & Callaghan, 2010; Schinkel-Ivy et al., 2013), as opposed to investigating the effects of thoracic ROM movement tasks on lumbar behaviours. Thoracic ROM movement tasks while maintaining a neutral low back (versus, for example, thoracic ROM tasks combined with trunk flexion) were selected for comparison to Upright to enable participants to focus on maximizing thoracic movement without also having to focus on attaining a specific hip angle. Further,

maintaining a neutral position of the lumbar spine minimized the influence of lumbar spine movement on the ROM attained in the thoracic spine (Nairn & Drake, 2014), and on muscle activation patterns in both regions. Finally, these types of movements are relatively common during activities of daily living (for example, brushing teeth or removing laundry from a washing machine), although it is likely that individuals would not consciously target those body positions, but rather use the movements as a means of accomplishing the outcome task.

Regarding co-contraction calculation, several approaches have grouped muscles to produce global co-contraction measures (Brown & McGill, 2008; D'Hooge et al., 2013; Granata et al., 2005a, b; Winby et al., 2013), as opposed to quantifying co-contraction between two muscles through the co-contraction index (Graham et al., 2014; Lewek et al., 2004; Nelson-Wong & Callaghan, 2010; Schinkel-Ivy et al., 2013). Although generalized flexor-extensor co-contraction measures have been recommended for the knee joint (Winby et al., 2013), these muscles function primarily as flexors or extensors. This approach may not be as suitable in the trunk, in which muscles contribute to multi-planar motion. Therefore, analyzing individual muscle pairings to identify common trends may constitute a more appropriate means of investigating trunk co-contraction.

The co-contraction magnitudes calculated in the present study were comparable to previously reported values using the CCI equation. Schinkel-Ivy et al. (2013) calculated co-contraction between various muscles in the trunk during prolonged sitting. Per minute over a 2 hour protocol, the average of all muscle pairings (120 in total) was approximately 2381%MVC, with CCIs ranging from 1186%MVC to 5344%MVC

(Schinkel-Ivy et al., 2013). Further, Nelson-Wong and Callaghan (2010) reported ranges of bilateral gluteus medius and global flexor-extensor co-contraction of approximately 1500%MVC to 2500%MVC per minute during 2 hours of standing. The values in the present study ranged from 134.12%MVC (left TR–right TR, MaxFlex) to 2781.97%MVC (left EO–right IO, males, MaxTwist). Considering the shorter lengths of the trials in the present study, as well as the tasks performed by participants (movements, versus low-level static sitting and standing), the results of the present study are comparable to Nelson-Wong and Callaghan (2010) and Schinkel-Ivy et al. (2013). The values presented in the present study represent approximately 1.3% to 13.9% of the maximum CCI that could be theoretically be obtained over 100 frames of data (200%MVC (maximum for one frame) multiplied by 100 frames = 20,000%MVC).

With respect to the direction of movement, Thelen et al. (1995) reported co-contraction ratios of 25-29%, 35-46%, and 46-58% during isometric trunk flexion, lateral bend, and axial twist, respectively. Similarly, Graham et al. (2014) observed that co-contraction was higher in asymmetric trunk flexion than symmetric flexion. The majority of the present results followed a similar trend, in that on average, the flexion and axial twist tasks demonstrated the lowest and highest CCIs, respectively, for both the maximum trunk and thoracic movement tasks in the upper musculature, and for the maximum trunk movement tasks in the lumbar musculature. The axial twist tasks likely required the muscles to contract against the forces of passive tissues and opposing muscles while holding the posture, as opposed to the flexion and lateral bend movement tasks, which would be assisted by gravity to an extent. The lumbar musculature exhibited different

trends for the thoracic movement tasks, in which the lowest and highest CCIs, on average, were identified for ThorBend (847.57%MVC) and ThorFlex (917.88%MVC). The lumbar flexion angles during the ThorFlex task provide a possible explanation, as the average lumbar flexion was approximately 22°. This would have created a greater moment around the lumbar spine than thoracic movement alone, thereby requiring greater levels of activation to maintain the posture. Conversely, the smaller moments in ThorBend and ThorTwist may have reduced the amount of activation necessary in the lumbar musculature to maintain the posture.

Although it is intuitive that lumbar co-contraction would differ between Upright and movement tasks, the extent of the difference was of interest, as typically, little weight or consequence is assigned to the thoracic spine. The CCIs of the lumbar musculature during the movement tasks ranged from approximately 16% (MaxFlex) to 87% (MaxTwist) greater than Upright, with the thoracic movement tasks displaying differences of 67% (ThorFlex), 45% (ThorBend), and 55% (ThorTwist). These findings suggest that with thoracic movement tasks, there may be a requirement for increased spinal stiffness and stability in the lumbar spine, which may be achieved through increased muscle stiffness resulting from co-contraction (van Dieen et al., 2003a). This was supported by the results of the correlation analysis, which showed numerous relationships between thoracic angles and both the lumbar ES and abdominal muscle activation levels and CCIs. Over time, greater levels of co-contraction, the corresponding increased metabolic cost (Cholewicki & McGill, 1996; Missenard et al., 2008), and resulting fatigue may introduce a cycling effect. Fatigue has been observed to impair

muscle coordination (Potvin & O'Brien, 1998), thereby reducing spinal stiffness and stability (Granata et al., 2004; Grondin & Potvin, 2009). In turn, co-contraction may be further increased to maintain an appropriate level of stability, contributing to additional fatigue.

When comparing the maximum trunk and thoracic movement task within each direction, greater co-contraction was identified in the thoracic movement task for all movement directions for the upper musculature and for flexion and lateral bend for the lumbar musculature. These findings suggest that although the lumbar spine remained in a neutral position, co-contraction in that region was higher than when the trunk moved to its full ROM. Ergonomic recommendations often focus on maintaining a neutral back (McGill, 1997), which is beneficial for minimizing injury risk related to movements near the end ROM in either loaded or unloaded conditions (McGill, 2007). Maintaining a neutral low back is critical and a valuable initial step in injury prevention. However, it must also be acknowledged that this is not a 'cure-all' solution for eliminating back injuries in the workplace, as maintaining a neutral low back while moving the thoracic spine may result in an increased risk of fatigue and injury over time due to increased co-contraction and the resulting muscular load. Further, this type of recommendation, if used as the only precaution in injury prevention, may provide a false sense of security to workers, management, and engineers. These results emphasize the importance of educating workers to maintain a relatively neutral trunk (both lumbar and thoracic), which may aid in reducing unnecessary co-contraction and the associated risk of long-term injury. While it is likely that most jobs and job tasks will require some movements

outside of a relatively neutral posture on occasion, maintaining non-neutral thoracic postures for long durations or high numbers of repetitions may still potentially impose an increased risk of injury, even though the low back remains in a neutral position. For jobs involving specific tasks which regularly necessitate these types of postures and movements, the use of short, frequent rest breaks may assist in minimizing the accumulation of fatigue and resulting consequences.

The findings of the present study were tempered by several methodological limitations. The sample of participants constituted a relatively homogeneous group of young individuals asymptomatic for back pain. Individuals with LBP tend to exhibit increased levels of co-contraction relative to healthy individuals during mid-range (D'Hooge et al., 2013) and full (Graham et al., 2014) trunk flexion. Therefore, a similar trend would be expected for the types of thoracic movement tasks performed for the present study, although the extent of that increase remains unknown. Further, the relatively novel nature of the thoracic movement tasks may have affected the maximum thoracic angles that participants were able to achieve. Although these types of movements are relatively common during activities of daily living (for example, brushing teeth or removing laundry from a washing machine), it is likely that individuals would not consciously target those body positions, but rather use the movements as a means of accomplishing the outcome task. Finally, the lumbar position was not externally constrained during the thoracic movement tasks, resulting in small amounts of lumbar movement in the same direction as the thoracic spine. A future direction of study may

entail an examination of the effects of leaning on surfaces of different heights on co-contraction in the trunk musculature.

In conclusion, muscle co-contraction in the lumbar region during thoracic motion tasks was greater than that of Upright by an average of 67%, 45%, and 55% for ThorFlex, ThorBend, and ThorTwist, respectively. In addition, weak to moderate significant positive correlations were identified between thoracic angles and activation measures (activation levels, co-contraction). Therefore, deviation of the thoracic region from a neutral, upright posture impacted lumbar co-contraction, providing insight into the interaction between posture of the thoracic spine and muscle activation behaviours in the lumbar spine. These results suggest that even with a neutral low back, thoracic movement tasks may be associated with increased metabolic cost and fatigue compared to Upright. As non-neutral thoracic spine postures increased co-contraction among the lumbar muscles, care must be taken to not simply recommend that workers maintain a neutral low back posture during work tasks as a sole means of attempting to decrease injury incidence. Rather, educating workers to maintain a neutral trunk (both lumbar and thoracic) may aid in reducing unnecessary co-contraction and the associated risk of long-term injury.

CHAPTER 8

General Discussion

CHAPTER 8

General Discussion

8.1 Global Research Contributions

The literature surrounding the thoracic spine is relatively sparse compared to the lumbar spine, specifically motion characteristics, muscle activation characteristics, and relationships in the motion and muscle activation both within the thoracic spine and between the lumbar and thoracic spine regions. Therefore, this dissertation aimed to quantify and evaluate thoracic spine characteristics during fundamental tasks relating to kinematic and muscle activation measures, and relationships in these characteristics within the thoracic spine and between the lumbar and thoracic spine regions. Specifically, the effects of adjacent segments, repeatability and reliability characteristics, relationships in motion and muscle activation, and the effects of thoracic movement were examined. The thoracic spine is typically represented as a single rigid segment or simply ignored for research, clinical, and/or ergonomic applications. This approach may have been adopted due to the presumed effects of the rib cage in terms of providing stability and restricting motion (Horton et al., 2005; Oda et al., 1996, 2002; Watkins et al., 2005). However, based on the findings of the five presented studies, it is concluded that the thoracic spine demonstrates differences in motion and muscle activation characteristics both along its length and relative to the lumbar spine, and also influences the behaviour of the lumbar spine. As such, the thoracic spine needs to be monitored or accounted for during the investigation of spinal mechanics, taking into consideration the kinematic and

activation changes that occur along its length as opposed to representing it as a single rigid entity. Knowledge of the behaviour of the thoracic spine, as well as the interactions between the thoracic spine and adjacent regions, provides the first step to more clearly understanding the behaviour of the spine as a whole, and potentially mechanisms of pain in the thoracic and lumbar spine regions. Studies comparing the present findings with individuals with LBP, and longitudinal studies to determine whether any differences are predisposing or adaptive to LBP, will be required in order to identify pain mechanisms. Clinical implications for this work may include the identification of aberrant spinal motion or activation patterns for qualitative assessments of motion or muscle activation. The results of this dissertation may also have implications for ergonomic assessment tools such as posture-matching-based approaches and digital human modeling, in how the thoracic spine is represented. Taken together, the results of these studies can aid in the further development of predictive joint loading models for the thoracic and lumbar spine regions. Specifically, these studies provide insight into the kinematic and muscle activation data necessary as inputs for the prediction of compression and shear forces in the thoracic spine, and the locations at which loading variables should be calculated. The development of such a model would enable the investigation of loading pathways along the length of the spine, as well as the relationship between loading variables and pain in both the thoracic and lumbar spine regions.

8.2 Specific Research Contributions

8.2.1 Study #1 Contributions: Repeatability of Kinematic and Electromyographical Measures During Standing and Trunk Motion: How Many Trials are Sufficient? (Chapter 3)

In Chapter 3, the repeatability and reliability characteristics of kinematic and EMG measures were investigated, with the intent of determining the minimum number of trials required to achieve repeatability and reliability. The repeatability and reliability of the majority of measures was relatively high, with 59%, 68%, 78%, 86%, and 91% of measures achieving repeatable and reliable values with two, three, four, five, and ten trials, respectively. The results of this study constitute recommendations regarding the minimum number of trials required for repeatable and reliable kinematic and EMG measures, which are intended to provide an acceptable trade-off between repeatable and reliable values and feasibility of the collection protocol. These recommendations provide a guideline for researchers to select the number of trials to be collected in an experimental protocol, depending on their research question and measures of interest as well as the level of repeatability and reliability acceptable for the research question.

8.2.2 Study #2 Contributions: Identification of Head and Arm Positions to Elicit Maximal Voluntary Trunk Range-of-Motion Measures (Chapter 4)

In Chapter 4, the head and arm positions that elicited the greatest voluntary ROM in various spine angle measures during MaxFlex, MaxBend, and MaxTwist were determined. It was concluded that an active head position elicited greater angles for all movements in the upper regions, while there was generally no effect for the lower and

global regions. Regarding arm positions, loose and abducted arms were generally preferable for MaxFlex and MaxTwist, respectively. For MaxBend, the crossed and loose arm positions were preferable for the upper and lower/global regions, respectively. The results provide insight into the interplay between the spine and the head and arms, and also enable the determination of whether the effects of head and arm movement are exclusive or local to the thoracic spine, or if head and arm positions exert a global influence over regions that are more removed. This knowledge is crucial to understanding how the trunk functions as a system, as opposed to individual, isolated regions. Further, this study highlights the importance of developing standardized positions during maximum trunk ROM trials, in order to elicit maximal voluntary angles in each plane for various spinal regions, which will be beneficial in both research and clinical contexts.

8.2.3 Study #3 Contributions: Quantification of the Trunk Part I: Which Motion Segments are Required to Sufficiently Characterize its Kinematic Behaviour? (Chapter 5)

In Chapter 5, the motion characteristics of the thoracic spine were examined in order to determine the set of segments necessary to sufficiently characterize the kinematics of the thoracic spine. A four-cluster marker set with clusters at the C₇, T₆, T₁₂, and L₅ vertebrae was sufficient to quantify motion for six of the seven movement tasks tested, which was fewer clusters than expected. This marker set may constitute best practices recommendations for measuring thoracic motion, to provide a trade-off between feasibility of instrumentation and data processing, and the ability to capture the necessary information relating to thoracic motion. These findings provide insight into the

relationships in motion between smaller regions within the thoracic spine, and between the thoracic and lumbar spine regions. Such an understanding is relevant to the development of predictive spine loading models, posture-matching-based approaches, and digital human models incorporating the thoracic spine. From a clinical perspective, this study also contributes qualitative information regarding functional motions of the spine and coordination at different spinal levels, which may aid in identifying aberrant spinal motion in patient populations.

8.2.4 Study #4 Contributions: Quantification of the Trunk Part II: Muscles Required to Represent Activation Characteristics During Range-of-Motion Tasks (Chapter 6)

In Chapter 6, the interactions between the thoracic and lumbar musculature were examined in order to better understand the behaviour of the trunk musculature, and to determine the superficial muscles that were necessary to adequately quantify the gross trunk muscle activation characteristics. It was concluded that between 10 and 14 of the 16 muscles tested were necessary to quantify the muscle activation characteristics of the superficial trunk muscles. The results emphasized the complexity and interaction of the neuromuscular characteristics both within the thoracic spine and between the lumbar and thoracic spine regions, and provided insight into the synergy of the trunk musculature that produces trunk movements in the three planes of motion. Further, a preliminary indication of the muscles that best represent the activation characteristics of the superficial trunk musculature has been obtained. The results also have implications for spine modeling in the thoracic and lumbar spine regions, with respect to identifying the muscles necessary to use as inputs into predictive joint loading models.

8.2.5 Study #5 Contributions: Does Thoracic Movement Influence Muscle Activation Patterns Around the Lumbar Spine? (Chapter 7)

In Chapter 7, the effects of thoracic movement on co-contraction in the lumbar spine were investigated. It was concluded that non-neutral thoracic postures elicited increased co-contraction in the lumbar spine compared to Upright by approximately 67% (ThorFlex), 45% (ThorBend), and 55% (ThorTwist), on average, and that thoracic angles were positively associated with activation measures in the lumbar spine. These findings provide insight into the interplay between the thoracic and lumbar spine regions by quantifying the extent of co-contraction in one region in response to changes in posture in another. That co-contraction in the thoracic movement tasks was substantially greater than that of Upright has potential clinical and occupational implications with respect to spine injury risk, as the additional levels of co-contraction may contribute to fatigue and long-term injury risk. Similarly, higher levels of co-contraction have been associated with pain development during prolonged, low-level exposures (Nelson-Wong & Callaghan, 2010; Schinkel-Ivy et al., 2013). It is commonly recommended in ergonomic practice for individuals to ‘maintain a neutral low back’. While maintaining a neutral low back is indeed crucial for back safety, it is also important to acknowledge that this is not a catch-all solution, and may in fact promote a false sense of safety in workers or employers. Therefore, workers should focus on maintaining a neutral posture of the whole trunk during work tasks to ensure that additional co-contraction is not being imposed due to non-neutral thoracic postures, and should take adequate rest breaks to delay the onset of fatigue.

8.3 General Limitations

Study-specific limitations are detailed in each of the individual chapters. There were, however, several limitations that were common across most or all studies. These included: a relatively homogeneous, young, asymptomatic sample of participants; the use of relatively standardized standing, maximum trunk ROM, and thoracic ROM tasks; and the nature of the skin-mounted spine cluster marker set used.

The data used to address the purposes for all five studies in this dissertation were collected from the same group of individuals. This may limit the applicability of the results to an extent, as the kinematic and EMG measures would have been related within each individual participant. However, varying subsets of trials were analyzed for each study (with the exceptions of Studies #3 and #4, which used the same subset of trials), using different analysis techniques, in order to minimize the impact of the same group of participants. Further, this group of participants was representative of a healthy, young population, with mean values for all measures examined in the five studies falling within the range of values previously reported in the literature. Therefore, the results should be reflective of this population and would not be expected to change with a different participant sample. The participants were relatively homogeneous with respect to age (range from 19.0 to 33.3 years), and had all been asymptomatic for back pain within the 12 months prior to collection. Reduced trunk ROM has been identified in older adults (Intolo et al., 2009; McGill et al., 1999), as have altered muscle activation characteristics (McGill et al., 1999). Associations have also been observed between LBP status and ROM (Hidalgo et al., 2012; Mayer et al., 1984), motion patterns (Marras et al., 1999;

Shum et al., 2005a, b; Wong & Lee, 2004), muscle activation (D’Hooge et al., 2013; Lariviere et al., 2000; Watson et al., 1997), and co-contraction (D’Hooge et al., 2013; Graham et al., 2014). Therefore, the results of the studies presented in this dissertation may not be generalizable to these populations.

The movement tasks assessed in the present series of studies consisted of standing postures, maximum trunk ROM movement tasks, and thoracic ROM movement tasks. Trunk and thoracic extension movement tasks were not included in the study due to instrumentation constraints. As well, with the marker cluster set, a maximally extended trunk posture would cause the marker clusters to touch or overlap, which would limit the system’s ability to distinguish between markers. Participants were tested in a highly controlled laboratory setting, and whether these results would apply to similar tasks performed in a field setting remains to be determined. The movement tasks that were tested were standardized in order to control the effects of motion of adjacent segments (head and arms) on the motion and muscle activation of the different regions in the spine. Participants were given specific instructions with regards to the positions of the head, arms, and knees, as well as the target position of the trunk. These measures were deemed to be necessary experimental controls. However, it is unknown if the results of the present studies would generalize to activities of daily living, functional tasks, or task-oriented activities (for example, lifting, putting on shoes, etc.). To assess more functional tasks, participants could be provided with instructions focusing on the task to be performed (for example, “lift the box”), with little to no indication of a preferred technique or final body position. As this approach would enable participants to select

their own movement strategies and means of completing a task, the conclusions may potentially vary from those drawn from the present studies. In addition, tasks encompassing different levels of effort (for example, picking up a light object such as a pen, compared to a weighted box) and greater contributions from the extremities would also be important to fully characterize motion and muscle activation characteristics during functional tasks.

Spinal motion was quantified through the use of skin-mounted marker clusters, thereby introducing small amounts of artefact from the movement of the skin relative to the underlying bone (Heneghan & Balanos, 2010; Leardini et al., 2005). While resources were not available to directly quantify the amount of soft tissue artefact, previous work has concluded that surface markers mounted over the spinous processes of the vertebrae represent the position of the spinous processes with very strong correlations (Morl & Blickhan, 2006), likely due to the tight bonding of the overlying connective tissue to the bone (Gal et al., 1997; Lundberg, 1996). Further, during the pilot stages of the study, the clusters were visually observed to be minimally affected by skin movement. With respect to the placements of the marker clusters, it would have been preferable to place clusters on adjacent or every second vertebra, to ensure that motion was monitored at as many levels as possible. However, this was not possible due to technical limitations of the Vicon motion capture system, in that it is a passive-reflective system. When markers were placed in very close proximity to each other, the system was not able to distinguish the individual markers. This has been identified as a limitation of cluster marker sets (as opposed to individual markers) by Ranavolo et al. (2013). Placing the marker clusters on

every third vertebra along the thoracic spine enabled the collection of data at the most vertebral sites, while still maintaining the integrity of the kinematic data. The results of the present study indicated that with clusters located at every third vertebra, it was still possible to eliminate some clusters for collection. Taken together with the results of Ranavolo et al. (2013), this suggests that additional clusters would not have been necessary and likely would not have changed the results of the present study in terms of the general landmarks or regions of interest for measuring motion along the spine.

8.4 Future Directions

Future work is necessary to address the limitations in Section 8.3. Additional studies are required to determine the extent to which the findings of these studies differ in populations such as individuals with LBP or older adults, as these populations have been shown to exhibit different motion and muscle activation characteristics than young individuals asymptomatic for back pain. Further, functional tasks such as activities of daily living should be investigated to determine whether the results of the studies are applicable beyond the controlled fundamental tasks of standing and ROM tasks. Ideally, an attempt should be made to verify the accuracy of the skin-mounted marker clusters employed in the present study using a medical imaging technique. Finally, kinetic data will aid in validating the results of the studies presented in Chapters 5 and 6, and in extending the results of the study presented in Chapter 7 to estimate the effects of non-neutral thoracic postures on spinal loading.

The thoracic spine demonstrates differences in motion and muscle activation characteristics both along its length and compared to the adjacent lumbar region, and therefore needs to be monitored or accounted for during the investigation of spinal mechanics. Knowledge of the behaviour of the thoracic spine and interactions between the thoracic and lumbar spine regions is crucial, in that it may help to more clearly understand the behaviour of the spine as a whole. In addition, comparison of the present findings to individuals with LBP and investigation of the links between altered motion and muscle activation characteristics and LBP may aid in a better understanding of pain mechanisms in the thoracic and lumbar spine regions. Clinically, the results may provide guidance for qualitative assessments of movement coordination or muscle activation, to aid in the identification of aberrant spinal motion or activation patterns. Taken together, the results of this dissertation can also aid in the development or extension of predictive joint loading models for the thoracic and lumbar spine regions, by providing insight into the kinematic and muscle activation data necessary as inputs for the prediction of compression and shear forces in the thoracic spine. The development of such a model would enable the investigation of loading pathways along the length of the spine, as well as the relationships between loading variables and pain in both the thoracic and lumbar spine regions.

8.5 Hypotheses Revisited

8.5.1 Global Thesis Objective

Purpose: To determine if it is necessary to monitor or account for the thoracic spine during the investigation of trunk and lumbar mechanics.

Hypothesis: It will be necessary to monitor or account for the kinematic and muscle activation characteristics of the thoracic spine during the investigation of trunk and lumbar mechanics.

The thoracic spine demonstrates differences in motion and muscle activation characteristics both along its length and compared to the lumbar spine, and also affects the behaviour of the lumbar spine. Therefore, the thoracic spine needs to be monitored or accounted for during the investigation of trunk and lumbar mechanics. Knowledge of the behaviour of the thoracic spine, as well as the interactions between the thoracic spine and adjacent regions, may help to more clearly define the behaviour of the spine as a whole. Ultimately, comparison of the present findings to individuals with LBP and investigation of the links between altered motion and muscle activation characteristics and LBP may provide insight into pain mechanisms in the thoracic and lumbar spine regions.

Verdict: Hypothesis accepted.

8.5.2 Specific Purposes

The specific purposes addressed by this dissertation were:

- 1. To evaluate the repeatability and reliability of kinematic and EMG measures, and to determine the minimum number of trials required to achieve repeatability and reliability.*

Hypothesis: 1a) The repeatability and reliability of both kinematic and EMG measures will be relatively high ($ICC > 0.90$; $SEM\% < 25\%$; no significant differences from other trial sets) during upright standing and maximum trunk ROM movement tasks. 1b) Kinematic measures will demonstrate higher repeatability and reliability than EMG measures.

Verdict: Hypothesis 1A accepted.

Verdict: Hypothesis 1B accepted.

The repeatability and reliability of most measures was very high (0.95 and 0.92 for all measures and all sets of trials for kinematic and EMG measures, respectively), resulting in 59%, 68%, 78%, 86%, and 91% of measures producing repeatable and reliable values with two, three, four, five, and ten trials, respectively. The repeatability and reliability of the EMG measures was slightly lower than that of the kinematic measures, although overall the EMG measures were still very high. This potentially suggests that while there may be differences in activation strategies between individuals, the strategies used by the same individual over a series of repetitions may be relatively consistent.

2. *To determine which head and arm positions enabled the greatest voluntary ROM in spine angle measures during maximum flexion, lateral bend, and axial twist.*

Hypothesis: 2a) The greatest angles will be elicited from the upper spinal regions (head, thoracic, and segmented thoracic measures) by the active head and crossed arm positions. 2b) The neutral head (aligned with the trunk) and loose arm positions will elicit the greatest angles for the lower and global regions (lumbar, trunk, and pelvis) for maximum flexion and bending, and neutral head and abducted arms for maximum twist.

Verdict: Hypothesis 2A accepted for maximum bend; rejected for maximum flex and maximum twist (arm position).

Verdict: Hypothesis 2B rejected (head position).

The results regarding the effects of head position agreed with the hypothesized results for the upper regions (head, cervico-thoracic, thoracic, upper-thoracic, mid-thoracic, and lower-thoracic), in that an active head tended to elicit greater angles for all three movement tasks. Generally, there was no effect of head position for the lower and global regions. Regarding arm positions, the hypothesis was supported for the MaxBend task, with greater angles for the upper regions with crossed arms and for the lower regions with loose arms. Conversely, for MaxFlex and MaxTwist, regions with differences due to arm position generally displayed greater angles with loose and abducted arms, respectively.

3. *To determine the set of segments necessary to sufficiently characterize the kinematics of the trunk and specifically the thoracic spine.*

Hypothesis: 3a) For each movement task examined, not all collected segments will be necessary to characterize the kinematics of the thoracic spine. 3b) In order to sufficiently characterize thoracic spine motion in all directions, a marker set consisting of five to six clusters will be required.

Verdict: Hypothesis 3A accepted.

Verdict: Hypothesis 3B rejected.

Marker clusters and locations were relatively consistent across the tested movement tasks. For the majority of movement tasks, a four-cluster marker set was

sufficient to capture the necessary information relating to thoracic motion, with clusters at the C₇, T₆, T₁₂, and L₅ vertebrae, which were fewer clusters than originally hypothesized. The only movement task for which this marker set was not sufficient was ThorTwist.

4. *To investigate the interactions between the thoracic and lumbar musculature, and to determine which superficial muscles were necessary to adequately capture the gross trunk muscle activation characteristics.*

Hypothesis: 4a) The majority of tested muscles will be required to quantify the muscle activation characteristics of the trunk. 4b) Muscles from both the anterior and posterior sides of the body will be required to quantify the gross trunk muscle activation characteristics.

Verdict: Hypothesis 4A accepted.

Verdict: Hypothesis 4B accepted.

For movement direction-specific recommendations, ten, thirteen, and twelve muscles were required to quantify the muscle activation characteristics of the trunk during flexion, lateral bend, and axial twist tasks, involving muscles from both the anterior and posterior sides of the body. Across all movement directions, four muscles (three abdominal, one back) were strongly related to at least one other muscle, and therefore these muscles could all be considered as options for elimination.

5. *To determine the extent of the increases in co-contraction in the lumbar musculature during deviation of the thoracic spine from an upright posture, and to determine whether a relationship exists between the angles of the thoracic spine and co-contraction within the lumbar spine.*

Hypothesis: 5a) Co-contraction in the lumbar spine will increase in response to non-neutral thoracic postures, compared to upright standing. 5b) Thoracic angles will be positively associated with increased co-contraction in the lumbar spine.

Verdict: Hypothesis 5A accepted.

Verdict: Hypothesis 5B accepted.

Increases in co-contraction were observed in the lumbar spine in response to thoracic movement, compared to Upright. On average, co-contraction in the lumbar musculature increased by approximately 67%, 45%, and 55% from Upright for the ThorFlex, ThorBend, and ThorTwist movement tasks. Significant, positive correlations of weak to moderate strength were identified between thoracic angles and activation measures in the lumbar spine.

8.6 General Conclusions

This dissertation quantified thoracic spine characteristics relating to kinematic and muscle activation measures, specifically repeatability and reliability, the effects of adjacent segments, relationships in motion and muscle activation, and co-contraction. Based on the findings of this dissertation, the thoracic spine demonstrates differences in motion and muscle activation characteristics both along its length and compared to the lumbar spine. Knowledge of the behaviour of the thoracic spine, as well as the interactions between the thoracic spine and adjacent regions, constitutes the first step to more clearly understanding the behaviour of the spine as a whole, with the ultimate goal of identifying mechanisms of pain in the thoracic and lumbar spine regions. The thoracic

spine is typically represented as a single rigid segment for research, clinical, and/or ergonomic applications. However, based on the findings of the five presented studies, it appears that the thoracic spine needs to be monitored or accounted for during the investigation of spinal mechanics, taking into consideration the kinematic and activation changes that occur along its length (as opposed to representing it as a single rigid entity).

References

Adams MA, Mannion AF, Dolan P. Personal risk factors for first-time low back pain.

Spine 1999;24(23):2497-505.

Alexander LA, Hancock E, Agouris I, Smith FW, MacSween A. The response of the

nucleus pulposus of the lumbar intervertebral discs to functionally loaded positions.

Spine 2007;32(14):1508-12.

Allison GT, Fukushima S. Estimating three-dimensional spinal repositioning error: The

impact of range, posture, and number of trials. Spine 2003;28(22):2510-6.

Alschuler KN, Neblett R, Wiggert E, Haig AJ, Geisser ME. Flexion-relaxation and

clinical features associated with chronic low back pain: A comparison of different

methods of quantifying flexion-relaxation. Clinical Journal of Pain 2009;25:760-6.

Andersson EA, Oddsson LIE, Grundström H, Nilsson J, Thorstensson A. EMG activities

of the quadratus lumborum and erector spinae muscles during flexion-relaxation and

other motor tasks. Clinical Biomechanics 1996;11(7):392-400.

Andriacchi T, Schultz A, Belytschko T, Galante J. A model for studies of mechanical

interactions between the human spine and rib cage. Journal of Biomechanics

1974;7:497-507.

Arlotta M, LoVasco G, McLean L. Selective recruitment of the lower fibers of the

trapezius muscle. Journal of Electromyography and Kinesiology 2011;21:403-10.

Astfalck RG, O'Sullivan PB, Straker LM, Smith AJ, Burnett A, Caneiro JP, et al. Sitting

postures and trunk muscle activity in adolescents with and without nonspecific

chronic low back pain. Spine 2010;35(14):1387-95.

- Atkinson G, Nevill AM. Statistical methods for assessing measurement error (reliability) in variables relevant to sports medicine. *Sports Medicine* 1998;26(4):217-38.
- Beneck GJ, Baker LL, Kulig K. Spectral analysis of EMG using intramuscular electrodes reveals non-linear fatigability characteristics in persons with chronic low back pain. *Journal of Electromyography and Kinesiology* 2013;23:70-7.
- Bigos SJ, Spengler DM, Martin NA, Zeh J, Fisher L, Nachemson A. Back injuries in industry: A retrospective study. III. Employee-related factors. *Spine* 1986;11(3):252-6.
- Bird AR, Payne CB. Foot function and low back pain. *The Foot* 1999;9:175-80.
- Brereton LC, McGill SM. Frequency response of spine extensors during rapid isometric contractions: Effects of muscle length and tension. *Journal of Electromyography and Kinesiology* 1998;8:227-32.
- Briggs AM, Bragge P, Smith AJ, Govil D, Straker LM. Prevalence and associated factors for thoracic spine pain in the adult working population: A literature review. *Journal of Occupational Health* 2009;51:177-92.
- Briggs AM, van Dieen H, Wrigley TV, Greig AM, Phillips B, Lo SK, et al. Thoracic kyphosis affects spinal loads and trunk muscle force. *Physical Therapy* 2007;87(5):595-607.
- Brown SHM, McGill SM. Co-activation alters the linear versus non-linear impression of the EMG-torque relationship of trunk muscles. *Journal of Biomechanics* 2008;41:491-7.

- Brown SHM, Vera-Garcia FJ, McGill SM. Effects of abdominal muscle coactivation on the externally preloaded trunk: Variations in motor control and its effect on spine stability. *Spine* 2006;31(13):E387-93.
- Bruce-Low S, Smith D, Burnet S, Fisher J, Bissell G, Webster L. One lumbar extension training session per week is sufficient for strength gains and reductions in pain in patients with chronic low back pain ergonomics. *Ergonomics* 2012;55(4):500-7.
- Burnett A, O'Sullivan P, Ankarberg L, Gooding M, Nelis R, Offermann F. Lower lumbar spine axial rotation is reduced in end-range sagittal postures when compared to a neutral spine posture. *Manual Therapy* 2008;13:300-6.
- Burnett A, O'Sullivan PB, Caneiro JP, Krug R, Bochmann F, Helgestad GW. An examination of the flexion-relaxation phenomenon in the cervical spine in lumbo-pelvic sitting. *Journal of Electromyography and Kinesiology* 2009;19(4):229-36.
- Busscher I, van Dieen JH, Kingma I, van der Veen AJ, Gijsbertus V, Veldhuizen AG. Biomechanical characteristics of different regions of the human spine: An in vitro study on multilevel spinal segments. *Spine* 2009;34(26):2858-64.
- C-Motion Research Biomechanics Wiki-Documentation. Marker set guidelines. Retrieved August 16, 2014, available [www.c-motion.com/v3dwiki/index.php?title=Marker Set Guidelines](http://www.c-motion.com/v3dwiki/index.php?title=Marker_Set_Guidelines).
- C-Motion Research Biomechanics Wiki-Documentation. Constructing the coordinate system. [www.c-motion.com/v3dwiki/index.php?title=Constructing the Segment Coordinate System](http://www.c-motion.com/v3dwiki/index.php?title=Constructing_the_Segment_Coordinate_System)

- Callaghan JP, Dunk NM. Examination of the flexion relaxation phenomenon in erector spinae muscles during short duration slumped sitting. *Clinical Biomechanics* 2002;17:353-60.
- Callaghan JP, McGill SM. Low back joint loading and kinematics during standing and unsupported sitting. *Ergonomics* 2001;44(3):280-94.
- Caneiro JP, O'Sullivan P, Burnett A, Barach A, O'Neil D, Tveit O, et al. The influence of different sitting postures on head/neck posture and muscle activity. *Manual Therapy* 2010;15:54-60.
- Carlsson H, Rasmussen-Barr E. Clinical screening tests for assessing movement control in non-specific low-back pain. A systematic review of intra- and inter-observer reliability studies. *Manual Therapy* 2013;18:103-10.
- Cavanaugh JT, Shinberg M, Ray L, Shipp KM, Kuchibhatla M, Schenkman M. Kinematic characterization of standing reach: Comparison of younger vs. older subjects. *Clinical Biomechanics* 1999;14:271-9.
- Centers for Disease Control and Prevention. Work-related musculoskeletal disorders. Retrieved July 16, 2014, available www.cdc.gov/workplacehealthpromotion/implementation/topics/disorders.html.
- Chan PY, Wong HK, Goh JCH. The repeatability of spinal motion of normal and scoliotic adolescents during walking. *Gait & Posture* 2006;24:219-28.
- Chatfield C. *The analysis of time series*. New York: Chapman and Hall; 1984.
- Cholewicki J, McGill SM. Mechanical stability of the in vivo lumbar spine: Implications for injury and chronic low back pain. *Clinical Biomechanics* 1996;11(1):1-15.

- Claus AP, Hides JA, Mosely GL, Hodges PW. Is 'ideal' sitting posture real?"
Measurement of spinal curves in four sitting postures. *Manual Therapy* 2009;14:404-8.
- Colloca CJ, Hinrichs RN. The biomechanical and clinical significance of the lumbar erector spinae flexion-relaxation phenomenon: A review of literature. *Journal of Manipulative and Physiological Therapeutics* 2005;28:623-31.
- Crosbie J, Kilbreath SL, Dylke E. The kinematics of the scapulae and spine during a lifting task. *Journal of Biomechanics* 2010;43:1302-9.
- Crosbie J, Kilbreath SL, Hollmann L, York S. Scapulohumeral rhythm and associated spinal motion. *Clinical Biomechanics* 2008;23:184-92.
- Csernatony Z, Molnar S, Hunya Z, Mano S, Kiss L. Biomechanical examination of the thoracic spine – The axial rotation moment and vertical loading capacity of the transverse process. *Journal of Orthopaedic Research* 2011;29:1904-9.
- D'Hooze R, Hodges P, Tsao H, Hall L, MacDonald D, Danneels L. Altered trunk muscle coordination during rapid trunk flexion in people in remission of recurrent low back pain. *Journal of Electromyography and Kinesiology* 2013;23:173-81.
- Dankaerts W, O'Sullivan P, Burnett A, Straker L, Davey P, Gupta R. Discriminating healthy controls and two clinical subgroups of nonspecific chronic low back pain patients using trunk muscle activation and lumbosacral kinematics of postures and movements: A statistical classification model. *Spine* 2009;34(15):1610-8.
- Dankaerts W, O'Sullivan PB, Burnett AF, Straker LM, Daneels LA. Repeatability of EMG measurements for trunk muscles during maximal and sub-maximal voluntary

- isometric contractions in health controls and CLBP patients. *Journal of Electromyography and Kinesiology* 2004;14(3):333-42.
- De Luca CJ. The use of surface electromyography in biomechanics. *Journal of Applied Biomechanics* 1997;13:135-63.
- Dos Santos CM, Ferreira G, Malacco PL, Sabino GS, de Souza Moraes GF, Felicio DC. Intra and inter examiner reliability and measurement error of goniometer and digital inclinometer use. *Revista Brasileira de Medicina do Esporte* 2012;18(1).
- Drake JDM, Callaghan JP. Do flexion/extension postures affect the in vivo passive lumbar spine response to applied axial twist moments? *Clinical Biomechanics* 2008;23(5):510-9.
- Drake JDM, Callaghan JP. Elimination of electrocardiogram contamination from electromyogram signals: An evaluation of currently used removal techniques. *Journal of Electromyography and Kinesiology* 2006;16:175-87.
- Drake JDM, Fischer SL, Brown SH, Callaghan JP. Do exercise balls provide a training advantage for trunk extensor exercises? A biomechanical evaluation. *Journal of Manipulative and Physiological Therapeutics* 2006;29(5):354-62.
- Dunk NM, Callaghan JP. Gender-based differences in postural responses to seated exposures. *Clinical Biomechanics* 2005;20:1101-10.
- Dunk NM, Callaghan JP. Lumbar spine movement patterns during prolonged sitting differentiate low back pain developers from matched asymptomatic controls. *Work* 2010;35:3-14.

- Dunk NM, Lalonde J, Callaghan JP. Implications for the use of postural analysis as a clinical diagnostic tool: Reliability of quantifying upright standing spinal postures from photographic images. *Journal of Manipulative & Physiological Therapeutics* 2005;28:386-92.
- Edmondston SJ, Aggerholm M, Elfving S, Flores N, Ng C, Smith R. Influence of posture on the range of axial rotation and coupled lateral flexion of the thoracic spine. *Journal of Manipulative and Physiological Therapeutics* 2007a;30:193-9.
- Edmondston SJ, Chan HY, Ngai GCW, Warren MLR, Williams JM, Glennon S. Postural neck pain: An investigation of habitual sitting posture, perception of 'good' posture and cervicothoracic kinaesthesia. *Manual Therapy* 2007b;12:363-71.
- Edmondston SJ, Sharp M, Symes A, Alhabib N, Allison GT. Changes in mechanical load and extensor muscle activity in the cervico-thoracic spine induced by sitting posture modification. *Ergonomics* 2011a;54(2):179-86.
- Edmondston SJ, Singer KP. Thoracic spine: Anatomical and biomechanical considerations for manual therapy. *Manual Therapy* 1997;2(3):132-43.
- Edmondston S, Waller R, Vallin P, Holthe A, Noebauer A, King E. Thoracic spine extension mobility in young adults: Influence of subject position and spinal curvature. *Journal of Orthopaedic & Sports Physical Therapy* 2011b;41(4):266-73.
- Esola MA, McClure PW, Fitzgerald GK, Siegler S. Analysis of lumbar spine and hip motion during forward bending in subjects with and without a history of low back pain. *Spine* 1996;21(1):71-8.

- Essendrop M, Maul I, Laubli T, Riihimaki H, Schibye B. Measures of low back function: A review of reproducibility studies. *Clinical Biomechanics* 2002;17:235-49.
- Essendrop M, Schibye B, Hansen K. Reliability of isometric muscle strength tests for the trunk, hands and shoulders. *International Journal of Industrial Ergonomics* 2001;28:379-87.
- Ferguson SA, Marras WS, Burr DL, Davis KG, Gupta P. Differences in motor recruitment and resulting kinematics between low back pain patients and asymptomatic participants during lifting exertions. *Clinical Biomechanics* 2004;19(10):992-9.
- Ferguson SA, Marras WS, Crowell RR. Three-dimensional functional capacity of normals and low back pain patients. *Proceedings of the Human Factors and Ergonomics Society 40th Annual Meeting* 1996a;40:737-41.
- Ferguson SA, Marras WS, Crowell RR. Dynamic low back functional motion capacity evaluation. *Journal of Occupational Rehabilitation* 1996b;6(4):203-14.
- Fujimori T, Iwasaki M, Nagamoto Y, Ishii T, Kashii M, Murase T, et al. Kinematics of the thoracic spine in trunk rotation: In vivo 3-dimensional analysis. *Spine* 2012;37(21):E1318-25.
- Fujimori T, Iwasaki M, Nagamoto Y, Matsuo Y, Ishii T, Sugiura T, et al. Kinematics of the thoracic spine in trunk lateral bending: In vivo three-dimensional analysis. *The Spine Journal* 2014 (in press).

- Gal J, Herzog W, Kawchuk G, Conway P, Zhang YT. Measurements of vertebral translations using bone pins, surface markers, and accelerometers. *Clinical Biomechanics* 1997;12(5):337-40.
- Geisser ME, Ranavaya M, Haig AJ, Roth RS, Zucker R, Ambroz C, et al. A meta-analytic review of surface electromyography among persons with low back pain and normal, healthy controls. *Journal of Pain* 2005;6(11):711-26.
- German RZ, Crompton AW, Thexton AJ. Variation in EMG activity: A hierarchical approach. *Integrative and Comparative Biology* 2008;48(2):283-93.
- Gibbons P, Tehan P. Muscle energy concepts and coupled motion of the spine. *Manual Therapy* 1998;3(2):95-101.
- Govindu NK, Babski-Reeves K. Effects of personal, psychosocial and occupational factors on low back pain severity in workers. *International Journal of Industrial Ergonomics* 2014;44:335-41.
- Graham RB, Oikawa LY, Ross GB. Comparing the local dynamic stability of trunk movements between varsity athletes with and without non-specific low back pain. *Journal of Biomechanics* 2014;47:1459-64.
- Granata KP, Lee PE, Franklin TC. Co-contraction recruitment and spinal load during isometric trunk flexion and extension. *Clinical Biomechanics* 2005a;20:1029-37.
- Granata K, Lee P, Franklin T. Co-contraction recruitment and spinal load during isometric pushing tasks. *Proceedings of the Human Factors and Ergonomics Society Annual Meeting* 2005b;49:1330-3.

- Granata KP, Marras WS. An EMG-assisted model of loads on the lumbar spine during asymmetric trunk extensions. *Journal of Biomechanics* 1993;26(12):1429-38.
- Granata KP, Marras WS. Cost-benefit of muscle cocontraction in protecting against spinal instability. *Spine* 2000;25(11):1398-404.
- Granata KP, Slota GP, Wilson SE. Influence of fatigue in neuromuscular control of spinal stability. *Human Factors* 2004;46(1):81-91.
- Gregersen GG, Lucas DB. An in vivo study of the axial rotation of the human thoracolumbar spine. *Journal of Bone & Joint Surgery* 1967;49:247-62.
- Gregory DE, Callaghan JP. Prolonged standing as a precursor for the development of low back discomfort: An investigation of possible mechanisms. *Gait & Posture* 2008;28:86-92.
- Gregory DE, Dunk NM, Callaghan JP. Stability ball versus office chair: Comparison of muscle activation and lumbar spine posture during prolonged sitting. *Human Factors* 2006;48(1):142-53.
- Gregory DE, Narula S, Howarth SJ, Russell C, Callaghan JP. The effect of fatigue on trunk muscle activation patterns and spine postures during simulated firefighting tasks. *Ergonomics* 2008;51(7):1032-41.
- Grondin DE, Potvin JR. Effects of trunk muscle fatigue and load timing on spinal responses during sudden hand loading. *Journal of Electromyography and Kinesiology* 2009;19:e237-45.

- Helsing E, Reigo T, McWilliam J, Spangfort E. Cervical and lumbar lordosis and thoracic kyphosis in 8, 11 and 15 year old children. *European Journal of Orthodontics* 1987;9:129-38.
- Heneghan NR, Balanos GM. Soft tissue artifact in the thoracic spine during axial rotation and arm elevation using ultrasound imaging: A descriptive study. *Manual Therapy* 2010;15:599-602.
- Hidalgo B, Gilliaux M, Poncin W, Detrembleur C. Reliability and validity of a kinematic spine model during active trunk movement in healthy subjects and patients with chronic non-specific low back pain. *Journal of Rehabilitation Medicine* 2012;44:756-63.
- Horton WC, Kraiwattanapong C, Akamaru T, Minamide A, Park JS, Park MS, et al. The role of the sternum, costosternal articulations, intervertebral disc, and facets in thoracic sagittal plane biomechanics. *Spine* 2005;30(18):2014-23.
- Howarth SJ, Beach TAC, Pearson AJ, Callaghan JP. Using sitting as a component of job rotation strategies: Are lifting/lowering kinetics and kinematics altered following prolonged sitting. *Applied Ergonomics* 2009;40:433-9.
- Howarth SJ, Glisic D, Lee JGB, Beach TAC. Does prolonged seated deskwork alter the lumbar flexion relaxation phenomenon? *Journal of Electromyography and Kinesiology* 2013;23:587-93.
- Hoy D, Brooks P, Blyth F, Buchbinder R. The epidemiology of low back pain. *Best Practice & Research Clinical Rheumatology* 2010;24:769-81.

- Hubley-Kozey CL, Vezina MJ. Differentiating temporal electromyographic waveforms between those with chronic low back pain and healthy controls. *Clinical Biomechanics* 2002;17:621-9.
- Intolo P, Milosavljevic S, Baxter DG, Carman AB, Pal P, Munn J. The effect of age on lumbar range of motion: A systematic review. *Manual Therapy* 2009;15:596-604.
- Jensen C, Vasseljen O, Westgaard RH. The influence of electrode position on bipolar surface electromyogram recordings of the upper trapezius muscle. *European Journal of Applied Physiology* 1993;67:266-73.
- Johnson MB, Cacciatore TW, Hamill J, Van Emmerik REA. Multi-segmental torso coordination during the transition from sitting to standing. *Clinical Biomechanics* 2010;25:199-205.
- Kaigle AM, Wessberg P, Hansson TH. Muscular and kinematic behaviour of the lumbar spine during flexion-extension. *Journal of Spinal Disorders* 1998;11(2):163-74.
- Kellis E, Arabatzi F, Papadopoulos C. Muscle co-activation around the knee in drop jumping using the co-contraction index. *Journal of Electromyography and Kinesiology* 2003;13:229-38.
- Knutson LM, Soderberg GL, Ballantyne BT, Clarke WR. A study of various normalization procedures for within day electromyographic data. *Journal of Electromyography and Kinesiology* 1994;4(1):47-59.
- Kopec JA, Sayre EC, Esdaile JM. Predictors of back pain in a general population cohort. *Spine* 2003;29(1):70-8.

- Kumar S, Fagarasanu M, Naraya Y, Prasad N. Measures of localized spinal muscle fatigue. *Ergonomics* 2006;49(11):1092-110.
- Kuo YL, Tully EA, Galea MP. Video analysis of sagittal spinal posture in healthy young and older adults. *Journal of Manipulative and Physiological Therapeutics* 2009;32:210-5.
- Lariviere C, Gagnon D, Genest K. Controlling for out-of-plane lumbar moments during unidirectional trunk efforts: Learning and reliability issues related to trunk muscle activation estimates. *Journal of Electromyography and Kinesiology* 2014;24:531-41.
- Lariviere C, Gagnon D, Loisel P. The comparison of trunk muscles EMG activation between participants with and without chronic low back pain during flexion-extension and lateral bending tasks. *Journal of Electromyography and Kinesiology* 2000;10(2):79-91.
- Lau KT, Cheung KY, Chan KB, Chan MH, Lo KY, Chiu TTW. Relationships between sagittal postures of thoracic and cervical spine, presence of neck pain, neck pain severity and disability. *Manual Therapy* 2010;15:457-62.
- Leardini A, Chiari L, Della Croce U, Cappozzo A. Human movement analysis using stereophotogrammetry Part 3. Soft tissue artifact assessment and compensation. *Gait and Posture* 2005;21:212-25.
- Lee LJ, Coppieters MW, Hodges PW. Differential activation of the thoracic multifidus and longissimus thoracis during trunk rotation. *Spine* 2005;30(8):870-6.

- Lee NG, Lee JA, Kim JB. A comparison of three-dimensional spine kinematics during multidirectional trunk movement between elderly subjects with degenerative spine disease and healthy young adults. *Journal of Physical Therapy Science*, 2013;25:21-6.
- Lee RYW, Wong TKT. Relationship between the movements of the lumbar spine and hip. *Human Movement Science* 2002;21:481-94.
- Lewek MD, Rudolph KS, Snyder-Mackler L. Control of frontal plane knee laxity during gait in patients with medial compartment knee osteoarthritis. *Osteoarthritis and Cartilage* 2004;12:745-51.
- Li L, Caldwell GE. Coefficient of cross correlation and the time domain correspondence. *Journal of Electromyography and Kinesiology* 1999;9:385-9.
- Lomond KV, Henry SM, Hitt JR, DeSarno MJ, Bunn JY. Altered postural responses persist following physical therapy of general versus specific trunk exercises in people with low back pain. *Manual Therapy* 2014;19:425-32.
- Lundberg A. On the use of bone and skin markers in kinematics research. *Human Movement Science* 1996;15:411-22.
- Makhsous M, Lin F, Bankard J, Hendrix RW, Hepler M, Press J. Biomechanical effects of sitting with adjustable ischial and lumbar support on occupational low back pain: Evaluation of sitting load and back muscle activity. *BMC Musculoskeletal Disorders*, 2009;10(17).
- Marras WS, Ferguson SA, Gupta P, Bose S, Parnianpour M, Kim JY, et al. The quantification of low back disorder using motion measures: Methodology and validation. *Spine* 1999;24(20):2091-100.

- Marras WS, Lavendar SA, Leurgans SE, Fathallah FA, Ferguson SA, Allread WG, et al. Biomechanical risk factors for occupationally related low back disorders. *Ergonomics* 1995;38(2):377-410.
- Marras WS, Lavendar SA, Leurgans SE, Rajulu SL, Allread WG, Fathallah FA, et al. The role of dynamic three-dimensional trunk motion in occupationally-related low back disorders: The effect of workplace factors, trunk position, and trunk motion characteristics on risk of injury. *Spine* 1993a;18(5):617-28.
- Marras WS, Parnianpour M, Ferguson SA, Kim JY, Crowell RR, Simon SR. Quantification and classification of low back disorders based on trunk motion. *Journal of Physical and Rehabilitation Medicine* 1993b;3:218-35.
- Marshall PWM, Patel H, Callaghan JP. Gluteus medius strength, endurance, and co-activation in the development of low back pain during prolonged standing. *Human Movement Science* 2011;30:63-73.
- Masset DF, Piette AG, Malchaire JB. Relation between functional characteristics of the trunk and the occurrence of low back pain: Associated risk factors. *Spine* 1998;23(3):359-65.
- Mayer TG, Tencer AF, Kristoferson S, Mooney V. Use of noninvasive techniques for quantification of spinal range-of-motion in normal subjects and chronic low-back dysfunction patients. *Spine* 1984;9(6):588-95.
- McGill SM. Electromyographic activity of the abdominal and low back musculature during the generation of isometric and dynamic axial trunk torque: implications for lumbar mechanics. *Journal of Orthopaedic Research* 1991;9(1):91-103.

- McGill SM. A myoelectrically based dynamic three-dimensional model to predict loads on lumbar spine tissues during lateral bending. *Journal of Biomechanics* 1992;25(4):395-414.
- McGill SM. The biomechanics of low back injury: Implications on current practice in industry and the clinic. *Journal of Biomechanics* 1997;30(5):465-75.
- McGill SM. *Low back disorders: Evidence-based prevention and rehabilitation*. 2nd ed. Champaign, IL: Human Kinetics, 2007.
- McGill SM, Grenier S, Kavcic N, Cholewicki J. Coordination of muscle activity to assure stability of the lumbar spine. *Journal of Electromyography & Kinesiology* 2003;13:353-9.
- McGill SM, Norman RW. Partitioning of the L4-L5 dynamic moment into disc, ligamentous, and muscular components during lifting. *Spine* 1986;11(7):666-78.
- McGill SM, Yingling VR, Peach JP. Three-dimensional kinematics and trunk muscle myoelectric activity in the elderly spine – a database compared to young people. *Clinical Biomechanics* 1999;14:389-95.
- McGregor AH, McCarthy ID, Hughes SP. Motion characteristics of the lumbar spine in the normal population. *Spine* 1995;20(22):2421-8.
- McLean L. The effect of postural correction on muscle activation amplitudes recorded from the cervicobrachial region. *Journal of Electromyography and Kinesiology* 2005;15(6):527-35.

- Mieritz RM, Hartvigsen J, Boyle E, Jakobsen MD, Aagaard P, Bronfort G. Lumbar motion changes in chronic low back pain patients: A secondary analysis of data from a randomized clinical trial. *The Spine Journal* 2014 (in press).
- Mirka GA, Marras WS. A stochastic model of trunk muscle coactivation during trunk bending. *Spine* 1993;18(11):1396-409.
- Missenard O, Mottet D, Perrey S. The role of cocontraction in the impairment of movement accuracy with fatigue. *Experimental Brain Research* 2008;185:151-6.
- Montgomery T, Boocock M, Hing W. The effects of spinal posture and pelvic fixation on trunk rotation range of motion. *Clinical Biomechanics* 2011;26:707-12.
- Moon OK, Kim SH, Lee SB, An HJ, Kim BK, Kim NJ, et al. Thoracic coupled motions of Korean men in good health in their 20s. *Journal of Physical Therapy Science* 2014;26:87-91.
- Morl F, Blickhan R. Three-dimensional relation of skin markers to lumbar vertebrae of healthy subjects in different postures measured by open MRI. *European Spine Journal* 2006;15:742-51.
- Morris JM, Benner G, Lucas DB. An electromyographic study of the intrinsic muscles of the back in man. *Journal of Anatomy* 1962;96(4):509-20.
- Nairn BC, Azar NR, Drake JDM. Transient pain developers show increased abdominal muscle activity during prolonged sitting. *Journal of Electromyography and Kinesiology* 2013a;23:1421-7.
- Nairn BC, Chisholm SR, Drake JDM. What is slumped sitting? A kinematic and electromyographical evaluation. *Manual Therapy* 2013b;18:498-505.

- Nairn BC, Drake JDM. Impact of lumbar spine posture on thoracic spine motion and muscle activation patterns. *Human Movement Science* 2014;37:1-11.
- Neblett R, Mayer TG, Brede E, Gatchel RJ. Correcting abnormal flexion-relaxation in chronic lumbar pain: Responsiveness to a new biofeedback training protocol. *Clinical Journal of Pain* 2010;26(5):403-9.
- Nelson-Wong E, Alex B, Csepe D, Lancaster D, Callaghan JP. Altered muscle recruitment during extension from trunk flexion in low back pain developers. *Clinical Biomechanics* 2012;27:994-8.
- Nelson-Wong E, Callaghan JP. Is muscle co-activation a predisposing factor for low back pain development during standing? A multifactorial approach for early identification of at-risk individuals. *Journal of Electromyography and Kinesiology* 2010;20:256-63.
- Nelson-Wong E, Callaghan JP. Transient low back pain development during standing predicts future clinical low back pain in previously asymptomatic individuals. *Spine* 2014;39(6):E379-83.
- Nelson-Wong E, Gregory DE, Winter DA, Callaghan JP. Gluteus medius muscle activation patterns as a predictor of low back pain during standing. *Clinical Biomechanics* 2008;23:545-53.
- Nelson-Wong E, Howarth SJ, Callaghan JP. Acute biomechanical responses to a prolonged standing exposure in a simulated occupational setting. *Ergonomics* 2010;53(9):1117-28.

- Nelson-Wong E, Howarth S, Winter DA, Callaghan JP. Application of autocorrelation and cross-correlation analyses in human movement and rehabilitation research. *Journal of Orthopaedic & Sports Physical Therapy* 2009;39(4):287-95.
- Nelson-Wong E, Poupore K, Ingvalson S, Dehmer K, Piatte A, Alexander S, et al. Neuromuscular strategies for lumbopelvic control during frontal and sagittal plane movement challenges differ between people with and without low back pain. *Journal of Electromyography and Kinesiology* 2013;23:1317-24.
- Ng JKF, Kippers V, Parnianpour M, Richardson CA. EMG activity normalization for trunk muscles in subjects with and without back pain. *Medicine & Science in Sports & Exercise* 2002;34(7):1082-6.
- Ng JKF, Parnianpour M, Kippers V, Richardson CA. Reliability of electromyographic and torque measures during isometric axial rotation exertions of the trunk. *Clinical Neurophysiology* 2003;114:2355-61.
- Norman R, Wells R, Neumann P, Frank J, Shannon H, Kerr M, et al. A comparison of peak vs cumulative physical work exposure risk factors for the reporting of low back pain in the automotive industry. *Clinical Biomechanics* 1998;13:561-73.
- O'Bryan S, Brown NAT, Billaut F, Rouffet DM. Changes in muscle coordination and power output during sprint cycling. *Neuroscience Letters* 2014;576:11-6.
- Oda I, Abumi K, Cunningham BW, Kaneda K, McAfee PC. An in vitro human cadaveric study investigating the biomechanical properties of the thoracic spine. *Spine* 2002;27(3):E64-70.

- Oda I, Abumi K, Lu D, Yasuhiro S, Kiyoshi K. Biomechanical role of the posterior elements, costovertebral joints, and rib cage in the stability of the thoracic spine. *Spine* 1996;21(12):1423-9.
- Oxland TR, Lin RM, Panjabi MM. Three-dimensional mechanical properties of the thoracolumbar junction. *Journal of Orthopaedic Research* 1992;10:573-80.
- Panjabi M, Yamamoto I, Oxland T, Crisco J. How does posture affect coupling in the lumbar spine? *Spine* 1989;14(9):1002-11.
- Panjabi MM, Brand RA, White AA. Mechanical properties of the human thoracic spine as shown by three-dimensional load-displacement curves. *Journal of Bone & Joint Surgery* 1976a;58:642-52.
- Panjabi MM, Brand RA, White AA. Three-dimensional flexibility and stiffness properties of the human thoracic spine. *Journal of Biomechanics* 1976b;9:185-92.
- Panjabi MM, Takata K, Goel V, Federico D, Oxland T, Duranceau J, et al. Thoracic human vertebrae: Quantitative three-dimensional anatomy. *Spine* 1991;16(8):888-901.
- Peach JP, Sutarno CG, McGill SM. Three-dimensional kinematics and trunk muscle myoelectric activity in the young lumbar spine: A database. *Archives of Physical Medicine and Rehabilitation* 1998;79:663-9.
- Pearcy MJ. Twisting mobility of the human back in flexed postures. *Spine* 1993;18(1):114-9.
- Pearcy MJ, Hindle RJ. New method for the non-invasive three-dimensional measurement of human back movement. *Clinical Biomechanics* 1989;4:73-9.

- Pearcy MJ, Tibrewal SB. Axial rotation and lateral bending in the normal lumbar spine measured by three-dimensional radiography. *Spine* 1984;9(6):582-7.
- Pitcher MJ, Behm DG, MacKinnon SN. Reliability of electromyographic and force measures during prone isometric back extension in subjects with and without low back pain. *Applied Physiology, Nutrition, and Metabolism* 2008;33:52-60.
- Pope MH, Goh KL, Magnusson ML. Spine ergonomics. *Annual Review of Biomedical Engineering* 2002;4:49-68.
- Potvin JR, O'Brien PR. Trunk muscle co-contraction increases during fatiguing, isometric, lateral bend exertions. *Spine* 1998;23(7):774-81.
- Preuss RA, Popovic MR. Three-dimensional spine kinematics during multidirectional, target-directed trunk movement in sitting. *Journal of Electromyography and Kinesiology* 2010;20:823-32.
- Radebold A, Cholewicki J, Polzhofer GK, Greene, HS. Impaired postural control of the lumbar spine is associated with delayed muscle response times in patients with chronic idiopathic low back pain. *Spine* 2001;26(7):724-30.
- Ranavolo A, Don R, Draicchio F, Bartolo M, Serrao M, Padua L, et al. Modelling the spine as a deformable body: Feasibility of reconstruction using an optoelectronic system. *Applied Ergonomics* 2013;44:192-9.
- Reeves NP, Popovich Jr. JM, Priess MC, Cholewicki J, Choi J, Radcliffe CJ. Reliability of assessing trunk motor control using position and force tracking and stabilization tasks. *Journal of Biomechanics* 2014;47:44-9.

- Roe C, Steingrimsdottir OA, Knardahl S, Bakke ES, Vollestad NK. Long-term repeatability of force, endurance time and muscle activity during isometric contractions. *Journal of Electromyography and Kinesiology* 2006;16:103-13.
- Roussouly P, Pinheiro-Franco JL. Sagittal parameters of the spine: Biomechanical approach. *European Spine Journal* 2011;20:S578-85.
- Rudolph KS, Axe MJ, Snyder-Mackler L. Dynamic stability after ACL injury: Who can hop? *Knee Surgery, Sports Traumatology, Arthroscopy* 2000;8:262-9.
- Schinkel-Ivy A, Nairn BC, Drake JDM. Investigation of trunk muscle co-contraction and its association with low back pain development during prolonged sitting. *Journal of Electromyography and Kinesiology* 2013;23:778-86.
- Schinkel-Ivy A, Pardisnia S, Drake JDM. Head and arm positions that elicit maximal voluntary trunk range-of-motion measures. *Journal of Applied Biomechanics* 2014 (accepted July 1, 2014).
- Shaffer HB, Lauder GV. Aquatic prey capture in ambystomatid salamanders: Patterns of variation in muscle activity. *Journal of Morphology* 1985;183:273-84.
- Shan X, Wei Y, Chen Z, Fan L, Shi W, Yang S. Effect of leg support on muscle cross-correlation of bilateral erector spinae during trunk flexion-extension performance. *Gait and Posture* 2014;39:161-5.
- Sheeran L, Sparkes V, Caterson B, Busse-Morris M, van Deursen R. Spinal position sense and trunk muscle activity during sitting and standing in nonspecific chronic low back pain. *Spine* 2012;37(8):E486-95.

- Shin G, Mirka GA. An in vivo assessment of the low back response to prolonged flexion: Interplay between active and passive tissues. *Clinical Biomechanics* 2007;22:965-71.
- Shum GLK, Crosbie J, Lee RYW. Effect of low back pain on the kinematics and joint coordination of the lumbar spine and hip during sit-to-stand and stand-to-sit. *Spine*. 2005a;30(17):1998-2004.
- Shum GLK, Crosbie J, Lee RYW. Symptomatic and asymptomatic movement coordination of the lumbar spine and hip during an everyday activity. *Spine*. 2005b;30(23):E697-702.
- Shum GLK, Crosbie J, Lee RYW. Movement coordination of the lumbar spine and hip during a picking up activity in low back pain subjects. *European Spine Journal* 2007;16:749-58.
- Sizer PS, Brismée J-M, Cook, C. Coupling behavior of the thoracic spine: A systematic review of the literature. *Journal of Manipulative and Physiological Therapeutics* 2007;30:390-9.
- Solomonow M, Baratta RV, Banks A, Freudenberger C, Zhou BH. Flexion-relaxation response to static lumbar flexion in males and females. *Clinical Biomechanics* 2003;18:273-9.
- Sparto PJ, Parnianpour M. Generalizability of trunk muscle EMG and spinal forces. *IEEE Engineering in Medicine and Biology Magazine* 2001;20(6):72-81.
- Stanley SK, Ghanayem AJ, Voronov LI, Havey RM, Paxinos O, Carandang G, et al. Flexion-extension response of the thoracolumbar spine under compressive follower preload. *Spine* 2004;29(22):E510-4.

- Stevens VK, Bouche KG, Mahieu NN, Cambier DC, Vanderstraeten GG, Danneels LA. Reliability of a functional clinical test battery evaluating postural control, proprioception and trunk muscle activity. *American Journal of Physical Medicine & Rehabilitation* 2006;85:727-36.
- Stevenson JM, Weber C, Smith JT, Dumas GA, Albert WJ. A longitudinal study of the development of low back pain in an industrial population. *Spine* 2001;26(12):1370-7.
- Stokes IAF, Gardner-Morse MG, Henry SM. Abdominal muscle activation increases lumbar spinal stability: Analysis of contributions of different muscle groups. *Clinical Biomechanics* 2011;26:797-803.
- Strahan AD, Burnett AF, Caneiro JP, Doyle MM, O'Sullivan PB, Goodman C. Differences in spinopelvic kinematics in sweep and scull ergometer rowing. *Clinical Journal of Sport Medicine* 2011;21(4):330-6.
- Swinscow TDV. Correlation and regression. In: *Statistics at square one*. 9th ed. London: BMJ Publishing Group, 1997. p. 75-85.
- Tawackoli W, Marco R, Liebschner MAK. The effect of compressive axial preload on the flexibility of the thoracolumbar spine. *Spine* 2004;29(9):988-93.
- Thelen DG, Schultz AB, Ashton-Miller JA. Co-contraction of lumbar muscles during the development of time-varying triaxial moments. *Journal of Orthopaedic Research* 1995;13:390-8.
- Theodoridis D, Ruston S. The effect of shoulder movements on thoracic spine 3D motion. *Clinical Biomechanics* 2002;17:418-21.

- Thiese MS, Hegmann KT, Wood EM, Garg A, Moore JS, Kapellusch JM, et al. Low-back pain ratings for lifetime, 1-month period, and point prevalences in a large occupational population. *Human Factors* 2014;56(1):86-97.
- Tissot F, Messing K, Stock S. Studying the relationship between low back pain and working postures among those who stand and those who sit most of the working day. *Ergonomics* 2009;52(11):1402-18.
- Tojima M, Ogata N, Yozu A, Sumitani M, Haga N. A novel three-dimensional motion analysis method for measuring the lumbar spine range of motion: Repeatability and reliability compared with an electrogoniometer. *Spine* 2013;38(14):849-906.
- Tortora GJ. *Principles of human anatomy*, 10th ed. Hoboken, NJ: John Wiley & Sons, Inc., 2005.
- Troke M, Schuit D, Petersen CM. Reliability of lumbar spinal palpation, range of motion, and determination of position. *BMC Musculoskeletal Disorders* 2007;8:103.
- Tsang SMH, Szeto GPY, Lee RYW. Normal kinematics of the neck: The interplay between the cervical and thoracic spines. *Manual Therapy* 2013;18(5):431-7.
- Van Dieen JH, Kingma I. Effects of antagonistic co-contraction on differences between electromyography based and optimization based estimates of spinal forces. *Ergonomics* 2005;48(4):411-26.
- Van Dieen JH, Kingma I, van der Bug JCE. Evidence for a role of antagonistic cocontraction in controlling trunk stiffness during lifting. *Journal of Biomechanics* 2003a;36:1829-36.

- Van Dieen JH, Selen LPJ, Cholewicki J. Trunk muscle activation in low-back pain patients, an analysis of the literature. *Journal of Electromyography and Kinesiology* 2003b;13:333-51.
- Van Herp G, Rowe P, Salter P, Paul JP. Three-dimensional lumbar spinal kinematics: A study of range of movement in 100 healthy subjects aged 20 to 60+ years. *Rheumatology* 2000;39:1337-40.
- Waters TR, Putz-Anderson V, Garg A, Fine LJ. Revised NIOSH equation for the design and evaluation of manual lifting tasks. *Ergonomics* 1993;36(7):749-76.
- Watkins R, Watkins R, Williams L, Ahlbrand S, Garcia R, Karamanian A, et al. Stability provided by the sternum and rib cage in the thoracic spine. *Spine* 2005;30(11):1283-6.
- Watson PJ, Booker CK, Main CJ, Chen ACN. Surface electromyography in the identification of chronic low back pain patients: The development of the flexion relaxation ratio. *Clinical Biomechanics* 1997;12(3):165-71.
- Webb NM, Shavelson RJ, Haertel EH. Reliability coefficients and generalizability theory. *Handbook of Statistics* 2006;26:81-124.
- Weir JP. Quantifying test-retest reliability using the intraclass correlation coefficient and the SEM. *Journal of Strength and Conditioning Research* 2005;19(1):231-40.
- White AA, Panjabi MM. *Clinical biomechanics of the spine*. 2nd ed. Philadelphia, PA: J.B. Lippincott Company, 1990.
- Willems JM, Jull GA, Ng JKF. An in vivo study of the primary and coupled rotations of the thoracic spine. *Clinical Biomechanics* 1996;11(6):311-6.

- Winby CR, Gerus P, Kirk TB, Lloyd DG. Correlation between EMG-based co-activation measures and medial and lateral compartment loads of the knee during gait. *Clinical Biomechanics* 2013;28:1014-9.
- Winter DA. *Biomechanics and motor control of human movement*, 3rd ed. Hoboken, NJ: John Wiley & Sons, 2005.
- Wong TKT, Lee RYW. Effects of low back pain on the relationship between the movements of the lumbar spine and hip. *Human Movement Science* 2004;23:21-34.
- Zipp P. Recommendations for the standardization of lead positions in surface electromyography. *European Journal of Applied Physiology and Occupational Physiology* 1982;50(1):41-54.

APPENDIX A

Participant Instructions for Experimental Tasks

APPENDIX A

Participant Instructions for Experimental Tasks

Table 40: Instructions given to participants prior to each trial with keywords describing the features of the task. ROM: range-of-motion.

Task	Instructions
<i>Standing (Figure 31)</i>	
Upright Standing	<ul style="list-style-type: none"> This trial will be 10 seconds of standing. Stand as you normally would, arms at your sides and looking straight ahead.
Slumped Standing	<ul style="list-style-type: none"> This trial will be a slump trial. Round out your shoulders and your whole back, looking straight ahead with your arms at your sides.
<i>Maximum Flexion (Figure 32)</i>	
Head: Active Arms: Crossed	<ul style="list-style-type: none"> This trial will be a full flexion straight forward. Put your chin to your chest then flex the trunk the rest of the way, with your arms crossed over your chest.
Head: Active Arms: Loose	<ul style="list-style-type: none"> This trial will be a full flexion straight forward. Put your chin to your chest then flex the trunk the rest of the way, with your arms hanging down to the floor.
Head: Neutral Arms: Crossed	<ul style="list-style-type: none"> This trial will be a full flexion straight forward. Keep your head in a neutral position in line with the trunk, with your arms crossed over your chest.
Head: Neutral Arms: Loose	<ul style="list-style-type: none"> This trial will be a full flexion straight forward. Keep your head in a neutral position in line with the trunk, with your arms hanging down to the floor.
<i>Maximum Lateral Bend (Figure 33)</i>	
Head: Active Arms: Crossed	<ul style="list-style-type: none"> This trial will be a full bend to the right. Put your ear to your shoulder then bend the trunk the rest of the way, with your arms crossed over your chest.
Head: Active Arms: Loose	<ul style="list-style-type: none"> This trial will be a full bend to the right. Put your ear to your shoulder then bend the trunk the rest of the way, with your right arm hanging down to the floor.
Head: Neutral Arms: Crossed	<ul style="list-style-type: none"> This trial will be a full bend to the right. Keep your head in a neutral position in line with the trunk, with your arms crossed over your chest.
Head: Neutral Arms: Loose	<ul style="list-style-type: none"> This trial will be a full bend to the right. Keep your head in a neutral position in line with the trunk, with your right arm hanging down to the floor.

Table 40 (cont.): Instructions given to participants prior to each trial with keywords describing the features of the task. ROM: range-of-motion.

Task	Instructions
<i>Maximum Axial Twist (Figure 34)</i>	
Head: Active Arms: Crossed	<ul style="list-style-type: none"> This trial will be a full twist to the right. Look over your shoulder then twist the trunk the rest of the way, with your arms crossed over your chest.
Head: Active Arms: Abducted	<ul style="list-style-type: none"> This trial will be a full twist to the right. Look over your shoulder then twist the trunk the rest of the way, with your arms straight out to the sides.
Head: Active Arms: Loose	<ul style="list-style-type: none"> This trial will be a full twist to the right. Look over your shoulder then twist the trunk the rest of the way, with your arms at your sides.
Head: Neutral Arms: Crossed	<ul style="list-style-type: none"> This trial will be a full twist to the right. Keep your head in a neutral position in line with the trunk, with your arms crossed over your chest.
Head: Neutral Arms: Abducted	<ul style="list-style-type: none"> This trial will be a full twist to the right. Keep your head in a neutral position in line with the trunk, with your arms straight out to the sides.
Head: Neutral Arms: Loose	<ul style="list-style-type: none"> This trial will be a full twist to the right. Keep your head in a neutral position in line with the trunk, with your arms at your sides.
<i>Thoracic ROM (Figure 35)</i>	
Thoracic Flexion	<ul style="list-style-type: none"> This trial will be thoracic flexion. Bend your chin to your chest, then continue rolling down the upper- and mid-back; keep the low back as neutral as you can. <p>Note: In thoracic flexion, the neck was flexed and the low back was kept as neutral as possible, as opposed to slumped standing, in which participants looked straight ahead and were asked to round out the shoulders and whole back.</p>
Thoracic Bend	<ul style="list-style-type: none"> This trial will be thoracic bend to the right. Bend your ear to your shoulder, then continue rolling down the upper- and mid-back; keep the low back as neutral as you can.
Thoracic Twist	<ul style="list-style-type: none"> This trial will be thoracic twist to the right. Look over your shoulder, then continue twisting the rest of the upper- and mid-back, keeping the low back as neutral as you can.

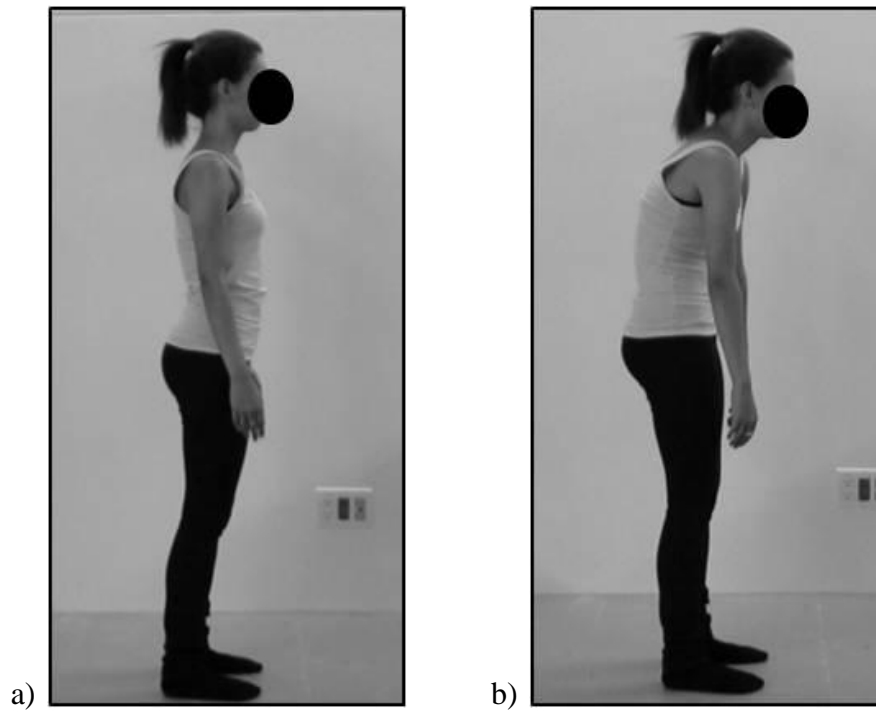


Figure 31: a) Upright standing; b) Slumped standing.

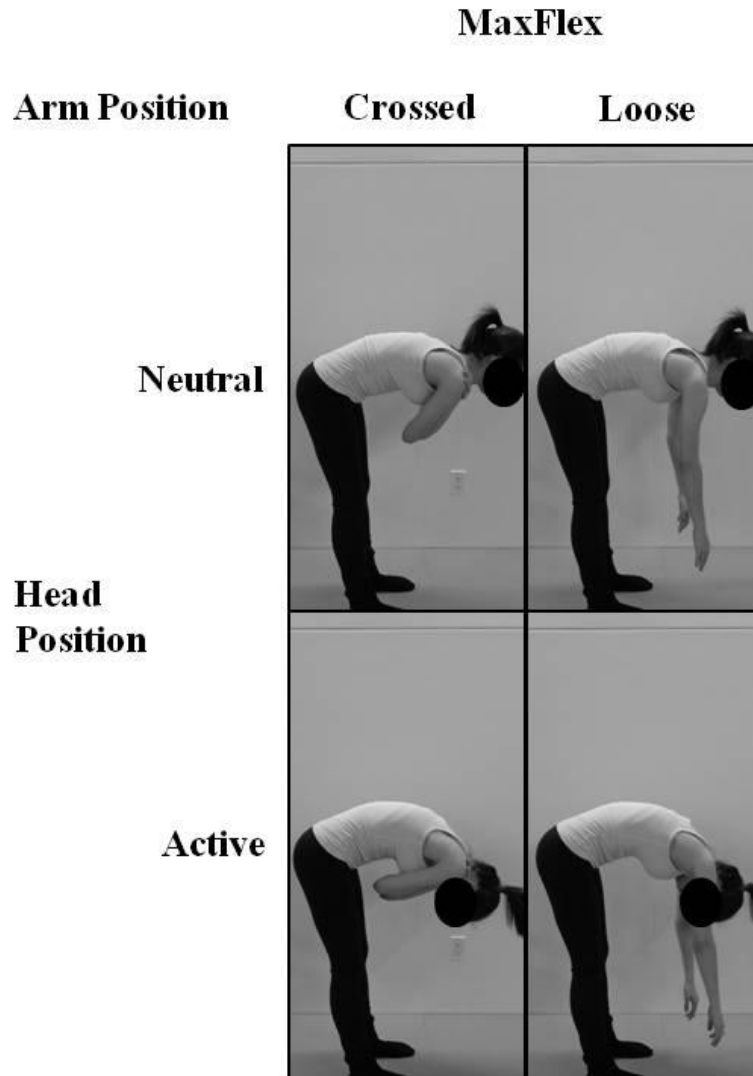


Figure 32: Combinations of head and arm positions used for MaxFlex (Adapted, by permission, from: Schinkel-Ivy A, Pardisnia S, Drake JDM. Head and arm positions that elicit maximal voluntary trunk range-of-motion measures. *Journal of Applied Biomechanics* 2014 (accepted July 1, 2014). Figure 1. © Human Kinetics, Inc.). Written copyright permission not required for self-authored work; refer to Appendix B.

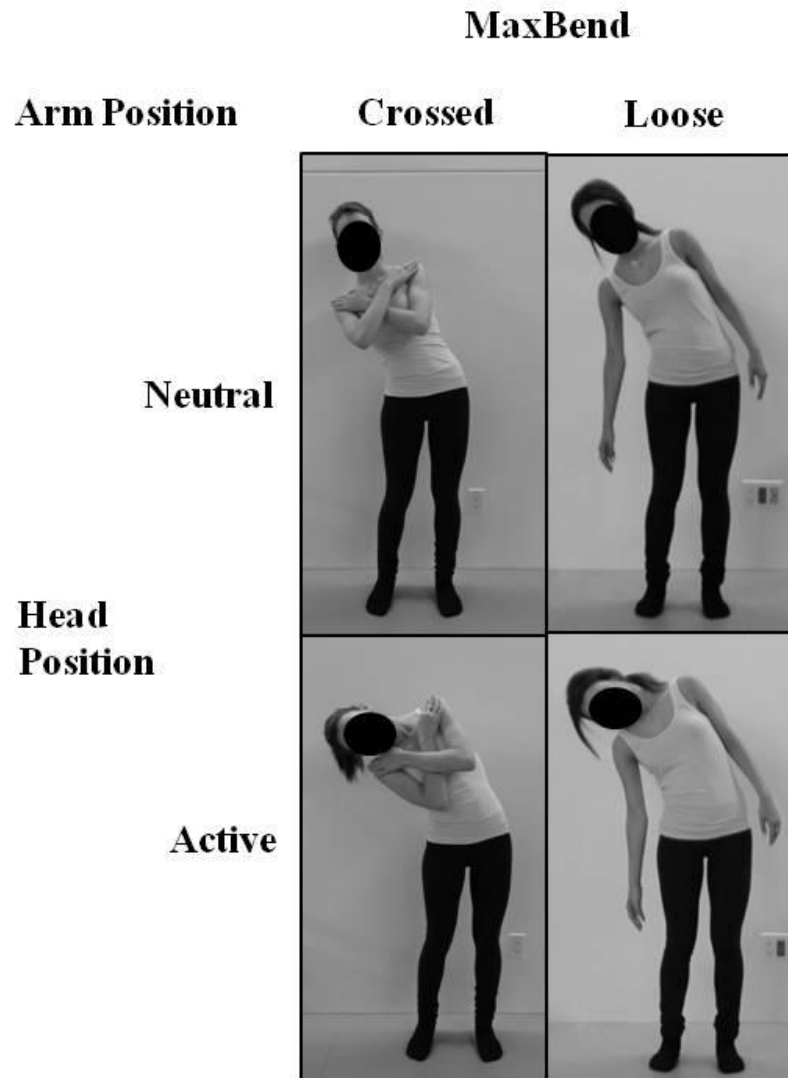


Figure 33: Combinations of head and arm positions used for MaxBend (Adapted, by permission, from: Schinkel-Ivy A, Pardisnia S, Drake JDM. Head and arm positions that elicit maximal voluntary trunk range-of-motion measures. *Journal of Applied Biomechanics* 2014 (accepted July 1, 2014). Figure 1. © Human Kinetics, Inc.). Written copyright permission not required for self-authored work; refer to Appendix B.

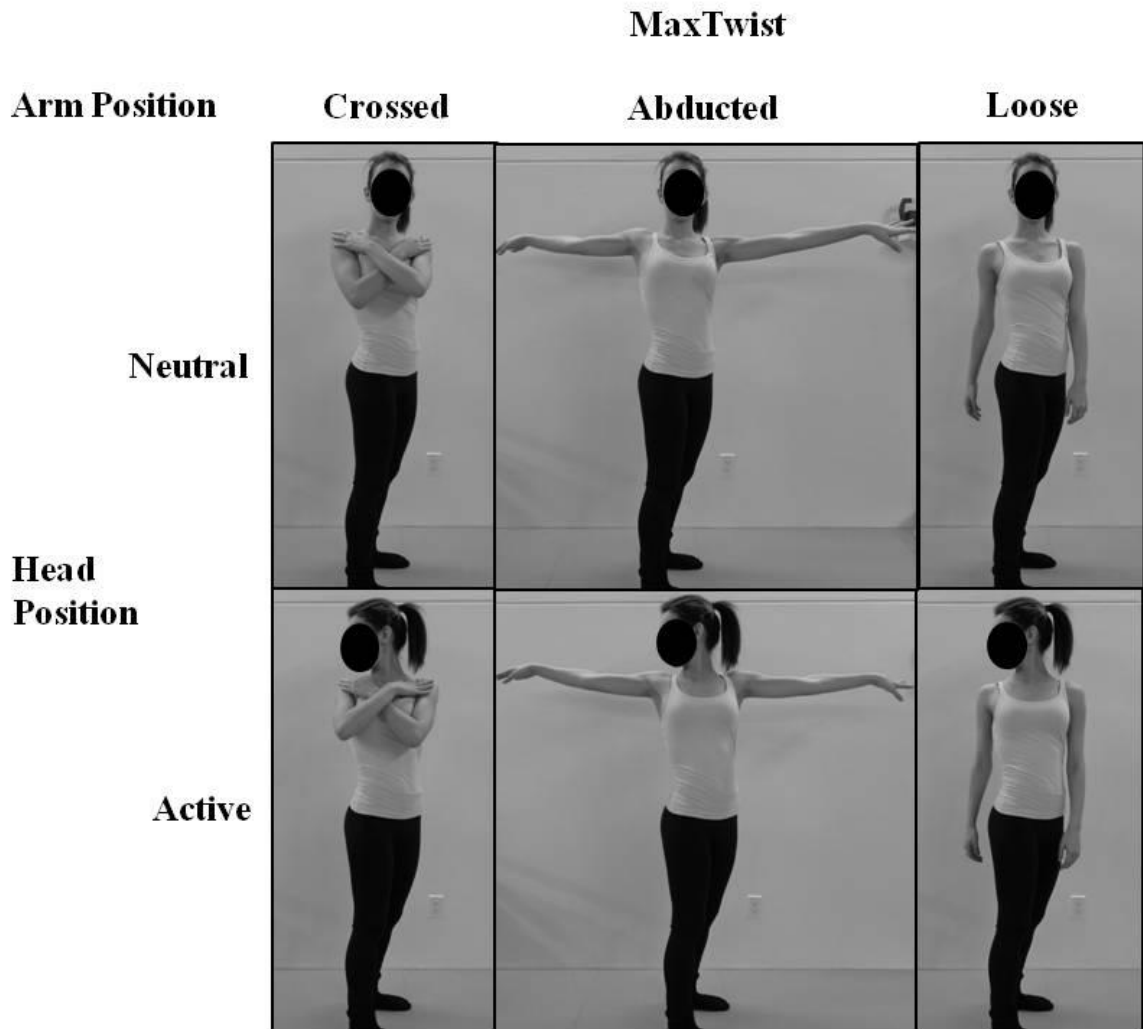


Figure 34: Combinations of head and arm positions used for MaxTwist (Adapted, by permission, from: Schinkel-Ivy A, Pardisnia S, Drake JDM. Head and arm positions that elicit maximal voluntary trunk range-of-motion measures. *Journal of Applied Biomechanics* 2014 (accepted July 1, 2014). Figure 1. © Human Kinetics, Inc.). Written copyright permission not required for self-authored work; refer to Appendix B.

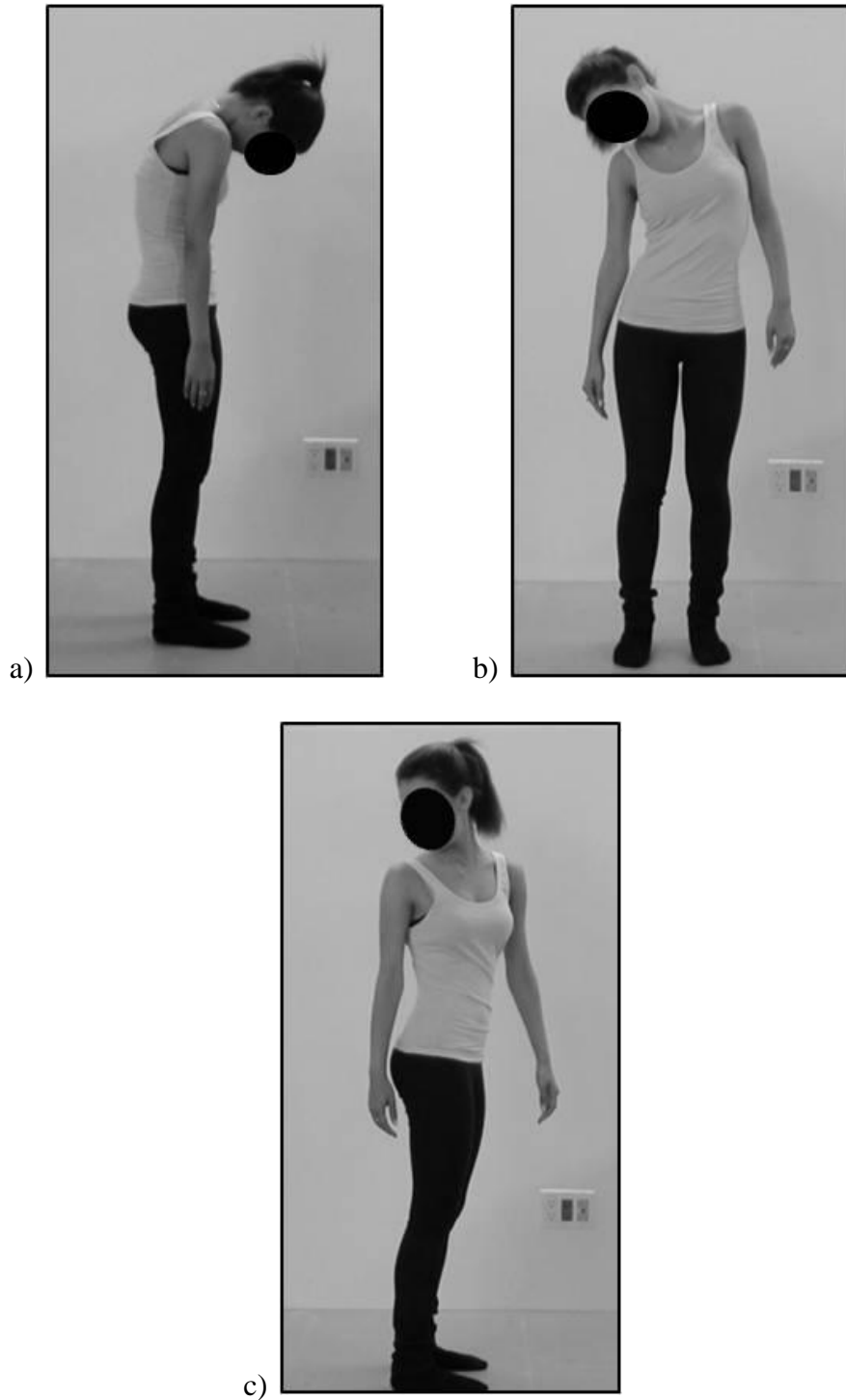


Figure 35: a) Thoracic flexion; b) Thoracic bend; c) Thoracic twist. Participants kept the low back as neutral as possible while moving the head and thoracic spine.

APPENDIX B

Copyright Permissions for Published Figures

APPENDIX B

Copyright Permissions for Published Figures

Copyright permission for:

Figure 1: Mean (*SD*) range-of-motion and neutral zone for axial rotation in four spinal regions (Busscher I, van Dieen JH, Kingma I, van der Veen AJ, Gijsbertus V, Veldhuizen AG. Biomechanical characteristics of different regions of the human spine: An in vitro study on multilevel spinal segments. *Spine* 2009;34(26):2858-64. Figure 2, page 2860).

WOLTERS KLUWER HEALTH LICENSE TERMS AND CONDITIONS

Sep 10, 2014

This is a License Agreement between Alison Schinkel ("You") and Wolters Kluwer Health ("Wolters Kluwer Health") provided by Copyright Clearance Center ("CCC"). The license consists of your order details, the terms and conditions provided by Wolters Kluwer Health, and the payment terms and conditions.

All payments must be made in full to CCC. For payment instructions, please see information listed at the bottom of this form.

License Number	3465501297645
License date	Sep 10, 2014
Licensed content publisher	Wolters Kluwer Health
Licensed content publication	Spine
Licensed content title	Biomechanical Characteristics of Different Regions of the Human Spine: An In Vitro Study on Multilevel Spinal Segments.

Licensed content author	Busscher, Iris; van Dieen, Jaap; Kingma, Idsart; van der Veen, Albert; Verkerke, Gijsbertus; MSc, PhD; Veldhuizen, Albert; MD, PhD
Licensed content date	Jan 1, 2009
Volume Number	34
Issue Number	26
Type of Use	Dissertation/Thesis
Requestor type	Individual
Portion	Figures/table/illustration
Number of figures/tables/illustrations	1
Figures/tables/illustrations used	Figure 2
Author of this Wolters Kluwer article	No
Title of your thesis / dissertation	Quantification and evaluation of the biomechanical behaviour of the trunk during fundamental tasks: Should the thoracic spine be considered?
Expected completion date	Oct 2014
Estimated size(pages)	320
Billing Type	Invoice
Billing address	616 Wilson Road North Oshawa, ON L1G6E9 Canada
Total	0.00 USD

Terms and Conditions

Terms and Conditions

1. A credit line will be prominently placed and include the author(s), title of article, title of journal, volume number, issue number and inclusive pages.
2. The requestor warrants that the material shall not be used in any manner which may be considered derogatory to the title, content, or authors of the material, or to Wolters Kluwer.
3. Permission granted is non-exclusive, and is valid throughout the world in the English language and the languages specified in your original request.
4. Wolters Kluwer cannot supply the requestor with the original artwork or a "clean copy."
5. Permission is valid if the borrowed material is original to a Wolters Kluwer imprint (Lippincott-Raven Publishers, Williams & Wilkins, Lea & Febiger, Harwal, Rapid Science, Little Brown & Company, Harper & Row Medical, American Journal of Nursing Co, and Urban & Schwarzenberg - English Language).
6. If you opt not to use the material requested above, please notify RightsLink or Wolters Kluwer Health/Lippincott Williams & Wilkins within 90 days of the original invoice date.
7. This permission does not apply to images that are credited to publications other than Wolters Kluwer journals. For images credited to non-Wolters Kluwer journal publications, you will need to obtain permission from the journal referenced in the figure or table legend or credit line before making any use of the image(s) or table(s).
8. Adaptations are protected by copyright, so if you would like to reuse material that we have adapted from another source, you will need not only our permission, but the permission of the rights holder of the original material. Similarly, if you want to reuse an adaptation of original LWW content that appears in another publisher's work, you will need our permission and that of the next publisher. The adaptation should be credited as follows: Adapted with permission from

Lippincott Williams and Wilkins/Wolters Kluwer Health: Book author, title, year of publication or Journal name, article author, title, reference citation, year of publication.

9. **Please note that modification of text within figures or full-text article is strictly forbidden.**
10. Please note that articles in the ahead-of-print stage of publication can be cited and the content may be re-used by including the date of access and the unique DOI number. Any final changes in manuscripts will be made at the time of print publication and will be reflected in the final electronic version of the issue. Disclaimer: Articles appearing in the Published Ahead-of-Print section have been peer-reviewed and accepted for publication in the relevant journal and posted online before print publication. Articles appearing as publish ahead-of-print may contain statements, opinions, and information that have errors in facts, figures, or interpretation. Accordingly, Lippincott Williams & Wilkins, the editors and authors and their respective employees are not responsible or liable for the use of any such inaccurate or misleading data, opinion or information contained in the articles in this section.
11. Permission is granted for a one time use only within 12 months from the date of this invoice. Rights herein do not apply to future reproductions, editions, revisions, or other derivative works. Once the 12-month term has expired, permission to renew must be submitted in writing.
12. The following statement needs to be added when reprinting the material in Open Access journals only: 'promotional and commercial use of the material in print, digital or mobile device format is prohibited without the permission from the publisher Lippincott Williams & Wilkins. Please contact journalpermissions@lww.com for further information♦.
13. In case of ***Disease Colon Rectum, Plastic Reconstructive Surgery, The Green Journal, Critical Care Medicine, Pediatric Critical Care Medicine, the American Heart Publications, the American Academy of Neurology*** the following guideline applies: no drug

brand/trade name or logo can be included in the same page as the material re-used

14. When requesting a permission to translate a full text article, Wolters Kluwer/Lippincott Williams & Wilkins requests to receive the pdf of the translated document
15. Other Terms and Conditions:

v1.9

You will be invoiced within 48 hours of this transaction date. You may pay your invoice by credit card upon receipt of the invoice for this transaction. Please follow instructions provided at that time.

To pay for this transaction now; please remit a copy of this document along with your payment. Payment should be in the form of a check or money order referencing your account number and this invoice number RLNK501399585. Make payments to "COPYRIGHT CLEARANCE CENTER" and send to:

Copyright Clearance Center

Dept 001

P.O. Box 843006

Boston, MA 02284-3006

Please disregard electronic and mailed copies if you remit payment in advance.

Questions? customer@copyright.com or +1-855-239-3415 (toll free in the US) or +1-978-646-2777.

Gratis licenses (referencing \$0 in the Total field) are free. Please retain this printable license for your reference. No payment is required.

Copyright permission for:

Figure 5: EMG amplitudes for the longissimus thoracis at T₅, T₈, and T₁₁ during neutral sitting and seated axial twist, normalized to the peak axial twist amplitude (Adapted from: Lee LJ, Coppieters MW, Hodges PW. Differential activation of the thoracic multifidus and longissimus thoracis during trunk rotation. Spine 2005;30(8):870-6. Figure 2b, page 872).

**WOLTERS KLUWER HEALTH LICENSE
TERMS AND CONDITIONS
Sep 11, 2014**

This is a License Agreement between Alison Schinkel ("You") and Wolters Kluwer Health ("Wolters Kluwer Health") provided by Copyright Clearance Center ("CCC"). The license consists of your order details, the terms and conditions provided by Wolters Kluwer Health, and the payment terms and conditions.

All payments must be made in full to CCC. For payment instructions, please see information listed at the bottom of this form.

License Number	3465910277786
License date	Sep 11, 2014
Licensed content publisher	Wolters Kluwer Health
Licensed content publication	Spine
Licensed content title	Differential Activation of the Thoracic Multifidus and Longissimus Thoracis During Trunk Rotation.
Licensed content author	Lee, Linda-Joy; Coppieters,

	Michel; Hodges, Paul
Licensed content date	Jan 1, 2005
Volume Number	30
Issue Number	8
Type of Use	Dissertation/Thesis
Requestor type	Individual
Portion	Figures/table/illustration
Number of figures/tables/illustrations	1
Figures/tables/illustrations used	Figure 2b
Author of this Wolters Kluwer article	No
Title of your thesis / dissertation	Quantification and evaluation of the biomechanical behaviour of the trunk during fundamental tasks: Should the thoracic spine be considered?
Expected completion date	Oct 2014
Estimated size(pages)	320
Billing Type	Invoice
Billing address	616 Wilson Road North Oshawa, ON L1G6E9 Canada
Total	0.00 USD
Terms and Conditions	

Terms and Conditions

1. A credit line will be prominently placed and include the author(s), title of article, title of journal, volume number, issue number and inclusive pages.
2. The requestor warrants that the material shall not be used in any manner which may be considered derogatory to the title, content, or authors of the material, or to Wolters Kluwer.
3. Permission granted is non-exclusive, and is valid throughout the world in the English language and the languages specified in your original request.
4. Wolters Kluwer cannot supply the requestor with the original artwork or a "clean copy."
5. Permission is valid if the borrowed material is original to a Wolters Kluwer imprint (Lippincott-Raven Publishers, Williams & Wilkins, Lea & Febiger, Harwal, Rapid Science, Little Brown & Company, Harper & Row Medical, American Journal of Nursing Co, and Urban & Schwarzenberg - English Language).
6. If you opt not to use the material requested above, please notify RightsLink or Wolters Kluwer Health/Lippincott Williams & Wilkins within 90 days of the original invoice date.
7. This permission does not apply to images that are credited to publications other than Wolters Kluwer journals. For images credited to non-Wolters Kluwer journal publications, you will need to obtain permission from the journal referenced in the figure or table legend or credit line before making any use of the image(s) or table(s).
8. Adaptations are protected by copyright, so if you would like to reuse material that we have adapted from another source, you will need not only our permission, but the permission of the rights holder of the original material. Similarly, if you want to reuse an adaptation of original LWW content that appears in another publisher's work, you will need our permission and that of the next publisher. The adaptation should be credited as follows: Adapted with permission from Lippincott Williams and Wilkins/Wolters Kluwer Health: Book author, title, year of publication or Journal name, article author, title, reference citation, year of publication.
9. **Please note that modification of text within figures or**

full-text article is strictly forbidden.

10. Please note that articles in the ahead-of-print stage of publication can be cited and the content may be re-used by including the date of access and the unique DOI number. Any final changes in manuscripts will be made at the time of print publication and will be reflected in the final electronic version of the issue. Disclaimer: Articles appearing in the Published Ahead-of-Print section have been peer-reviewed and accepted for publication in the relevant journal and posted online before print publication. Articles appearing as publish ahead-of-print may contain statements, opinions, and information that have errors in facts, figures, or interpretation. Accordingly, Lippincott Williams & Wilkins, the editors and authors and their respective employees are not responsible or liable for the use of any such inaccurate or misleading data, opinion or information contained in the articles in this section.
11. Permission is granted for a one time use only within 12 months from the date of this invoice. Rights herein do not apply to future reproductions, editions, revisions, or other derivative works. Once the 12-month term has expired, permission to renew must be submitted in writing.
12. The following statement needs to be added when reprinting the material in Open Access journals only: 'promotional and commercial use of the material in print, digital or mobile device format is prohibited without the permission from the publisher Lippincott Williams & Wilkins. Please contact journalpermissions@lww.com for further information♦.
13. In case of ***Disease Colon Rectum, Plastic Reconstructive Surgery, The Green Journal, Critical Care Medicine, Pediatric Critical Care Medicine, the American Heart Publications, the American Academy of Neurology*** the following guideline applies: no drug brand/trade name or logo can be included in the same page as the material re-used
14. When requesting a permission to translate a full text article, Wolters Kluwer/Lippincott Williams & Wilkins requests

to receive the pdf of the translated document
15. Other Terms and Conditions:

v1.9

You will be invoiced within 48 hours of this transaction date. You may pay your invoice by credit card upon receipt of the invoice for this transaction. Please follow instructions provided at that time.

To pay for this transaction now; please remit a copy of this document along with your payment. Payment should be in the form of a check or money order referencing your account number and this invoice number RLNK501400315. Make payments to "COPYRIGHT CLEARANCE CENTER" and send to:

**Copyright Clearance Center
Dept 001**

P.O. Box 843006

Boston, MA 02284-3006

Please disregard electronic and mailed copies if you remit payment in advance.

Questions? customercare@copyright.com or +1-855-239-3415 (toll free in the US) or +1-978-646-2777.

Gratis licenses (referencing \$0 in the Total field) are free. Please retain this printable license for your reference. No payment is required.

Copyright permission for:

Figure 7: Previous marker setup used to calculate a general thoracic angle (angle between T₁, T₅, and T₁₀) (Claus AP, Hides JA, Mosely GL, Hodges PW. Is 'ideal' sitting posture real?" Measurement of spinal curves in four sitting postures. Manual Therapy 2009;14:404-8. Figure 1, page 405).

ELSEVIER LICENSE TERMS AND CONDITIONS

Sep 10, 2014

This is a License Agreement between Alison Schinkel ("You") and Elsevier ("Elsevier") provided by Copyright Clearance Center ("CCC"). The license consists of your order details, the terms and conditions provided by Elsevier, and the payment terms and conditions.

All payments must be made in full to CCC. For payment instructions, please see information listed at the bottom of this form.

Supplier	Elsevier Limited The Boulevard, Langford Lane Kidlington, Oxford, OX5 1GB, UK
Registered Company Number	1982084
Customer name	Alison Schinkel
Customer address	616 Wilson Road North Oshawa, ON L1G6E9
License number	3465491230566
License date	Sep 10, 2014
Licensed content publisher	Elsevier

Licensed content publication	Manual Therapy
Licensed content title	Is 'ideal' sitting posture real?: Measurement of spinal curves in four sitting postures
Licensed content author	Andrew P. Claus,Julie A. Hides,G. Lorimer Moseley,Paul W. Hodges
Licensed content date	August 2009
Licensed content volume number	14
Licensed content issue number	4
Number of pages	5
Start Page	404
End Page	408
Type of Use	reuse in a thesis/dissertation
Portion	figures/tables/illustrations
Number of figures/tables/illustrations	1
Format	both print and electronic
Are you the author of this Elsevier article?	No
Will you be translating?	No
Title of your thesis/dissertation	Quantification and evaluation of the biomechanical behaviour of the trunk during fundamental tasks: Should the thoracic spine be considered?
Expected completion date	Oct 2014
Estimated size (number of pages)	320

Elsevier VAT number	GB 494 6272 12
Permissions price	0.00 USD
VAT/Local Sales Tax	0.00 USD / 0.00 GBP
Total	0.00 USD
Terms and Conditions	

INTRODUCTION

1. The publisher for this copyrighted material is Elsevier. By clicking "accept" in connection with completing this licensing transaction, you agree that the following terms and conditions apply to this transaction (along with the Billing and Payment terms and conditions established by Copyright Clearance Center, Inc. ("CCC"), at the time that you opened your Rightslink account and that are available at any time at <http://myaccount.copyright.com>).

GENERAL TERMS

2. Elsevier hereby grants you permission to reproduce the aforementioned material subject to the terms and conditions indicated.

3. Acknowledgement: If any part of the material to be used (for example, figures) has appeared in our publication with credit or acknowledgement to another source, permission must also be sought from that source. If such permission is not obtained then that material may not be included in your publication/copies. Suitable acknowledgement to the source must be made, either as a footnote or in a reference list at the end of your publication, as follows:

“Reprinted from Publication title, Vol /edition number, Author(s), Title of article / title of chapter, Pages No., Copyright (Year), with permission from Elsevier [OR APPLICABLE SOCIETY COPYRIGHT OWNER].” Also Lancet special credit - “Reprinted from The Lancet, Vol. number, Author(s), Title of article, Pages No., Copyright (Year), with permission from Elsevier.”

4. Reproduction of this material is confined to the purpose and/or media for which permission is hereby given.

5. Altering/Modifying Material: Not Permitted. However figures and illustrations may be altered/adapted minimally to serve your work. Any other abbreviations, additions, deletions and/or any other alterations shall be made only with prior written authorization of

Elsevier Ltd. (Please contact Elsevier at permissions@elsevier.com)

6. If the permission fee for the requested use of our material is waived in this instance, please be advised that your future requests for Elsevier materials may attract a fee.

7. **Reservation of Rights:** Publisher reserves all rights not specifically granted in the combination of (i) the license details provided by you and accepted in the course of this licensing transaction, (ii) these terms and conditions and (iii) CCC's Billing and Payment terms and conditions.

8. **License Contingent Upon Payment:** While you may exercise the rights licensed immediately upon issuance of the license at the end of the licensing process for the transaction, provided that you have disclosed complete and accurate details of your proposed use, no license is finally effective unless and until full payment is received from you (either by publisher or by CCC) as provided in CCC's Billing and Payment terms and conditions. If full payment is not received on a timely basis, then any license preliminarily granted shall be deemed automatically revoked and shall be void as if never granted. Further, in the event that you breach any of these terms and conditions or any of CCC's Billing and Payment terms and conditions, the license is automatically revoked and shall be void as if never granted. Use of materials as described in a revoked license, as well as any use of the materials beyond the scope of an unrevoked license, may constitute copyright infringement and publisher reserves the right to take any and all action to protect its copyright in the materials.

9. **Warranties:** Publisher makes no representations or warranties with respect to the licensed material.

10. **Indemnity:** You hereby indemnify and agree to hold harmless publisher and CCC, and their respective officers, directors, employees and agents, from and against any and all claims arising out of your use of the licensed material other than as specifically authorized pursuant to this license.

11. **No Transfer of License:** This license is personal to you and may not be sublicensed, assigned, or transferred by you to any other person without publisher's written permission.

12. **No Amendment Except in Writing:** This license may not be amended except in a writing signed by both parties (or, in the case of publisher, by CCC on publisher's behalf).

13. **Objection to Contrary Terms:** Publisher hereby objects to any terms contained in any purchase order, acknowledgment, check endorsement or other writing prepared by you, which terms are inconsistent with these terms and conditions or CCC's Billing and Payment terms and conditions. These terms and conditions, together with CCC's Billing and Payment terms and conditions (which are incorporated herein), comprise the entire

agreement between you and publisher (and CCC) concerning this licensing transaction. In the event of any conflict between your obligations established by these terms and conditions and those established by CCC's Billing and Payment terms and conditions, these terms and conditions shall control.

14. **Revocation:** Elsevier or Copyright Clearance Center may deny the permissions described in this License at their sole discretion, for any reason or no reason, with a full refund payable to you. Notice of such denial will be made using the contact information provided by you. Failure to receive such notice will not alter or invalidate the denial. In no event will Elsevier or Copyright Clearance Center be responsible or liable for any costs, expenses or damage incurred by you as a result of a denial of your permission request, other than a refund of the amount(s) paid by you to Elsevier and/or Copyright Clearance Center for denied permissions.

LIMITED LICENSE

The following terms and conditions apply only to specific license types:

15. **Translation:** This permission is granted for non-exclusive world **English** rights only unless your license was granted for translation rights. If you licensed translation rights you may only translate this content into the languages you requested. A professional translator must perform all translations and reproduce the content word for word preserving the integrity of the article. If this license is to re-use 1 or 2 figures then permission is granted for non-exclusive world rights in all languages.

16. **Posting licensed content on any Website:** The following terms and conditions apply as follows: Licensing material from an Elsevier journal: All content posted to the web site must maintain the copyright information line on the bottom of each image; A hyper-text must be included to the Homepage of the journal from which you are licensing at <http://www.sciencedirect.com/science/journal/xxxxx> or the Elsevier homepage for books at <http://www.elsevier.com>; Central Storage: This license does not include permission for a scanned version of the material to be stored in a central repository such as that provided by Heron/XanEdu.

Licensing material from an Elsevier book: A hyper-text link must be included to the Elsevier homepage at <http://www.elsevier.com>. All content posted to the web site must maintain the copyright information line on the bottom of each image.

Posting licensed content on Electronic reserve: In addition to the above the following clauses are applicable: The web site must be password-protected and made available only to bona fide students registered on a relevant course. This permission is granted for 1 year

only. You may obtain a new license for future website posting.

For journal authors: the following clauses are applicable in addition to the above: Permission granted is limited to the author accepted manuscript version* of your paper.

***Accepted Author Manuscript (AAM) Definition:** An accepted author manuscript (AAM) is the author's version of the manuscript of an article that has been accepted for publication and which may include any author-incorporated changes suggested through the processes of submission processing, peer review, and editor-author communications. AAMs do not include other publisher value-added contributions such as copy-editing, formatting, technical enhancements and (if relevant) pagination.

You are not allowed to download and post the published journal article (whether PDF or HTML, proof or final version), nor may you scan the printed edition to create an electronic version. A hyper-text must be included to the Homepage of the journal from which you are licensing at <http://www.sciencedirect.com/science/journal/xxxxx>. As part of our normal production process, you will receive an e-mail notice when your article appears on Elsevier's online service ScienceDirect (www.sciencedirect.com). That e-mail will include the article's Digital Object Identifier (DOI). This number provides the electronic link to the published article and should be included in the posting of your personal version. We ask that you wait until you receive this e-mail and have the DOI to do any posting.

Posting to a repository: Authors may post their AAM immediately to their employer's institutional repository for internal use only and may make their manuscript publically available after the journal-specific embargo period has ended.

Please also refer to [Elsevier's Article Posting Policy](#) for further information.

18. **For book authors** the following clauses are applicable in addition to the above: Authors are permitted to place a brief summary of their work online only.. You are not allowed to download and post the published electronic version of your chapter, nor may you scan the printed edition to create an electronic version. **Posting to a repository:** Authors are permitted to post a summary of their chapter only in their institution's repository.

20. **Thesis/Dissertation:** If your license is for use in a thesis/dissertation your thesis may be submitted to your institution in either print or electronic form. Should your thesis be published commercially, please reapply for permission. These requirements include permission for the Library and Archives of Canada to supply single copies, on demand, of the complete thesis and include permission for UMI to supply single copies, on demand, of the complete thesis. Should your thesis be published commercially, please reapply for permission.

Elsevier Open Access Terms and Conditions

Elsevier publishes Open Access articles in both its Open Access journals and via its Open Access articles option in subscription journals.

Authors publishing in an Open Access journal or who choose to make their article Open Access in an Elsevier subscription journal select one of the following Creative Commons user licenses, which define how a reader may reuse their work: Creative Commons Attribution License (CC BY), Creative Commons Attribution – Non Commercial - ShareAlike (CC BY NC SA) and Creative Commons Attribution – Non Commercial – No Derivatives (CC BY NC ND)

Terms & Conditions applicable to all Elsevier Open Access articles:

Any reuse of the article must not represent the author as endorsing the adaptation of the article nor should the article be modified in such a way as to damage the author's honour or reputation.

The author(s) must be appropriately credited.

If any part of the material to be used (for example, figures) has appeared in our publication with credit or acknowledgement to another source it is the responsibility of the user to ensure their reuse complies with the terms and conditions determined by the rights holder.

Additional Terms & Conditions applicable to each Creative Commons user license:

CC BY: You may distribute and copy the article, create extracts, abstracts, and other revised versions, adaptations or derivative works of or from an article (such as a translation), to include in a collective work (such as an anthology), to text or data mine the article, including for commercial purposes without permission from Elsevier

CC BY NC SA: For non-commercial purposes you may distribute and copy the article, create extracts, abstracts and other revised versions, adaptations or derivative works of or from an article (such as a translation), to include in a collective work (such as an anthology), to text and data mine the article and license new adaptations or creations under identical terms without permission from Elsevier

CC BY NC ND: For non-commercial purposes you may distribute and copy the article and include it in a collective work (such as an anthology), provided you do not alter or modify the article, without permission from Elsevier

Any commercial reuse of Open Access articles published with a CC BY NC SA or CC BY NC ND license requires permission from Elsevier and will be subject to a fee.

Commercial reuse includes:

- Promotional purposes (advertising or marketing)
- Commercial exploitation (e.g. a product for sale or loan)
- Systematic distribution (for a fee or free of charge)

Please refer to [Elsevier's Open Access Policy](#) for further information.

21. Other Conditions:

v1.6

You will be invoiced within 48 hours of this transaction date. You may pay your invoice by credit card upon receipt of the invoice for this transaction. Please follow instructions provided at that time.

To pay for this transaction now; please remit a copy of this document along with your payment. Payment should be in the form of a check or money order referencing your account number and this invoice number RLNK501399556. Make payments to "COPYRIGHT CLEARANCE CENTER" and send to:

**Copyright Clearance Center
Dept 001**

P.O. Box 843006

Boston, MA 02284-3006

Please disregard electronic and mailed copies if you remit payment in advance.

Questions? customercare@copyright.com or +1-855-239-3415 (toll free in the US) or +1-978-646-2777.

Gratis licenses (referencing \$0 in the Total field) are free. Please retain this printable license for your reference. No payment is required.

Copyright permission for:

Figure 8: Previous marker setup used to calculate angles for four thoracic regions (T₃, T₆, T₉, and T₁₂) (Preuss RA, Popovic MR. Three-dimensional spine kinematics during multidirectional, target-directed trunk movement in sitting. Journal of Electromyography and Kinesiology 2010;20:823-32. Figure 1c, page 824).

ELSEVIER LICENSE TERMS AND CONDITIONS

Sep 10, 2014

This is a License Agreement between Alison Schinkel ("You") and Elsevier ("Elsevier") provided by Copyright Clearance Center ("CCC"). The license consists of your order details, the terms and conditions provided by Elsevier, and the payment terms and conditions.

All payments must be made in full to CCC. For payment instructions, please see information listed at the bottom of this form.

Supplier	Elsevier Limited The Boulevard, Langford Lane Kidlington, Oxford, OX5 1GB, UK
Registered Company Number	1982084
Customer name	Alison Schinkel
Customer address	616 Wilson Road North Oshawa, ON L1G6E9
License number	3465500051279
License date	Sep 10, 2014
Licensed content publisher	Elsevier
Licensed content publication	Journal of Electromyography and Kinesiology

Licensed content title	Three-dimensional spine kinematics during multidirectional, target-directed trunk movement in sitting
Licensed content author	Richard A. Preuss, Milos R. Popovic
Licensed content date	October 2010
Licensed content volume number	20
Licensed content issue number	5
Number of pages	10
Start Page	823
End Page	832
Type of Use	reuse in a thesis/dissertation
Intended publisher of new work	other
Portion	figures/tables/illustrations
Number of figures/tables/illustrations	1
Format	both print and electronic
Are you the author of this Elsevier article?	No
Will you be translating?	No
Title of your thesis/dissertation	Quantification and evaluation of the biomechanical behaviour of the trunk during fundamental tasks: Should the thoracic spine be considered?
Expected completion date	Oct 2014

Estimated size (number of pages)	320
Elsevier VAT number	GB 494 6272 12
Permissions price	0.00 USD
VAT/Local Sales Tax	0.00 USD / 0.00 GBP
Total	0.00 USD

Terms and Conditions

INTRODUCTION

1. The publisher for this copyrighted material is Elsevier. By clicking "accept" in connection with completing this licensing transaction, you agree that the following terms and conditions apply to this transaction (along with the Billing and Payment terms and conditions established by Copyright Clearance Center, Inc. ("CCC"), at the time that you opened your Rightslink account and that are available at any time at <http://myaccount.copyright.com>).

GENERAL TERMS

2. Elsevier hereby grants you permission to reproduce the aforementioned material subject to the terms and conditions indicated.

3. Acknowledgement: If any part of the material to be used (for example, figures) has appeared in our publication with credit or acknowledgement to another source, permission must also be sought from that source. If such permission is not obtained then that material may not be included in your publication/copies. Suitable acknowledgement to the source must be made, either as a footnote or in a reference list at the end of your publication, as follows:

“Reprinted from Publication title, Vol /edition number, Author(s), Title of article / title of chapter, Pages No., Copyright (Year), with permission from Elsevier [OR APPLICABLE SOCIETY COPYRIGHT OWNER].” Also Lancet special credit - “Reprinted from The Lancet, Vol. number, Author(s), Title of article, Pages No., Copyright (Year), with permission from Elsevier.”

4. Reproduction of this material is confined to the purpose and/or media for which permission is hereby given.

5. Altering/Modifying Material: Not Permitted. However figures and illustrations may be

altered/adapted minimally to serve your work. Any other abbreviations, additions, deletions and/or any other alterations shall be made only with prior written authorization of Elsevier Ltd. (Please contact Elsevier at permissions@elsevier.com)

6. If the permission fee for the requested use of our material is waived in this instance, please be advised that your future requests for Elsevier materials may attract a fee.

7. **Reservation of Rights:** Publisher reserves all rights not specifically granted in the combination of (i) the license details provided by you and accepted in the course of this licensing transaction, (ii) these terms and conditions and (iii) CCC's Billing and Payment terms and conditions.

8. **License Contingent Upon Payment:** While you may exercise the rights licensed immediately upon issuance of the license at the end of the licensing process for the transaction, provided that you have disclosed complete and accurate details of your proposed use, no license is finally effective unless and until full payment is received from you (either by publisher or by CCC) as provided in CCC's Billing and Payment terms and conditions. If full payment is not received on a timely basis, then any license preliminarily granted shall be deemed automatically revoked and shall be void as if never granted. Further, in the event that you breach any of these terms and conditions or any of CCC's Billing and Payment terms and conditions, the license is automatically revoked and shall be void as if never granted. Use of materials as described in a revoked license, as well as any use of the materials beyond the scope of an unrevoked license, may constitute copyright infringement and publisher reserves the right to take any and all action to protect its copyright in the materials.

9. **Warranties:** Publisher makes no representations or warranties with respect to the licensed material.

10. **Indemnity:** You hereby indemnify and agree to hold harmless publisher and CCC, and their respective officers, directors, employees and agents, from and against any and all claims arising out of your use of the licensed material other than as specifically authorized pursuant to this license.

11. **No Transfer of License:** This license is personal to you and may not be sublicensed, assigned, or transferred by you to any other person without publisher's written permission.

12. **No Amendment Except in Writing:** This license may not be amended except in a writing signed by both parties (or, in the case of publisher, by CCC on publisher's behalf).

13. **Objection to Contrary Terms:** Publisher hereby objects to any terms contained in any purchase order, acknowledgment, check endorsement or other writing prepared by you, which terms are inconsistent with these terms and conditions or CCC's Billing and

Payment terms and conditions. These terms and conditions, together with CCC's Billing and Payment terms and conditions (which are incorporated herein), comprise the entire agreement between you and publisher (and CCC) concerning this licensing transaction. In the event of any conflict between your obligations established by these terms and conditions and those established by CCC's Billing and Payment terms and conditions, these terms and conditions shall control.

14. **Revocation:** Elsevier or Copyright Clearance Center may deny the permissions described in this License at their sole discretion, for any reason or no reason, with a full refund payable to you. Notice of such denial will be made using the contact information provided by you. Failure to receive such notice will not alter or invalidate the denial. In no event will Elsevier or Copyright Clearance Center be responsible or liable for any costs, expenses or damage incurred by you as a result of a denial of your permission request, other than a refund of the amount(s) paid by you to Elsevier and/or Copyright Clearance Center for denied permissions.

LIMITED LICENSE

The following terms and conditions apply only to specific license types:

15. **Translation:** This permission is granted for non-exclusive world **English** rights only unless your license was granted for translation rights. If you licensed translation rights you may only translate this content into the languages you requested. A professional translator must perform all translations and reproduce the content word for word preserving the integrity of the article. If this license is to re-use 1 or 2 figures then permission is granted for non-exclusive world rights in all languages.

16. **Posting licensed content on any Website:** The following terms and conditions apply as follows: Licensing material from an Elsevier journal: All content posted to the web site must maintain the copyright information line on the bottom of each image; A hyper-text must be included to the Homepage of the journal from which you are licensing at <http://www.sciencedirect.com/science/journal/xxxxx> or the Elsevier homepage for books at <http://www.elsevier.com>; Central Storage: This license does not include permission for a scanned version of the material to be stored in a central repository such as that provided by Heron/XanEdu.

Licensing material from an Elsevier book: A hyper-text link must be included to the Elsevier homepage at <http://www.elsevier.com> . All content posted to the web site must maintain the copyright information line on the bottom of each image.

Posting licensed content on Electronic reserve: In addition to the above the following clauses are applicable: The web site must be password-protected and made available only

to bona fide students registered on a relevant course. This permission is granted for 1 year only. You may obtain a new license for future website posting.

For journal authors: the following clauses are applicable in addition to the above: Permission granted is limited to the author accepted manuscript version* of your paper.

***Accepted Author Manuscript (AAM) Definition:** An accepted author manuscript (AAM) is the author's version of the manuscript of an article that has been accepted for publication and which may include any author-incorporated changes suggested through the processes of submission processing, peer review, and editor-author communications. AAMs do not include other publisher value-added contributions such as copy-editing, formatting, technical enhancements and (if relevant) pagination.

You are not allowed to download and post the published journal article (whether PDF or HTML, proof or final version), nor may you scan the printed edition to create an electronic version. A hyper-text must be included to the Homepage of the journal from which you are licensing at <http://www.sciencedirect.com/science/journal/xxxxx>. As part of our normal production process, you will receive an e-mail notice when your article appears on Elsevier's online service ScienceDirect (www.sciencedirect.com). That e-mail will include the article's Digital Object Identifier (DOI). This number provides the electronic link to the published article and should be included in the posting of your personal version. We ask that you wait until you receive this e-mail and have the DOI to do any posting.

Posting to a repository: Authors may post their AAM immediately to their employer's institutional repository for internal use only and may make their manuscript publically available after the journal-specific embargo period has ended.

Please also refer to [Elsevier's Article Posting Policy](#) for further information.

18. **For book authors** the following clauses are applicable in addition to the above: Authors are permitted to place a brief summary of their work online only.. You are not allowed to download and post the published electronic version of your chapter, nor may you scan the printed edition to create an electronic version. **Posting to a repository:** Authors are permitted to post a summary of their chapter only in their institution's repository.

20. **Thesis/Dissertation:** If your license is for use in a thesis/dissertation your thesis may be submitted to your institution in either print or electronic form. Should your thesis be published commercially, please reapply for permission. These requirements include permission for the Library and Archives of Canada to supply single copies, on demand, of the complete thesis and include permission for UMI to supply single copies, on demand, of the complete thesis. Should your thesis be published commercially, please reapply for

permission.

Elsevier Open Access Terms and Conditions

Elsevier publishes Open Access articles in both its Open Access journals and via its Open Access articles option in subscription journals.

Authors publishing in an Open Access journal or who choose to make their article Open Access in an Elsevier subscription journal select one of the following Creative Commons user licenses, which define how a reader may reuse their work: Creative Commons Attribution License (CC BY), Creative Commons Attribution – Non Commercial - ShareAlike (CC BY NC SA) and Creative Commons Attribution – Non Commercial – No Derivatives (CC BY NC ND)

Terms & Conditions applicable to all Elsevier Open Access articles:

Any reuse of the article must not represent the author as endorsing the adaptation of the article nor should the article be modified in such a way as to damage the author's honour or reputation.

The author(s) must be appropriately credited.

If any part of the material to be used (for example, figures) has appeared in our publication with credit or acknowledgement to another source it is the responsibility of the user to ensure their reuse complies with the terms and conditions determined by the rights holder.

Additional Terms & Conditions applicable to each Creative Commons user license:

CC BY: You may distribute and copy the article, create extracts, abstracts, and other revised versions, adaptations or derivative works of or from an article (such as a translation), to include in a collective work (such as an anthology), to text or data mine the article, including for commercial purposes without permission from Elsevier

CC BY NC SA: For non-commercial purposes you may distribute and copy the article, create extracts, abstracts and other revised versions, adaptations or derivative works of or from an article (such as a translation), to include in a collective work (such as an anthology), to text and data mine the article and license new adaptations or creations under identical terms without permission from Elsevier

CC BY NC ND: For non-commercial purposes you may distribute and copy the article and include it in a collective work (such as an anthology), provided you do not alter or

modify the article, without permission from Elsevier

Any commercial reuse of Open Access articles published with a CC BY NC SA or CC BY NC ND license requires permission from Elsevier and will be subject to a fee.

Commercial reuse includes:

- Promotional purposes (advertising or marketing)
- Commercial exploitation (e.g. a product for sale or loan)
- Systematic distribution (for a fee or free of charge)

Please refer to [Elsevier's Open Access Policy](#) for further information.

21. Other Conditions:

v1.6

You will be invoiced within 48 hours of this transaction date. You may pay your invoice by credit card upon receipt of the invoice for this transaction. Please follow instructions provided at that time.

To pay for this transaction now; please remit a copy of this document along with your payment. Payment should be in the form of a check or money order referencing your account number and this invoice number RLNK501399563. Make payments to "COPYRIGHT CLEARANCE CENTER" and send to:

Copyright Clearance Center

Dept 001

P.O. Box 843006

Boston, MA 02284-3006

Please disregard electronic and mailed copies if you remit payment in advance.

Questions? customer care@copyright.com or +1-855-239-3415 (toll free in the US) or +1-978-646-2777.

Gratis licenses (referencing \$0 in the Total field) are free. Please retain this printable license for your reference. No payment is required.

Figure 9: Marker setup in the sagittal view. IC: iliac crest (Adapted, by permission, from: Schinkel-Ivy A, Pardisnia S, Drake JDM. Head and arm positions that elicit maximal voluntary trunk range-of-motion measures. *Journal of Applied Biomechanics* 2014 (accepted July 1, 2014). Figure 2a. © Human Kinetics, Inc.).

Figure 12: Collapsed 3D sagittal view of the markers in Visual3D. ASIS: anterior superior iliac spine; GT: greater trochanter; IC: iliac crest (Adapted, by permission, from: Schinkel-Ivy A, Pardisnia S, Drake JDM. Head and arm positions that elicit maximal voluntary trunk range-of-motion measures. *Journal of Applied Biomechanics* 2014 (accepted July 1, 2014). Figure 2b. © Human Kinetics, Inc.).

Figure 13: Collapsed 3D sagittal view of the markers representing the method by which each measure was calculated. The angles represented in this collapsed 3D sagittal view are the equivalent of flexion-extension angles (Adapted, by permission, from: Schinkel-Ivy A, Pardisnia S, Drake JDM. Head and arm positions that elicit maximal voluntary trunk range-of-motion measures. *Journal of Applied Biomechanics* 2014 (accepted July 1, 2014). Figure 2c. © Human Kinetics, Inc.).

Figure 16, 32: Combinations of head and arm positions used for MaxFlex (Adapted, by permission, from: Schinkel-Ivy A, Pardisnia S, Drake JDM. Head and arm positions that elicit maximal voluntary trunk range-of-motion measures. *Journal of Applied Biomechanics* 2014 (accepted July 1, 2014). Figure 1. © Human Kinetics, Inc.).

Figure 17, 33: Combinations of head and arm positions used for MaxBend (Adapted, by permission, from: Schinkel-Ivy A, Pardisnia S, Drake JDM. Head and arm positions that elicit maximal voluntary trunk range-of-motion measures. *Journal of Applied Biomechanics* 2014 (accepted July 1, 2014). Figure 1. © Human Kinetics, Inc.).

Figure 18, 34: Combinations of head and arm positions used for MaxTwist (Adapted, by permission, from: Schinkel-Ivy A, Pardisnia S, Drake JDM. Head and arm positions that elicit maximal voluntary trunk range-of-motion measures. *Journal of Applied Biomechanics* 2014 (accepted July 1, 2014). Figure 1. © Human Kinetics, Inc.).

Figure 19: Collapsed 3D sagittal view of the markers for a visual representation of how each angle was calculated. The angles represented in this collapsed 3D sagittal view are the equivalent of flexion-extension angles. CT: cervico-thoracic; UT: upper-thoracic; MT: mid-thoracic; LT: lower-thoracic (Adapted, by permission, from: Schinkel-Ivy A, Pardisnia S, Drake JDM. Head and arm positions that elicit maximal voluntary trunk range-of-motion measures. *Journal of Applied Biomechanics* 2014 (accepted July 1, 2014). Figure 2c. © Human Kinetics, Inc.).

Figure 29: Collapsed 3D sagittal view of the markers representing the methods by which each angle was calculated. The angles represented in this collapsed 3D sagittal view are the equivalent of flexion-extension angles (Adapted, by permission, from: Schinkel-Ivy A, Pardisnia S, Drake JDM. Head and arm positions that elicit maximal

voluntary trunk range-of-motion measures. *Journal of Applied Biomechanics* 2014 (accepted July 1, 2014). Figure 2c. © Human Kinetics, Inc.).



Alison Schinkel <alisonschinkel@gmail.com>

Question regarding copyright permissions for a self-authored work

Permissions Mailbox <permissions@hkusa.com>

Fri, Sep 12, 2014 at 4:23 PM

To: "alisonschinkel@gmail.com" <alisonschinkel@gmail.com>

Hi Alison,

The author transfer of copyright form for *Journal of Applied Biomechanics* includes the following statement:

The authors explicitly reserve the following rights:

- The right to use original figures and tables in future publications, provided explicit acknowledgment is made of their initial appearance in this journal.

Please use the following credit lines (or similar) and copyright statement adjacent to the figures (adding first/middle initials for your coauthors):

Adapted, by permission, from A. Schinkel-Ivy, [?] Pardisnia, and [?] Drake, 2014, "Head and arm positions that elicit maximal voluntary trunk range-of-motion measures," *Journal of Applied Biomechanics* (in press). © Human Kinetics, Inc.

Thanks for checking with us. If there's anything else I can help you with, please don't hesitate to ask.

Best,

Martha

Martha Gullo

Senior Permissions Manager
Human Kinetics, Inc.
www.humankinetics.com
P: 217-351-5076 ext. 2223
F: 217-351-2674
E: marthag@hkusa.com

Figure 30: The final marker set recommendation that was appropriate for the greatest number of movement tasks (6 of 7) (Adapted from: Schinkel-Ivy A, Drake JDM. Quantification of the trunk: Which motion segments are required to sufficiently characterize its kinematic behaviour? Journal of Electromyography and Kinesiology (in review, manuscript ID JEK-D-14-00129.R1). Figure 1).



Alison Schinkel <alisonschinkel@gmail.com>

Question regarding permissions for in-review work

Permissions Helpdesk <permissionshelpdesk@elsevier.com>

Wed, Sep 10, 2014
at 3:35 PM

To: Alison Schinkel <alisonschinkel@gmail.com>

Dear Alison:

Permission is covered by the rights you retain as an Elsevier journal author as outlined at <http://www.elsevier.com/journal-authors/author-rights-and-responsibilities>, which include Inclusion in a thesis or dissertation, provided that proper acknowledgement is given to the original source of publication. As this is a retained right, no written permission is necessary. If you have any questions, please let me know. Best of luck with your dissertation.

Regards,

Hop

Hop Wechsler

Permissions Helpdesk Manager

Elsevier

1600 John F. Kennedy Boulevard

Suite 1800

Philadelphia, PA 19103-2899

Tel: +1-215-239-3520

Mobile: +1-215-900-5674

Fax: +1-215-239-3805

E-mail: h.wechsler@elsevier.com

Contact the Permissions Helpdesk:

+1-800-523-4069 x 3808 permissionshelpdesk@elsevier.com

APPENDIX C

Setup of Coordinate Systems

APPENDIX C

Setup of Coordinate Systems

Laboratory Coordinate System

The laboratory coordinate system was defined based on a Vicon calibration wand (Vicon MX, Vicon Systems Ltd., Oxford, UK). The selected origin in the centre of the laboratory was marked with painter's tape, and for each collection, the origin was defined at this same location. Within the associated Nexus software (version 1.6.1; Vicon MX, Vicon Systems Ltd., Oxford, UK), the X axis was defined as the medio-lateral axis; the Y axis was defined as the antero-posterior axis; and the Z axis was defined as the supero-inferior axis, in line with gravity. Participants were positioned such that the positive directions in each axis were to their right (X axis), forward (Y axis), and up (Z axis) (Figure 34). Marks were made on the floor of the laboratory to define the antero-posterior location of the toes (in line with the origin) to ensure that each participant stood at the same location relative to the origin.



Figure 36: Orientation of the participant relative to the laboratory coordinate system.

Model Setup and Local Coordinate Systems

Within Visual3D v.4 (C-Motion, Inc., Germantown, USA), local coordinate systems were assigned to the head, trunk, pelvis, and each marker clusters (C₇, T₃, T₆, T₉, T₁₂, and L₅) (Figure 35). To assign a local coordinate system to the marker clusters, the right marker was arbitrarily defined as the lateral marker, while the left marker was defined as the medial marker (C-Motion Research Biomechanics Wiki-Documentation: Marker Set Guidelines, www.c-motion.com/v3dwiki/index.php?title=Marker_Set_Guidelines). The same convention (right: lateral, left: medial) was employed for the head, trunk, and pelvis.

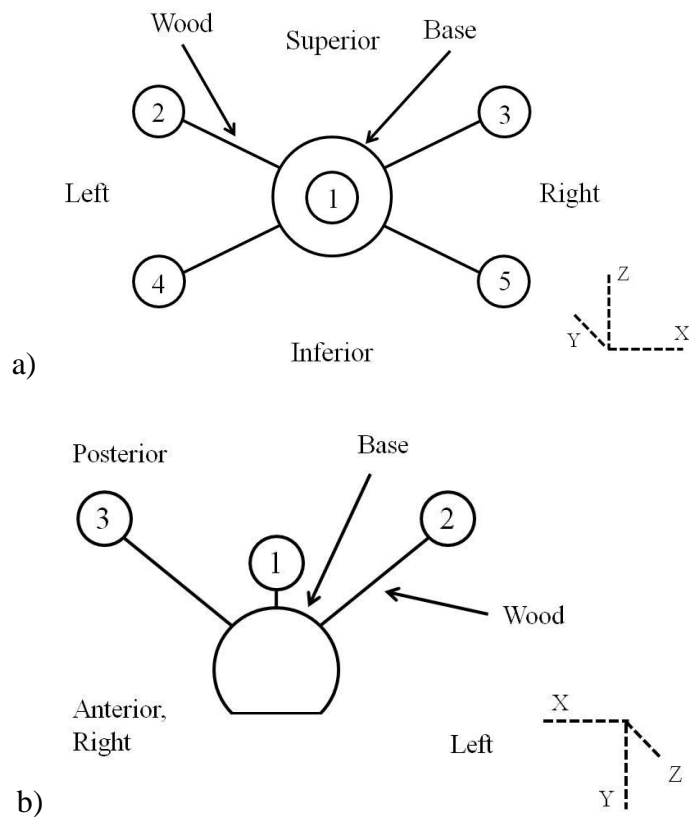


Figure 37: a) Posterior view of a cluster when adhered to the skin over the spine. b) Top view of a cluster when adhered to the skin over the spine.

Segment coordinate systems were defined as per C-Motion Research Biomechanics Wiki-Documentation (Constructing the Segment Coordinate System, [www.c-motion.com/v3dwiki/index.php?title=Constructing the Segment Coordinate System](http://www.c-motion.com/v3dwiki/index.php?title=Constructing_the_Segment_Coordinate_System)). The Z axis passed through the midpoint of the distance between the two proximal and two distal endpoints. The plane of the proximal and distal markers also defined the frontal (X-Z) plane. The cross-product of the Z axis and the line connecting the two proximal markers determined the Y axis. Finally, the cross-product of the Y and Z axes was calculated to define the X axis, producing a set of orthogonal axes in which

rotation around the X axis represented flexion-extension, rotation around the Y axis represented lateral bend, and rotation around the Z axis represented axial twist. The orientation of the segment coordinate systems were aligned with the laboratory coordinate system, with the positive directions for each axis were the right (X axis), forward (Y axis), and up (Z axis). The head, trunk, and pelvis were all defined as per C-Motion Research Biomechanics Wiki-Documentation (Marker Set Guidelines, www.c-motion.com/v3dwiki/index.php?title=Marker_Set_Guidelines), and the coordinate systems for the clusters were defined using the same convention (Table 41).

Table 41: Markers used to define the endpoints of each segment and cluster. The midpoint of the two proximal markers and the two distal markers were used to create the Z axis.

Segment	Proximal Endpoints	Distal Endpoints
Head	Left, right acromia	Markers posterior to the ear, left and right sides
Clusters	Cluster markers #4, #5	Cluster markers #2, #3
Trunk	Left, right iliac crests	Left, right acromia
Pelvis	Left, right iliac crests	Left, right greater trochanters

APPENDIX D

Exemplar Kinematic and EMG Data

APPENDIX D

Exemplar Kinematic and EMG Data

CT: Cervico-thoracic region.
EO: External oblique.
IO: Internal oblique.
L/R: Left/right.
LD: Latissimus dorsi.
LES: Lumbar erector spinae.
LT: Lower-thoracic region.
LTES: Lower-thoracic erector spinae.
MT: Mid-thoracic region.
RA: Rectus abdominis.
TR: Upper trapezius.
UT: Upper-thoracic region.
UTES: Upper-thoracic erector spinae.

Chapter 3

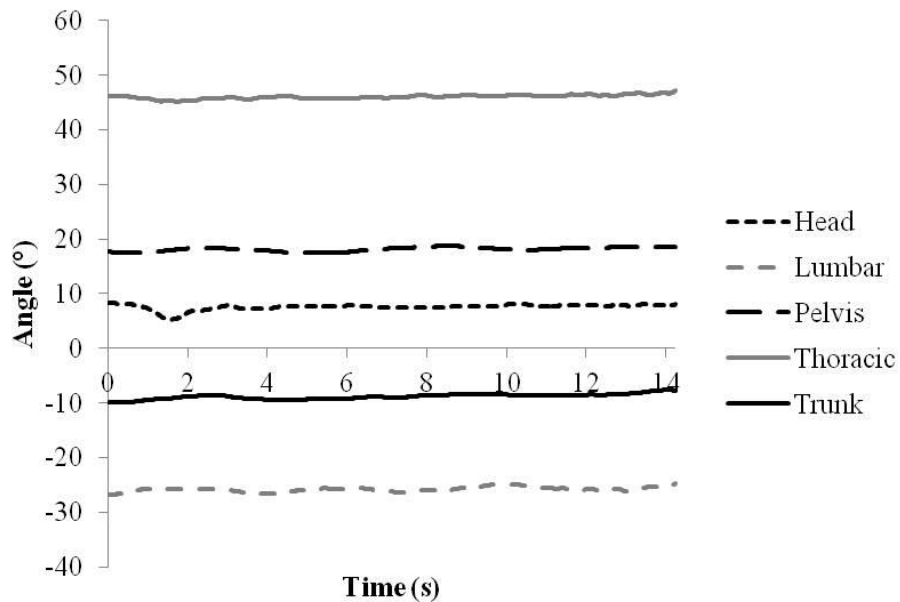


Figure 38: Sample time series data set of head, lumbar, pelvis, thoracic, and trunk flexion-extension angles during upright standing.

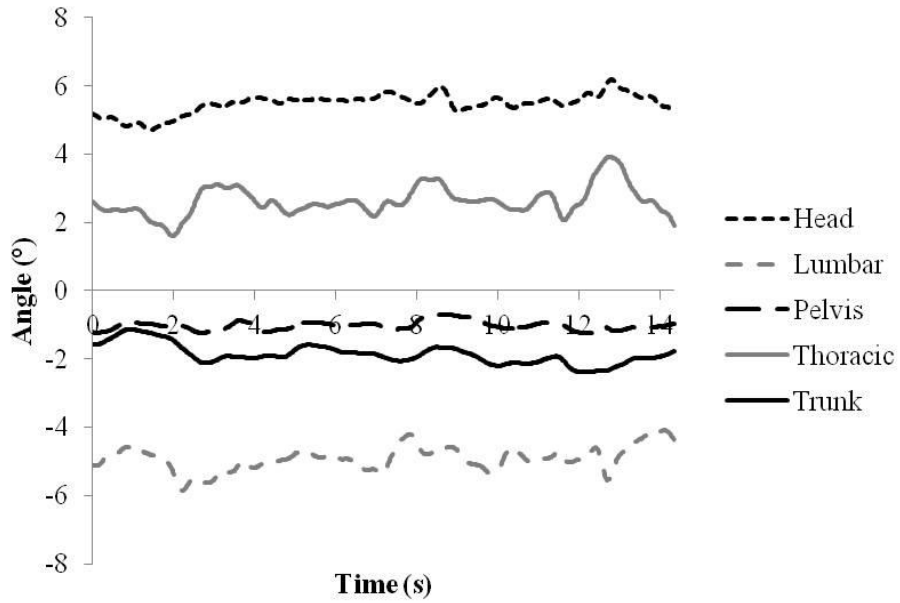


Figure 39: Sample time series data set of head, lumbar, pelvis, thoracic, and trunk lateral bend angles during upright standing.

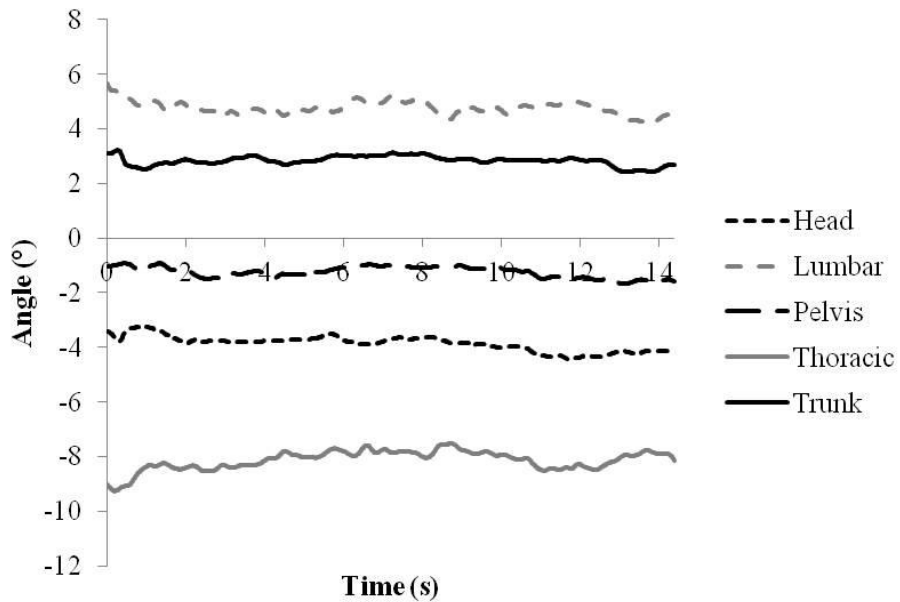


Figure 40: Sample time series data set of head, lumbar, pelvis, thoracic, and trunk axial twist angles during upright standing.

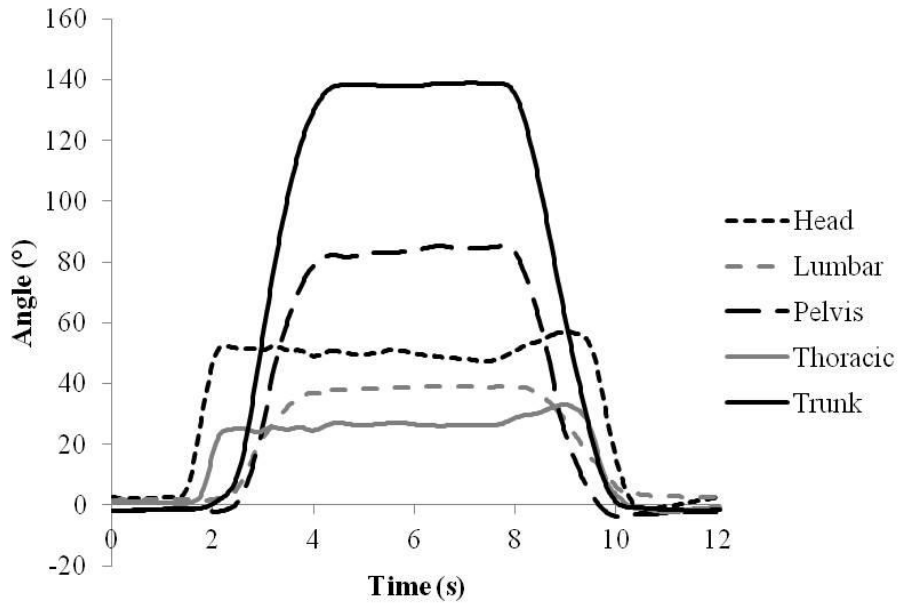


Figure 41: Sample time series data set of head, lumbar, pelvis, thoracic, and trunk flexion angles during MaxFlex.

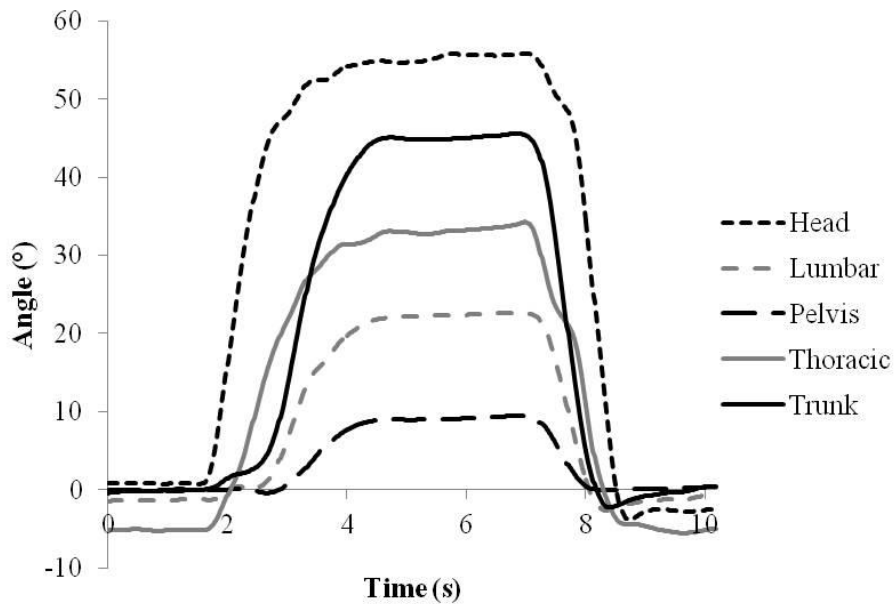


Figure 42: Sample time series data set of head, lumbar, pelvis, thoracic, and trunk lateral bend angles during MaxBend.

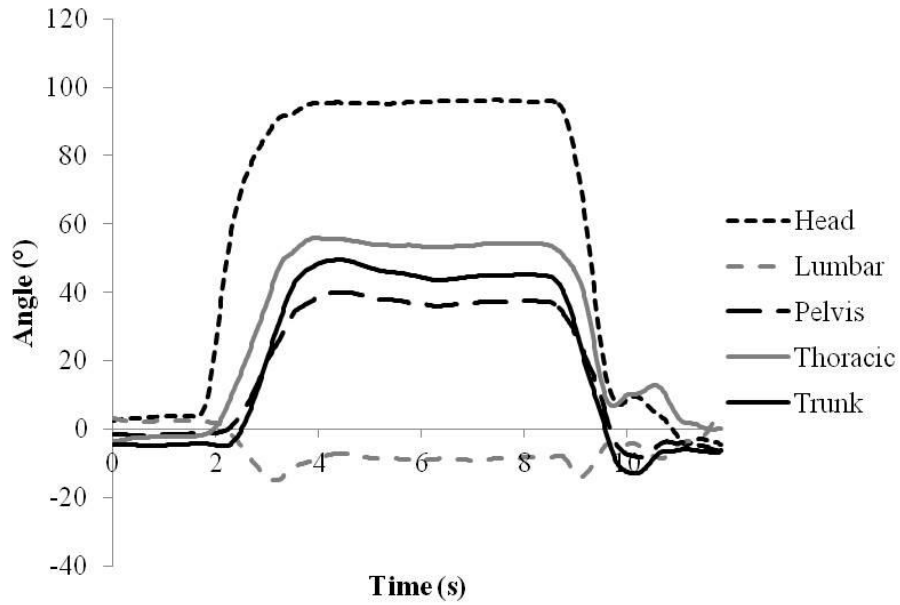


Figure 43: Sample time series data set of head, lumbar, pelvis, thoracic, and trunk axial twist angles during MaxTwist.

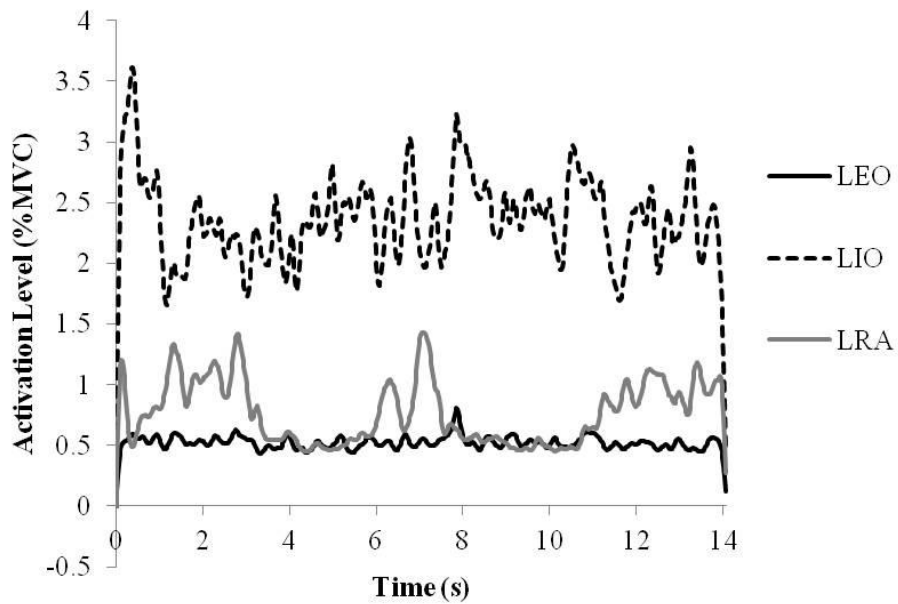


Figure 44: Sample time series data set of LEO, LIO, and LRA during upright standing.

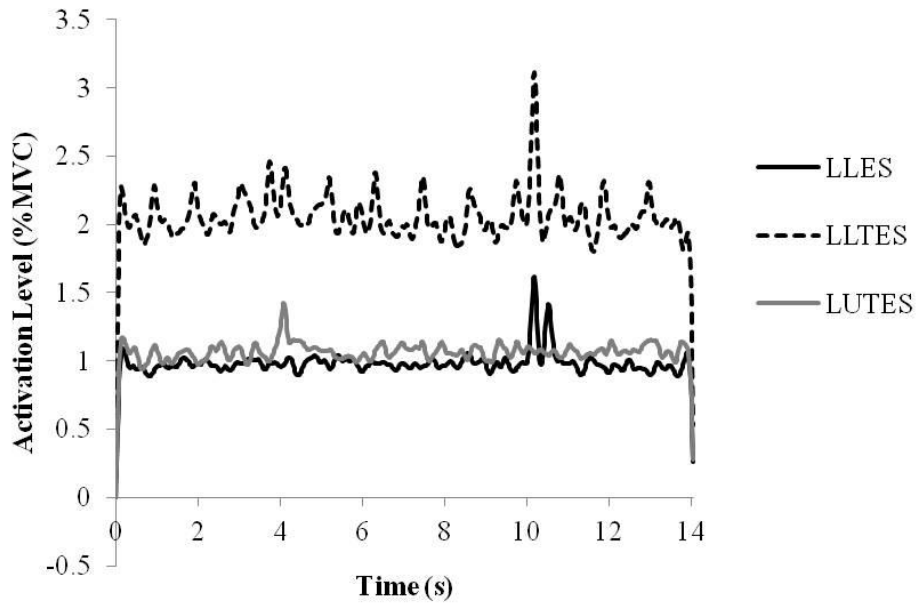


Figure 45: Sample time series data set of LLES, LLTES, and LUTES during upright standing.

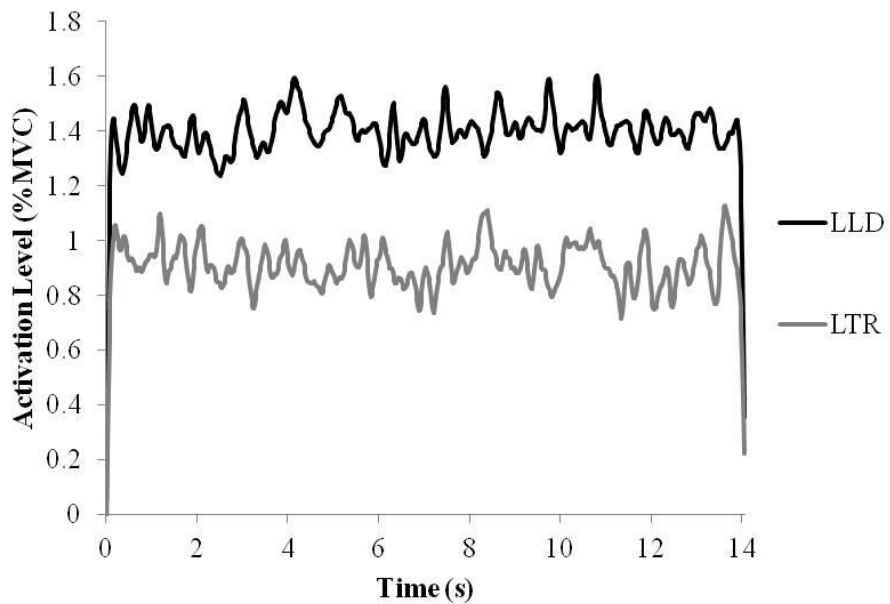


Figure 46: Sample time series data set of LLD and LTR during upright standing.

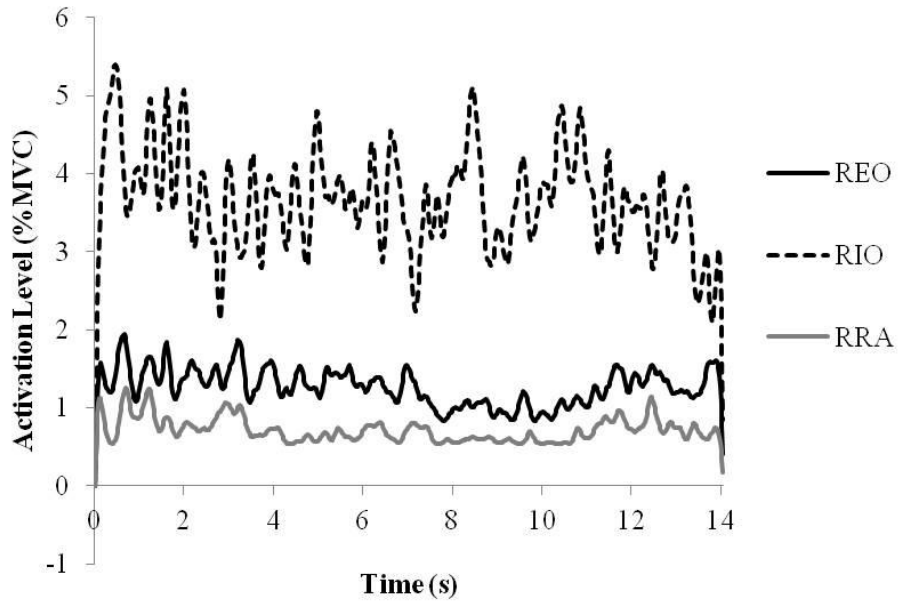


Figure 47: Sample time series data set of REO, RIO, and RRA during upright standing.

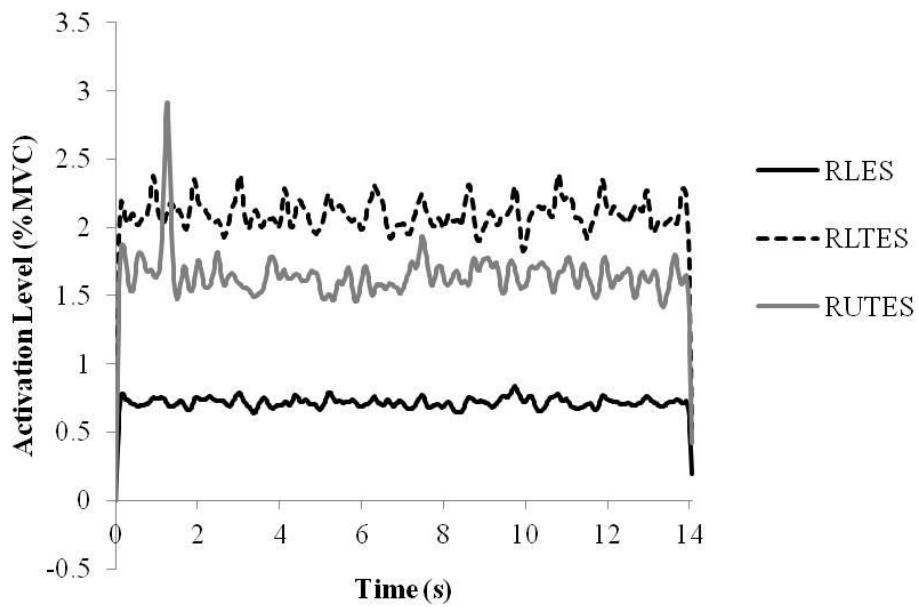


Figure 48: Sample time series data set of RLES, RLTES, and RUTES during upright standing.

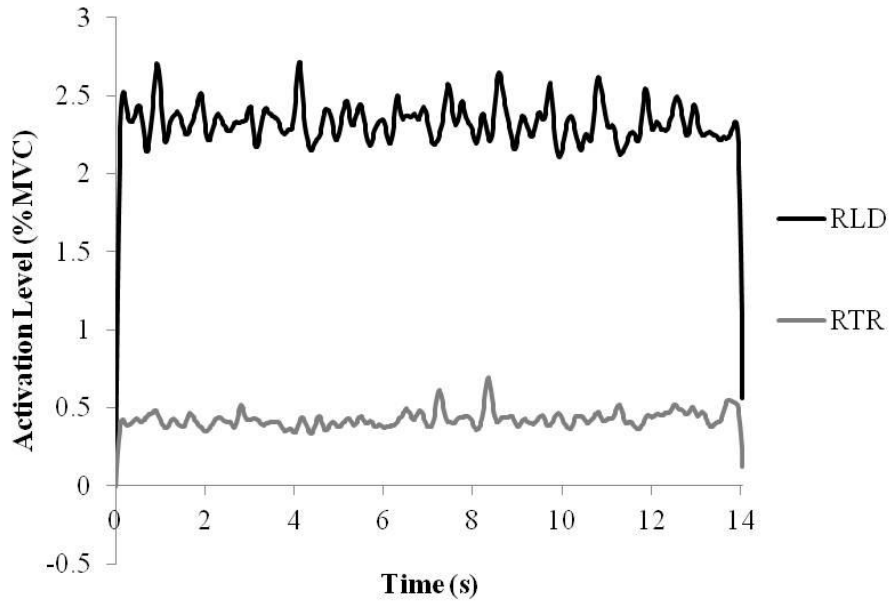


Figure 49: Sample time series data set of RLD and RTR during upright standing.

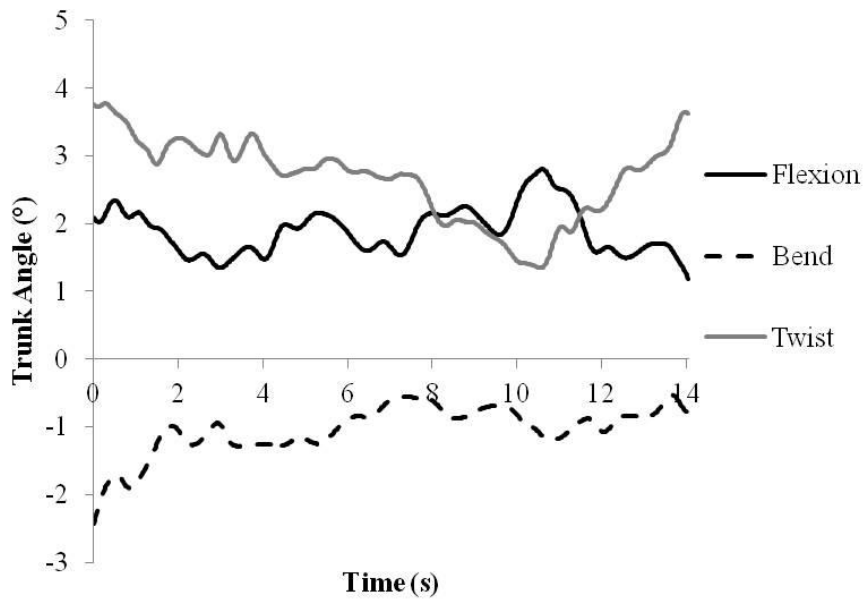


Figure 50: Time series data set of trunk angles in the flexion-extension, lateral bend, and axial twist directions during upright standing, as context for the EMG time series data sets.

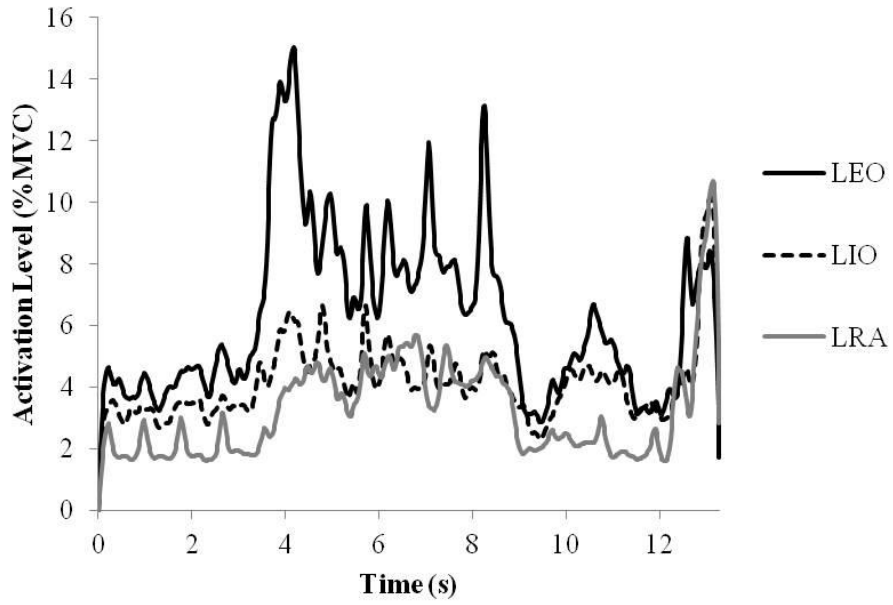


Figure 51: Sample time series data set of LEO, LIO, and LRA during MaxFlex.

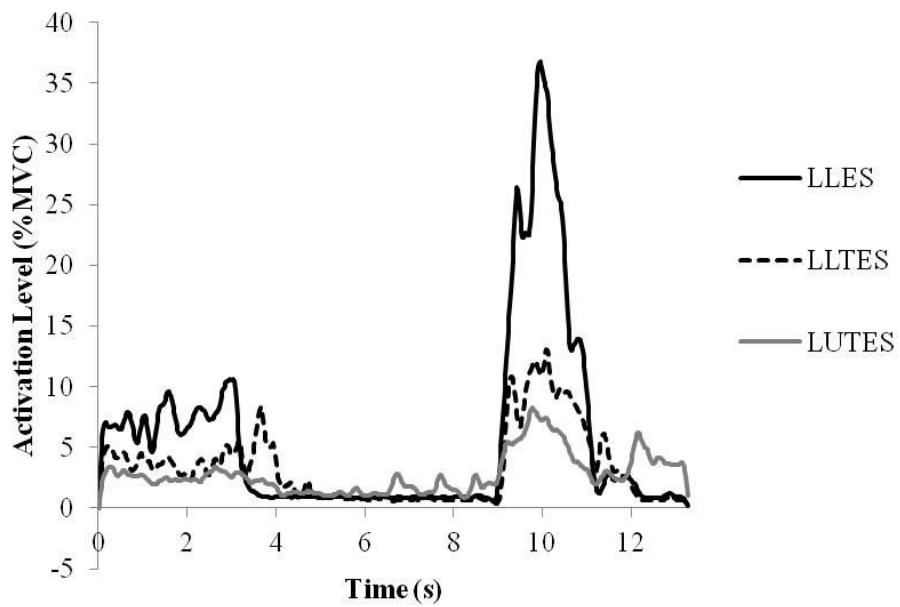


Figure 52: Sample time series data set of LLES, LLTES, and LUTES during MaxFlex.

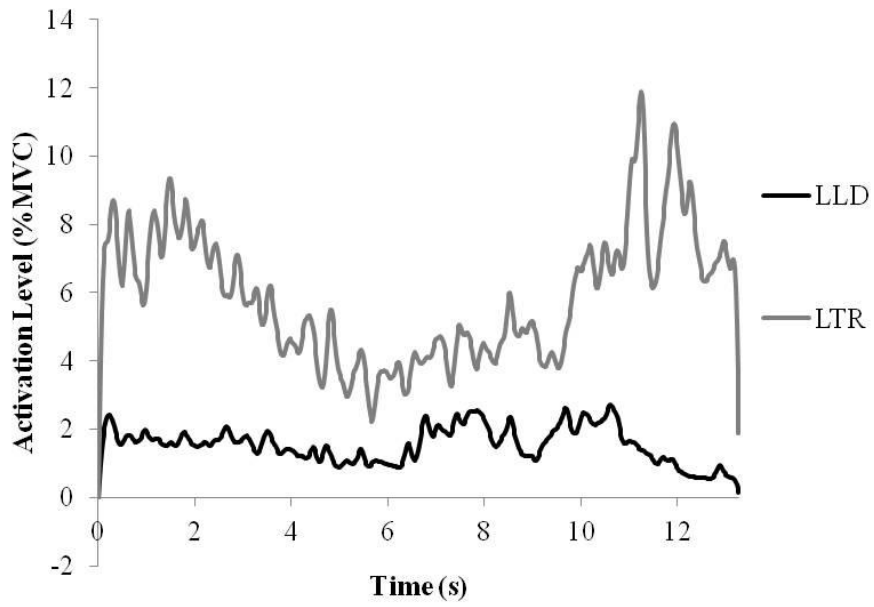


Figure 53: Sample time series data set of LLD and LTR during MaxFlex.

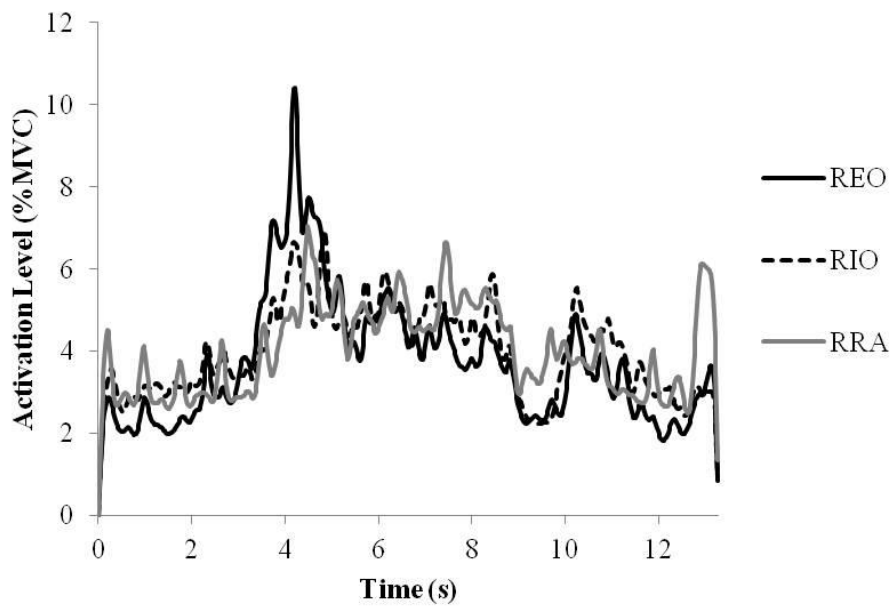


Figure 54: Sample time series data set of REO, RIO, and RRA during MaxFlex.

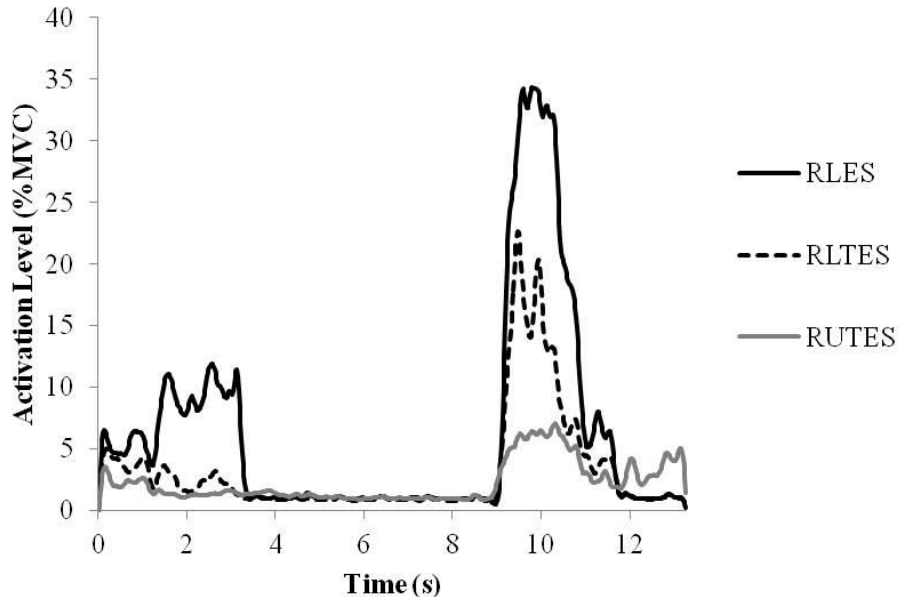


Figure 55: Sample time series data set of RLES, RLTES, and RUTES during MaxFlex.

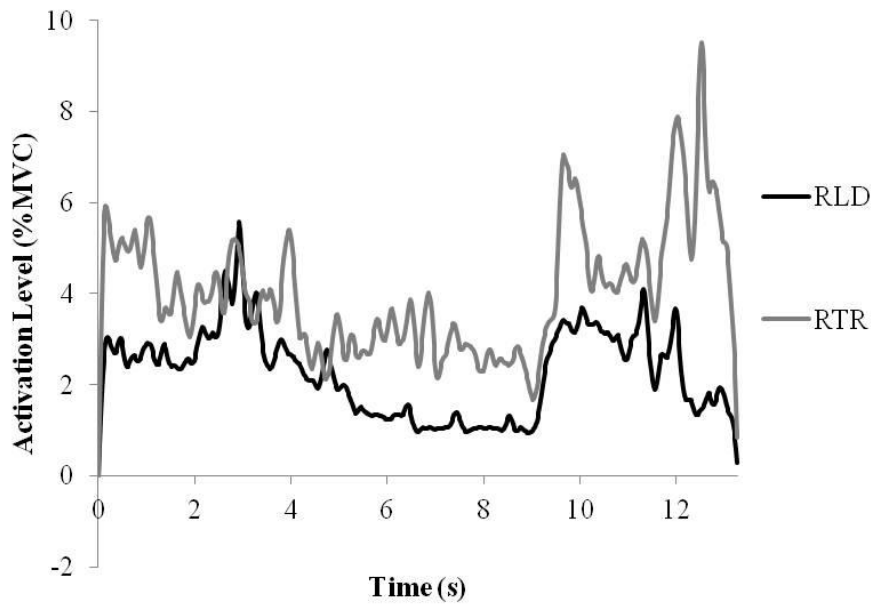


Figure 56: Sample time series data set of RLD and RTR during MaxFlex.

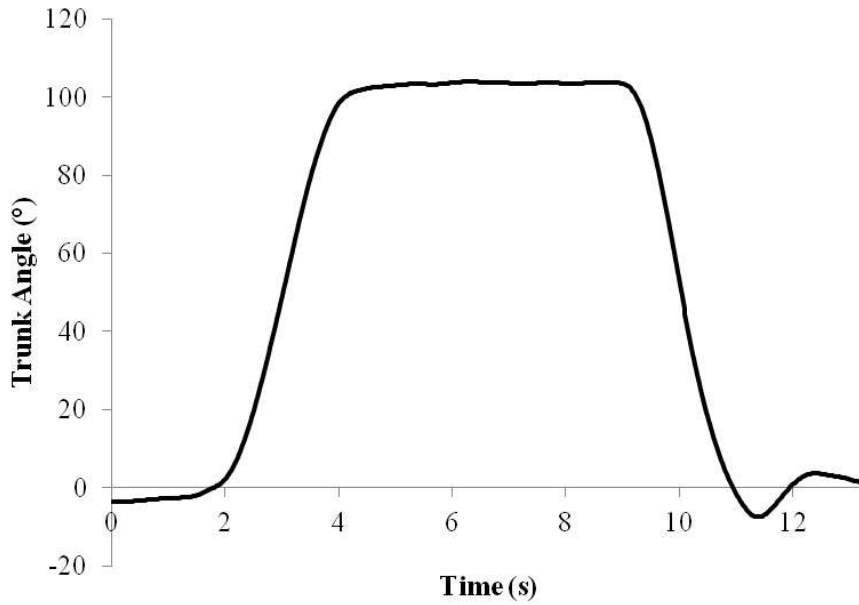


Figure 57: Time series data set of trunk flexion angles during MaxFlex, as context for the EMG time series data sets.

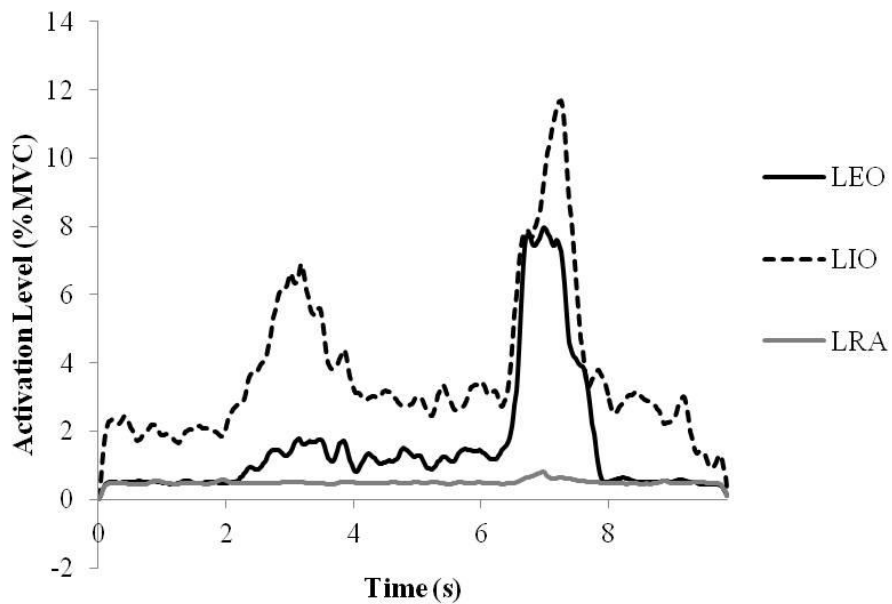


Figure 58: Sample time series data set of LEO, LIO, and LRA during MaxBend.

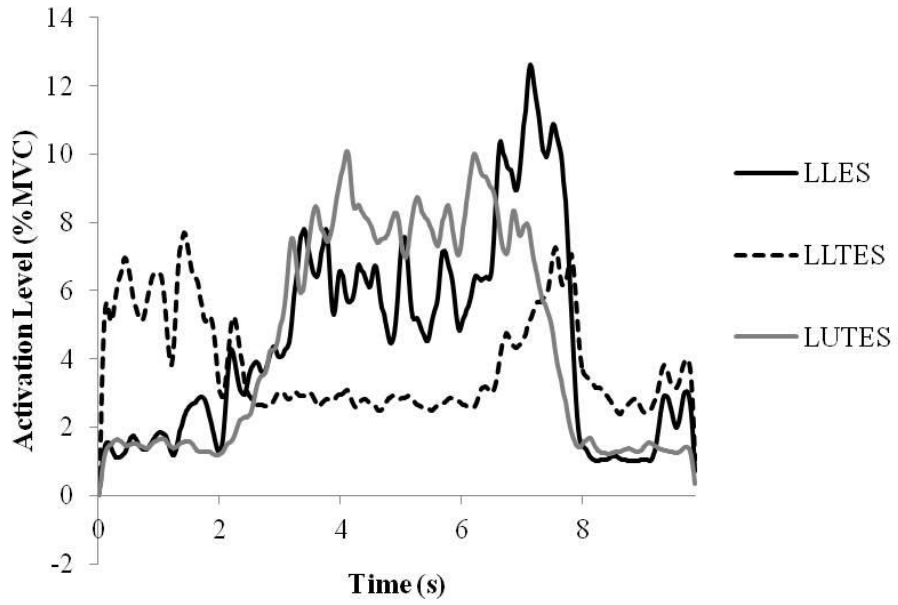


Figure 59: Sample time series data set of LLES, LLTES, and LUTES during MaxBend.

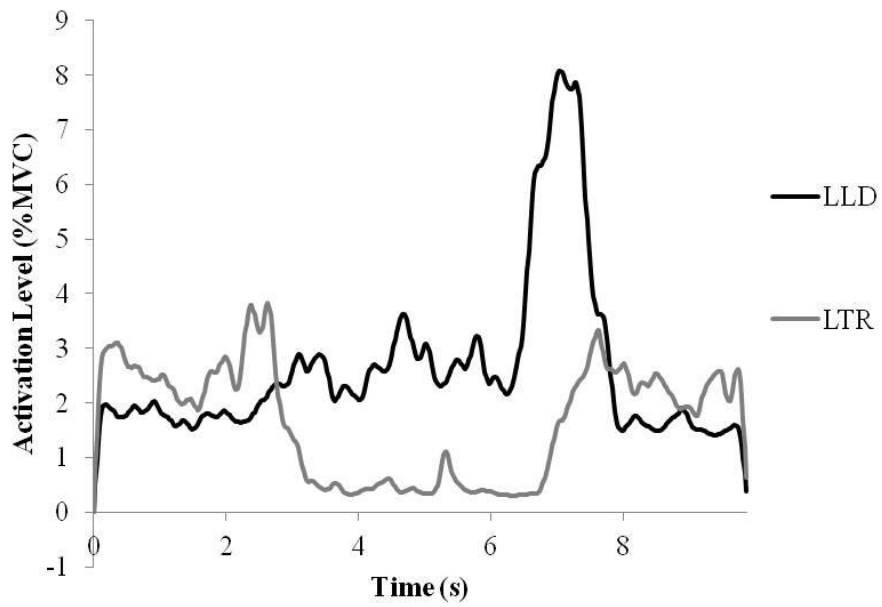


Figure 60: Sample time series data set of LLD and LTR during MaxBend.

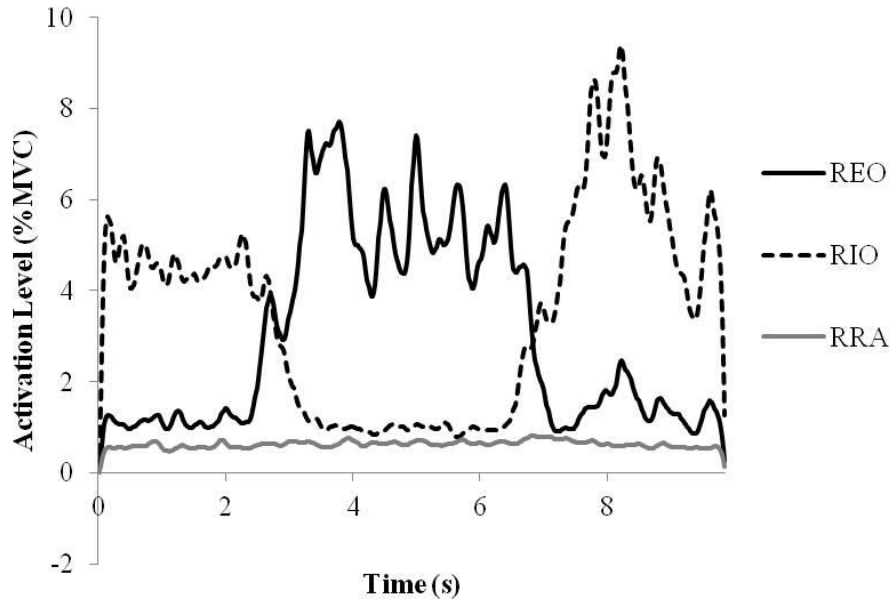


Figure 61: Sample time series data set of REO, RIO, and RRA during MaxBend.

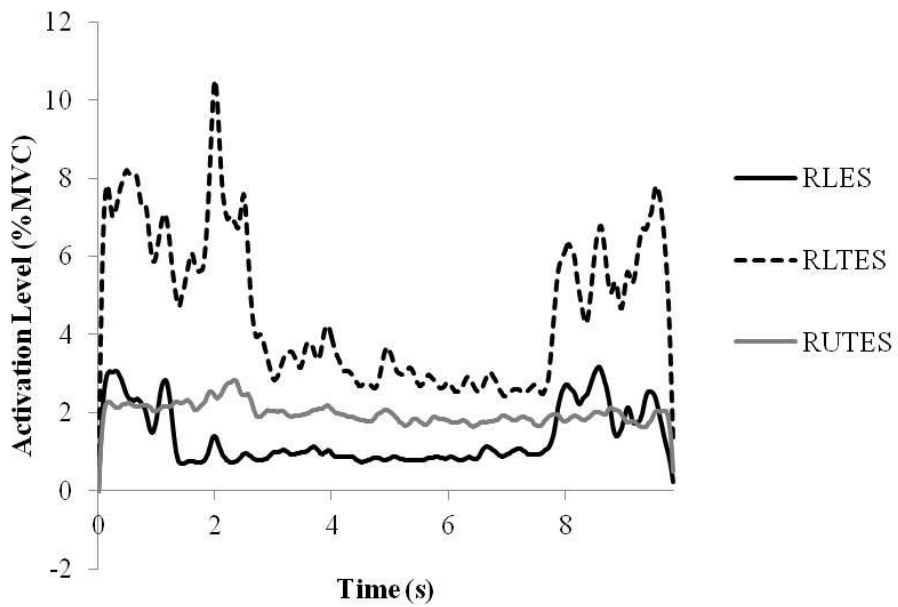


Figure 62: Sample time series data set of RLES, RLTES, and RUTES during MaxBend.

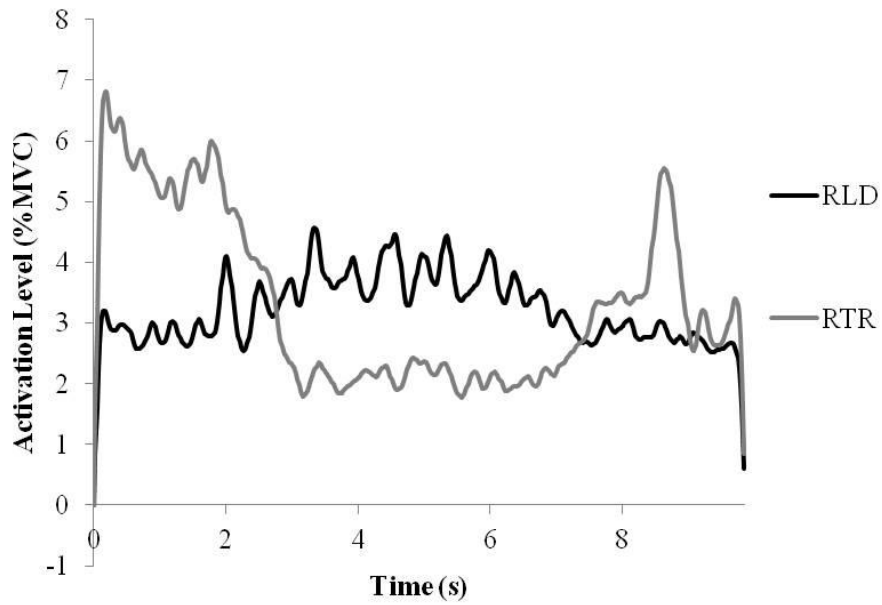


Figure 63: Sample time series data set of RLD and RTR during MaxBend.

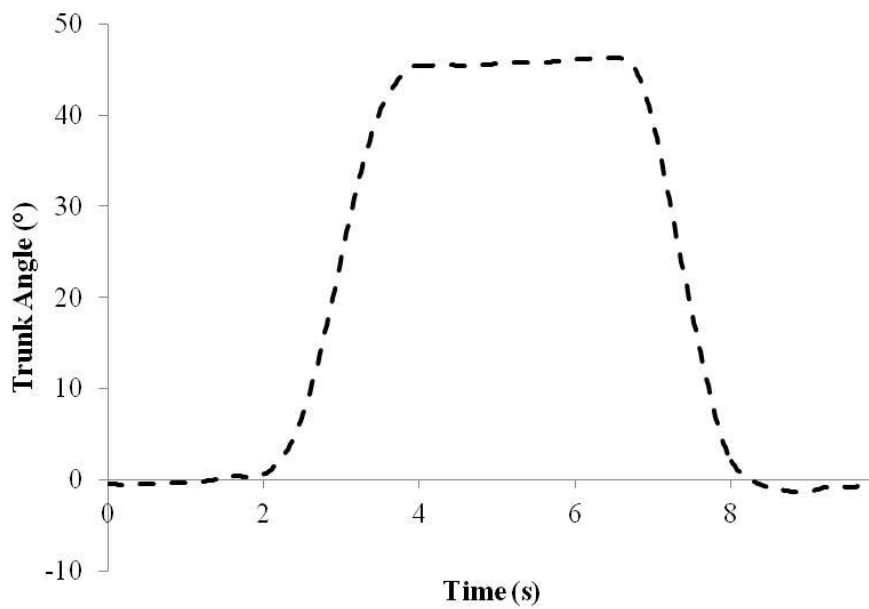


Figure 64: Time series data set of trunk lateral bend angles during MaxBend, as context for the EMG time series data sets.

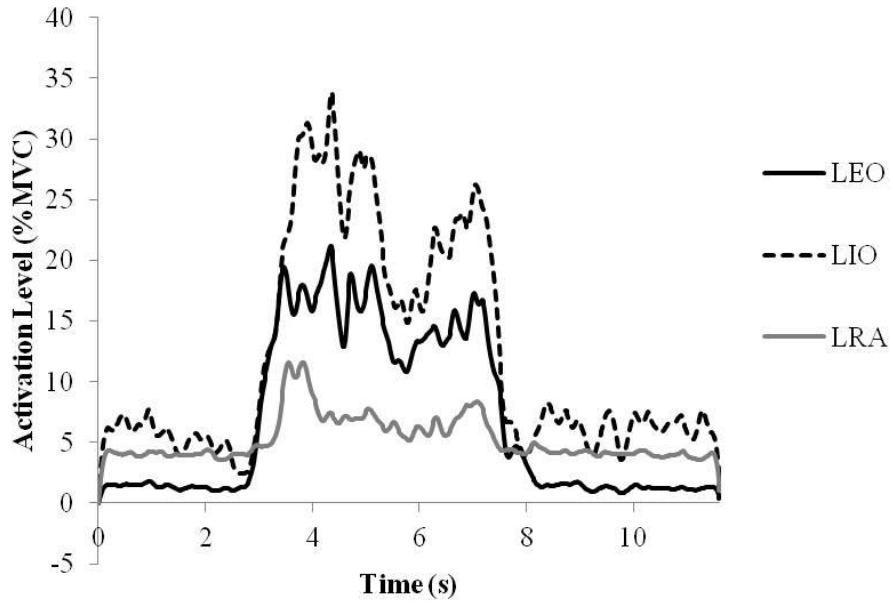


Figure 65: Sample time series data set of LEO, LIO, and LRA during MaxTwist.

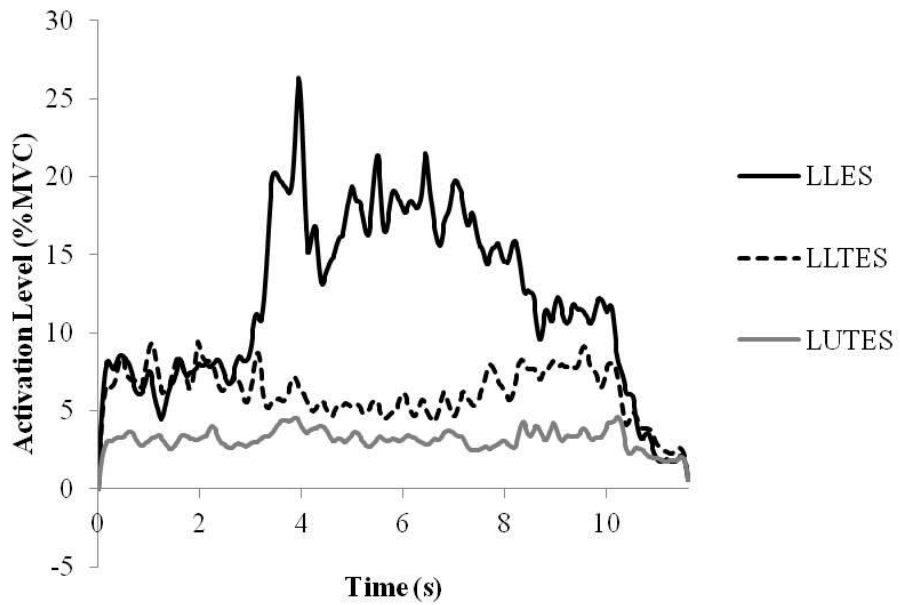


Figure 66: Sample time series data set of LLES, LLTES, and LUTES during MaxTwist.

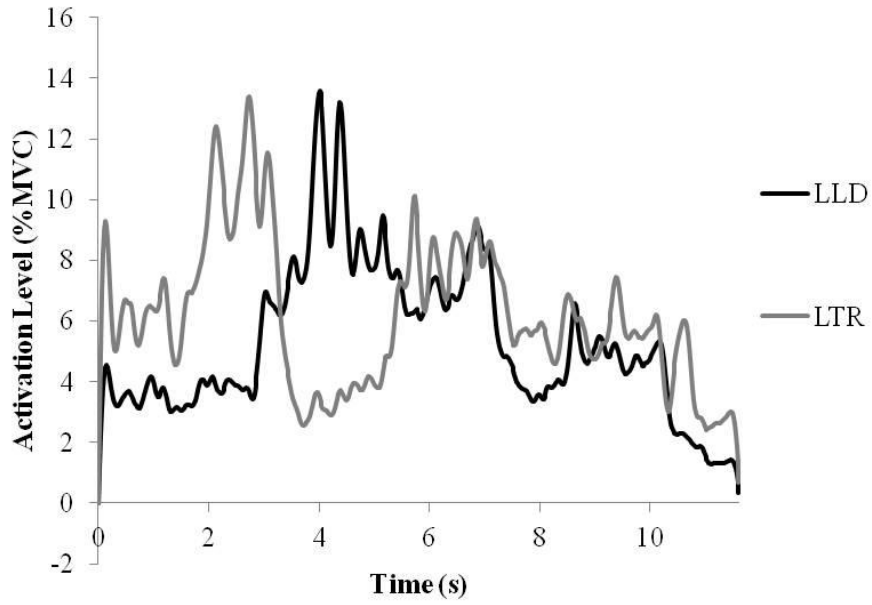


Figure 67: Sample time series data set of LLD and LTR during MaxTwist.

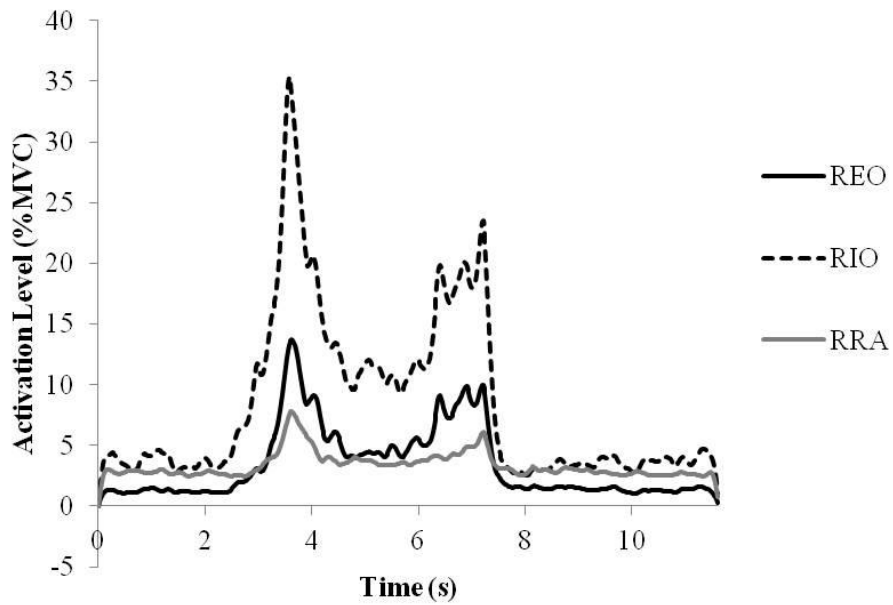


Figure 68: Sample time series data set of REO, RIO, and RRA during MaxTwist.

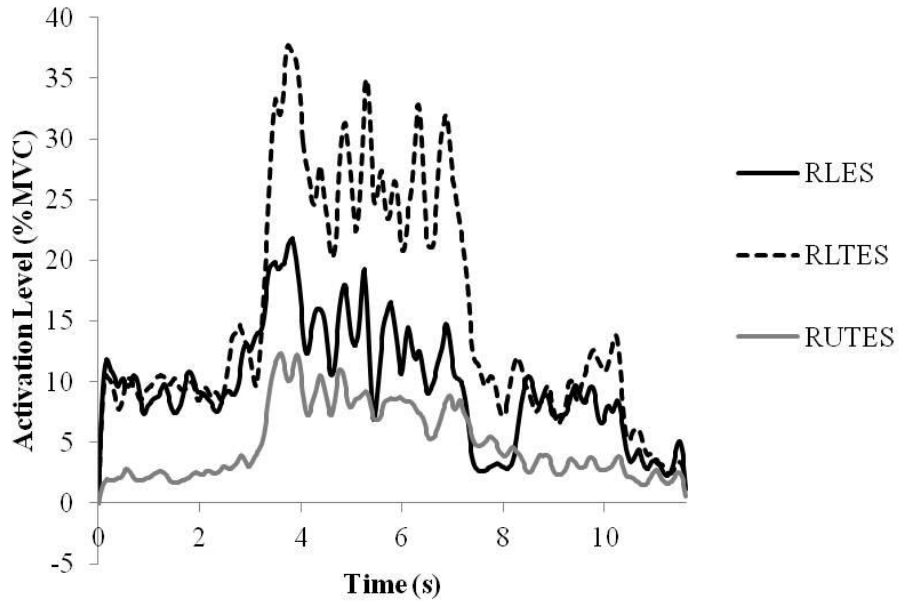


Figure 69: Sample time series data set of RLES, RLTES, and RUTES during MaxTwist.

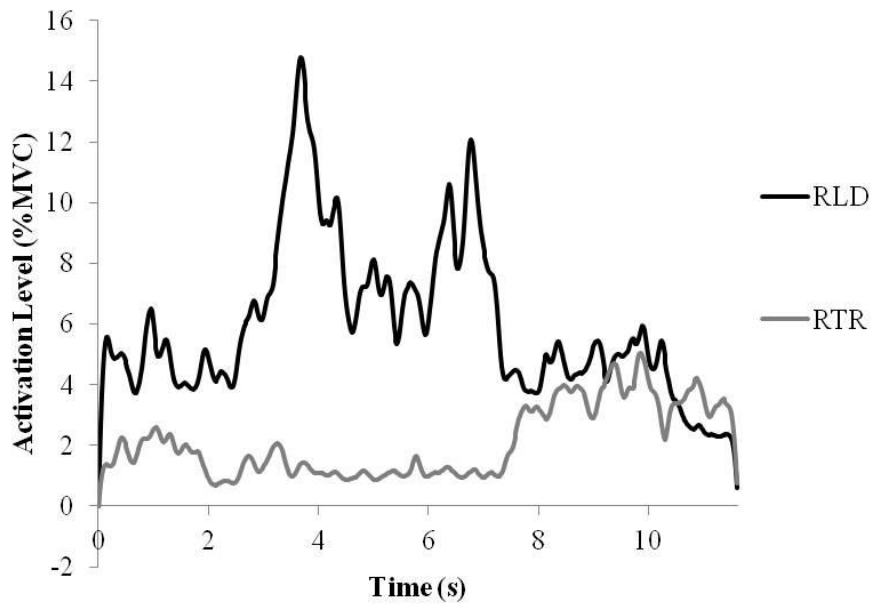


Figure 70: Sample time series data set of RLD and RTR during MaxTwist.

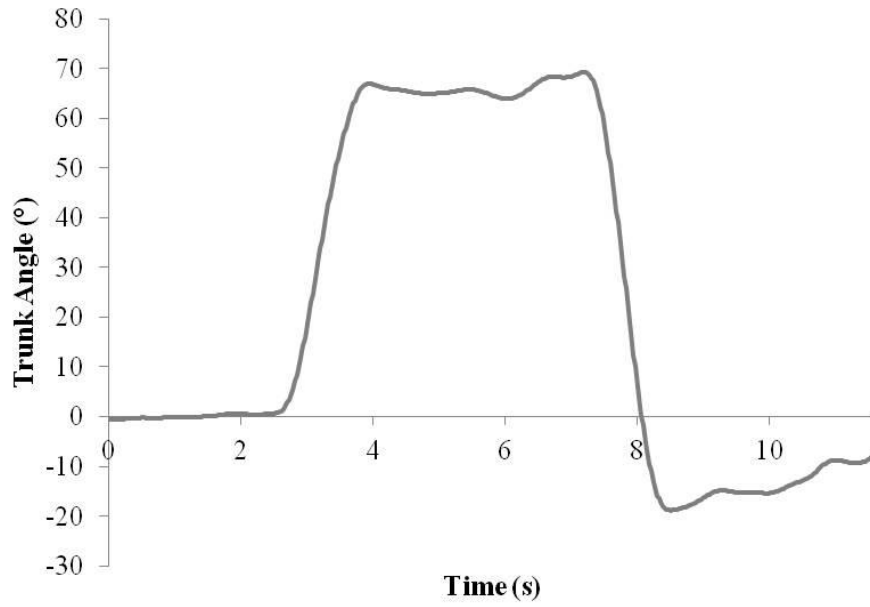


Figure 71: Time series data set of trunk axial angles during MaxTwist, as context for the EMG time series data sets.

Chapter 4

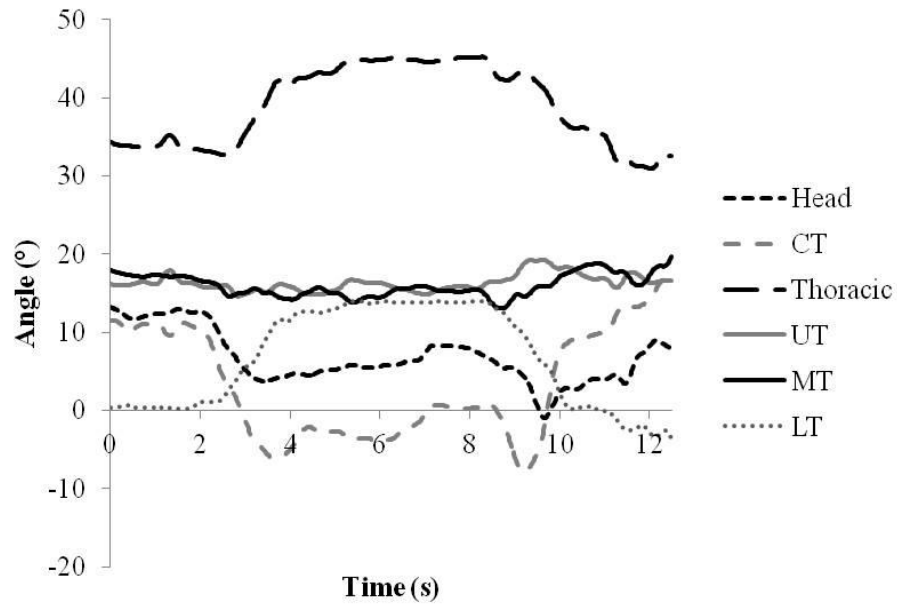


Figure 72: Sample time series data set of the head, CT, thoracic, UT, MT, and LT flexion angles during MaxFlex (neutral head, crossed arms).

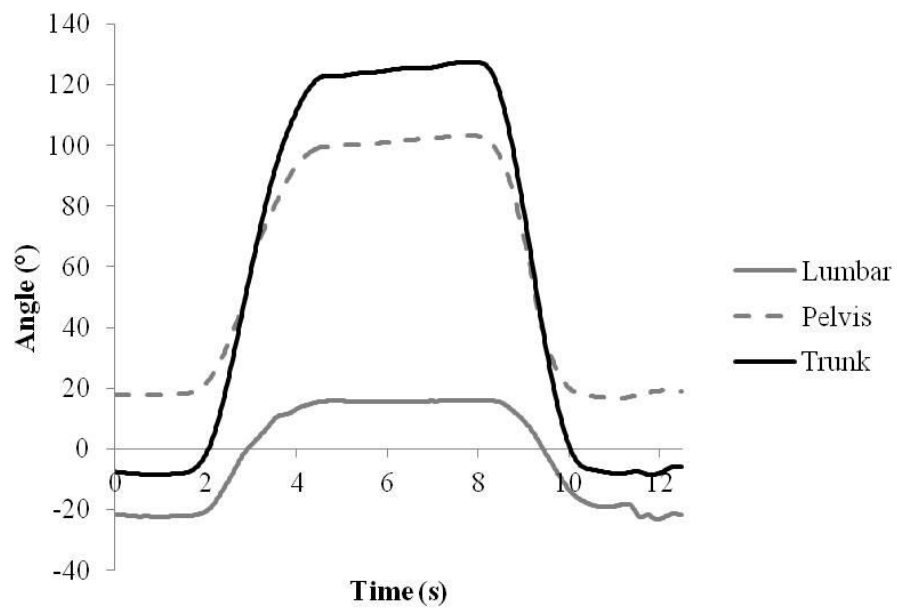


Figure 73: Sample time series data set of the lumbar, pelvis, and trunk flexion angles during MaxFlex (neutral head, crossed arms).

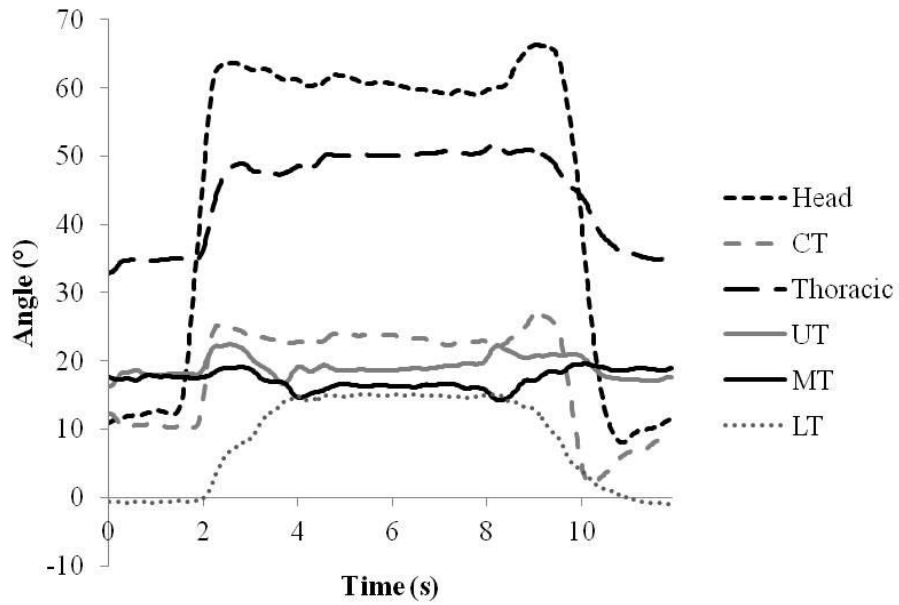


Figure 74: Sample time series data set of the head, CT, thoracic, UT, MT, and LT flexion angles during MaxFlex (active head, crossed arms).

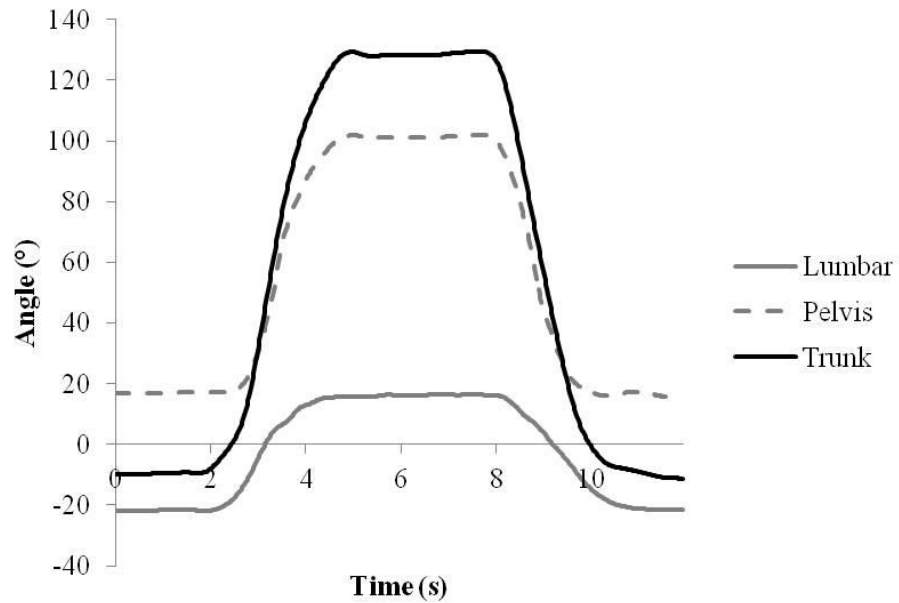


Figure 75: Sample time series data set of the lumbar, pelvis, and trunk flexion angles during MaxFlex (active head, crossed arms).

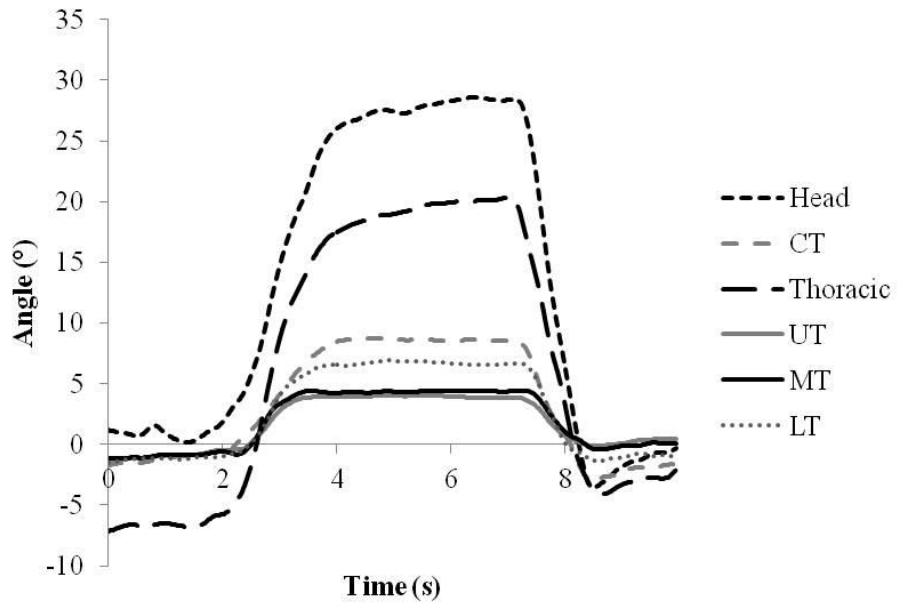


Figure 76: Sample time series data set of the head, CT, thoracic, UT, MT, and LT lateral bend angles during MaxBend (neutral head, crossed arms).

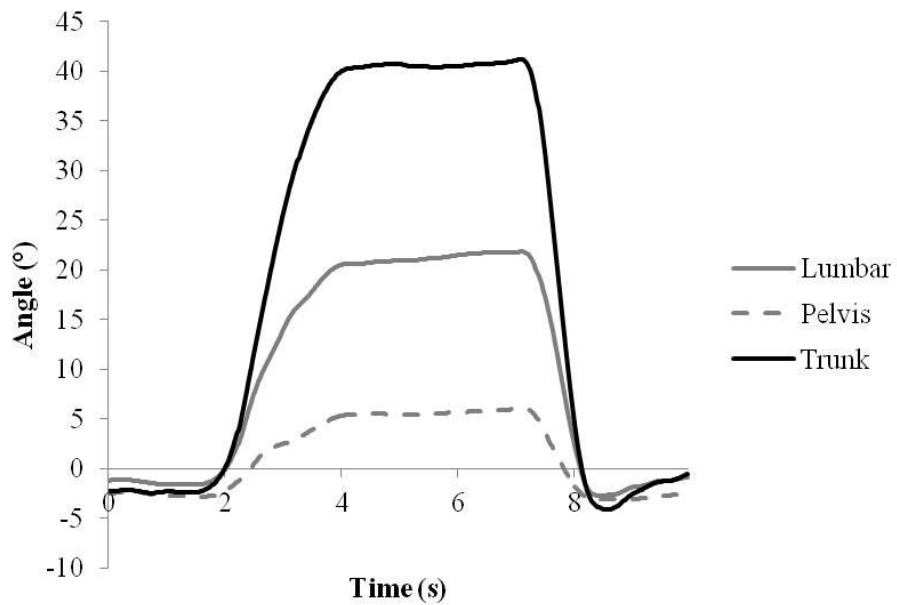


Figure 77: Sample time series data set of the lumbar, pelvis, and trunk lateral bend angles during MaxBend (neutral head, crossed arms).

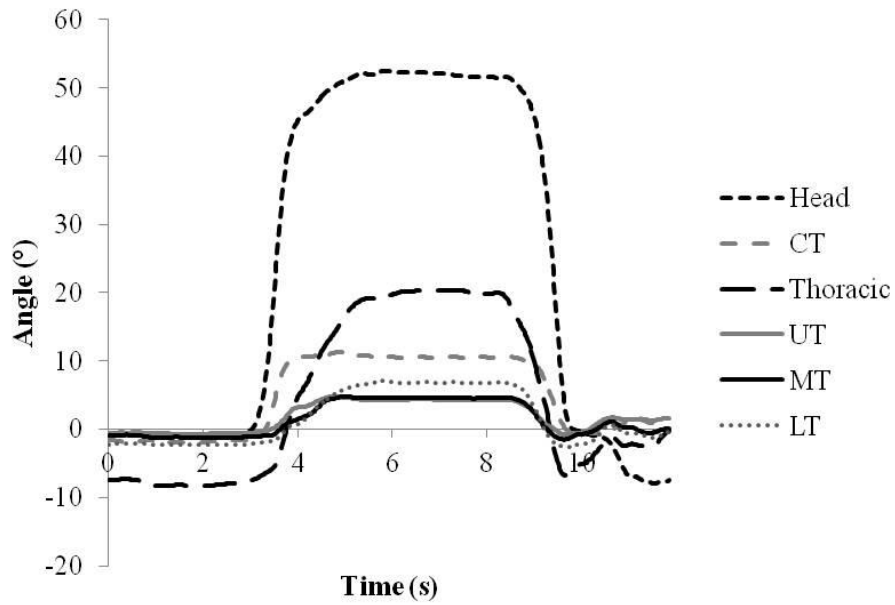


Figure 78: Sample time series data set of the head, CT, thoracic, UT, MT, and LT lateral bend angles during MaxBend (active head, crossed arms).

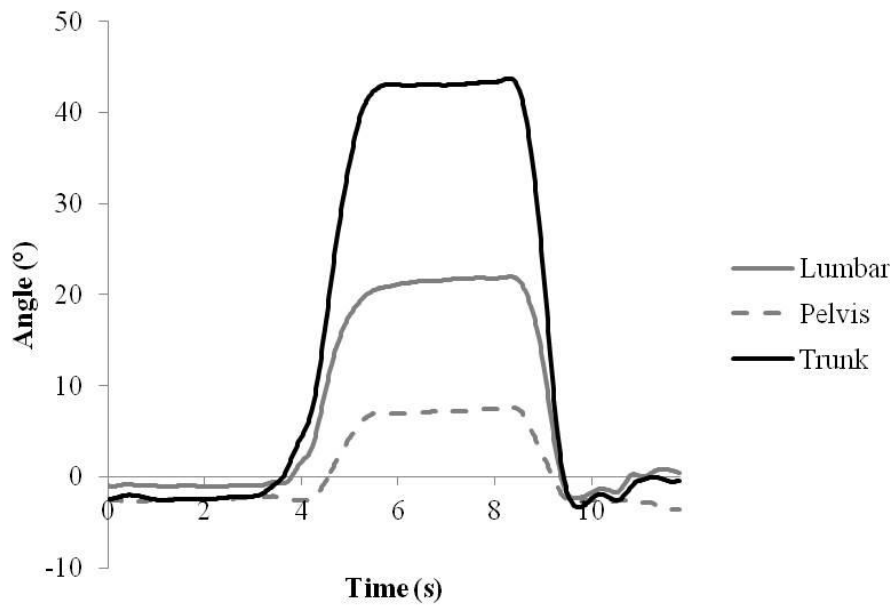


Figure 79: Sample time series data set of the lumbar, pelvis, and trunk lateral bend angles during MaxBend (active head, crossed arms).

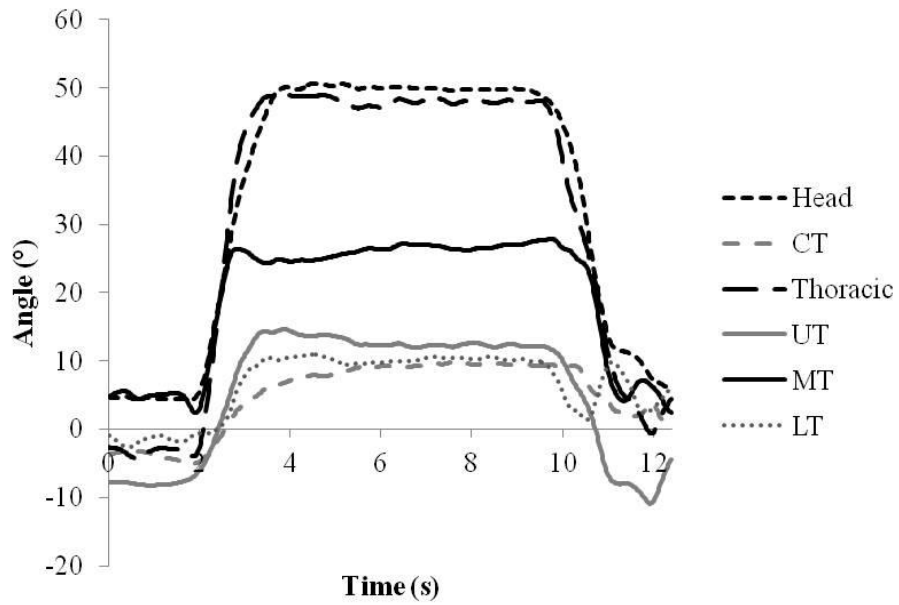


Figure 80: Sample time series data set of the head, CT, thoracic, UT, MT, and LT axial twist angles during MaxTwist (neutral head, crossed arms).

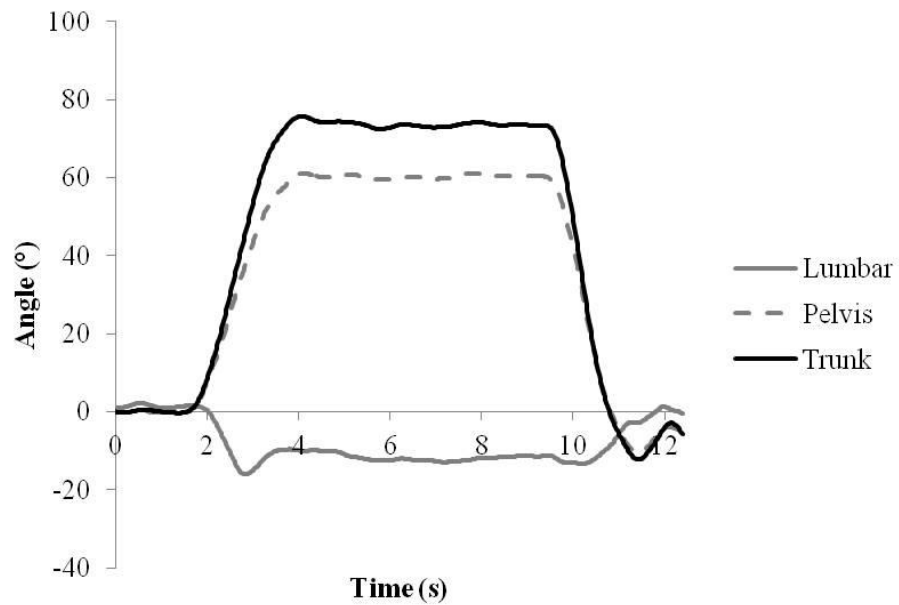


Figure 81: Sample time series data set of the lumbar, pelvis, and trunk axial twist angles during MaxTwist (neutral head, crossed arms).

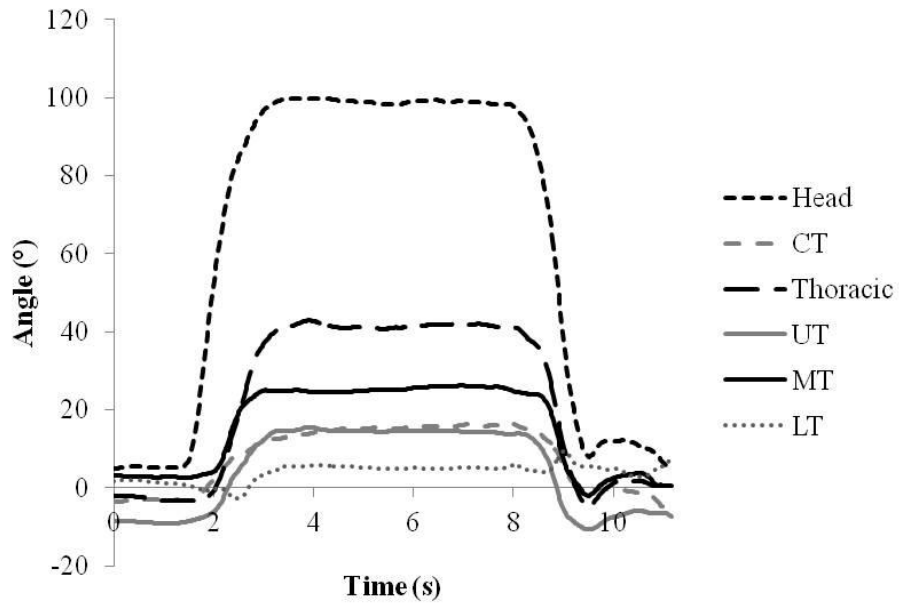


Figure 82: Sample time series data set of the head, CT, thoracic, UT, MT, and LT axial twist angles during MaxTwist (active head, crossed arms).

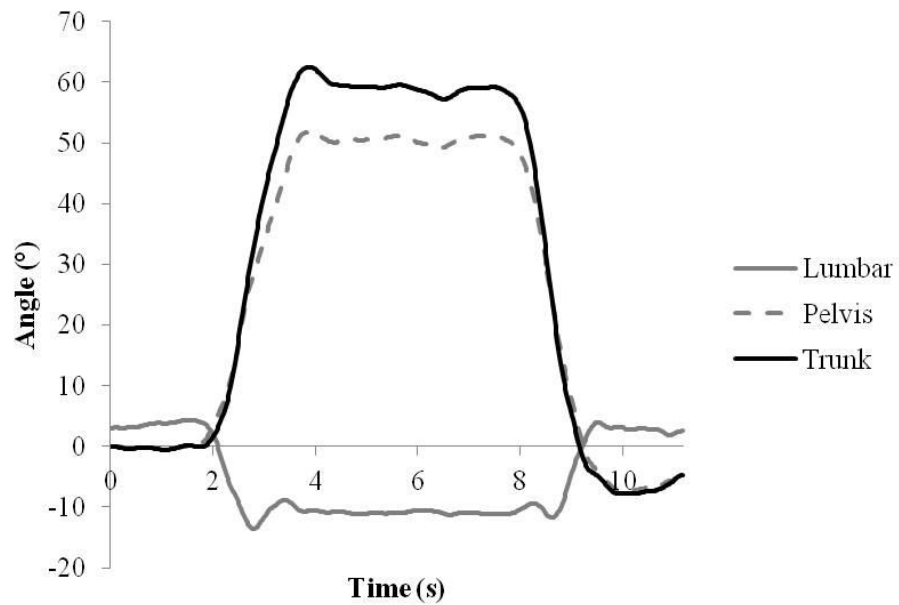


Figure 83: Sample time series data set of the lumbar, pelvis, and trunk axial twist angles during MaxTwist (active head, crossed arms).

Chapter 5

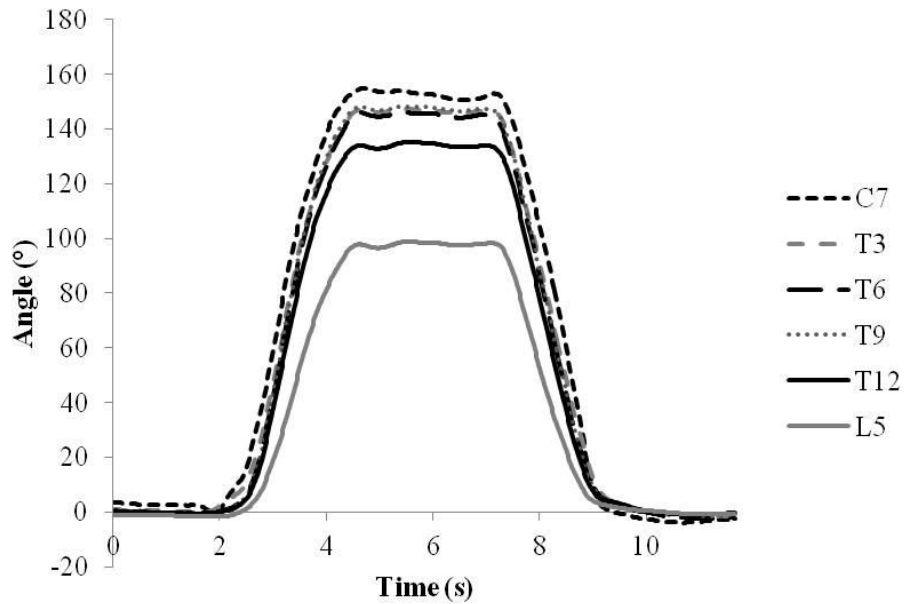


Figure 84: Sample time series data set of the flexion angles of the C₇, T₃, T₆, T₉, T₁₂, and L₅ clusters during MaxFlex.

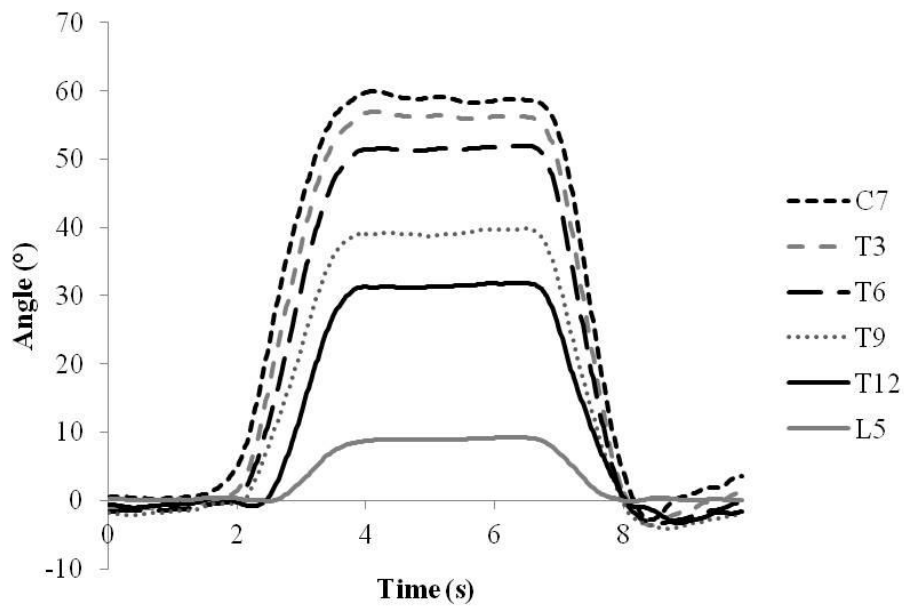


Figure 85: Sample time series data set of the lateral bend angles of the C₇, T₃, T₆, T₉, T₁₂, and L₅ clusters during MaxBend.

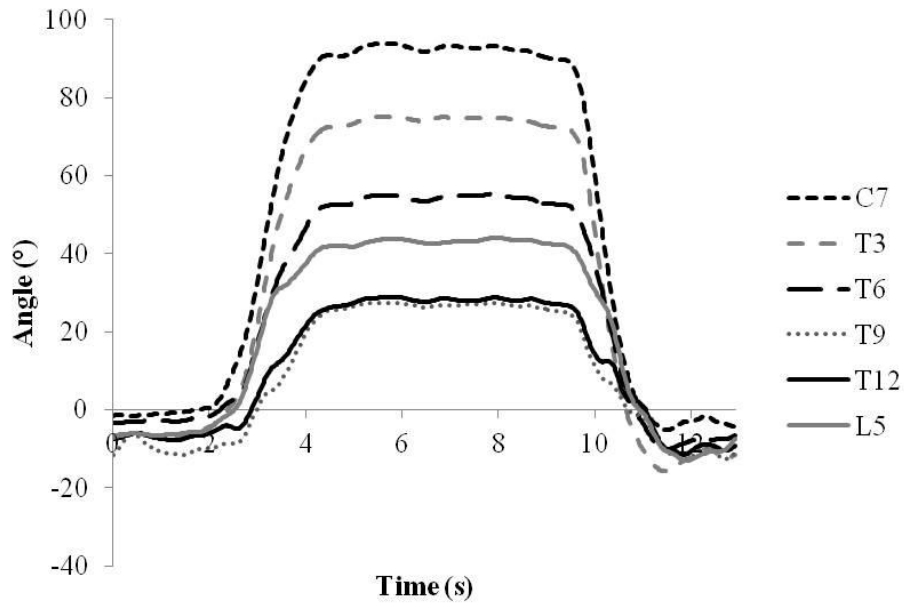


Figure 86: Sample time series data set of the axial twist angles of the C₇, T₃, T₆, T₉, T₁₂, and L₅ clusters during MaxTwist.

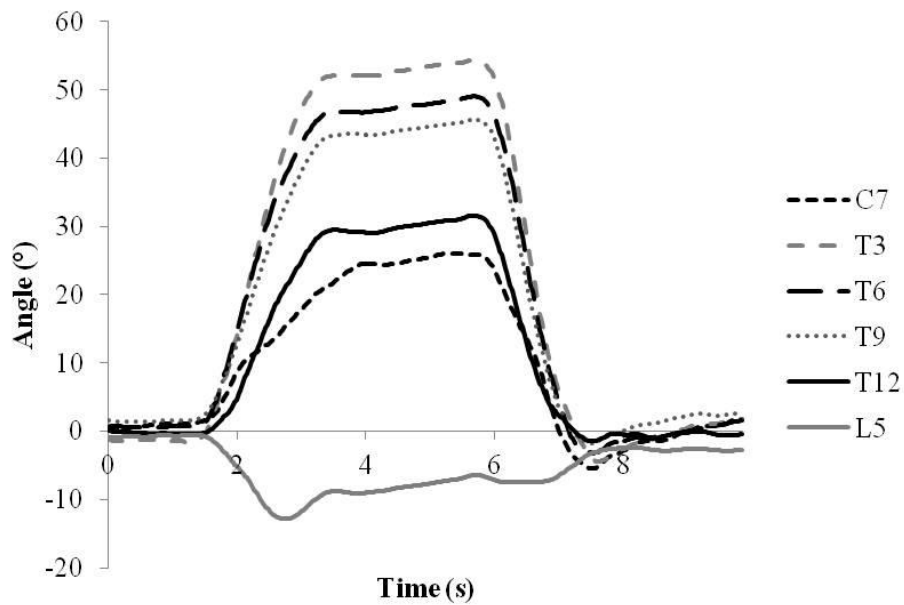


Figure 87: Sample time series data set of the flexion angles of the C₇, T₃, T₆, T₉, T₁₂, and L₅ clusters during Slump.

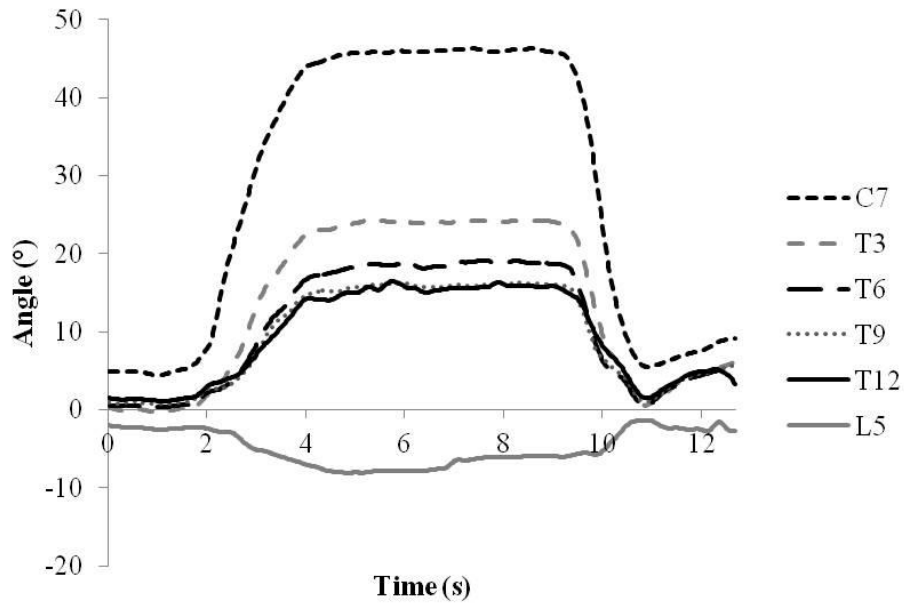


Figure 88: Sample time series data set of the flexion angles of the C₇, T₃, T₆, T₉, T₁₂, and L₅ clusters during ThorFlex.

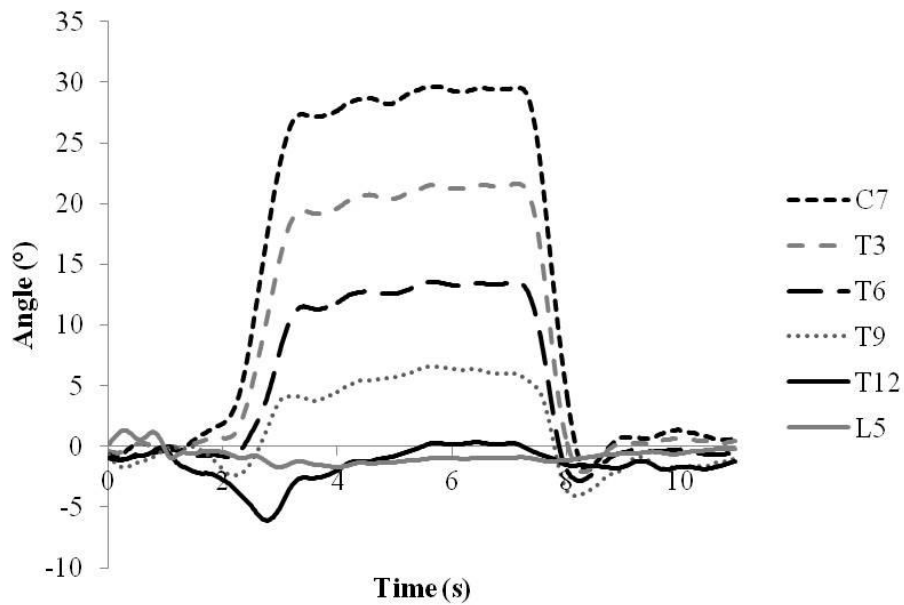


Figure 89: Sample time series data set of the lateral bend angles of the C₇, T₃, T₆, T₉, T₁₂, and L₅ clusters during ThorBend.

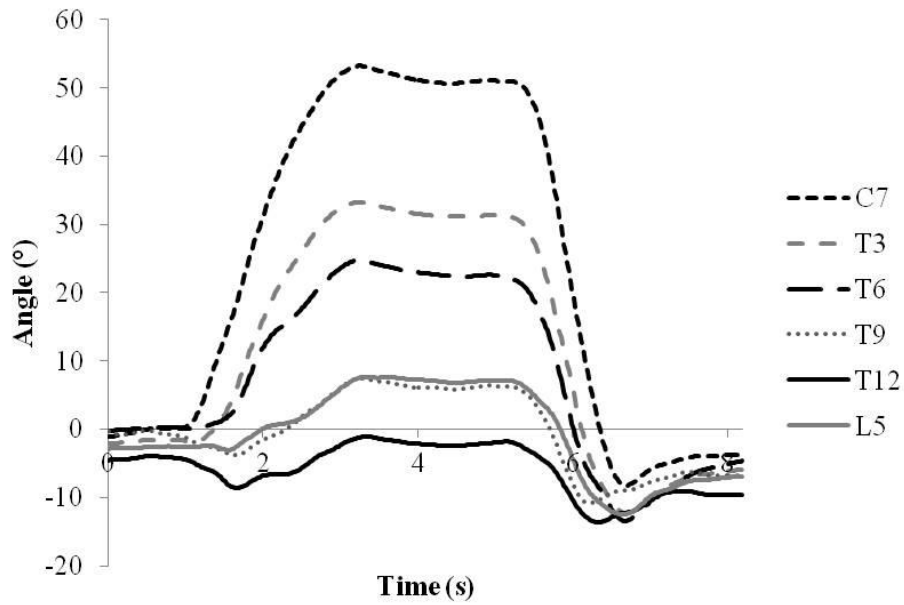


Figure 90: Sample time series data set of the axial twist angles of the C₇, T₃, T₆, T₉, T₁₂, and L₅ clusters during ThorTwist.

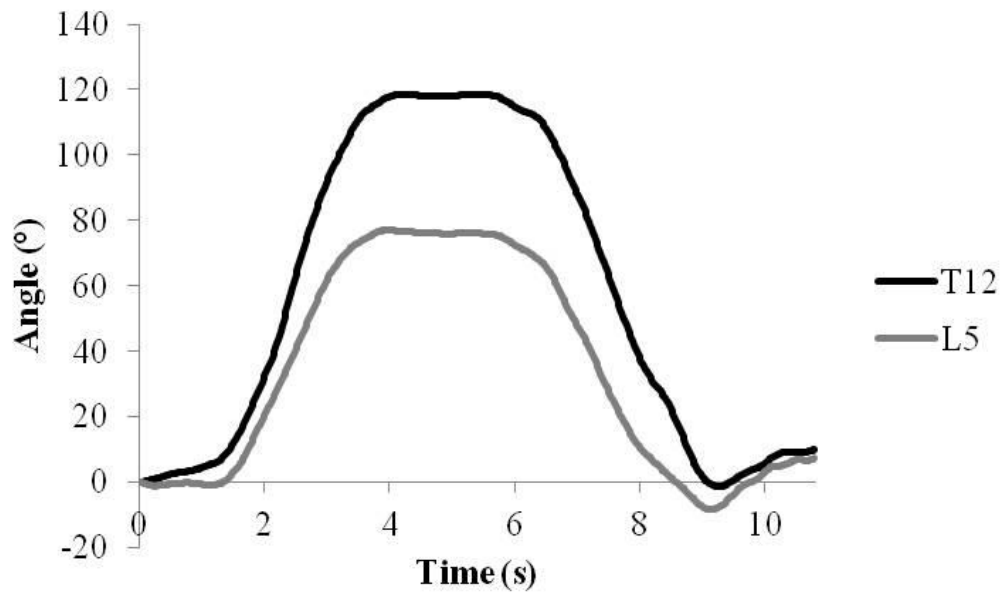


Figure 91: Sample time series of the flexion angles of the T₁₂ and L₅ clusters during MaxFlex, used for the sample cross-correlation in Figure 92.

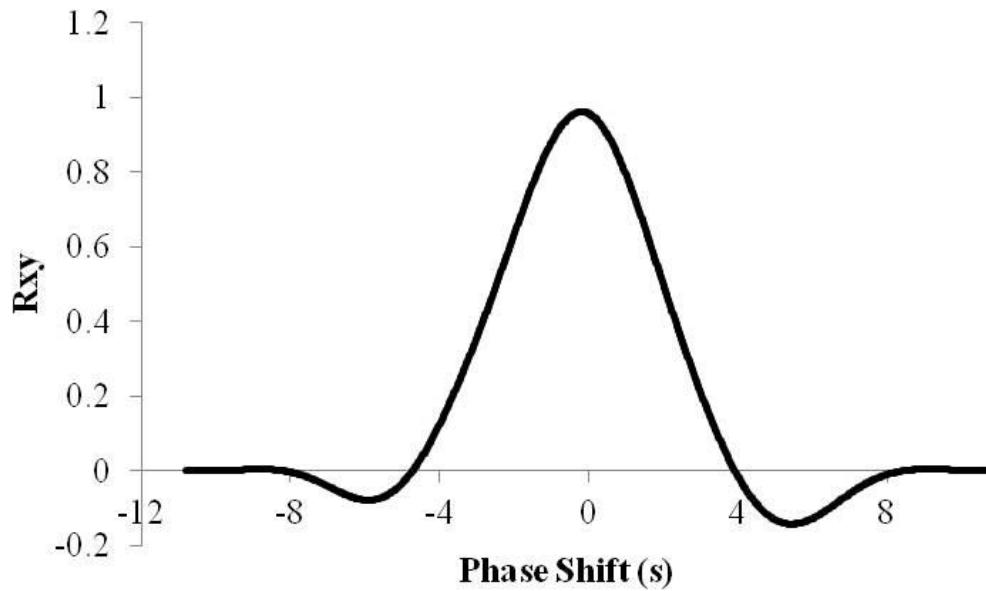


Figure 92: Output of the cross-correlation performed between the T_{12} and L_5 flexion angles during MaxFlex (shown in Figure 91). Positive values indicate that the clusters were moving in the same direction.

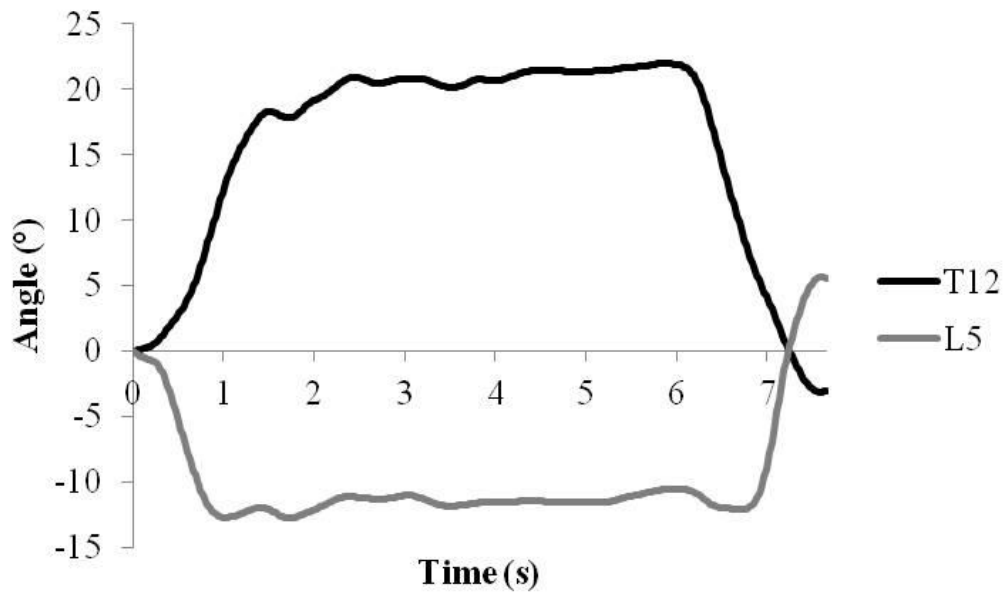


Figure 93: Sample time series of the flexion angles of the T_{12} and L_5 clusters during Slump, used for the sample cross-correlation in Figure 94.

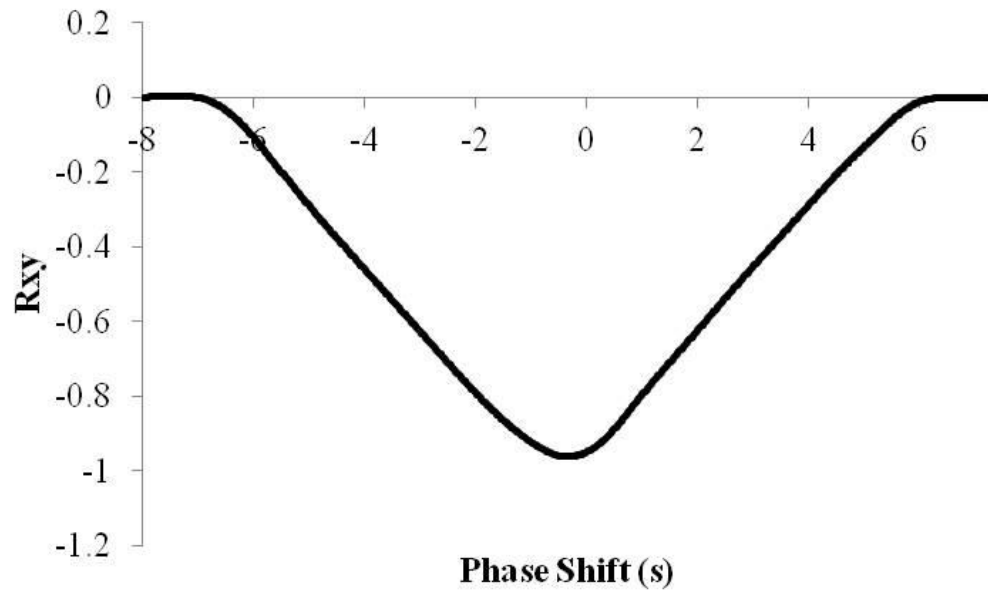


Figure 94: Output of the cross-correlation performed between the T₁₂ and L₅ flexion angles during Slump (shown in Figure 93). Negative values indicate that the clusters were moving in opposite directions.

Chapter 6

Note: For sample time series data sets for MaxFlex, MaxBend, and MaxTwist, refer to Appendix D, Chapter 3.

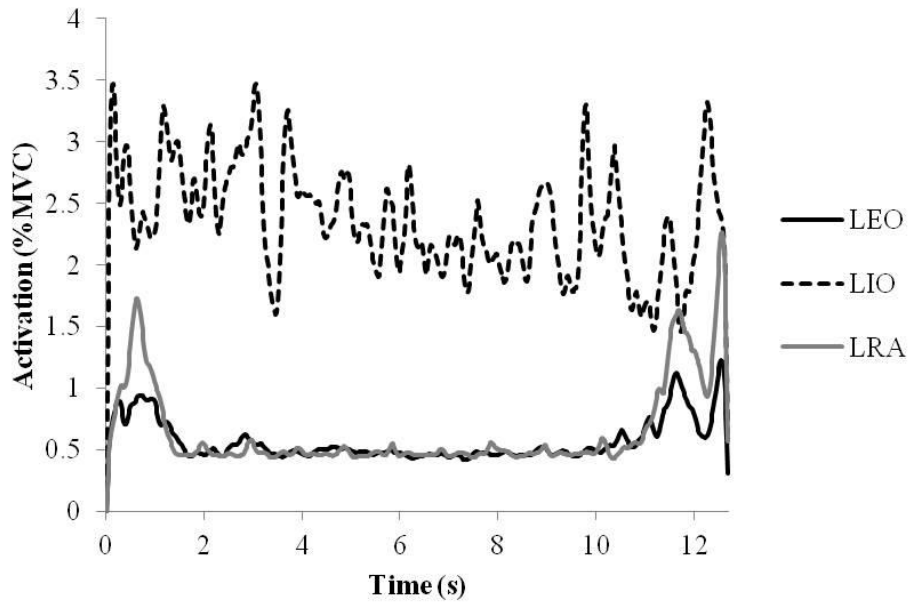


Figure 95: Sample time series data set of LEO, LIO, and LRA during Slump.

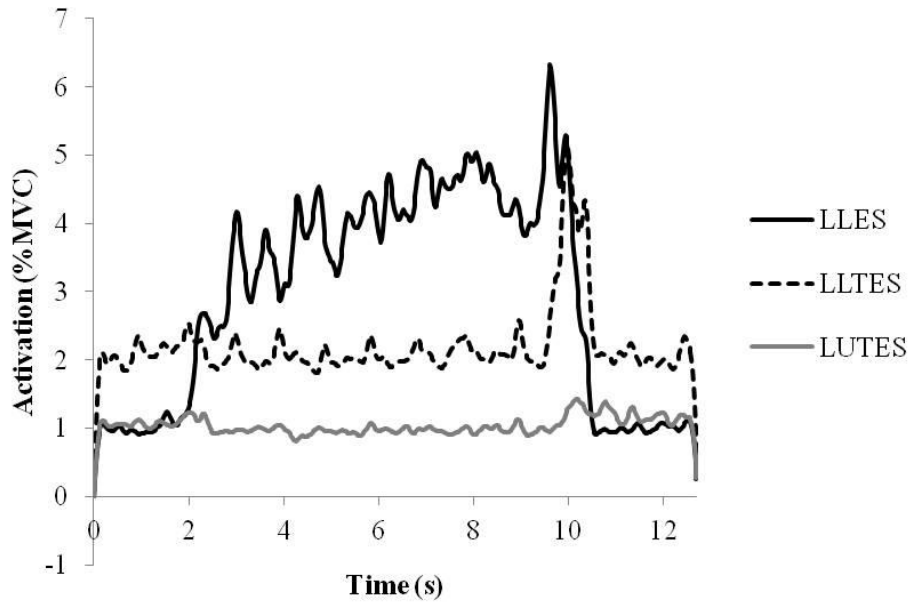


Figure 96: Sample time series data set of LLES, LLTES, and LUTES during Slump.

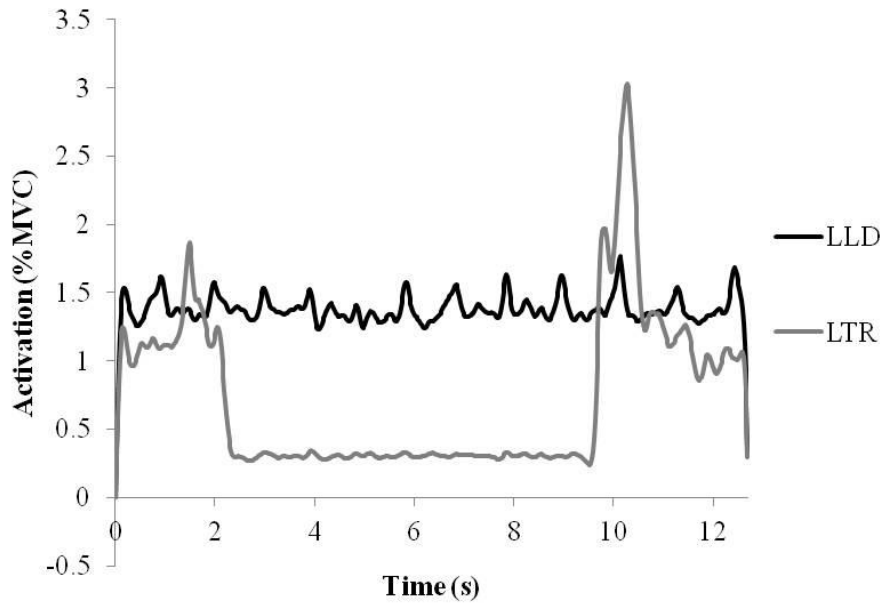


Figure 97: Sample time series data set of LLD and LTR during Slump.

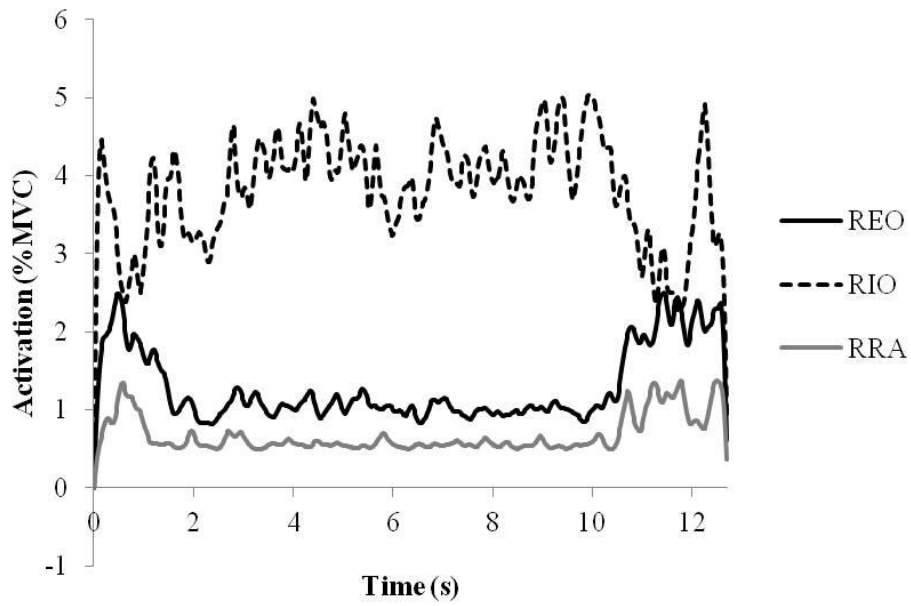


Figure 98: Sample time series data set of REO, RIO, and RRA during Slump.

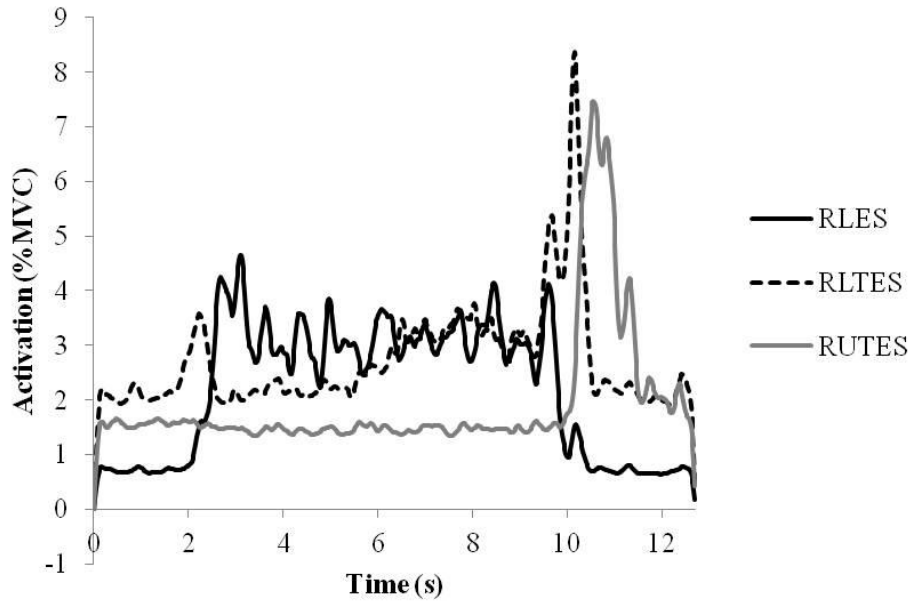


Figure 99: Sample time series data set of RLES, RLTES, and RUTES during Slump.

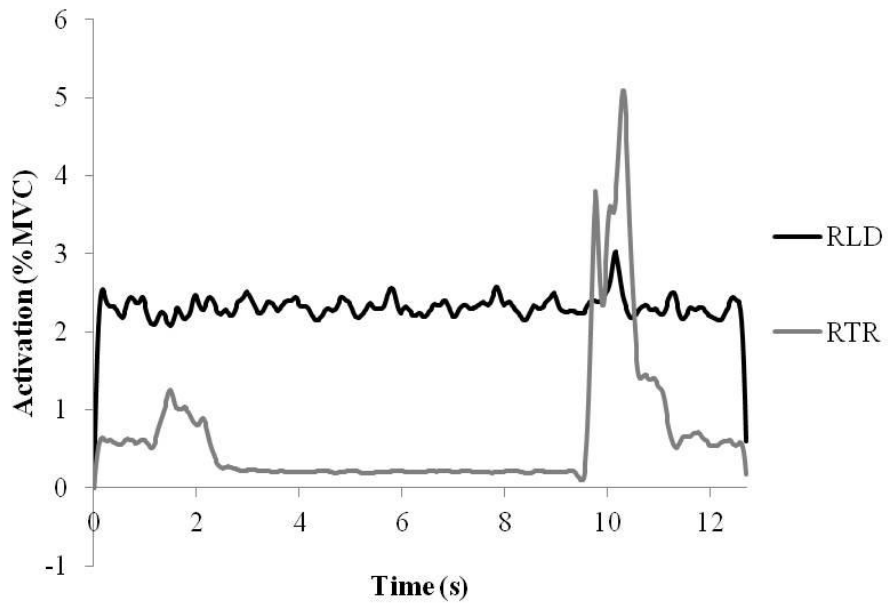


Figure 100: Sample time series data set of RLD and RTR during Slump.

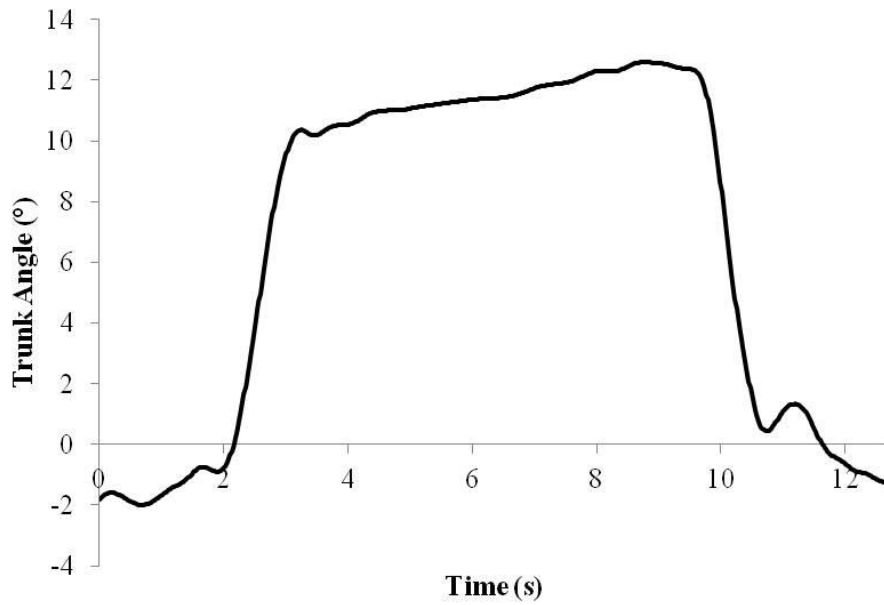


Figure 101: Time series data set of trunk flexion angles during Slump, as context for the EMG time series data sets.

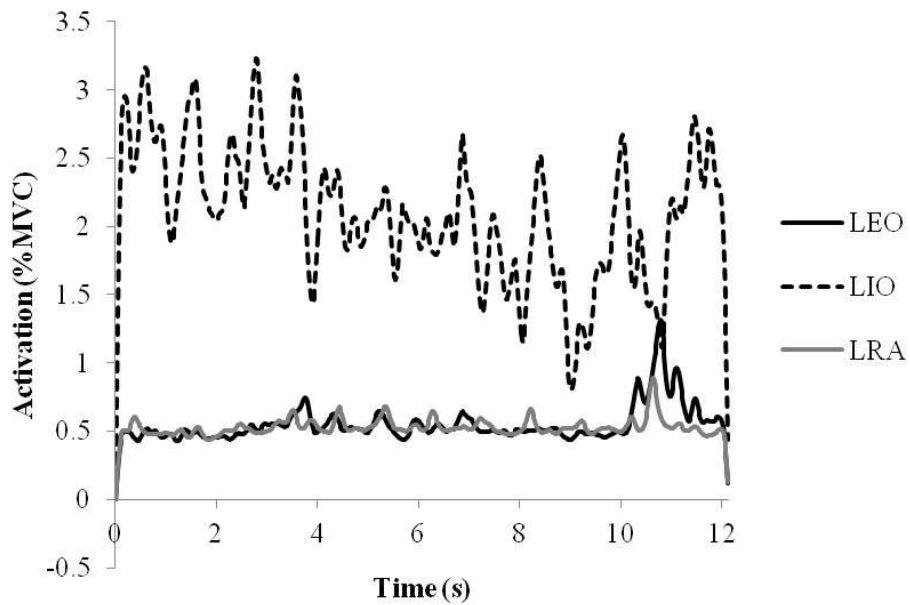


Figure 102: Sample time series data set of LEO, LIO, and LRA during ThorFlex.

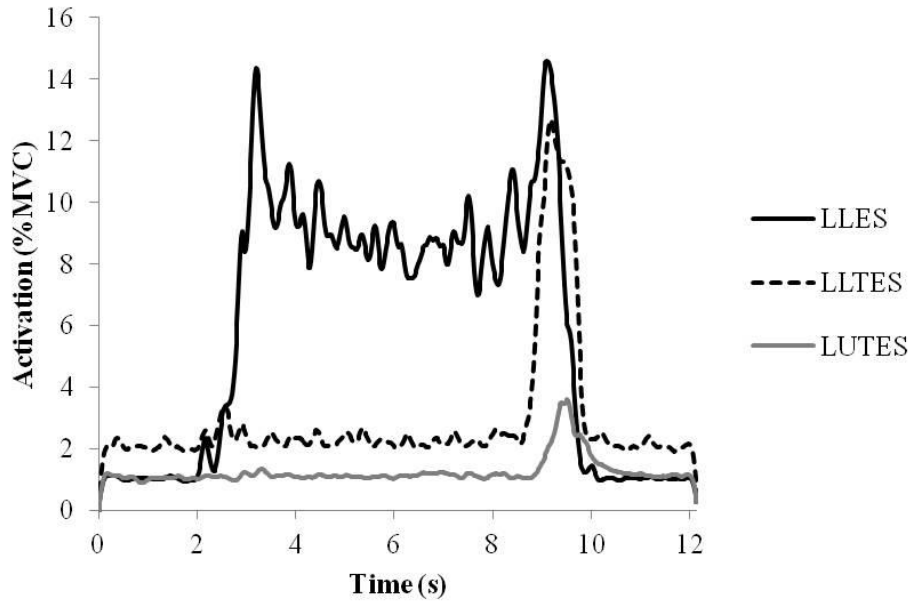


Figure 103: Sample time series data set of LLES, LLTES, and LUTES during ThorFlex.

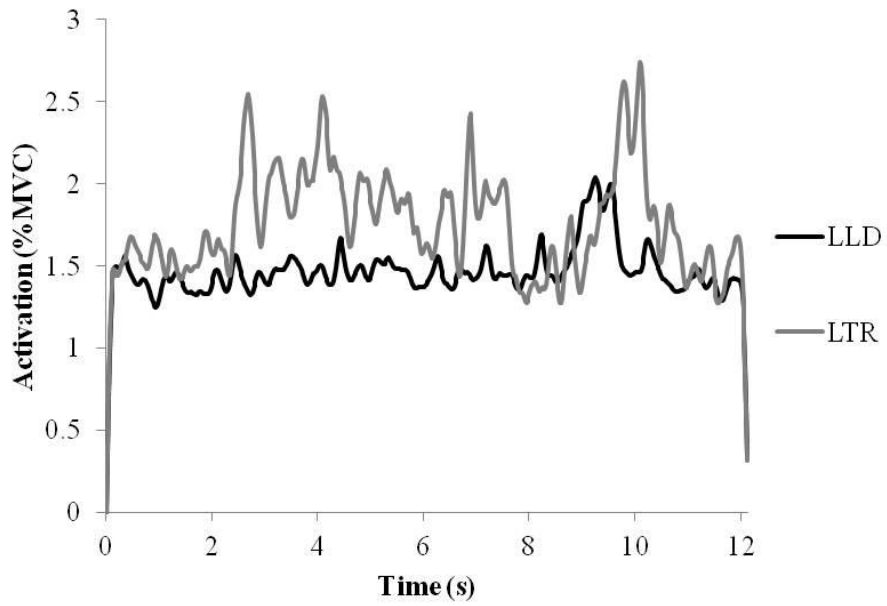


Figure 104: Sample time series data set of LLD and LTR during ThorFlex.

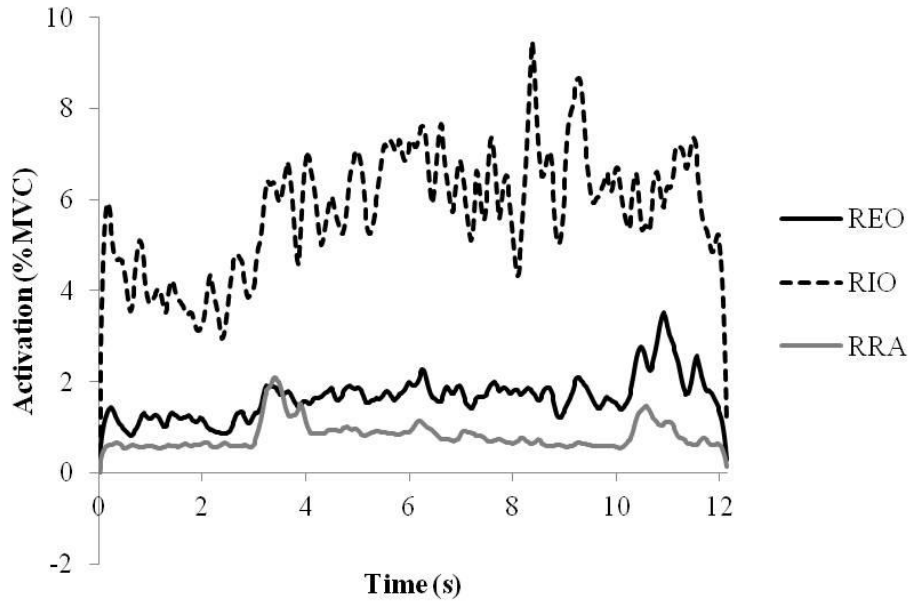


Figure 105: Sample time series data set of REO, RIO, and RRA during ThorFlex.

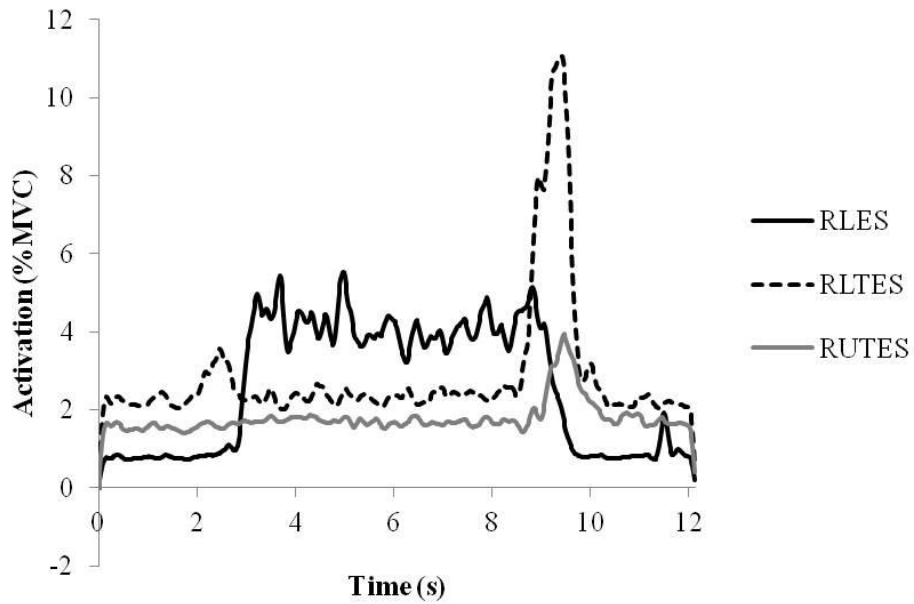


Figure 106: Sample time series data set of RLES, RLTES, and RUTES during ThorFlex.

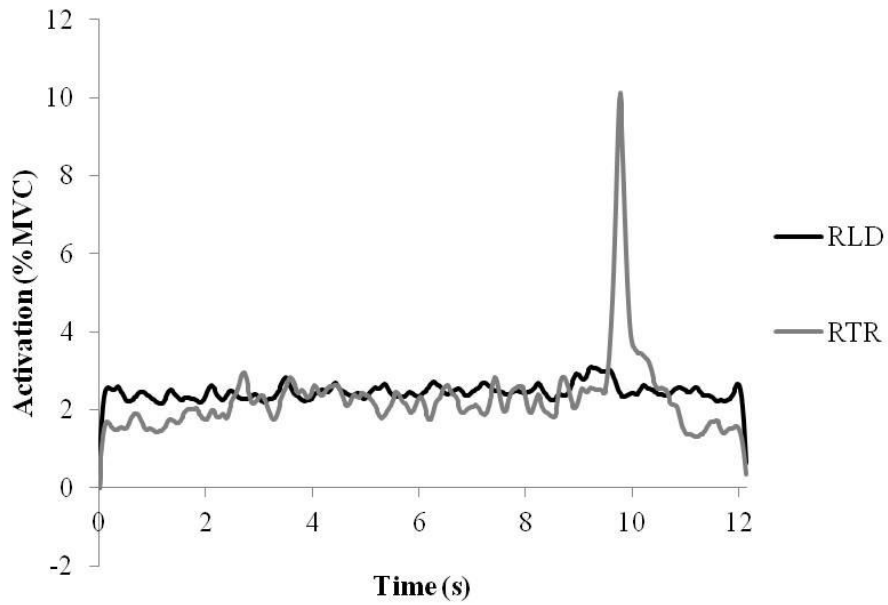


Figure 107: Sample time series data set of RLD and RTR during ThorFlex.

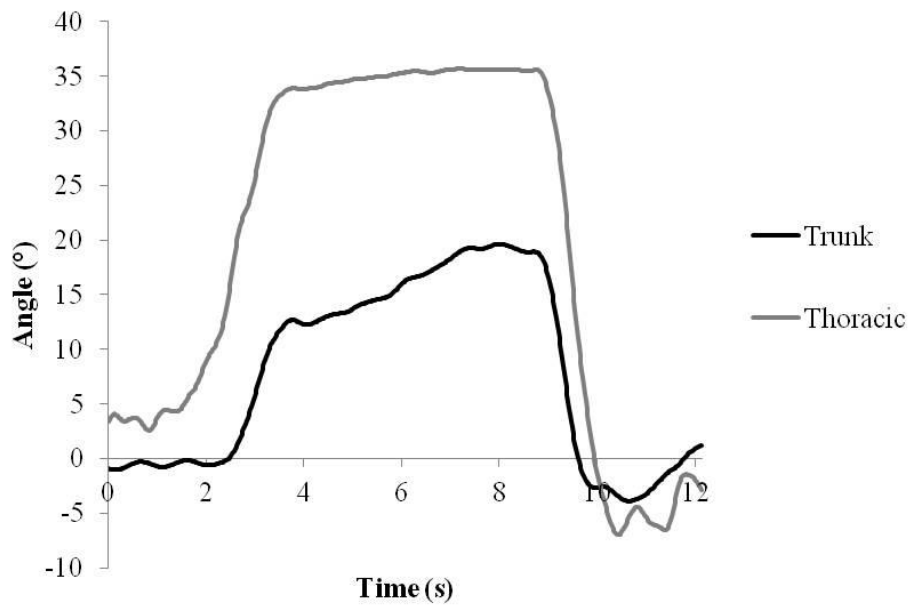


Figure 108: Time series data set of trunk and thoracic flexion angles during ThorFlex, as context for the EMG time series data sets.

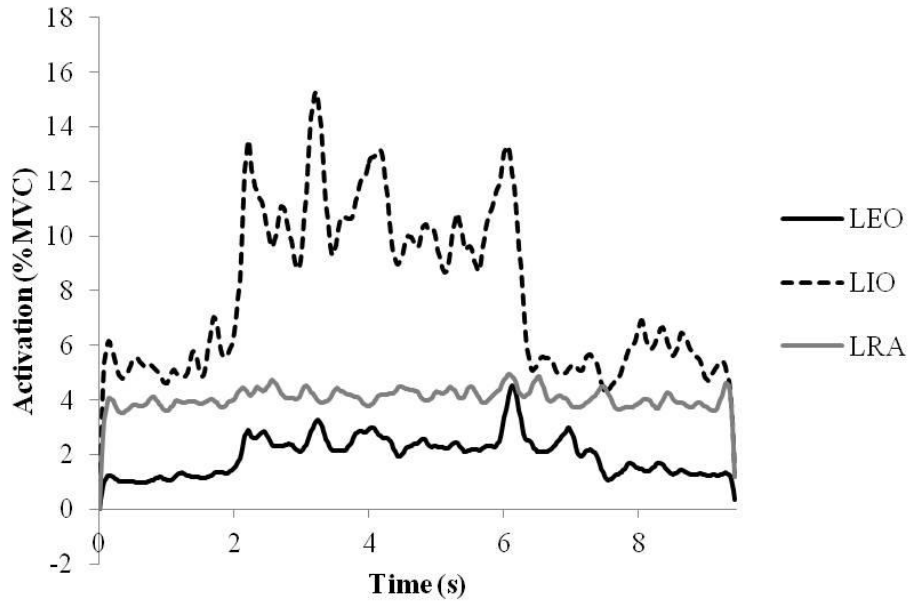


Figure 109: Sample time series data set of LEO, LIO, and LRA during ThorBend.

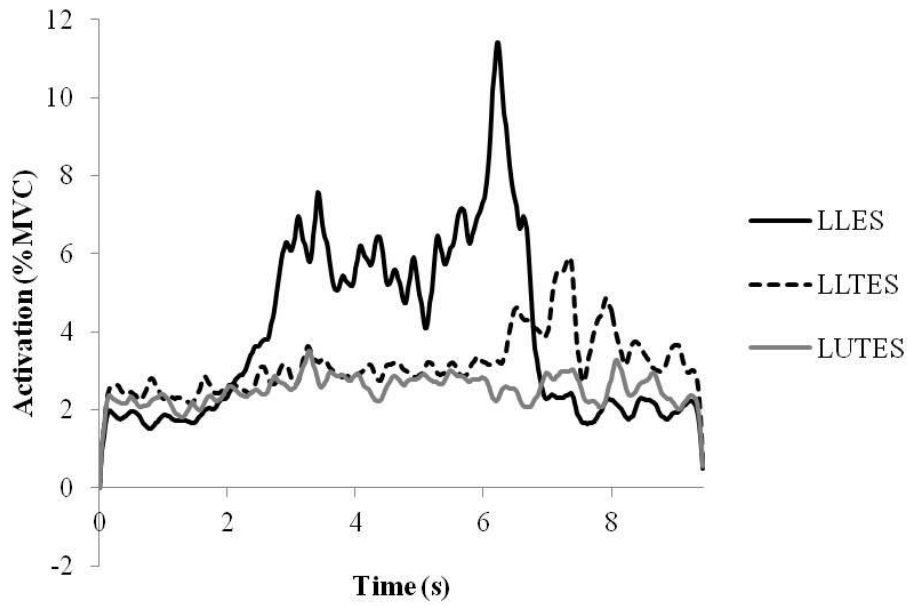


Figure 110: Sample time series data set of LLES, LLTES, and LUTES during ThorBend.

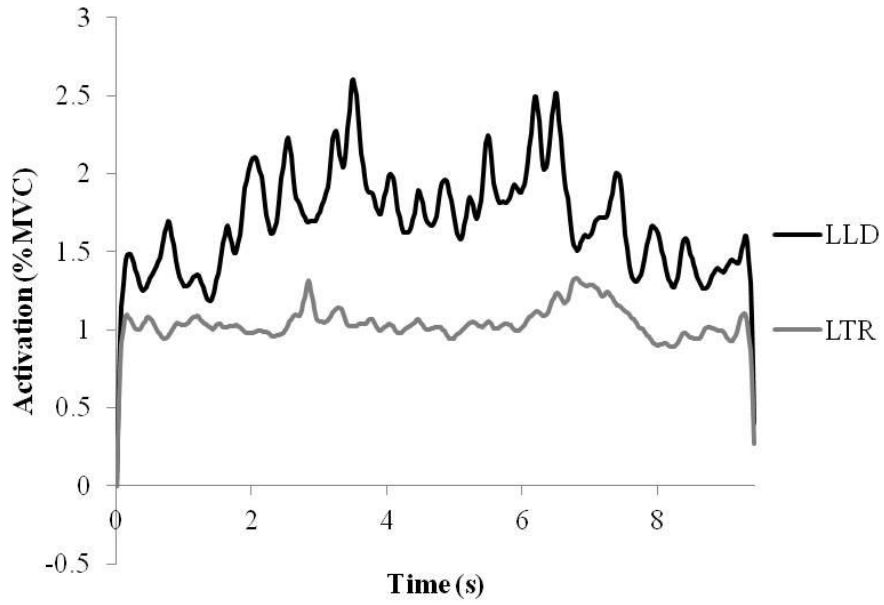


Figure 111: Sample time series data set of LLD and LTR during ThorBend.

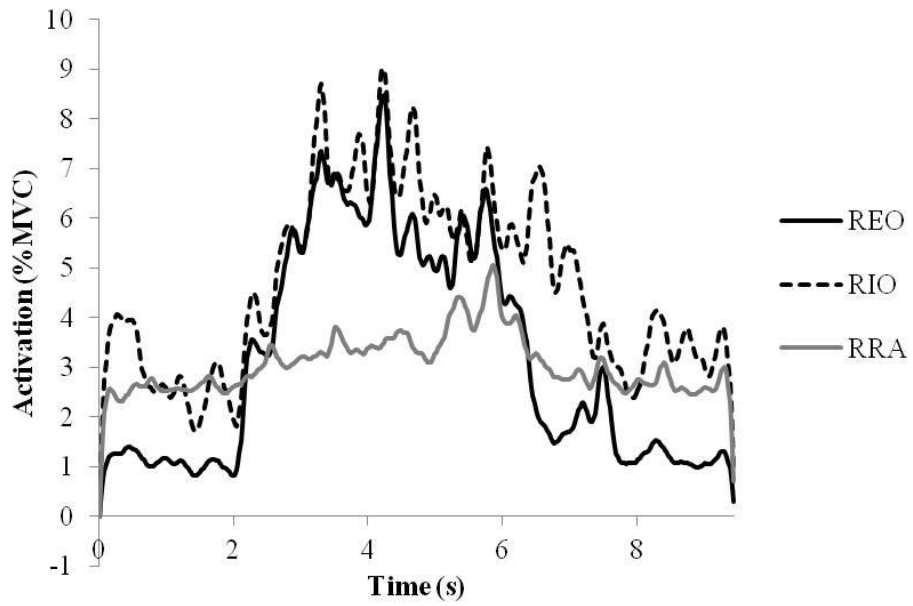


Figure 112: Sample time series data set of REO, RIO, and RRA during ThorBend.

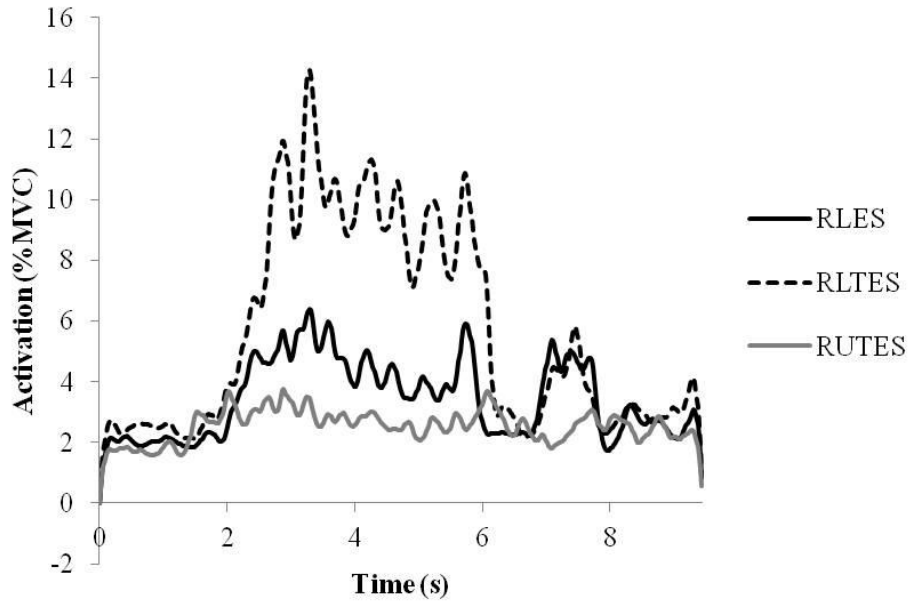


Figure 113: Sample time series data set of RLES, RLTES, and RUTES during ThorBend.

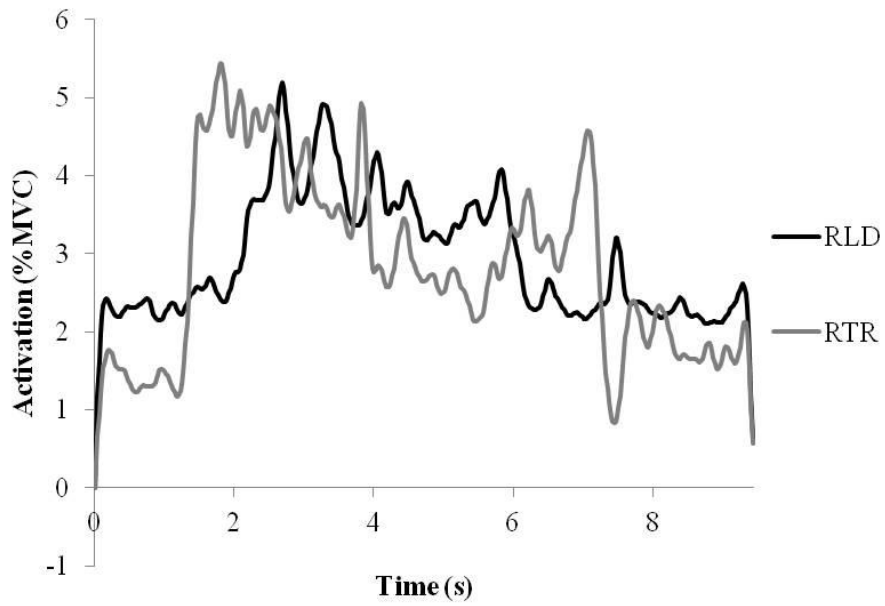


Figure 114: Sample time series data set of RLD and RTR during ThorBend.

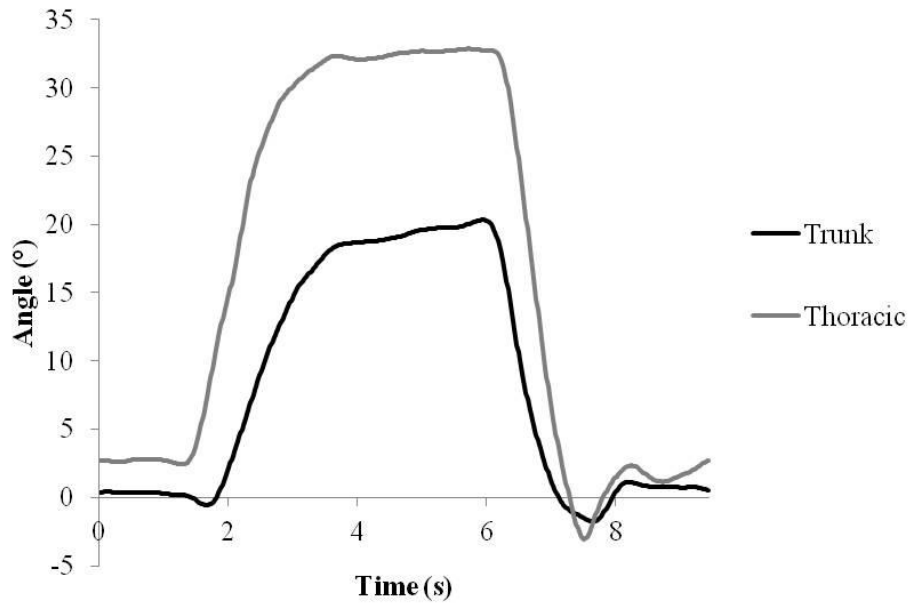


Figure 115: Time series data set of trunk and thoracic lateral bend angles during ThorBend, as context for the EMG time series data sets.

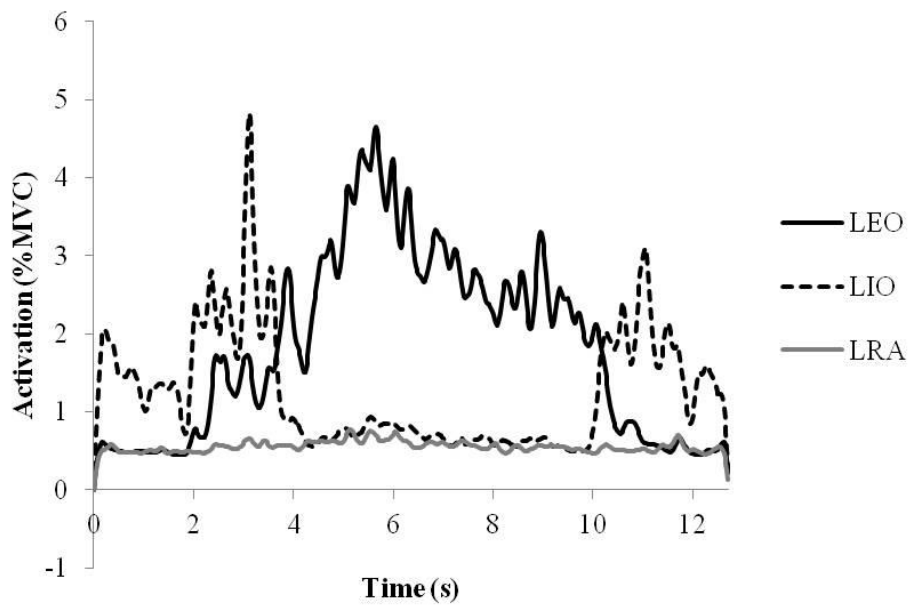


Figure 116: Sample time series data set of LEO, LIO, and LRA during ThorTwist.

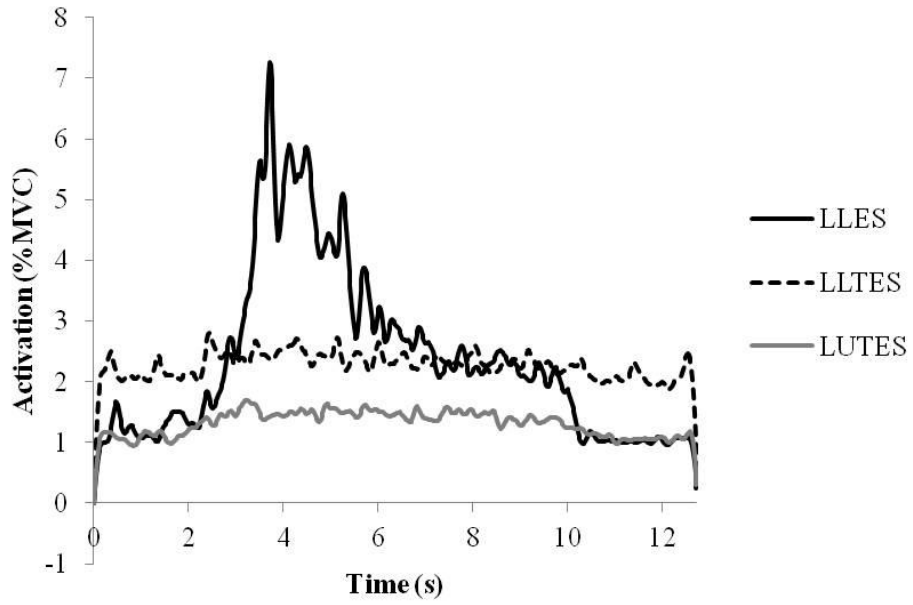


Figure 117: Sample time series data set of LEO, LIO, and LRA during ThorTwist.

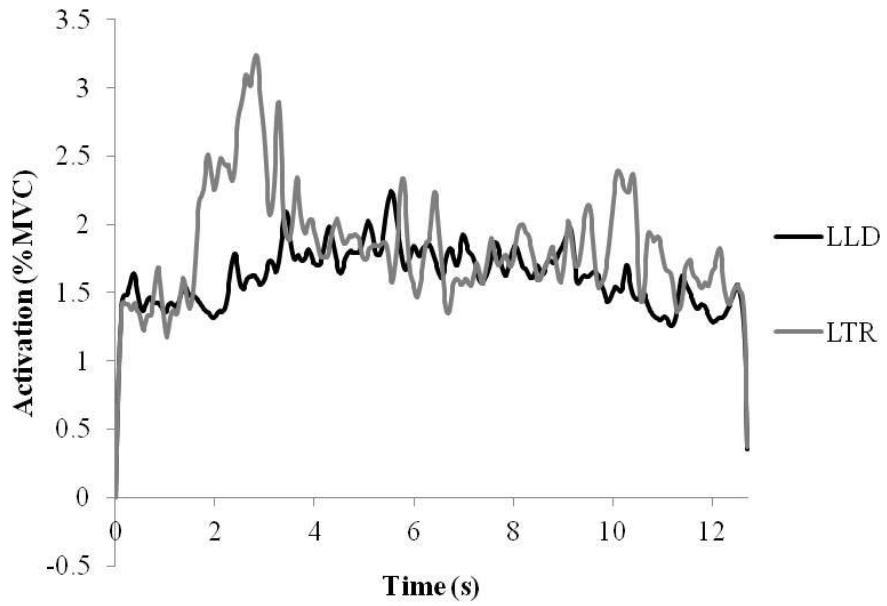


Figure 118: Sample time series data set of LLD and LTR during ThorTwist.

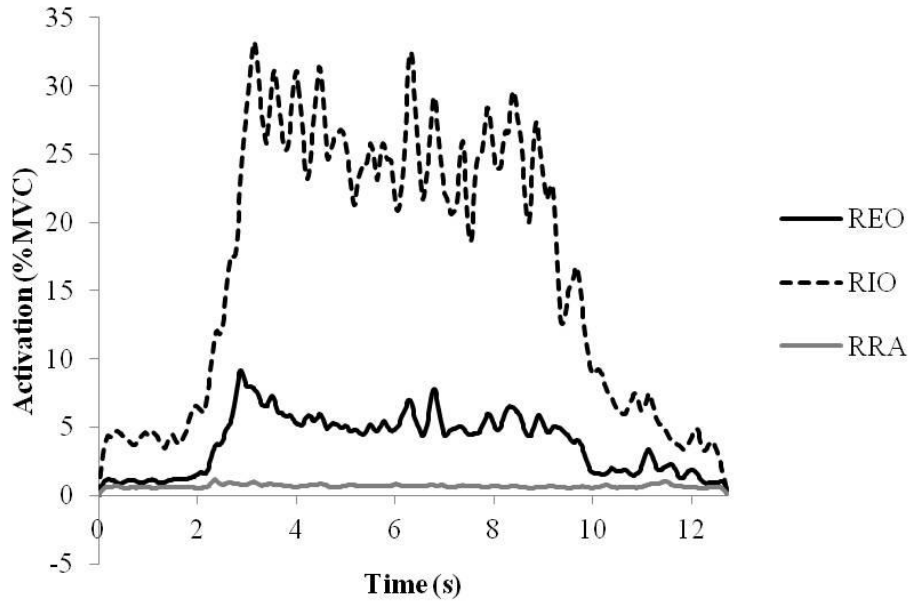


Figure 119: Sample time series data set of REO, RIO, and RRA during ThorTwist.

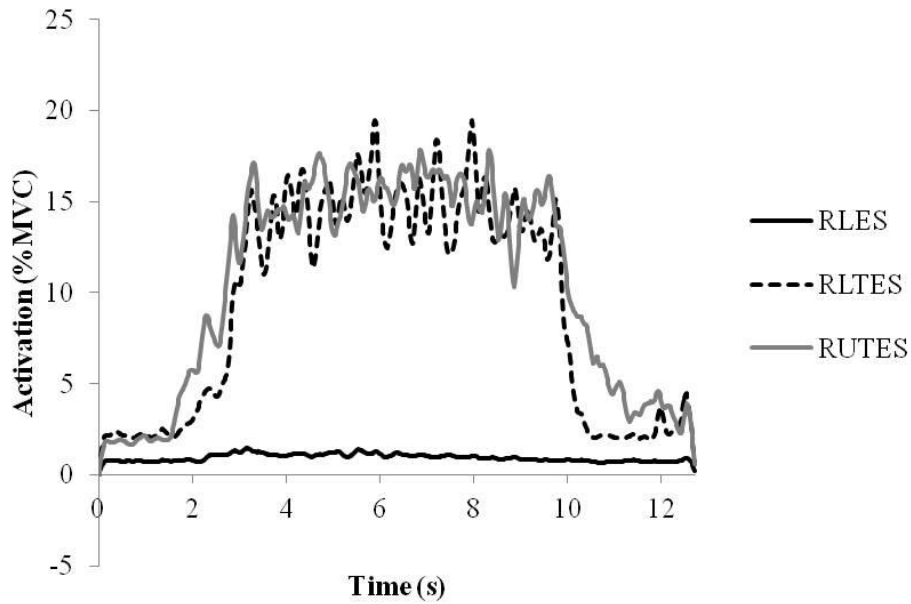


Figure 120: Sample time series data set of RLES, RLTES, and RUTES during ThorTwist.

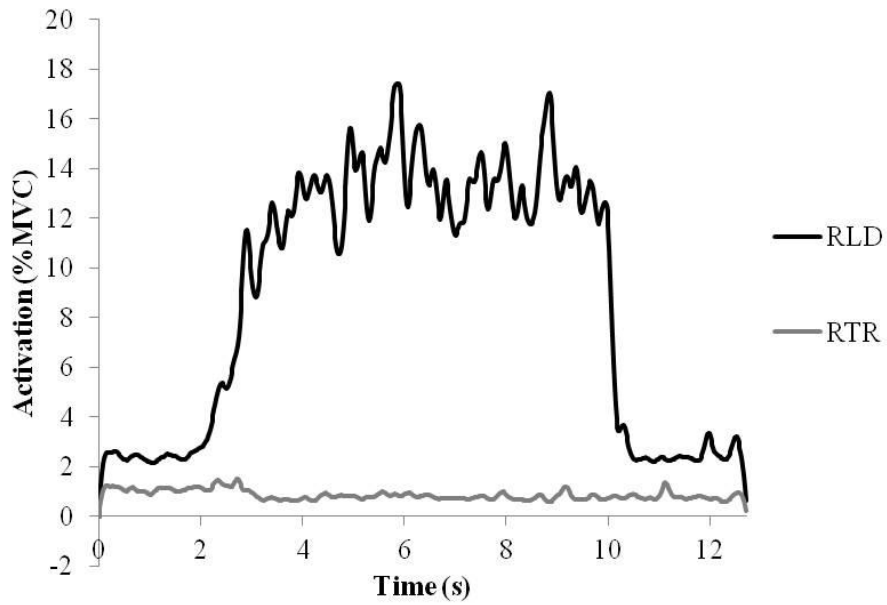


Figure 121: Sample time series data set of RLD and RTR during ThorTwist.

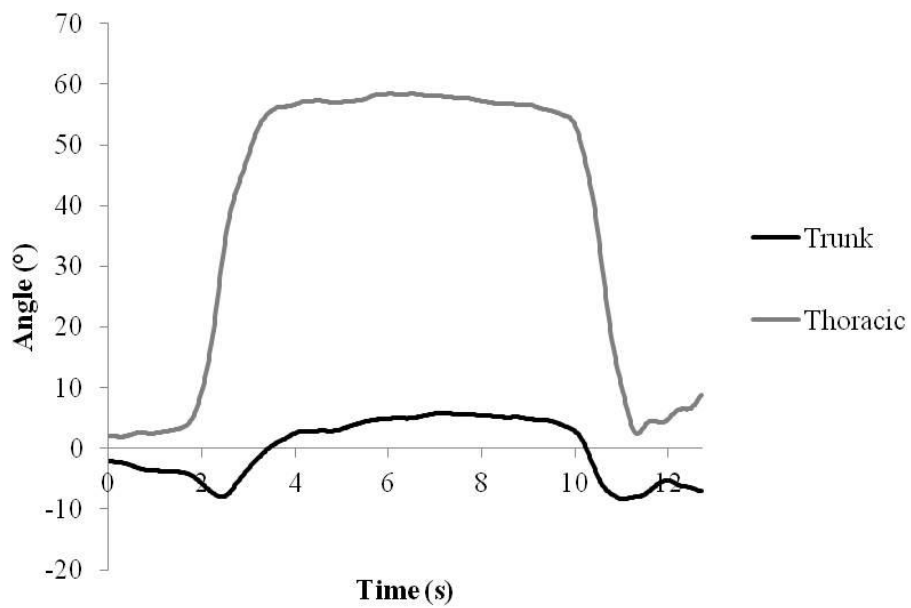


Figure 122: Time series data set of trunk and thoracic axial twist angles during ThorTwist, as context for the EMG time series data sets.

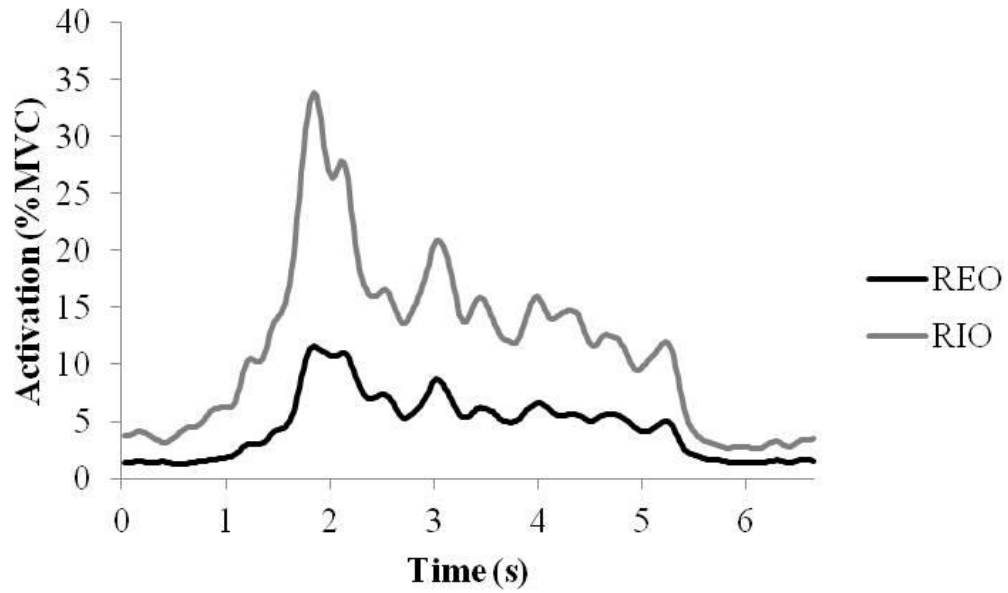


Figure 123: Sample time series of the activation of REO and RIO during MaxTwist, used for the sample cross-correlation in Figure 124.

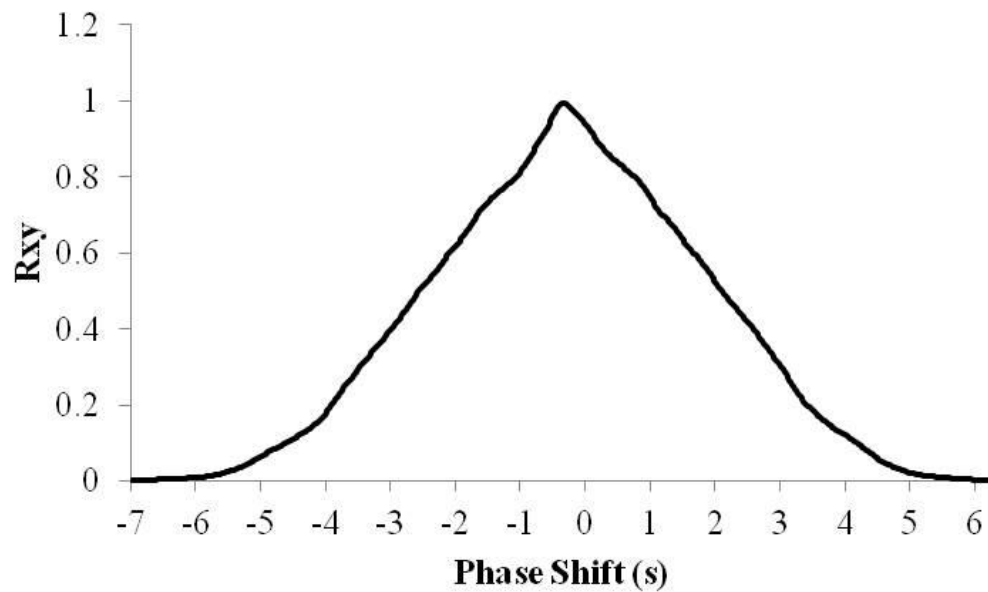


Figure 124: Output of the cross-correlation performed between REO and RIO during MaxTwist (as shown in Figure 123). Positive values indicate that the muscles were activating at the same time.

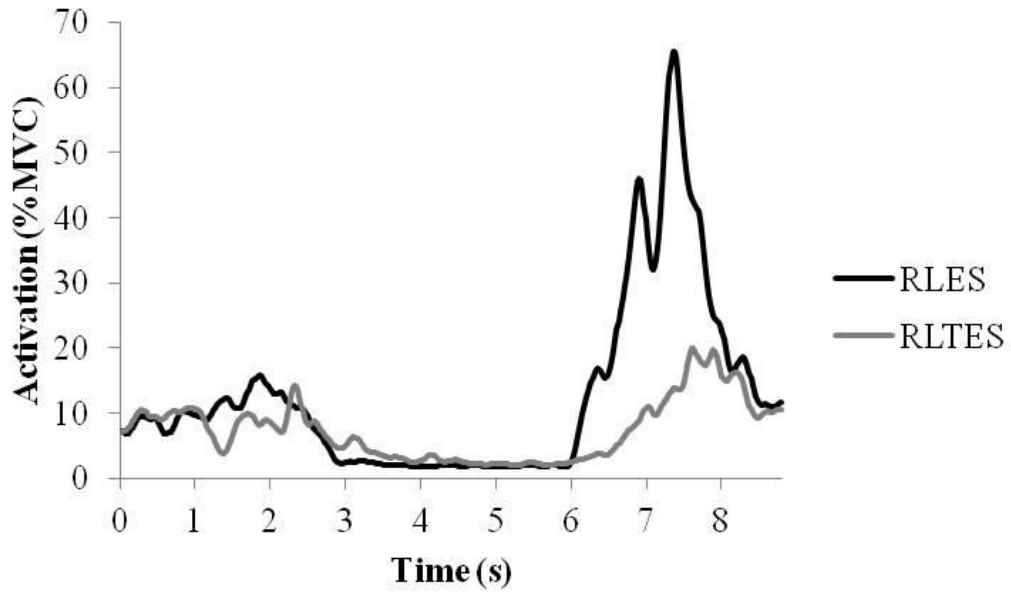


Figure 125: Sample time series of the activation of RLES and RLTES during MaxFlex, used for the sample cross-correlation in Figure 126.

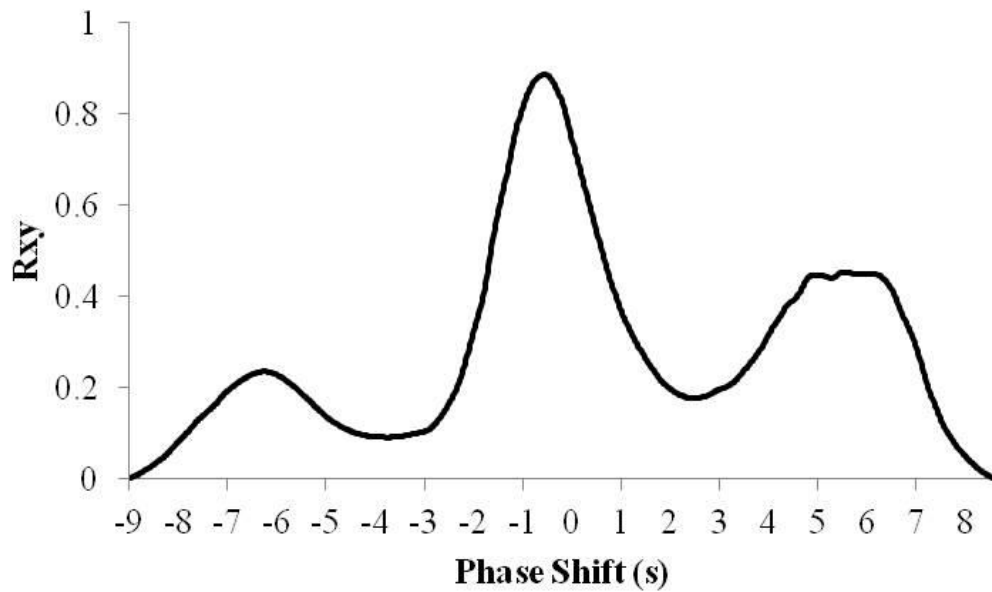


Figure 126: Output of the cross-correlation performed between REO and RIO during MaxTwist (as shown in Figure 125). Positive values indicate that the muscles were activating at the same time.